The Bombay Salesian Society's

Don Bosco Institute of Technology

Department of Electronics and Telecommunication



PubTech

volume 5.0

Research Papers based on Final Year Projects

Academic Year 2023 - 2024

Principal's Message



Dear Readers,

It is with great pride and enthusiasm that I welcome you to this special edition of "PubTech, Vol. 5" featuring a collection of technical papers based on the exceptional final year project work from the Electronics and Telecommunication (EXTC) Department.

The culmination of an engineering student's academic journey is marked by the final year project - a testament to their hard work, innovative thinking, and technical acumen. The projects showcased in this edition exemplify the dedication, creativity, and expertise of our students and faculty.

I am immensely proud of our students for their remarkable achievements and their ability to translate theoretical knowledge into practical solutions. Their work, guided by our dedicated faculty, reflects the high standards of academic excellence that DBIT upholds. The technical papers in this edition of "PubTech" are a testament to their ingenuity and potential to make significant contributions to the field of Electronics and Telecommunications.

I extend my heartfelt congratulations to all the students and faculty members who have contributed to this publication. Your relentless pursuit of knowledge and excellence is truly commendable. I am confident that the insights and innovations shared through these papers will inspire and benefit fellow students, researchers, and industry professionals.
Together, let us celebrate the achievements of our students and look forward to a future filled with groundbreaking discoveries and technological advancements.

Warm regards,

Dr. Sudhakar S. Mande

Principal

HOD's Message



Greetings of the Day!

It is with great pride and enthusiasm that I introduce PubTech 5.0, a compilation of research papers based on the final year projects of AY-2023-24. It is a testament to the remarkable work done by our students in collaboration with their research guides. This collection not only highlights the intellectual rigor and creativity of our students but also underscores the pivotal role of mentorship in academic and professional development.

The projects featured in this booklet cover a diverse array of disciplines and topics, reflecting the broad spectrum of interests and expertise within our department. These projects were very much appreciated by Industry professionals and external peers from academia during "INNOVEX-2024", the annual project exhibition and competition.

I extend my heartfelt congratulations to all the students and their research guides whose work has been published. Your dedication, hard work, and collaborative spirit are truly commendable. I also express my gratitude to Ms. Madhavi Pednekar for her meticulous efforts in bringing this compilation to life.

I hope that this work will serve as an inspiration to current and future students, as well as to researchers and practitioners in the wider academic community. May it encourage continued exploration, foster new collaborations, and contribute to the advancement of knowledge in various fields.

Thank you for being a part of this journey and for celebrating the achievements of our talented researchers and their mentors.

Ms. Namita Agarwal,

HOD, EXTC Department.

PubTech Vol. 5 Team



Ms. Madhavi S. Pednekar
B.E. Project Coordinator, Dept. of EXTC



Mr. Jero Royston Poobalarayan
Student, Dept. of EXTC

CONTENTS

1. Design and Development of a Metasurface Antenna for Sensing Applications. 01
2. Design and Development of a Metasurface Based C-Band Phase Shifter. 07
3. Smart Water Management using LoRaWAN. 13
4. Advanced Navigational System for Accurate GPS Localization. 24
5. Development of a Container GPS Tracking System to Enhance Supply Chain Security. 30
6. Design of a LiDAR System using Optisim Scans. 36
7. Design and Development of Duplexer for GSM Applications. 42
8. Analysis and Comparison of Methods of Speech Recognition Using Neural Network. 50
9. Implementation of Mesh Topology for IoT Network. 56
10. Multi-Object Detection in Operation Theatre. 61
11. Design and Development of a Ultra-Wide Band Antenna Configuration For Radio Jamming Applications. 64
12. Real Time ICU Patient Monitoring & Visualisation of Critical Parameters of Patients Health for Hospital Professionals. 71
13. Design and Implementation of Low Power MAC Unit for Image Processing on FPGA. 79

PUBLISHED AND ACCEPTED PAPERS

1. Evaluating the Effectiveness of Machine Learning Models for Early Diagnosis of Chronic Kidney Disease. 85
2. Design of Web based Student Information System. 90
3. A-eye: Attendance Monitoring using Face Detection and Recognition from CCTV Footage. 95

Design and Development of a Metasurface Antenna for Sensing Applications

Rakshita Khantwal[1], Suraj Kumar[2], Ashwini Kotrashetti[3], Freda Carvalho[4]
[1]*Department of Electronics and Telecommunication Engineering*
[1]*The Bombay Salesian Society's, Don Bosco Institute Of Technology, University of Mumbai, Mumbai India*
[1]*khantwalrakshita@gmail.com,* [2]*surajkumarskd123@gmail.com* [3]*ashwinikotrashetti@dbit.in,* [4]*freda@dbit.in*

***Abstract*—In this paper, the design and development of a metasurface antenna operating within the 2.4GHz ISM (Industrial, Scientific, and Medical) band is discussed, targeting a 10dB return loss and a minimum gain of 10dB across the operational bandwidth. Metasurfaces, characterized by their engineered subwavelength elements, offer remarkable accuracy in controlling electromagnetic waves. This study capitalizes on the unique properties of metasurfaces to create a high-performance antenna system for sensing applications. The outcomes of this research contribute to the advancement of metasurface antenna technology, offering innovative solutions for sensing applications across diverse fields such as healthcare, environmental monitoring, and industrial automation.**

***Index Terms*—Metasurface antenna, 2.4GHz ISM band, return loss, gain, sensing applications**

I. Introduction

The demand for wireless sensing systems operating at the Industrial, Scientific, and Medical (ISM) frequency band is steadily increasing due to their widespread applications in various fields. Microwave sensors have become popular over the last few years. Their contactless sensing capability, real-time detection ability, accuracy in measurement, ease of fabrication, and robustness have made them one of the fundamental choices in smart sensing applications. In addition, having a higher operational frequency reduces their footprint, and their planar structure allows them to integrate easily with wireless communication systems [1], [2].

A metasurface antenna is a type of antenna that employs a metasurface to control and manipulate electromagnetic waves. Metasurfaces are artificially engineered structures consisting of sub-wavelength-sized elements or metamaterials that are designed to control the propagation of electromagnetic waves in unconventional ways [3].

These artificial, nanostructured (subwavelenth) surfaces have the ability to control and engineer the behavior of electromagnetic waves in unprecedented ways, revolutionizing various industries such as telecommunications, imaging, and sensing. Metasurfaces offer unique opportunities to manipulate the properties of electromagnetic waves, enabling applications that were once considered impossible or extremely challenging [4].

Metasurface antennas offer high sensitivity and specificity in detecting biological molecules and biomarkers. By functionalizing the surface of the metasurface with specific receptors or ligands, they can selectively capture target biomolecules such as proteins, DNA, and RNA. Metasurface antennas are also being explored for the rapid and sensitive detection of viruses and other pathogens. Similar to bio-sensing applications, the surface of the metasurface can be functionalized with receptors or antibodies that specifically bind to viral particles. Metasurface antennas can also be deployed for environmental monitoring applications, including the detection of pollutants, toxins, and harmful substances in air, water, and soil. By functionalizing the antenna surface with appropriate sensing elements [5].

Research into metamaterials and metasurfaces has experienced explosive growth over the last two decades, evident in various metrics. Special sessions on these topics are now commonplace at major international meetings across several communities, and entire conferences are dedicated to them (for example, the Metamaterials conference is now in its fourteenth edition). Currently, hundreds of research groups worldwide are actively pursuing "meta" research programs, with several institutional networks and funding mechanisms established solely for advancing this science and technology. Tens of thousands of articles have been published at an astonishing rate in leading journals across multiple research communities [6].

Unlike traditional bulky optical components, metasurfaces are ultra thin and lightweight, offering a platform for the development of compact and efficient devices. Some of its application fields are:

- Remote sensing in weather monitoring, environmental sensing, and agricultural monitoring. The ability of metasurface to control radiation patterns and beam steering can enhance the precision and coverage of remote sensing systems.
- Wireless sensing networks for applications like structural health monitoring, where they enable the detection of cracks, deformations, or other anomalies in buildings, bridges, and infrastructure.
- Security and surveillance applications, such as intrusion detection and perimeter monitoring, by enabling better control of radar and communication systems.
- Metasurface antennas can improve the resolution and performance of radar and imaging systems. By controlling the direction and focus of electromagnetic waves,

they can enhance object detection, tracking, and imaging capabilities, which are valuable in fields like security, defense, and autonomous vehicles.
Metasurfaces, a recent development in nanophotonics, revolutionize light manipulation by replacing bulky optical components with ultrathin, flat counterparts, over 10,000 times thinner. Since their first demonstration in 2011, they've sparked immense interest in consumer optics and electronics industries. Notably, metasurface-enabled bioimaging and biosensing tools have emerged, showcasing novel applications. This review article delves into the cutting-edge of this technology, offering an interdisciplinary perspective. Topics covered include metasurfaces for chiral imaging, endoscopic optical coherence tomography, fluorescent imaging, super-resolution imaging, magnetic resonance imaging, quantitative phase imaging, and sensing of antibodies, proteins, DNAs, cells, and cancer biomarkers. Future directions explore application-specific biomedical metasurfaces and bioinspired metasurface devices. Perspectives on challenges, opportunities, and translational biomedical devices in metasurfaces and biophotonics are also discussed. [7].

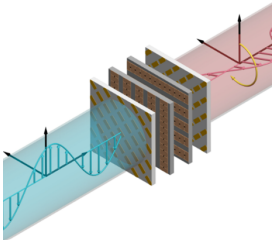


Fig. 1. Metasurface manipulating electromagnetic wave's phase [8]

A. Motivation

To create a sensing metasurface antenna operating at the ISM frequency of 2.4 GHz. The antenna will transmit and receive signals at 2.4 GHz, and the received signals will be analyzed. Any changes detected by the antenna will result in a change in the spectrum properties, which can be further analyzed. The proliferation of IoT devices and wireless sensor networks has opened up new possibilities for collecting data in diverse environments. Metasurface antennas offer a compact and versatile platform for integrating sensing capabilities into existing communication networks, enabling seamless data collection and analysis across various applications, including smart cities, environmental monitoring, and healthcare. In an increasingly interconnected and data-driven world, there is a need for innovative solutions to address emerging challenges, such as cybersecurity threats, environmental pollution, and public health crises. A sensing metasurface antenna offers a versatile platform for addressing these challenges by providing real-time monitoring and analysis capabilities, enabling proactive responses to potential risks and disruptions.

II. Methodology

- Assessing the problem to enlist the antenna specifications, assessing the problem and enlisting antenna specifications based on application requirements, environmental considerations, system integration needs, regulatory standards, and stakeholder input. Identify the specific application for which the antenna will be used.
- Identifying the type of antenna design through a literature survey: involves reviewing existing research papers, articles, textbooks, patents, and other scholarly sources to understand the various antenna designs that have been proposed or implemented for specific applications.
- Design of metasurface antenna: antenna involves the integration of metasurface technology into the antenna structure to achieve desired electromagnetic properties and performance characteristics.
- By simulating metasurface antennas, designers can efficiently explore design options, understand the electromagnetic behavior, and predict performance characteristics before fabricating physical prototypes, thereby saving time and resources in the design process.
- Analyzing and optimizing antenna designs for specific parameters, involves a systematic process to evaluate the performance of an antenna design and refine it to meet desired specifications.
- Layout and getber of antenna design, The geometry of the antenna refers to its physical shape and structure. This includes elements such as the radiating elements (e.g., dipole arms, patch dimensions), ground plane, feed structure.
- Designing a mechanism to feed antenna elements involves, creating a structure or system that efficiently transfers electromagnetic energy from the transmission line to the radiating elements of the antenna.
- Creating a metasurface antenna element array, involves designing and arranging individual metasurface elements in a two-dimensional array to achieve desired electromagnetic properties and antenna performance.
- Creating power divider to feed all metasurface units, Design a power divider or feeding network to distribute electromagnetic energy from the transmission line to all metasurface units within the antenna array..
- Optimization of metasurface antenna size, Optimize the size of the metasurface antenna to meet performance requirements while minimizing physical dimensions.
- Fabrication of antenna, Fabricate the metasurface antenna using appropriate manufacturing techniques and materials.
- Testing of antenna, Conduct experimental testing of the fabricated antenna to evaluate its performance in real-world conditions.
- comparison of simulated and measured results, Compare simulated results obtained from HFSS simulation software with measured results obtained through experimental testing.

A. Software Used

Ansys HFSS (high-frequency structure simulator) is used to make this project. It is a powerful electromagnetic simulator software developed by Ansys for simulating and analysing high frequency antennas, electronics components, RF/microwave circuits. HFSS is a versatile and comprehensive electromagnetic simulation tool used across various industries, including telecommunications, aerospace, automotive, electronics, and defense, for the design and analysis of high-frequency electromagnetic devices and systems.

III. Implementation of Metasurface Unit Cell

At the base of the antenna structure, a microstrip line is present with a FR-4 substrate positioned on top of it. Overlying this substrate is a copper sheet with a slot. This gives rise to an aperture coupled microstrip line. Subsequently, another layer of FR-4 substrate is on the copper sheet. Positioned at the apex of this configuration is a star patch. The thickness of copper sheet is 0.035mm and both the FR-4 substrates have thickness of 0.8mm. This is seen in single unit cell side view i.e. Fig.2

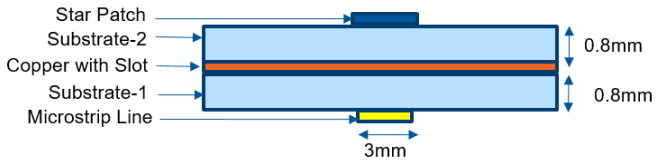


Fig. 2. Single unit cell side view.

Unit cell refers to the basic repeating structure within a larger antenna array or metamaterial. The unit cell is typically a small geometric shape or structure that is replicated across the entire antenna array to achieve the desired radiation pattern. Dimension of the antenna is lambda/5 i.e each side is equal to 25mm. The star patch has 12 edges. A unit cell is seen in the top view in Fig.3

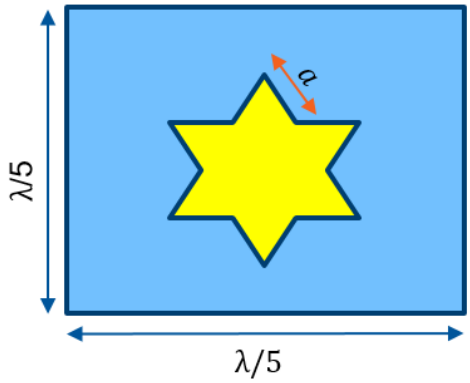


Fig. 3. Single unit cell top view.

A. Feeding Mechanism

The microstrip line excites the structure with electromagnetic wave. Microstripline has dimension of 15.16*3 mm. Slot present on the copper sheet gives path to the electromagnetic wave to excite the star patch. The slot dimensions are 1.3*22mm and the stub length is equal to 1.15mm which is an important parameter of the antenna as shown in Fig.4 When the stub is matched, maximum power transfer takes place with minimum reflections.

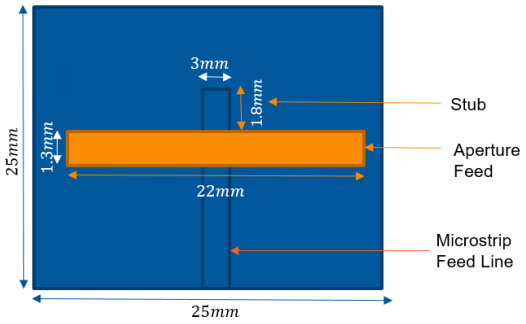


Fig. 4. Feeding mechanism for a single unit cell.

The ground plane, situated between two substrates, is designed with a slot to enable aperture feeding. This configuration facilitates the use of a microstrip feed line positioned beneath the ground plane, allowing for radiation through the slot to excite the radiating patch located above it. This aperture feeding mechanism enables efficient transmission of electromagnetic signals from the feed line to the radiating patch, facilitating effective communication or radiation performance in the system.

Simulation Results

B. Single unit metasurface without reflector

The top view of single unit metasurface and its back feeding is as shown in Fig. 5. The antenna exhibited a return loss of 41.43 dB and operated within a bandwidth of 120 MHz which covers the ISM band of operation as shown in Fig. 6. However, its gain is measured to be 6.25 dBi, with radiation predominantly directed downwards as shown in Fig.7

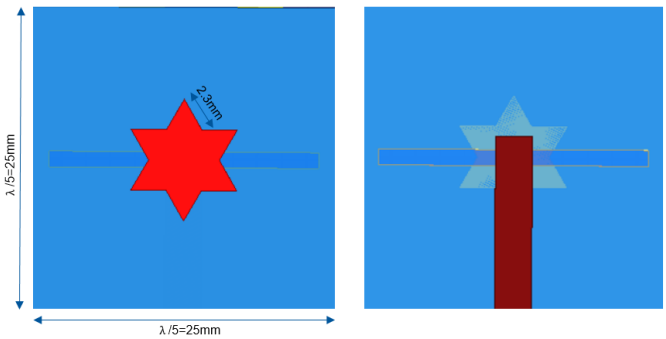


Fig. 5. Top view of unit cell with back feeding.

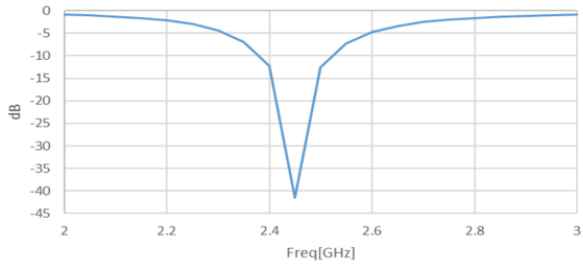


Fig. 6. Return loss of single unit metasurface without reflector.

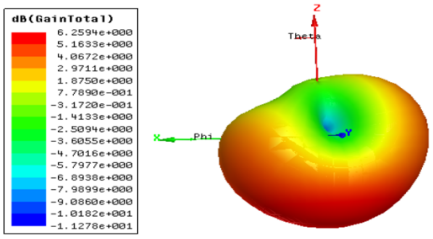
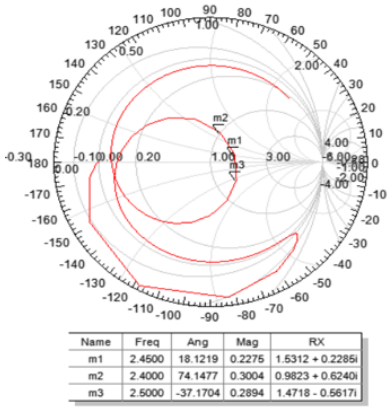


Fig. 7. Gain of single unit metasurface without reflector.



Name	Freq	Ang	Mag	RX
m1	2.4500	18.1219	0.2275	1.5312 + 0.2285i
m2	2.4000	74.1477	0.3004	0.9823 + 0.6240i
m3	2.5000	-37.1704	0.2894	1.4718 - 0.5617i

Fig. 8. Smith chart of single unit metasurface without reflector.

C. Single Unit Metasurface with Reflector

In an effort to optimize performance, a reflector was subsequently added to the antenna system. The reflector was placed at a distance of 1mm from the antenna with a thickness of 2mm. This adjustment resulted in a reduction of gain to 3.79 dBi, but with radiation now directing primarily in the forward direction. The antenna now operates within a bandwidth of 150 MHz with a return loss of 16.4dB. It suggest that the addition of the reflector slightly decreased the gain but also improved the overall performance of the antenna by redirecting the radiation towards the desired direction.

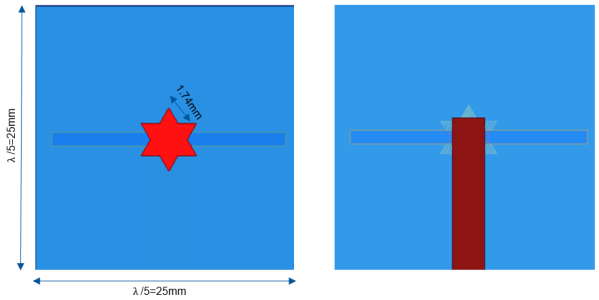


Fig. 9. Unit cell star patch with back feeding.

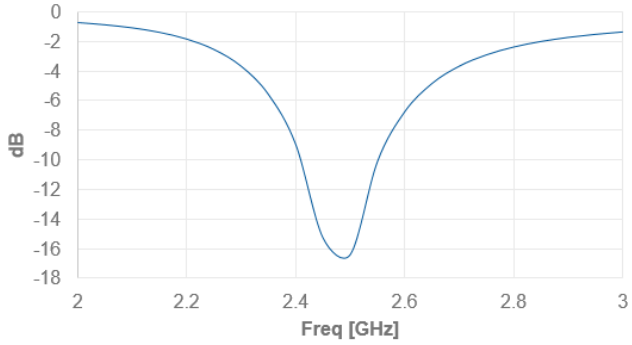


Fig. 10. Return loss of single unit metasurface with reflector.

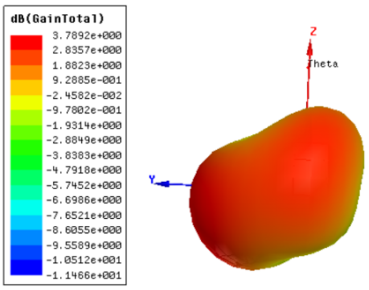
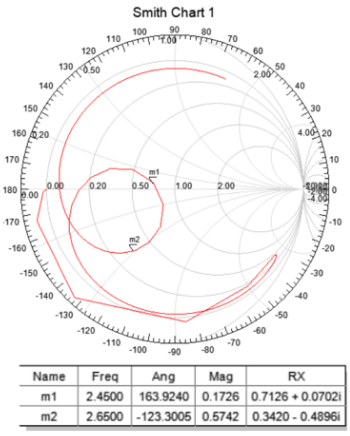


Fig. 11. Gain of single unit metasurface with reflector.



Name	Freq	Ang	Mag	RX
m1	2.4500	163.9240	0.1726	0.7126 + 0.0702i
m2	2.6500	-123.3005	0.5742	0.3420 - 0.4896i

Fig. 12. Smith chart of single unit metasurface with reflector.

D. 1x2 Array Metasurface with Reflector

Arrays consist of multiple antenna elements arranged in a specific geometric configuration, allowing constructive interference to boost the overall signal strength in the desired direction. In this case, a 1x2 array configuration was implemented. This configuration aimed to improve the gain while maintaining other desirable characteristics. Figure below shows the top view and bottom view of the 1x2 array.

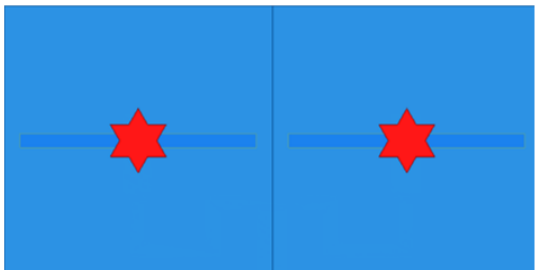


Fig. 13. Top view of 1x2 array metasurface with reflector.

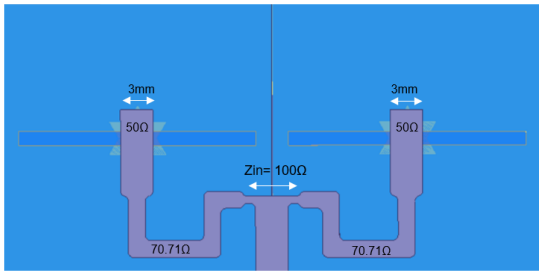


Fig. 14. Bottom view of 1x2 array metasurface with reflector.

The spacing between two elements is called the phase path and the phase path decides the phase shift. The input impedance (Zin) is 100 ohm, but the antenna is designed for 50 ohm impedance i.e Zout= 50ohm. So, to achieve this, a quarter-wave transformer is used. Its electrical length of the quarter wave transformer is Lamda g/4, that is equivalent to 14.9mm. Its impedence is equal to 70.71 ohm

$$Z = \sqrt{Zin.Zout}Z = \sqrt{100 * 50} = 70.71ohm$$

The table for impedance and corresponding width of the microstrip line is as shown below.

TABLE I
IMPEDANCE AND EQUIVALENT WIDTH OF TRANSMISSION LINE

Impedance(ohm)	Width of Transmission Line (mm)
50	3
70.71	1.57
100	0.66

Implementation of the array configuration, increased the effective aperture of antenna and it allowed better directivity showing improvements in the antenna's performance. The gain was significantly enhanced, measuring at 9.29 dBi as shown in Fig. 16, approximately equal to the requirement of 10 dB set forth in the initial design criteria. The operational bandwidth is of 138 MHz as shown in Fig. 15, allowing broader range of frequencies covering the ISM band of operation.

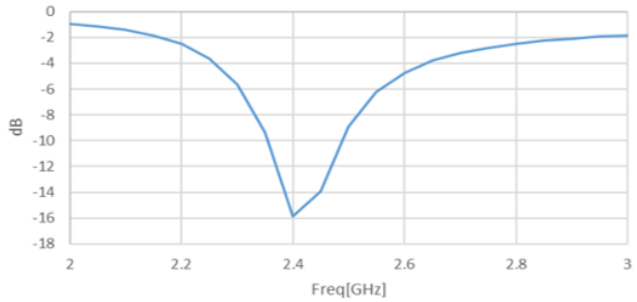


Fig. 15. Return loss of 1x2 array metasurface with reflector.

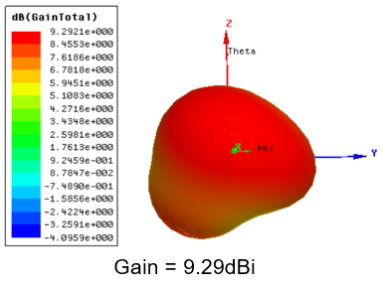


Fig. 16. Gain of 1x2 array metasurface with reflector.

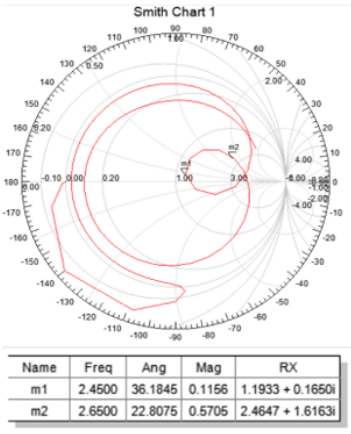


Fig. 17. Smith chart of 1x2 array metasurface with reflector.

IV. Conclusion and Future Scope

In this project, design of a metasurface antenna operating within the 2.4GHz ISM band, aiming for a 10dB return loss and a minimum gain of 10dB across the operational bandwidth. The results obtained showcase the effectiveness of different configurations in achieving the desired performance metrics. Single unit of metasurface antenna, with periodicity of lamda/5 equivalent to 25mm the measured return loss of 41.43 dB and operational bandwidth of 150 MHz. Gain of 6.25 dBi is achieved for a single unit, the radiation pattern predominantly directs downward. A reflector is introduced below the metasurface which result in forward radiation but with reduced gain of 3.79dBi. Further, a 1x2 array configuration is observed which results in a gain of 9.29 dBi at 2.4 GHz and Bandwidth of 200MHz. A corporate feeding technique with matched quaterwave transformer is used to feed the radiation elements in the array configuration.

It is observed as number of array elements are increased, gain increases. Hence, the array elements can be increased to meet the required gain. This enhancement is attributed to the increased effective aperture of the antenna, enabling better directivity and broader coverage of frequencies within the ISM band.

References

[1] Anu Bhargava and Mike Zoltowski. Sensors and wireless communication for medical care. In *14th International Workshop on Database and Expert Systems Applications, 2003. Proceedings.*, pages 956–960. IEEE, 2003.

[2] Parikha Mehrotra, Baibhab Chatterjee, and Shreyas Sen. Em-wave biosensors: A review of rf, microwave, mm-wave and optical sensing. *Sensors*, 19(5):1013, 2019.

[3] Jin Qin, Shibin Jiang, Zhanshan Wang, Xinbin Cheng, Baojun Li, Yuzhi Shi, Din Ping Tsai, Ai Qun Liu, Wei Huang, and Weiming Zhu. Metasurface micro/nano-optical sensors: principles and applications. *ACS nano*, 16(8):11598–11618, 2022.

[4] Zhanni Wu, Younes Ra'di, and Anthony Grbic. Tunable metasurfaces: A polarization rotator design. *Phys. Rev. X*, 9:011036, Feb 2019.

[5] Shawana Tabassum, SK Nayemuzzaman, Manish Kala, Akhilesh Kumar Mishra, and Satyendra Kumar Mishra. Metasurfaces for sensing applications: Gas, bio and chemical. *Sensors*, 22(18):6896, 2022.

[6] Ashwin K Iyer, Andrea Alu, and Ariel Epstein. Metamaterials and metasurfaces—historical context, recent advances, and future directions. *IEEE Transactions on Antennas and Propagation*, 68(3):1223–1231, 2020.

[7] Shuyan Zhang, Chi Lok Wong, Shuwen Zeng, Renzhe Bi, Kolvyn Tai, Kishan Dholakia, and Malini Olivo. Metasurfaces for biomedical applications: imaging and sensing from a nanophotonics perspective. *Nanophotonics*, 10(1):259–293, 2020.

[8] Zhanni Wu, Younes Ra'di, and Anthony Grbic. Tunable metasurfaces: A polarization rotator design. *Physical Review X*, 9(1):011036, 2019.

Design and Development of A Metasurface Based C-Band Phase Shifter

Shruti Gokhale[1], Umer Shaikh[2], Freda Carvalho[3], Ashwini Kotrashetti[4]
[1]*Department of Electronics and Telecommunication Engineering*
[1]*The Bombay Salesian Society's, Don Bosco Institute Of Technology, University of Mumbai, Mumbai India*
[1]*g.shrutigokhale@gmail.com,* [2]*shaikhumer1526@gmail.com,* [3]*freda@dbit.in,* [4]*ashwini@dbit.in*

***Abstract*—In this paper, a research of C band Phase Shifters based on Metasurface is proposed. The unit cell of the proposed metasurface consists of a lattice made of Omega shaped geometric patterns etched on an FR4 substrate of 1.68 mm thickness. This phase shifters bring in phase shifting properties with attenuation as low as 1dB over C band ie 4 GHz to 8 GHz . The geometrical dimensions of the Omega structure have been varied to study their impact on the reflection and transmission characteristics of the phase shifter. The phase shifters vary in design implementation of Omega structure. Compact, cost efficient, energy efficient frequency independent C band phase shifters are attempted in this work. The proposed metasurface based phase shifter can be useful for antenna systems, wireless communication, radar systems, signal processing, etc.**

***Index Terms*—metasurface, phase shifter, c band, return loss, insertion loss**

I. Introduction

Metasurfaces have gained a lot of research attention owing to their ability to orchestrate electromagnetic waves. They are array of subwavelength inclusions that can be densely arranged and allow the fields to be engineered with much better spatial resolution, it has recently become widely understood, thanks to the development of the concept of metamaterials, that a design of subwavelength inclusions can grant a more profound control of electromagnetic waves by planer structures. [1] Such inclusions, in general, have both electric and magnetic polarizations, and thus provide complete control over reflected and transmitted waves, opening up new possibilities for microwave and optical systems. Until recently, all such planar metamaterial structures were referred to as metasurfaces. They cater to a range of applications such as antennas, cloaking, absorbers, filters, polarization converters, phase shifters, etc. Planar slotted metallic metasurfaces with strip loading have been studied as bandpass filters (BPF) . Some interesting work is presented for the development of metasurface based filters, one such is that of a metasurface based waveguide filter that utilizes metal bars to form metasurface. This filter has its passband till the Ku band; however, such filters are non-planar Abstract - In this paper, a planar metasurface based broadband low pass filter has been proposed for up to X-band. The unit cell of the proposed metasurface consists of a lattice made of Omega shaped geometric patterns etched on an FR4 substrate. The geometrical dimensions of the Omega structure have been varied to study their impact on the reflection and transmission characteristics of the filter. The structure provides insertion losses of less than 3 dB up to 12.5 GHz for a linear phase shift and constant minimum group delay throughout the passband. The proposed metasurface based filter can be useful for weather forecasting, earth exploration services, airport surface detection equipment (ASDE) systems, etc. [1] They cater to a range of applications such as antennas, cloaking, absorbers, filters, polarization converters, phase shifters, etc.

A metasurface phase shifter is a type of phase shifter that employs a metasurface to control and manipulate electromagnetic waves. Metasurfaces are artificially engineered structures consisting of sub-wavelength-sized elements or metamaterials that are designed to control the propagation of electromagnetic waves in unconventional ways. [2]

These artificial, nanostructured (subwavelength) surfaces have the ability to control and engineer the behavior of electromagnetic waves in unprecedented ways, revolutionizing various industries such as telecommunications, imaging, and sensing. Metasurfaces offer unique opportunities to manipulate the properties of electromagnetic waves, enabling applications that were once considered impossible or extremely challenging. [3].

Research into metamaterials and metasurfaces has experienced explosive growth over the last two decades, evident in various metrics. Special sessions on these topics are now commonplace at major international meetings across several communities, and entire conferences are dedicated to them (for example, the Metamaterials conference is now in its fourteenth edition). Currently, hundreds of research groups worldwide are actively pursuing "meta" research programs, with several institutional networks and funding mechanisms established solely for advancing this science and technology. Tens of thousands of articles have been published at an astonishing rate in leading journals across multiple research communities. [4]

Unlike traditional bulky optical components, metasurfaces are ultra thin and lightweight, offering a platform for the development of compact and efficient devices. Some of its application fields are:

- Remote sensing in weather monitoring, environmental sensing, and agricultural monitoring. The ability of metasurface to control radiation patterns and beam steering can enhance the precision and coverage of remote sensing systems.

- Wireless sensing networks for applications like structural health monitoring, where they enable the detection of cracks, deformations, or other anomalies in buildings, bridges, and infrastructure.
- Security and surveillance applications, such as intrusion detection and perimeter monitoring, by enabling better control of radar and communication systems.
- Metasurface antennas can improve the resolution and performance of radar and imaging systems. By controlling the direction and focus of electromagnetic waves, they can enhance object detection, tracking, and imaging capabilities, which are valuable in fields like security, defense, and autonomous vehicles.
  Metasurfaces, a recent development in nanophotonics, revolutionize light manipulation by replacing bulky optical components with ultrathin, flat counterparts, over 10,000 times thinner. Since their first demonstration in 2011, they've sparked immense interest in consumer optics and electronics industries. Notably, metasurface-enabled bioimaging and biosensing tools have emerged, showcasing novel applications. This review article delves into the cutting-edge of this technology, offering an interdisciplinary perspective. Topics covered include metasurfaces for chiral imaging, endoscopic optical coherence tomography, fluorescent imaging, super-resolution imaging, magnetic resonance imaging, quantitative phase imaging, and sensing of antibodies, proteins, DNAs, cells, and cancer biomarkers. Future directions explore application-specific biomedical metasurfaces and bioinspired metasurface devices. Perspectives on challenges, opportunities, and translational biomedical devices in metasurfaces and biophotonics are also discussed. [5]

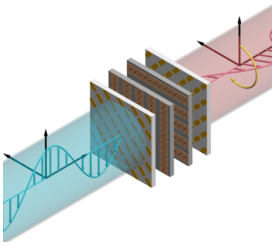


Fig. 1. Metasurface Manipulating Electromagnetic Wave's Phase [6]

A. Motivation

To create a metasurface Phase Shifter operating at the C - Bnad frequency of 4 -8 GHz. The surface will possess phase shifting and controlling abilities between 4 to 8 GHz with low insertion loss at 1dB and return loss at 10dB. The sub wavelength inclusions can be densely arranged and allow the fields to be engineered with much better spatial resolution, thus it has recently be- come widely understood. Thanks to the development of the concept of meta- materials, that a design of subwavelength inclusions can grant a more profound control of electromagnetic waves by planer structures. Such inclusions, in general, have both electric and magnetic polarization, and thus provide complete control over reflected and transmitted waves, opening up new possibilities for microwave and optical systems.

B. Scope of the Project

A metasurface phase shifter is designed so to achieve a phase shift over C - band and to achieve low insertion and return loss. The phase shifter is designed, simulated and will be fabricated and tested over C - band 4 to 8 GHz with insertion loss as low as 1dB and return loss close to 10 dB.

- Designing for low insertion and return loss : the primary goal of designing a metasurface phase shifter is to optimise its performance and achieve low insertion and return loss.
- Incorporating a excitation mode as floqute ports into the design is as the design is periodic and frequency selective, essential for ensuring controlled excitation.
- Simulation: Prior to fabrication, the designed metasurface antenna undergoes rigorous simulation using Ansys HFSS software.

II. Methodology

- Assess problem for metasurface specs, including app requirements, integration, standards, and stakeholder input. Identify specific application for phase shifter use.
- Identify metasurface design type via literature review: review papers, patents, etc., to understand existing designs and their characteristics.
- Design metasurface Phase shifter, integrating tech into antenna for desired properties and performance.
- Simulate metasurface Phase Shifters to explore design options, predict behavior, and save time/resources.
- Analyze and optimize metasurface designs for specific parameters to refine and meet desired specs.
- Design mechanism to excite phase shifter elements, efficiently transferring energy from transmission line to radiating elements.
- Create metasurface phase shifter element array, arranging elements for desired properties affecting parameters like directivity.
- Create power divider to feed all metasurface units, distributing energy within the surface array.
- Fabricate metasurface phase shifter using appropriate techniques and materials.
- Test fabricated surface to evaluate real-world performance.
- Compare simulated and measured results to identify discrepancies and improve simulation accuracy.

A. Software Used

Ansys HFSS (high-frequency structure simulator) is used to make this project. It is a powerful electromagnetic simulator software developed by Ansys for simulating and analysing high frequency antennas, electronics components,

RF/microwave circuits. HFSS is a versatile and comprehensive electromagnetic simulation tool used across various industries, including telecommunications, aerospace, automotive, electronics, and defense, for the design and analysis of high-frequency electromagnetic devices and systems. CST STUDIO SUITE is used to make this project. It is a widely used software package for electromagnetic simulation and analysis. It's used in various industries, including electronics, communications, and RF engineering.

B. Hardware Used

FR-4, or Flame Retardant 4, is a common type of material used for manufacturing printed circuit boards (PCBs). In antenna design, FR-4 PCBs are used to fabricate the antenna structure, including the radiating elements, feed network, and ground plane. The dielectric properties of FR-4 substrate affect the impedance matching, bandwidth, and radiation characteristics of the antenna. Microstrip lines are a common feeding technique used to feed RF/microwave signals to antennas and other components on PCBs. microstrip lines are used to connect the feeding network (e.g., power divider, matching network) to the radiating elements of the antenna.

III. Implementation of Metasurface Unit Cell

At the base of the MML (Metasurface Microstrip Line) structure, a microstrip line is present with a FR-4 substrate positioned below. This gives rise to an aperture coupled microstrip line. Subsequently, another layer of FR-4 substrate is on the copper sheet. Positioned at the apex of this configuration is a star patch. A unit cell is be seen in Fig. 2. Unit cell refers to the basic repeating structure within a larger antenna array or metamaterial. The unit cell is typically a small geometric shape or structure that is replicated across the entire antenna array to achieve the desired pattern.

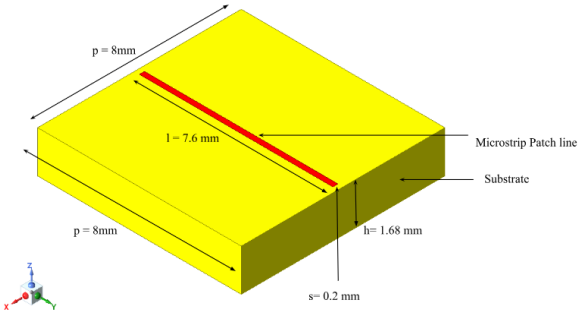


Fig. 2. Single Unit Cell of MML Isometric view

The method by which the metasurface elements of a metasurface phase shifter are stimulated or energised to produce the required phase shift or other electromagnetic properties is known as the excitation mechanism. The usefulness, efficiency, and performance of the phase shifter are all determined by this mechanism.

A number of variables, including the required phase shift range, operating frequency, power handling capacity, integration needs, and overall system design considerations, influence the choice of excitation mechanism. Engineers frequently choose the excitation mechanism for a metasurface phase shifter based on its particular application and performance objectives.

In Fig. 3, the floquet port excites the structure, via the terminal top and bottom ends of the structure, the excitation ports are applied on a vacuum box which surrounds the entire unit cell structure.

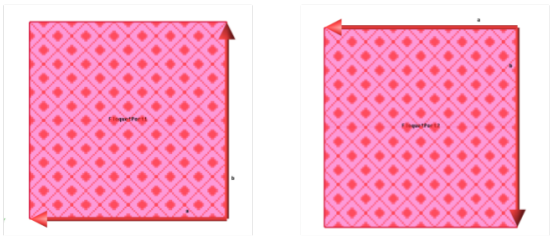


Fig. 3. Excitation mechanism for a Single Unit Cell

IV. Theoretical Calculations and Simulation Results

A. Calculation for MML

Phase shift (θ) calculation is done with the following mentioned formula, where β represents phase constant and l is length. By knowing this difference, we obtain the phase shift in terms of length.

$$\theta = \beta l - \beta l^{'} \tag{1}$$

$$\frac{2\pi l}{\lambda} l$$

Here, β l represents the phase shift at 8 GHz and $\beta l^{'}$ represents the phase shift at 4 GHz.
Therefore,

$$\theta = [\frac{2\pi l}{\lambda} - \frac{2\pi l^{'}}{\lambda^{'}}] \tag{2}$$

$$\theta = l[\frac{2\pi}{\lambda} - \frac{2\pi}{\lambda^{'}}] \tag{3}$$

$$\theta = 7.6[\frac{2\pi}{3.75} - \frac{2\pi}{7.5}] \tag{4}$$

$$\theta = 6.36 \tag{5}$$

Therefore, Phase Shift is 6.36°/1mm.

$$\theta = 6.36/7.6 \tag{6}$$

Therefore, Total Phase Shift is 48.33°.
Thus, the phase shift obtained by this simple MML structure is 12.08°/1 GHz and 6.36°/1mm.

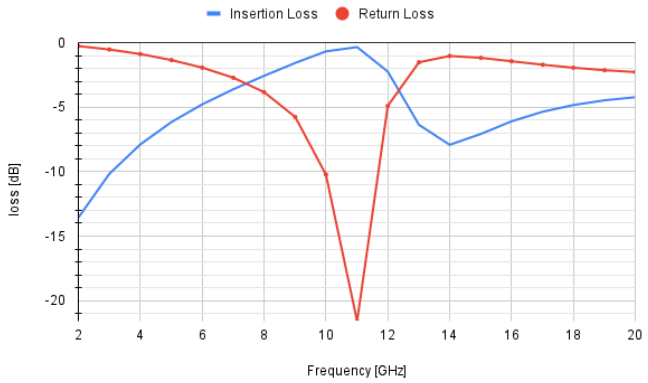


Fig. 4. Return Loss and Insertion loss

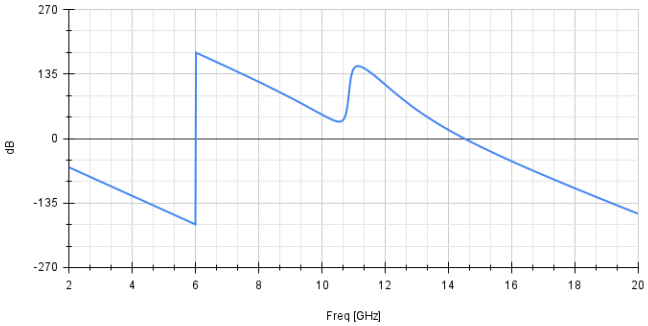


Fig. 5. Phase Shift in MMI over 2 to 20 GHz

B. Omega Phase Shifter Design

A Metasurface based Omega structured phase shifter with low insertion loss and C band characteristic exhibiting low frequency dependency of transmittance phase shift is attempted in this work. The metasurface unit cell shown in Fig. 5.3, is designed at 4 GHz to 8 GHz on a FR4 substrate with thickness of 1.68 mm. The lattice of the proposed metasurface consists of an Omega structure of copper on top of FR4 substrate.

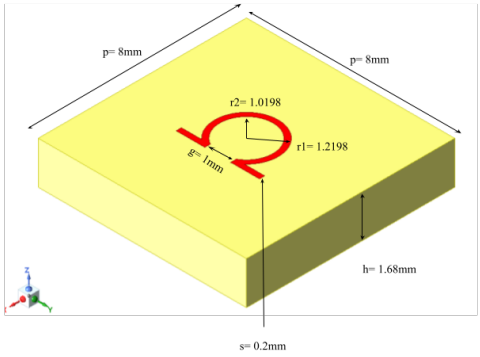


Fig. 6. Isometric view of omega design

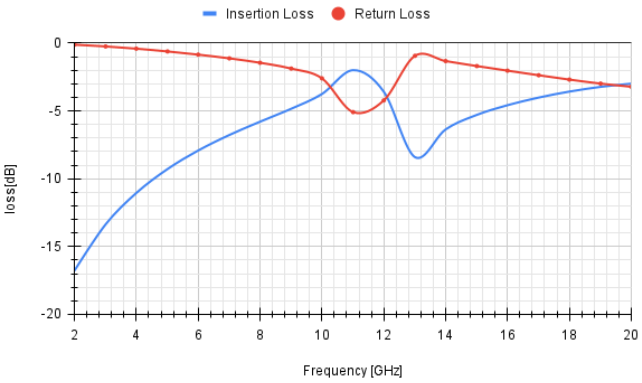


Fig. 7. omega insertion and return loss

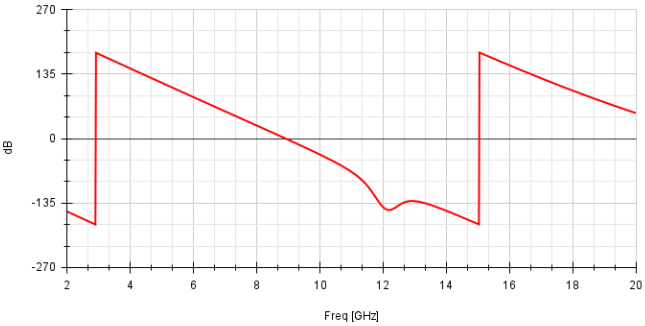


Fig. 8. Phase shift in Omega design over 2 to 20 GHz

C. Double Omega 1

The desired phase shift is expected between 4 to 8 GHz while trying to achieve a insertion loss of 10dB and return loss of 1dB. In figure Fig. 5.6, the repetative design analysis is done and the most optimum double omega strucutre (both omega's facing same direction) is reported. keeping all the dimensions same.

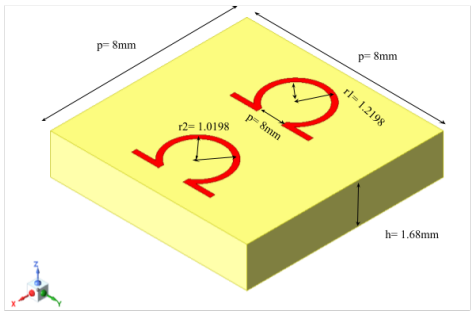


Fig. 9. Double Omega 1 design isometric view

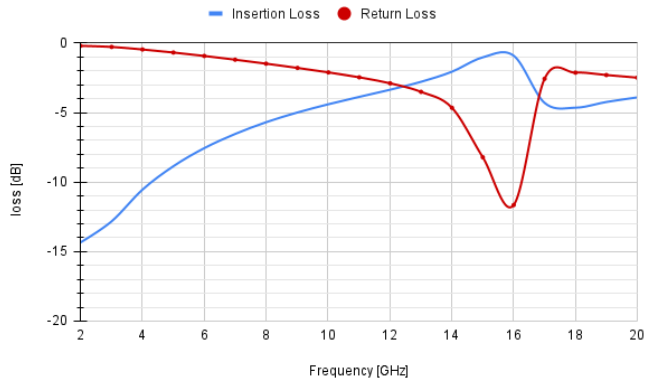


Fig. 10. Double Omega 1 insertion loss and return loss

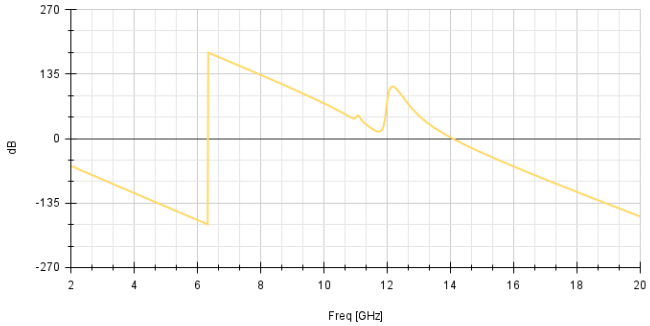


Fig. 11. Double Omega 1 Design Phase Shift

D. Double Omega 2

After achieving better and more promising results in Double Omega 1 design, keeping the parameters same, we designed double omega 2 (both omega facing opposite sides).Dimension are kept same.

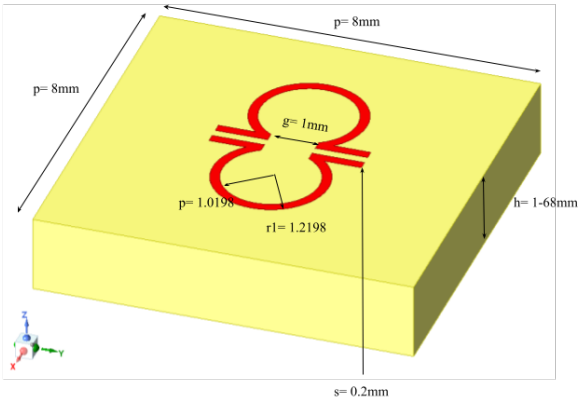


Fig. 12. Double Omega 2 design isometric view

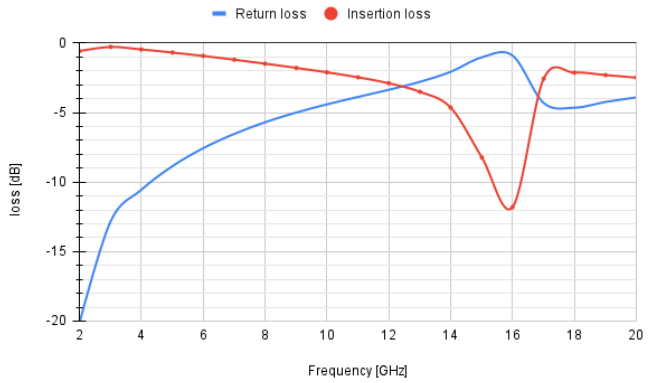


Fig. 13. Double Omega 2 insertion loss and return loss

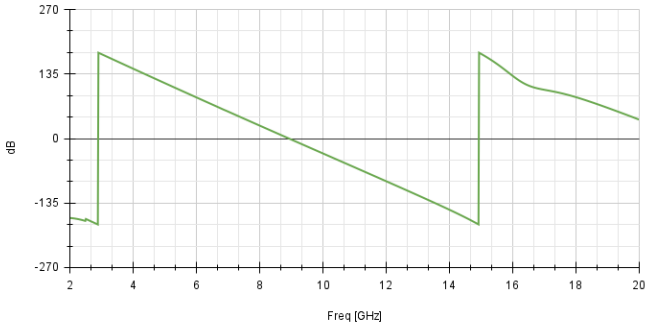


Fig. 14. Double Omega 2 insertion loss and return loss

V. Loss and Phase Shift Comparision

TABLE I
Comparison Table

No.	Design	Phase Shift	Insertion Loss	Return Loss
1	MML	26.55 GHz	-0.31 dB	-21.08 dB
2	Omega	29.75 GHz	-1.99 dB	-5.08 dB
3	Double Omega 1	29.5 GHz	-1.02 dB	-11.65 dB
4	Double Omega 2	29.625 GHz	-0.89 dB	-11.80 dB

The TABLE 1, illustrates how the previously mentioned designs (MML, Omega, Double Omega 1 and Double Omgea 2) perform in terms of phase shifting, insertion loss, and return loss. From the table, we can see that the design labeled as 'Omega' provides superior phase shift- ing capabilities, while the design labeled as 'Double Omega 2' exhibits better insertion loss performance. Additionally, the design marked as 'Omega' demonstrates superior return loss characteristics.

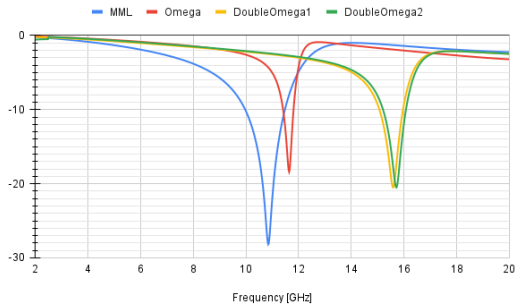


Fig. 15. Return loss comparison of all proposed designs

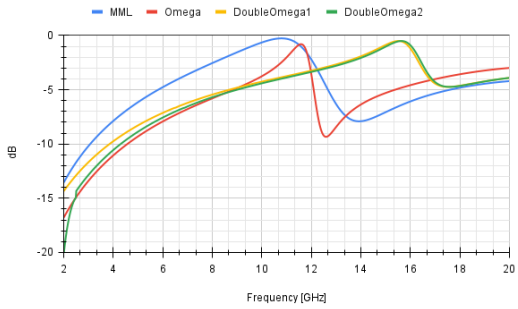


Fig. 16. Insertion loss comparison of all proposed designs

REFERENCES

[1] Sadanand Chauhan, Solomon Stephen, Freda Carvalho, Ashwini Kotrashetti, Sambit Ghosh, and Somak Bhattacharyya. Design and analysis of a compact metasurface based filter for broadband performance. In *2022 IEEE Region 10 Symposium (TENSYMP)*, pages 1–5. IEEE, 2022.

[2] Jin Qin, Shibin Jiang, Zhanshan Wang, Xinbin Cheng, Baojun Li, Yuzhi Shi, Din Ping Tsai, Ai Qun Liu, Wei Huang, and Weiming Zhu. Metasurface micro/nano-optical sensors: principles and applications. *ACS nano*, 16(8):11598–11618, 2022.

[3] Zhanni Wu, Younes Ra'di, and Anthony Grbic. Tunable metasurfaces: A polarization rotator design. *Phys. Rev. X*, 9:011036, Feb 2019.

[4] Ashwin K Iyer, Andrea Alu, and Ariel Epstein. Metamaterials and metasurfaces—historical context, recent advances, and future directions. *IEEE Transactions on Antennas and Propagation*, 68(3):1223–1231, 2020.

[5] Shawana Tabassum, SK Nayemuzzaman, Manish Kala, Akhilesh Kumar Mishra, and Satyendra Kumar Mishra. Metasurfaces for sensing applications: Gas, bio and chemical. *Sensors*, 22(18):6896, 2022.

[6] Zhanni Wu, Younes Ra'di, and Anthony Grbic. Tunable metasurfaces: A polarization rotator design. *Physical Review X*, 9(1):011036, 2019.

Smart Water Management using LoRaWAN

Benish Christo[1], Simran Koparkar[2], Deep Patel[3], Leroy Rodrigues[4] and Poonam Chakraborty[5]
[1]*Department of Electronics and Telecommunication Engineering*
[1]*The Bombay Salesian Society's, Don Bosco Institute Of Technology, University of Mumbai, Mumbai India*
[1]*benish.christo@gmail.com,* [2]*simransantosh22@gmail.com,* [3]*pateldeep.24520@gmail.com,* [4]*lr.leroyrod@gmail.com,* [5]*poonam@dbit.in*

***Abstract*—The Smart Water Management System presents a sophisticated solution for the efficient management of water distribution by harnessing the capabilities of LoRaWAN technology. The system employs LoRa modules to establish robust, long-range communication channels essential for remote monitoring and control. Use of sensors for pressure sensing, level detection, and volume measurement, alongside microcontrollers such as Arduino and STM32, helps the system achieve comprehensive data acquisition capabilities.**

Central to the approach is the utilization of sensor fusion facilitated by microcontrollers for accurate and real-time analysis of critical parameters. This includes continuous monitoring of volume, pressure variations, and water level measurements. The gathered data undergoes an analysis algorithms implemented on the microcontrollers, enabling insights into water distribution patterns and demand fluctuations.

The Seamless integration and synchronization of LoRa modules, precise interfacing with STM32 microcontrollers, rigorous sensor calibration to ensure data accuracy and reliability were the key challenges addressed. By optimizing water distribution, the system contributes to sustainable resource management, minimizing wastage, and enhancing overall resilience. The aim is to provide a scalable and adaptable solution that can be implemented in diverse urban and rural water management contexts to address the growing challenges of water scarcity and infrastructure optimization.

***Index Terms*—Water Management System, LoRaWAN Technology, Remote Monitoring and Control, Sensor Fusion, Micro controllers, (Arduino, STM32), Data Acquisition, Real-time Analysis, Water Distribution Patterns.**

I. Introduction

In recent years, there has been a growing recognition of the need for sustainable management of water resources, driven by factors such as population growth, urbanization, industrialization, and climate change [1] [14]. These challenges have underscored the importance of adopting innovative technologies to enhance the efficiency, reliability, and sustainability of water management practices [2]. In this context, the emergence of smart water management systems leveraging Internet of Things (IoT) technologies has garnered significant attention as a promising solution to address the complexities of modern water systems [3] [17].

In the context of smart water management, IoT technologies offer transformative capabilities by enabling real-time monitoring, predictive analytics, and remote control of water distribution networks [6]. By integrating the appropraiate sensors, communication networks, and data analytics, the smart water management systems provide the user with actionable insights which will help optimize resource allocation, detect anomalies, and mitigate risks [5].

The motivation behind the development of smart water management systems stems from the urgent need to address the challenges facing water management authorities and policymakers worldwide [13]. Traditional approaches to water management often rely on manual monitoring, periodic inspections, and reactive maintenance, leading to inefficiencies and suboptimal resource allocation. Moreover, the lack of real-time data and actionable insights hinders the ability of water authorities to respond effectively to emergencies such as leaks, contamination incidents, and supply disruptions [6].

The scope of the project encompasses the design, development, and implementation of a smart water management system using Long Range Wide Area Network (LoRaWAN) technology [1]. This includes selection and integration of appropriate sensors, communication devices, and data processing algorithms to create a scalable and adaptable infrastructure. The system will be capable of monitoring water flow, pressure, quality, and temperature in real-time, enabling timely intervention and optimization of water distribution networks [14].

Additionally, the project will involve the deployment of LoRaWAN gateways to establish connectivity and enable seamless communication between the sensors and a central monitoring platform [3]. The platform will provide users with access to actionable insights, visualization tools, and remote control functionalities to facilitate informed decision-making and proactive management of water resources [6].

While the primary focus is on urban water management, the system's modular design allows for potential expansion into other domains such as agriculture, industrial processes, and environmental monitoring []. By keeping the scope flexible , the aim is to create a solution that can be customized to meet the diverse needs of different environments.

Under the guidance of Mr. Quentin Desouza at QDnet Technologies, the industry collaborator for the project, the problem statement devised is:

"Developing a Smart Water Management System using

LoRaWAN to address water scarcity and improve resource allocation through real-time data collection."

II. Literature Survey

A. Introduction

In recent years, the integration of Internet of Things (IoT) technologies in water management has emerged as a promising approach to address challenges such as water scarcity, inefficient water usage, and infrastructure maintenance. This literature survey aims to explore the applications of LoRaWAN technology in smart water management, including smart metering, network infrastructure analysis, specific applications, and economic viability studies.

The introduction sets the stage for understanding the significance of IoT technologies in addressing water management challenges. It underscores the pivotal role of smart water grid networks, IoT applications in water usage and conservation, fog computing, LoRaWAN technologies, smart agriculture, smart waste management, and the economic viability of smart water metering systems [1] [14] [6].

Water scarcity and pollution have become pressing global concerns, necessitating innovative solutions to manage water resources effectively. Traditional water management approaches are often inefficient and lack real-time insights into water distribution, consumption patterns, and infrastructure integrity. In this context, IoT technologies offer promising avenues for transforming water management practices, enabling smarter, more efficient, and sustainable solutions.

B. IoT Technologies for Water Management

The adoption of IoT technologies offers unprecedented opportunities to improve water management practices. These technologies enable real-time monitoring, data collection, and analysis, leading to more efficient water usage and better decision-making. Within the realm of IoT technologies, Low-Power Wide-Area Network (LPWAN) technologies like LoRaWAN stand out for their ability to connect remote devices over long distances with minimal power consumption.

1) LoRaWAN Technology: LoRaWAN, short for Long Range Wide Area Network, is a wireless communication protocol designed for long-range communication between IoT devices and gateways. It operates on unlicensed radio bands, making it cost-effective and suitable for various applications, including smart water management. LoRaWAN technology utilizes star-of-stars network topology, enabling millions of devices to connect to a single gateway, making it ideal for large-scale deployments in water management systems.

C. Applications of LoRaWAN in Smart Water Management

Smart water grid networks and management systems represent a paradigm shift in water supply management, leveraging IoT technologies such as LoRaWAN to enhance efficiency, reliability, and sustainability. These systems enable utilities to monitor, analyze, and optimize water distribution in real-time, thereby improving service delivery and reducing water loss. The integration of IoT technology in water usage and conservation spans various domains, including agriculture, urban water management, and industrial processes. IoT-enabled solutions offer opportunities to optimize water usage, minimize wastage, and promote sustainable practices across diverse sectors.

1) Smart Metering: Smart metering is one of the prominent applications of LoRaWAN technology in water management. These studies explore the deployment of smart water meters equipped with LoRaWAN connectivity for accurate and real-time monitoring of water usage. By leveraging LoRaWAN, these systems enable utilities and consumers to track water consumption, detect leaks, and optimize usage patterns, leading to improved efficiency and conservation of water resources.

- An integrated IoT architecture for smart metering using next-generation sensor for water management based on LoRaWAN technology: A pilot study [17]
- A comparative study of LoRaWAN, Sigfox, and NB-IoT for smart water grid [9]
- Potable water management with integrated Fog computing and LoRaWAN technologies [3]
- IoT devices and applications based on LoRa/LoRaWAN [7]

2) Network Infrastructure and Capacity Analysis: Efficient network infrastructure is crucial for the successful implementation of IoT solutions in water management. These studies focus on the design, routing strategies, and capacity analysis of LoRaWAN networks tailored for smart water grids. By optimizing network architectures and protocols, these research efforts aim to enhance network reliability, scalability, and performance, ensuring seamless communication between devices and gateways.

- Routing strategies for LoRaWAN multi-hop networks: A survey and an SDN-based solution for smart water grid [10]
- LoRaWAN network capacity analysis for smart water grid [8]

3) Specific Applications: Beyond smart metering, LoRaWAN technology finds application in various aspects of water management, including water quality monitoring, irrigation control, and waste management. These studies demonstrate the versatility of LoRaWAN in addressing specific challenges faced by different stakeholders in the water sector, from agricultural producers to urban utilities.

- Smart water grid management using LPWAN IoT technology [16]
- Smart water quality monitoring and metering using LoRa for smart villages [11]
- A LoRaWAN IoT system for smart agriculture for vine water status determination [18]
- Smart control and energy efficiency in irrigation systems using LoRaWAN [15]

- Design and empirical validation of a LoRaWAN IoT smart irrigation system [6]
- Design of an energy-efficient LoRaWAN-based smart IoT water meter for African municipalities [12]
- Smart water management system in urban areas using LoRA technology [19]
- A multi-layer LoRaWAN infrastructure for smart waste management [5]

D. Economic Viability and Implementation Challenges

Despite the potential benefits of LoRaWAN-based solutions, challenges such as economic viability, regulatory compliance, and interoperability need to be addressed for successful deployment. These studies investigate the economic feasibility, implementation strategies, and regulatory implications of deploying LoRaWAN-enabled systems in water management contexts.

- Exploring the economic viability of LoRaWAN-based smart water meters for sustainable water management [13]
- Development and implementation of a smart water metering system based on LoRa technology [14]
- A smart water grid network for water supply management systems [1]
- Implementation of a LoRaWAN-based smart agriculture decision support system for optimum crop yield [4]

1) Precision Agriculture: Precision agriculture integrates IoT sensors, satellite imagery, and data analytics to monitor and manage crop production processes with unprecedented precision [4]. By collecting and analyzing data on soil moisture (SM), nutrient levels (NL), weather patterns (WP), and crop health (CH), precision agriculture systems enable farmers to tailor inputs such as water (W), fertilizer (F), and pesticides (P) to specific crop requirements. This targeted approach minimizes input wastage, optimizes resource use, and maximizes yields (Y), leading to improved profitability (P_{agri}) and sustainability.

$$Y = f(SM, NL, WP, CH)$$

$$P_{agri} = Y - \sum_{i=1}^{n} (W_i + F_i + P_i)$$

2) Resource Efficiency: IoT-enabled smart irrigation systems optimize water usage by delivering the right amount of water to crops at the right time [6]. These systems employ sensors to monitor soil moisture levels (SM), weather conditions (WC), and plant water requirements (WR), allowing for precise irrigation scheduling and control. By minimizing water wastage, runoff, and leaching, smart irrigation systems conserve water resources, protect soil health, and mitigate environmental degradation. Additionally, by reducing energy consumption associated with pumping and distribution, these systems contribute to overall resource efficiency and sustainability.

$$WR = f(SM, WC)$$

$$Efficiency = \frac{Water\_Utilized}{Water\_Available}$$

3) Cost-benefit Analysis: A comprehensive cost-benefit analysis (CBA) is essential for evaluating the economic viability and return on investment of smart water metering systems [13]. This analysis should consider both tangible costs (C_t) and benefits (B_t), as well as intangible ones, such as:

- Hardware Procurement: The initial cost of purchasing smart water meters and associated equipment.
- Installation: Expenses related to deploying the meters and integrating them into existing water infrastructure.
- Maintenance: Ongoing costs for upkeep, repairs, and upgrades of the metering system.
- Data Management: Investments in software, storage, and personnel required to collect, process, and analyze meter data.
- Customer Service: Resources allocated to handle inquiries, support, and billing associated with the new system.

On the benefits side, tangible gains may include:

- Water Conservation: Reductions in water loss due to leaks, theft, or inefficient usage, leading to cost savings.
- Operational Efficiency: Streamlined meter reading processes and improved accuracy in billing, reducing administrative costs.
- Revenue Generation: Potential for new revenue streams through value-added services, such as leak detection or consumption analytics.

Intangible benefits could encompass:

- Improved Customer Satisfaction: Enhanced service reliability and transparency, fostering trust and loyalty among customers.
- Environmental Impact: Positive effects on water resource management and conservation, contributing to sustainability goals.

By quantifying these costs and benefits, the cost-benefit analysis provides a structured framework for decision-makers to assess the financial viability and long-term impacts of smart water metering initiatives. The formula for calculating the net outcome (CBA) is:

$$CBA = B_t - C_t$$

Where B_t represents the total benefits accrued from the smart water metering system, and C_t denotes the total costs incurred in its implementation and operation.

E. Summary

The literature survey underscores the extensive array of applications for LoRaWAN technology in the realm of smart water management. It traverses a spectrum of utilities from smart metering to niche applications like irrigation control and waste management. While these studies illuminate the

potential of LoRaWAN to overhaul water management practices, they also emphasize the need for further research to tackle implementation hurdles and optimize the advantages of IoT technologies in ensuring sustainable water usage and conservation.

The amalgamation of diverse research fragments in the literature survey provides profound insights into the multifaceted role of IoT technologies in mitigating water management challenges and nurturing sustainable development. By synthesizing findings from various studies, this conclusion accentuates the transformative capacity of IoT solutions and underscores their significance in shaping the trajectory of water management practices.

One of the paramount insights gleaned from the literature is the indispensable role played by smart water grid networks and management systems in revolutionizing water supply management [1] [14]. These systems harness IoT technologies, notably LoRaWAN, to facilitate real-time monitoring, efficient distribution, and equitable access to clean water resources. By deploying IoT sensors across water distribution networks, utilities can swiftly detect leakages, optimize water flow, and uphold infrastructure integrity [1].

Furthermore, IoT applications in water usage and conservation present promising avenues for maximizing resource efficiency and advocating sustainable practices across various sectors [2] [6]. Smart irrigation systems, equipped with IoT sensors, adeptly optimize water usage in agriculture by continuously monitoring soil moisture levels, weather conditions, and crop requirements [6]. Similarly, smart water meters furnish real-time data on consumption patterns, empowering utilities and consumers alike to identify avenues for conservation and efficiency enhancements [2].

Additionally, fog computing and LoRaWAN technologies emerge as pivotal enablers for real-time analytics and decision-making in water management systems [3] [17]. Fog computing minimizes latency, while LoRaWAN furnishes a low-power, wide-range communication infrastructure for transmitting sensor data across expansive geographic areas [17]. This synergy facilitates local data processing, swift response to critical events, and real-time optimization of resource allocation by utilities [3].

In agriculture, IoT-enabled smart agriculture and irrigation systems offer avenues for precision farming and resource optimization [4] [6]. By amalgamating IoT sensors, satellite imagery, and data analytics, precision agriculture systems empower farmers to monitor soil conditions, weather patterns, and crop health with unparalleled precision [4]. This data-centric approach minimizes input wastage, maximizes yields, and fosters environmental sustainability in agricultural practices [6].

Likewise, in waste management, IoT technologies expedite optimized waste collection, recycling, and resource allocation [5]. Smart waste management systems leverage IoT sensors and data analytics to monitor waste generation patterns, fine-tune collection routes, and curtail environmental impact [5]. By furnishing real-time insights into waste volumes, fill levels, and collection schedules, these systems enhance operational efficiency, diminish costs, and foster sustainable waste management practices [5].

Nevertheless, notwithstanding the potential benefits of IoT technologies in water management, a plethora of challenges persist [14] [13]. These challenges encompass concerns regarding data privacy and security, interoperability issues, legacy system integration, and compliance with regulatory frameworks [14]. Utilities and stakeholders confront the task of navigating these complexities while ensuring alignment with strategic objectives, stakeholder expectations, and financial constraints [13]. Effective project management, collaboration, and risk mitigation strategies emerge as imperative for mitigating implementation risks and optimizing project outcomes [14].

Thus, the literature survey brings to the forefront the transformative potential of IoT technologies in tackling water management challenges and nurturing sustainable development. By harnessing IoT solutions, stakeholders can streamline resource allocation, enhance operational efficiency, and champion environmental sustainability in water management systems. However, successful implementation necessitates the adept negotiation of various technical, organizational, and regulatory obstacles. Through strategic planning, collaboration, and innovation, stakeholders can harness the prowess of IoT technologies to craft a more resilient, efficient, and sustainable water future.

III. Sensor Testing

In this chapter, the focus is on the testing phase of sensors integrated into the Smart Water Management System using LoRaWAN. The objective is to ensure accurate and reliable sensor performance under various conditions for effective water management. Discuss calibration, fine-tuning, validation, integration testing, and performance evaluation.

A. Calibration of Sensors

Calibration ensures sensor accuracy by adjusting their outputs to match expected values for parameters like pressure, flow rate, and water levels. It involves generating calibration curves based on known reference values and making adjustments to minimize errors.

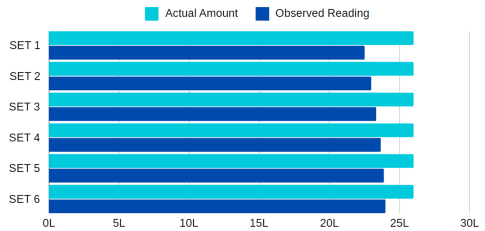


Fig. 1. FLOW METER PERFORMANCE ANALYSIS

TABLE I
SENSOR TESTING: FLOW METER

Sr. No.	Actual Distance	Observed Reading	Accuracy
1	25L	22.51L	90.04%
2	25L	22.98L	91.92%
3	25L	23.34L	93.36%
4	25L	23.66L	93.44%
5	25L	23.78L	95.15%
5	25L	24.28L	97.12%

B. Fine-Tuning of Sensor Parameters

Fine-tuning optimizes sensor performance by adjusting parameters like sensitivity and resolution. This enhances response time, reduces noise, and increases measurement precision.

C. Validation of Sensor Readings

Validation compares sensor data with reference values to assess accuracy and reliability. Field testing, comparative analysis, and data integrity checks ensure sensors perform well under real-world conditions.

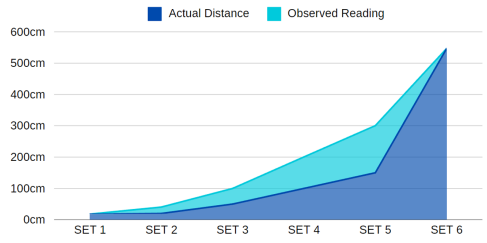


Fig. 2. ULTRASONIC LEVEL SENSOR PERFORMANCE ANALYSIS

TABLE II
SENSOR TESTING: ULTRASONIC LEVEL SENSOR

Sr. No.	Actual Distance	Observed Reading	Accuracy
1	18cm	835cm	0.00%
2	20cm	20.34cm	98.32%
3	50cm	49.86cm	99.72%
4	100cm	100.53cm	99.47%
5	150cm	150.48cm	99.68%
5	548cm	835cm	0.00%

D. Integration Testing

Integration testing verifies seamless sensor integration with the system architecture. It includes testing communication protocols, interoperability, and reliability to ensure smooth operation.

E. Performance Evaluation

Performance evaluation assesses sensor accuracy, reliability, response time, and data transmission efficiency. It provides insights into sensor effectiveness and guides optimization efforts.

IV. LORA COMMUNICATION

In this chapter, the intricate workings of LoRa communication, a pivotal component of the Smart Water Management System are understood. LoRa, an abbreviation for Long Range, represents a wireless communication technology renowned for its extensive range and low power consumption. Within the framework of the system, LoRa serves as the backbone, facilitating the transmission of crucial data from sensors to the central monitoring unit. This chapter aims to comprehensively elucidate the various facets of LoRa communication, spanning system architecture, data transmission, security protocols, and considerations for network scalability and coverage.

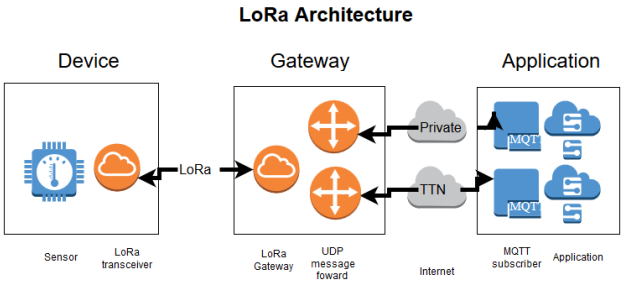


Fig. 3. Illustration of LoRa Communication System Architecture

A. Introduction to LoRa Communication

1) System Architecture: The architecture of a LoRa communication system encompasses several key elements, including end devices, gateways, and a network server. End devices, typically equipped with LoRa transceivers, serve as data collection points, gathering information from sensors deployed across the water distribution network. These devices then transmit the collected data to nearby gateways, which act as intermediaries responsible for relaying the information to the central network server. The network server, in turn, receives, processes, and stores the transmitted data, enabling comprehensive monitoring and analysis.

2) Data Transmission: Central to the functionality of LoRa communication is its ability to facilitate long-range data transmission while consuming minimal power. This feat is achieved through the utilization of chirp spread spectrum modulation, a technique that enables data packets to traverse extended distances while maintaining low power consumption. Data packets are transmitted across multiple frequency channels, ensuring robust communication even in environments plagued by interference and noise. The modulation techniques employed, coupled with carefully calibrated transmission parameters, collectively contribute to the efficiency and reliability of data transmission within the LoRa network.

TABLE III
COMPARISON OF LORAWAN SECURITY FEATURES

Security Feature	Description
End-to-End Encryption	Ensures data confidentiality
Authentication Mechanisms	Verifies device identity

B. Security Measures in LoRa Communication

1) End-to-End Encryption: Security lies at the heart of LoRa communication, safeguarding sensitive data against unauthorized access and tampering. To this end, LoRaWAN incorporates robust end-to-end encryption mechanisms, ensuring that data transmitted between end devices and the network server remains confidential and secure. Each end device is equipped with unique session keys, which are utilized to encrypt data packets prior to transmission. Upon reception, the network server utilizes the corresponding keys to decrypt and process the received data, thus safeguarding the integrity of the transmitted information.

2) Authentication Mechanisms: Authentication mechanisms serve as the first line of defense against unauthorized access within the LoRaWAN network. End devices undergo rigorous authentication procedures to verify their identity and establish secure communication channels with the network server. Authentication typically involves the exchange of cryptographic credentials, including pre-shared keys or digital certificates, thereby ensuring that only authorized devices are granted access to the network. By enforcing stringent authentication protocols, LoRaWAN mitigates the risk of malicious entities infiltrating the network and compromising data integrity.

C. Network Scalability and Coverage

1) Network Planning: Effective network planning is imperative to ensure optimal coverage and scalability within LoRaWAN deployments. This entails meticulous site selection, gateway placement, and frequency allocation to maximize network coverage and capacity. By strategically positioning gateways and optimizing channel utilization, network planners can mitigate potential interference issues and enhance the overall robustness of the network infrastructure.

2) Range Extension Techniques: Range extension techniques play a pivotal role in extending the coverage of LoRaWAN networks, particularly in scenarios where long-distance communication is imperative. Techniques such as signal amplification, antenna optimization, and relay node deployment are commonly employed to enhance the reach and reliability of communication. Through the judicious application of range extension strategies, network operators can effectively bridge communication gaps and ensure seamless connectivity across diverse terrains and environments.

V. Design and Proposed System

In this chapter, the crucial phase of designing and prototyping for a smart water management systems is studied. Here, the process of translating conceptual ideas into tangible solutions, focusing on the architecture, component selection, and prototyping of hardware and software modules is outlined. By exploring iterative process of design and refinement, the aim is to create scalable and effective solutions for addressing all the water management challenges. Through meticulous planning, innovative problem-solving, and rigorous testing, a robust system that optimizes water usage and promotes sustainability is developed.

A. Design Details

Designing a system requires attention to hardware layout, sensor placement, communication protocols, power management, user interface, and scalability:

- Hardware Layout: Organize components compactly to minimize interference and damage.
- Sensor Placement: Position sensors strategically for accurate data collection.
- Communication Protocols: Use LoRaWAN for reliable long-range communication.
- Power Management: Implement power-saving techniques and consider renewable energy sources.
- User Interface: Develop a user-friendly interface for monitoring and control.
- Scalability and Flexibility: Design the system to easily expand and adapt to future needs.

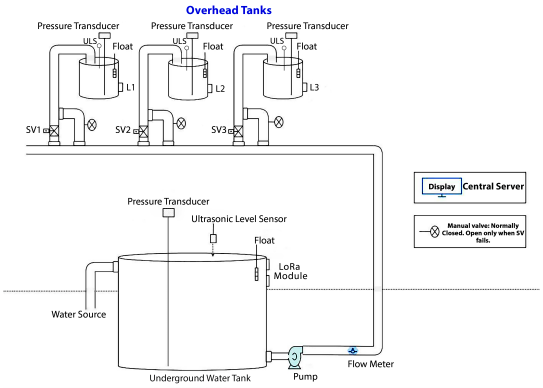


Fig. 4. Block Diagram

B. Proposed System/Methodology/Framework/Algorithm

The methodology section describes how we're going to build a smart water management system using the components we've discussed. It outlines the steps to be taken to assemble the hardware, write the software, and test the system to make sure it works correctly. First, all the necessary components, including the Arduino Uno R3, STM32 Nucleo F411RE, LoRa SX1278 module, BMP180 sensor, and YF S201 sensor are to be bought.

Any additional components and tools if needed, such as wires, breadboards, and a computer for programming are all gathered. Next, the hardware is assembled by connecting the sensors and modules to the microcontrollers according to the specifications provided by the manufacturers, double-checking all the connections to make sure everything is connected properly and securely.

Once the hardware is assembled, the software that will run on the microcontrollers is written. This will involve writing code to read data from the sensors, process the data, and send

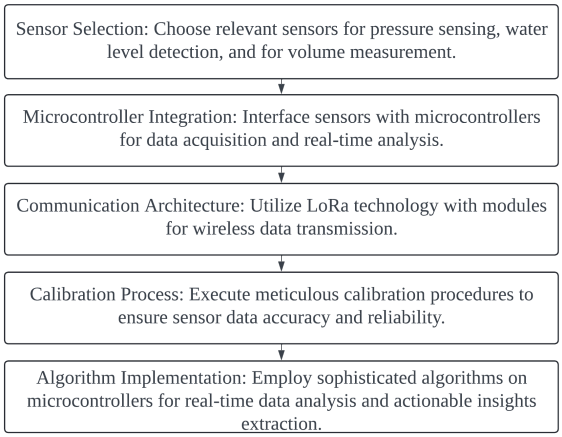


Fig. 5. Methodology

it wirelessly using the LoRa SX1278 module. Also writing the code to receive and interpret the data on the receiving end.

After the software is written, the system is tested to make sure it works correctly, simulating different scenarios and conditions to see how the system responds, making any necessary adjustments or improvements along the way.

Once we're satisfied that the system is working as intended, deploying it in the field and monitor its performance over time. The collected data from the sensors is analyzed to evaluate the effectiveness of the system and identify any areas for improvement.

By following this methodology, a reliable and efficient smart water management system that helps conserve water, reduce waste, can be built which ensure access to clean water for all.

VI. Prototype

The prototype model acts as a tangible manifestation of a proposed solution, providing a hands-on platform to validate ideas, experiment with functionality, and solicit feedback prior to full-scale deployment. It encompasses various stages, including meticulous design and development, seamless integration of components, rigorous testing to ensure functionality and reliability, iterative improvements based on testing outcomes and stakeholder input, thorough documentation to capture insights and decisions, and engaging stakeholder evaluation to gauge usability and effectiveness. This iterative process enables refining the solution iteratively, mitigate risks, and ultimately deliver a robust and reliable final product.

VII. Implementation

This chapter delves into the practical aspect of building a smart water management system. It discusses the implementation of various components, including hardware setup, software development, integration of sensors and communication modules, testing procedures, deployment, and monitoring. Each subsection provides detailed insights into the implementation process, supported by illustrations, diagrams, tables, and figures where applicable.

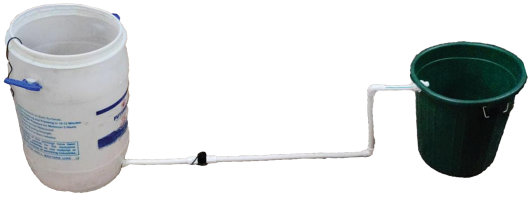


Fig. 6. Prototype Model

A. Hardware Setup

The hardware setup forms the backbone of a smart water management system, comprising the integration of microcontrollers, sensors, communication modules, and power sources. The process involves several steps to ensure proper assembly and connectivity of components.

To initiate the setup, begin by connecting the Arduino Uno R3 and STM32 Nucleo F411RE microcontrollers to the computer using USB cables. Install essential development environments such as Arduino IDE and STM32CubeIDE to facilitate programming and configuration.

Subsequently, mount the LoRa SX1278 module onto both microcontrollers, ensuring alignment and secure connection of communication pins. Carefully connect the BMP180 sensor to one microcontroller and the YF S201 sensor to the other, utilizing jumper wires to establish electrical connections between the components.

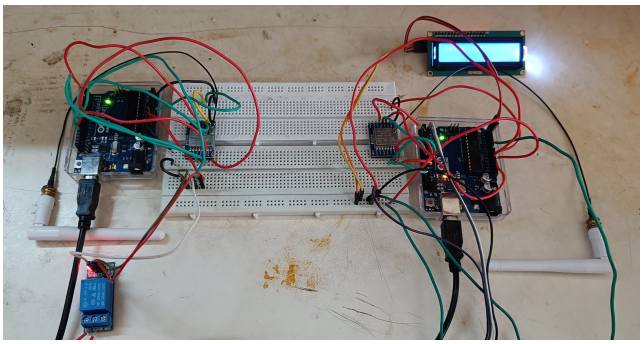


Fig. 7. Hardware Setup Diagram

Power provision is essential for the system's operation. Connect a 5V power source, such as a USB power adapter or battery pack, to each microcontroller. Verify the power supply to all components and conduct thorough checks for any loose connections or hardware malfunctions.

This meticulous hardware setup lays the groundwork for the smart water management system, enabling seamless communication between sensors and microcontrollers while ensuring reliable power distribution for uninterrupted operation.

B. Software Development for Smart Water Management

Software development forms the backbone of the smart water management system, enabling seamless communication

between hardware components, data processing, and implementation of control logic. The development process is characterized by meticulous planning, coding, and testing to ensure the reliability, efficiency, and scalability of the system.

1) Firmware Development: The firmware development phase commences with the writing of code for microcontrollers such as the Arduino Uno R3 and the STM32 Nucleo F411RE. Programming languages like C/C++ are utilized, along with libraries provided by the microcontroller manufacturers to facilitate hardware interaction.

For the Arduino Uno R3, firmware is crafted to initialize the LoRa SX1278 module, acquire data from sensors like the BMP180, and transmit this data over the LoRaWAN network. Robust error handling and data validation mechanisms are implemented to guarantee the integrity and accuracy of transmitted data.

Similarly, firmware for the STM32 Nucleo F411RE involves initializing the LoRa SX1278 module, capturing data from sensors like the YF S201, and receiving data transmitted by the Arduino Uno R3. Advanced logic is integrated to analyze incoming data, identify anomalies, and trigger appropriate responses such as alerts or adjustments in water flow rates.

2) Best Practices and Standards: Throughout the software development life cycle, adherence to industry best practices is paramount. Code organization, documentation, and version control are rigorously maintained to ensure the clarity, comprehensibility, and maintainability of the firmware.

Structured code organization enhances readability and facilitates future modifications or enhancements. Thorough documentation captures key insights, design decisions, and implementation details, serving as a valuable resource for developers and stakeholders alike. Version control systems enable collaboration, track changes, and ensure the stability of the codebase across iterations.

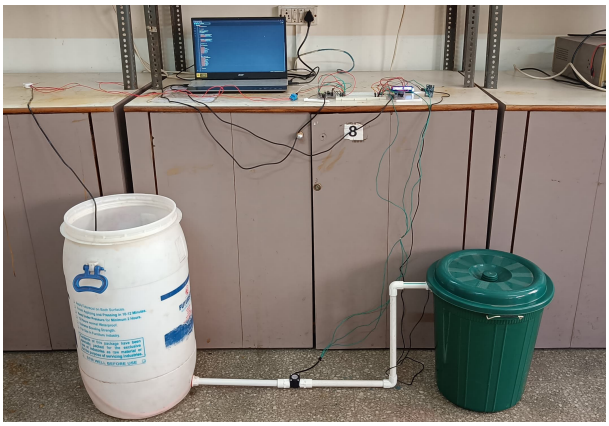


Fig. 8. Hardware Setup Diagram

3) Testing and Iterative Refinement: Testing forms an integral part of the software development process, encompassing unit testing, integration testing, and system testing. Test cases are meticulously designed to validate the functionality, performance, and reliability of the firmware under diverse scenarios and conditions.

Feedback gathered from testing iterations guides iterative refinements, driving continuous improvement and optimization of the software. An agile approach allows for flexibility and responsiveness to evolving requirements, ensuring that the firmware remains aligned with the dynamic needs of the smart water management system.

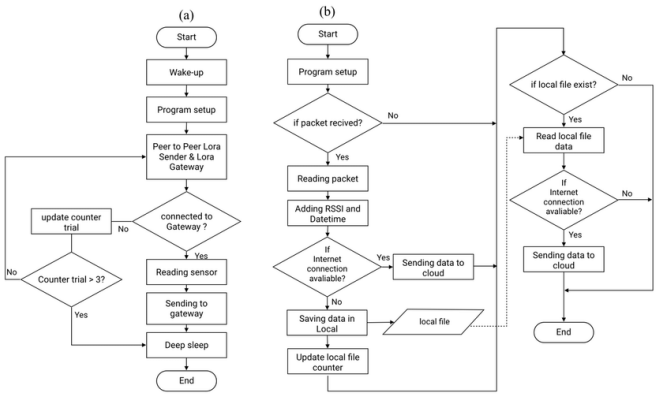


Fig. 9. Software Development Flowchart

By adhering to rigorous development practices and embracing a culture of continuous improvement, delivering firmware solutions that are robust, efficient, and resilient, are important, laying the foundation for a sustainable and effective smart water management infrastructure.

C. Integration of Sensors and Communication Modules

The integration of sensors and communication modules involves configuring the hardware and software to enable seamless interaction between these components, beginning with configuring the LoRa SX1278 module on both the Arduino Uno R3 and the STM32 Nucleo F411RE, setting parameters such as frequency, spreading factor, and transmission power to ensure optimal communication performance.

Next, calibration of the BMP180 sensor and the YF S201 sensor is done to ensure accurate measurement and detection of atmospheric pressure, temperature, and water flow rate, respectively. The sensors are verified, to check if they are functioning correctly and providing reliable data readings within the expected range.

Once the sensors are calibrated, communication between the microcontrollers and the sensors is established, configuring the necessary communication protocols, such as I2C or SPI, and implementing data exchange mechanisms in the firmware. The sensor data readings are validated to ensure that they are transmitted and received accurately by the respective microcontrollers.

Finally, integration testing is conducted to verify the overall functionality of the system, including sensor data acquisition, wireless communication, and error handling. Various scenarios and conditions are simulated to assess the robustness and

reliability of the system, making any necessary adjustments or optimizations.

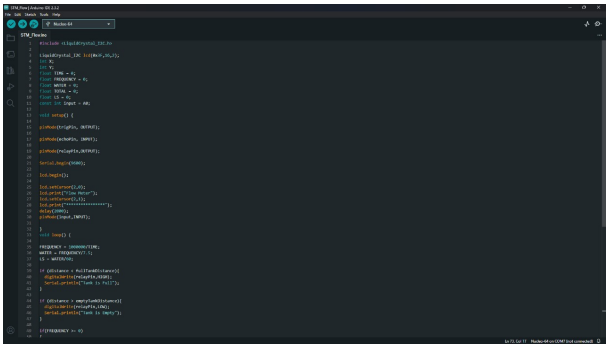


Fig. 10. Integration of Sensors and Communication Modules

D. Testing Procedures

Testing procedures are fundamental for validating the functionality, performance, and reliability of the smart water management system under varied operating conditions. A comprehensive testing plan is devised, covering functional, performance, and reliability aspects.

Functional testing verifies the correct operation of each system component. This includes testing sensor readings, microcontroller communication, data transmission via the LoRaWAN network, and the execution of control logic. The system's responses to different stimuli and inputs, such as changes in sensor readings or network conditions, are thoroughly examined.

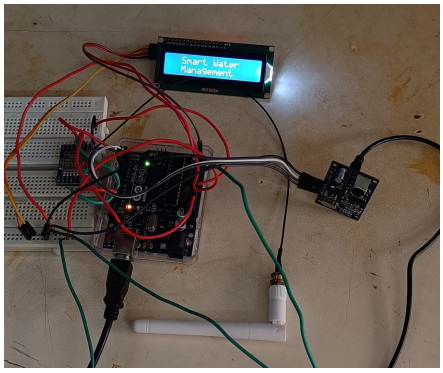


Fig. 11. Testing Procedures Overview

Performance testing is focused on assessing the speed, responsiveness, and efficiency of the system. Key performance metrics, including data transmission latency, sensor data acquisition rate, and power consumption, are measured. The system's performance is evaluated across various loads and usage scenarios to identify potential bottlenecks or limitations.

Reliability testing evaluates the system's ability to maintain continuous and predictable operation over time. Extended testing periods are employed to monitor for signs of degradation, malfunction, or failure. Adverse conditions, such as temperature extremes or network congestion, are simulated to assess the system's resilience and fault tolerance.

Throughout the testing process, meticulous documentation of test cases, procedures, and results is maintained. This comprehensive record of findings guides iterative design and implementation improvements. Based on test results, optimizations are made to enhance the overall quality and reliability of the system.

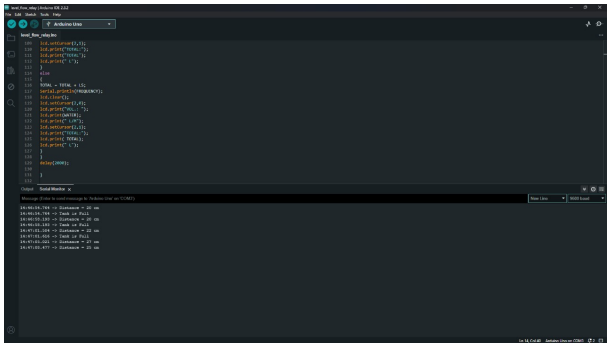


Fig. 12. Hardware Setup Diagram

E. Deployment and Monitoring

Deployment and monitoring entail the implementation of a smart water management system in real-world settings and the continuous assessment of its functionality and efficiency over time. This process involves meticulous planning, considering factors such as site selection, environmental variables, and network coverage to ensure optimal system performance.

Following deployment, remote monitoring capabilities are established to oversee the system's operation and performance from a central control center. Data visualization tools and dashboards are employed to present real-time sensor data, network status, and system health indicators. Alerts and notifications are configured to promptly notify operators of any detected issues or irregularities requiring attention.



Fig. 13. Deployment and Monitoring Process

The ongoing monitoring phase involves the systematic evaluation of the system's performance and the accumulation of data to assess its efficacy in water resource management. Data analysis techniques are applied to identify trends, patterns, and areas necessitating improvement. Insights derived from this analysis inform adjustments to system operations, resource

allocation optimization, and the implementation of predictive maintenance strategies.

Throughout the deployment and monitoring process, stakeholders are kept informed through regular communication channels, receiving updates on system performance and opportunities for feedback on potential enhancements. Emphasis is placed on user satisfaction, system reliability, and sustainability, driving continuous efforts to enhance the smart water management system.

VIII. Result and Analysis

In this chapter, the comprehensive analysis of the implementation and testing outcomes of the smart water management system is discussed. Through a meticulous examination of various components, the aim is to evaluate the system's performance in managing water resources effectively. Each section provides an in-depth exploration of different facets of the results, supplemented by figures, images, and tables where necessary.

A. Sensor Data Analysis

The sensor data analysis segment focuses on deciphering the trends, patterns, and anomalies present in the data collected by the smart water management system. By scrutinizing these insights, a nuanced understanding of water usage dynamics is achieved.

1) Temporal and Spatial Analysis: Temporal analysis involves dissecting how water usage patterns evolve over time, from hourly to weekly scales. Concurrently, spatial analysis entails mapping sensor data onto geographical representations or floor plans to discern the spatial distribution of water usage. This process aids in pinpointing areas of high consumption, potential leakages, or inefficiencies, thereby facilitating targeted optimization strategies (Figure **??**).

B. System Performance Evaluation

The system performance evaluation segment assesses the efficacy of the smart water management system across various metrics, including data accuracy, reliability, and efficiency. Through this assessment, the aim is to gauge the system's alignment with its objectives and identify areas for improvement.

1) Data Accuracy and Reliability: Data accuracy and reliability are paramount for robust decision-making. By juxtaposing sensor readings against ground truth values obtained from manual measurements or reference instruments, quantify deviations using metrics such as mean absolute error (MAE) or root mean square error (RMSE).

2) Efficiency: Efficiency encompasses the system's ability to achieve its objectives while minimizing resource consumption. By evaluating factors such as data transmission latency, power consumption, and network utilization, how effectively the system optimizes resource allocation and maximizes performance is assessed (Figure **??**).

C. Impact Assessment

The impact assessment section elucidates the ramifications of deploying a smart water management system on stakeholders and the environment. By weighing the benefits, challenges, and environmental implications, the aim is to provide a holistic understanding of the system's influence.

1) Benefits and Challenges: The benefits of the system extend across various domains, including water conservation, cost reduction, and decision-making enhancement. Conversely, deployment poses challenges and barriers to adoption, such as technical hurdles, regulatory constraints, financial limitations, or organizational resistance.

2) Environmental Impact: The environmental impact analysis scrutinizes how the system contributes to sustainability goals. By assessing factors such as water conservation, energy efficiency, and carbon emissions reduction, gauge the system's alignment with environmental objectives (Figure **??**).

IX. Conclusion and Future Work

This comprehensive conclusion serves as a synthesis of the findings, insights, and implications garnered from the study on smart water management systems. It encapsulates key discoveries, implementation insights, testing outcomes, and results analysis, illuminating the transformative potential of these systems for water resource management. Furthermore, it underscores the broader implications for societal benefits and environmental sustainability, advocating for the widespread adoption of smart water management systems to address pressing water challenges. Looking ahead, the section outlines potential avenues for further research and innovation, identifying emerging technologies, research gaps, and strategic priorities to propel the field forward. Ultimately, the study emphasizes the critical role of technology and collaboration in building a more resilient and sustainable future for water management.

A. Future Directions

This subsection outlines potential areas for further research, innovation, and implementation in smart water management, focusing on emerging technologies, research gaps, and strategic priorities.

1. Advanced Sensor Technologies: Research could focus on developing sensors capturing granular data on water quality, quantity, and distribution, like hyperspectral imaging or nanotechnology-based sensors.

2. Data Analytics and Machine Learning: Leveraging large data volumes, predictive models could forecast water demand, identify leakages, and optimize water distribution networks.

3. IoT and Edge Computing: Integrating IoT devices and edge computing can enhance system efficiency and responsiveness by decentralizing data processing tasks.

4. Water-Energy Nexus: Exploring interdependencies between water and energy systems could lead to integrated models optimizing resource allocation while minimizing environmental impacts.

5. Policy and Governance Frameworks: Developing frameworks incentivizing investment in smart water technologies and ensuring equitable access to water resources is crucial.

6. Community Engagement and Capacity Building: Empowering communities to participate in water conservation efforts through participatory approaches and educational programs is essential.

7. Resilience and Adaptation Strategies: Exploring decentralized water treatment systems, nature-based solutions, and resilient infrastructure design can enhance system resilience.

By addressing these areas, future research can advance smart water management, promoting efficiency, sustainability, and resilience in water resource management.

REFERENCES

[1] A. A. Ali, S. M. Saadi, T. M. Mahmood, and S. A. Mostafa, "A smart water grid network for water supply management systems," *Bulletin of Electrical Engineering and Informatics*, vol. 11, no. 3, pp. 1706–1714, 2022.

[2] I. Andrić, A. Vrsalović, T. Perković, M. A. Čuvić, and P. Šolić, "Iot approach towards smart water usage," *Journal of cleaner production*, vol. 367, p. 133065, 2022.

[3] H. Arkian, D. Giouroukis, P. S. Junior, and G. Pierre, "Potable water management with integrated fog computing and lorawan technologies," *IEEE IoT Newsletter*, pp. 1–3, 2020.

[4] J. Arshad, M. Aziz, A. A. Al-Huqail, M. H. u. Zaman, M. Husnain, A. U. Rehman, and M. Shafiq, "Implementation of a lorawan based smart agriculture decision support system for optimum crop yield," *Sustainability*, vol. 14, no. 2, p. 827, 2022.

[5] D. Baldo, A. Mecocci, S. Parrino, G. Peruzzi, and A. Pozzebon, "A multi-layer lorawan infrastructure for smart waste management," *Sensors*, vol. 21, no. 8, p. 2600, 2021.

[6] P. Fraga-Lamas, M. Celaya-Echarri, L. Azpilicueta, P. Lopez-Iturri, F. Falcone, and T. M. Fernández-Caramés, "Design and empirical validation of a lorawan iot smart irrigation system," in *Proceedings*, vol. 42, no. 1. MDPI, 2019, p. 62.

[7] O. Khutsoane, B. Isong, and A. M. Abu-Mahfouz, "Iot devices and applications based on lora/lorawan," in *IECON 2017-43rd Annual Conference of the IEEE Industrial Electronics Society*. IEEE, 2017, pp. 6107–6112.

[8] Y. Lalle, L. Fourati, M. Fourati, and J.P.Barraca, "Lorawan network capacity analysis for smart water grid," in *12th International Symposium on Communication Systems, Networks and Digital Signal Processing (CSNDSP)*. IEEE, 2020, pp. 1–6.

[9] Y. Lalle, L. C. Fourati, M. Fourati, and J. P. Barraca, "A comparative study of lorawan, sigfox, and nb-iot for smart water grid," in *2019 Global Information Infrastructure and Networking Symposium (GIIS)*. IEEE, 2019, pp. 1–6.

[10] Y. Lalle, M. Fourati, L. C. Fourati, and J. P. Barraca, "Routing strategies for lorawan multi-hop networks: A survey and an sdn-based solution for smart water grid," *IEEE Access*, vol. 9, pp. 168 624–168 647, 2021.

[11] A. M. Manoharan and V. Rathinasabapathy, "Smart water quality monitoring and metering using lora for smart villages," in *2018 2nd International Conference on Smart Grid and Smart Cities (ICSGSC)*. IEEE, 2018, pp. 57–61.

[12] E. Migabo, K. Djouani, and A. Kurien, "Design of an energy efficient lorawan-based smart iot water meter for african municipalities," in *2021 International Conference on Electrical, Computer and Energy Technologies (ICECET)*. IEEE, 2021, pp. 1–6.

[13] A. P. Murdan and A. Hardin, "Exploring the economic viability of lorawan based smart water meters for sustainable water management," in *IRC Conference on Science, Engineering and Technology*. Springer, 2023, pp. 216–225.

[14] H. P. Nguyen, V. P. Nguyen, M. H. Nguyen, and M. P. Lê, "Development and implementation of smart water metering system based on lora technology," *VNUHCM Journal of Engineering and Technology*, vol. 5, no. 1, pp. 1342–1370, 2022.

[15] F. Sánchez-Sutil and A. Cano-Ortega, "Smart control and energy efficiency in irrigation systems using lorawan," *Sensors*, vol. 21, no. 21, p. 7041, 2021.

[16] M. Saravanan, A. Das, and V. Iyer, "Smart water grid management using lpwan iot technology," in *2017 Global Internet of Things Summit (GIoTS)*. IEEE, 2017, pp. 1–6.

[17] V. Slaný, A. Lučanský, P. Koudelka, J. Mareček, E. Krčálová, and R. Martínek, "An integrated iot architecture for smart metering using next generation sensor for water management based on lorawan technology: A pilot study," *Sensors*, vol. 20, no. 17, p. 4712, 2020.

[18] A. Valente, C. Costa, L. Pereira, B. Soares, J. Lima, and S. Soares, "A lorawan iot system for smart agriculture for vine water status determination," *Agriculture*, vol. 12, no. 10, p. 1695, 2022.

[19] P. Yeram, N. Gonsalvez, C. D'Souza, E. Abraham, and V. Patil, "Smart water management system in urban areas using lora technology," in *Proceedings of the 3rd International Conference on Advances in Science & Technology (ICAST)*, 2020.

Advanced Navigational System for Accurate GPS Localization

Adarsh Rao, Lovely Varshney, Gouresh Sankhe, Abhishek Waghmare, Dr. Ashwini Kotrashetti

Department of Electronics and Telecommunication Engineering
The Bombay Salesian Society's, Don Bosco Institute of Technology, University of Mumbai, Mumbai, India

120adarsh0004@dbit.in, 120varshney0025@dbit.in, 120gouresh0011@dbit.in, 120abhishek0030@dbit.in

***Abstract*—In this Project, a system is developed that integrates Global Navigation Satellite Systems (GNSS) with Real-Time Kinematic (RTK) technology to achieve accurate localization of an object up to 10 cm using ZED-F9P-04B Ublox Module and the STM32WLE5CCU6 development board. This combination enables precise positioning and real-time navigation for a moving object, with support from a fixed base station. The project's setup involves a fixed base station positioned at a known location, while the rover acts as the moving object. Both are equipped with GNSS and LoRa modules for communication. The base station continuously sends correction data to the rover, allowing for accurate coordinate calculations even in challenging environments.These coordinates are then used for real-time navigation along predefined routes, allowing for tracking and display of the object's path. Extensive testing was conducted across various locations, including urban areas, open spaces, and over water bodies. The system's reliability and robustness were demonstrated across different urban settings and times of the day. This integration of GNSS with RTK technology offers potential applications in precise localization and real-time navigation across various fields.**

Index Terms—GPS, RTK, RTCM, GNSS, NTRIP,

I. Introduction

The Global Positioning System (GPS) is a satellite-based navigation that uses satellites to help us find where we are and what time it is, is crucial for modern navigation.But it's not accurate, especially when we need really precise measurements, like in construction or farming.GPS accuracy can vary but is typically around 5–10 meters for civilian users and more accurate for military applications. To make it better, some countries have made their own satellite systems, like Europe's Galileo, Russia's GLONASS, and China's BeiDou, which work alongside GPS to make positioning even more accurate. These systems not only give us more coverage but also improve accuracy, especially in places like cities where tall buildings can block GPS signals. To make GPS even more precise,Advance Techniques like Differential GPS (DGPS) and RealTime Kinematics (RTK) are used.They can improve accuracy within a few centimeters. DGPS uses special ground stations to correct GPS signals, making them more accurate, sometimes just a few centimeters off. RTK takes it a step further by using a network of fixed base stations to send real-time corrections to moving devices, making them super accurate, down to the centimeter. This kind of accuracy is really important in lots of areas, like making maps, driving self-

driving cars, flying planes, farming, and helping in emergencies. For example, in farming, knowing exactly where to plant seeds or apply fertilizer can make a big difference in how well the crops grow. And in emergencies, being able to quickly find and help people can save lives. So, making GPS and other positioning technologies are as accurate as possible is super important for lots of different reasons. By improving these technologies, we can make the world a safer, more efficient place for everyone.

II. Methodology

A. NTRIP

Networked Transport of RTCM via Internet Protocol or NTRIP is a recently developed application-level protocol streaming Global Navigation Satellite System (GNSS) data over the Internet by the Federal Agency for Cartography and Geodesy of Germany. NTRIP enables the streaming of DGPS or RTK correction data for the stationary and mobile users via Internet by using GPRS or other modern communication technologies (EDGE, or UMTS), allowing simultaneous PC, Laptop, PDA, or receiver connections to a broadcasting host. RTK GPS technology provides extremely precise location information, down to a few centimeters and relied on short-range radio links between a fixed base station and a mobile rover to transmit correction data. However, NTRIP takes advantage of the widespread availability of internet connectivity to transmit these corrections over long distances. By using the internet as the transport medium, NTRIP allows RTK correction data to be streamed from base stations to rovers, enabling real-time positioning over large geographic areas.

B. Components of the NTRIP System

The NTRIP system comprises 4 primary components:

- NTRIP Source:The NtripSource is a GNSS receiver that provides continuous GNSS data such as RTCM-104 corrections that refer to a known or specific location. A US organization, the Radio Technical Commission for Maritime Services (RTCM), works within a special Committee No. 104 (SC104) with standards for real time

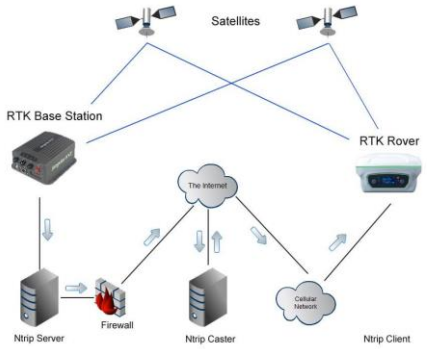


Fig. 1. Components of NTRIP

transfer of observations of satellite-based navigation systems for differential applications. The special committee is responsible for RTCM standards for differential GNSS. The HTTP-based TCP protocol NTRIP is currently undergoing this procedure via the special committee No. 104 to become a worldwide standard.

- NTRIP Server: NtripServer is software running on a conventional PC that sends correction data from a GNSS receiver (COM-port) to a third installation (from NtripSource to NtripCaster). As an example, NTRIP could be used within a virtual reference network where the protocol is able to transport RTCM data. The RTCM corrections could be taken into consideration at the user's approximate position. As an example, this virtual reference station data is comparable with a NtripSource that could be transmitted by one of the Ntrip components, the NtripServer. As a summary the NtripServer transports GNSS data of an NtripSource (GNSS receiver) directly to the NtripCaster. Before doing this in the described way the NtripServer sends a request to the mountpoint via HTTP. After the connection is established, the data can be sent via TCP/IP.
- NTRIP Caster: The NtripCaster is in general a HTTP server and acts, as already described, as a broadcaster integrated between the data sources (NtripServer) and the datareceiver (the NtripClients). The NtripCaster receives data streams from NtripServers (generated by NtripSources) and manages, for example, the handling of mountpoints for NtripSources, passwords, billing, and access.
- NTRIP Client: Devices receiving the information flows transmitted by the Caster. End devices are considered personal computers, tablets, mobile phones, GNSS receivers, among others.It also sends request messages to the caster to receive data.After Ntrip Client logs in, Ntrip Caster sends GNSS correction data to it.

C. Advantages of NTRIP

Real-time GNSS correction data provided by NTRIP enables high accuracy compared to standalone GNSS receivers. By continuously receiving correction updates from nearby base stations, rovers can achieve centimeter-level positioning accuracy even in challenging environments. NTRIP correction data can be obtained from multiple reference stations, providing wide coverage over large geographic areas. This enables users to perform highprecision positioning tasks such as land surveying, precision agriculture, and infrastructure monitoring. NTRIP can support a large number of GNSS receivers simultaneously, making it scalable for large-scale projects requiring high precision. Whether deploying a single rover or a fleet of vehicles, NTRIP efficiently delivers correction data to all connected receivers, ensuring consistent positioning performance across the entire project area.

III. IMPLEMENTATION

A. Block Diagram

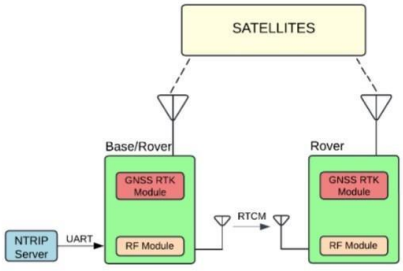


Fig. 2. Block Diagram

The block diagram consists of two separate parts: the rover section and the base section. Each of these sections includes a GNSS RTK Module (ZED-F9P-UBLOX) and an RF LoRa module (STM32WLECJ) respectively. The GNSS RTK Module's antenna continuously receives signals from satellites. At the base, we have connected an NTRIP server. The NTRIP service accurately determines the location of the base. Once the base achieves a fixed location, its NTRIP service disconnects. After achieving a fixed position, the base begins to transmit RTCM corrected messages to the rover via the RF LoRa Module. Using these corrected RTCM messages, the rover computes its precise location, achieving centimeterlevel accuracy.

B. Working

The working begins with the base station, a stationary device equipped with a GPS receiver. This receiver communicates with satellites orbiting the Earth to determine the base station's initial coordinates. These satellites, part of a

network maintained by various countries, continuously transmit signals containing precise timing and positioning information. By receiving signals from multiple satellites and performing calculations based on the time it takes for these signals to arrive, the GPS receiver can find its position on the Earth's surface. This initial position serves as the starting point for the entire process. However, the initial position obtained is not perfectly accurate. Accuracy can be influenced by various factors such as atmospheric conditions, signal interference, and the geometry of satellite constellations. To address these challenges and further enhance accuracy, the base station connects to a service known as NTRIP (Networked Transport of RTCM via Internet Protocol). NTRIP acts as a bridge between the base station and a network of reference stations equipped with high-precision GPS receivers. These reference stations continuously monitor their positions and compare them to known coordinates, allowing them to detect any deviations or errors. Through the NTRIP service, the base station receives correction data generated by these reference stations. This correction data contains precise information about any discrepancies between the actual position of the reference stations and their calculated positions. The base station then performs computations based on the GPS coordinates it receives and the correction data obtained from NTRIP. With its position refined and optimized through the correction data obtained from NTRIP, the base station now sends RTCM data to a rover. A rover is a mobile device equipped with its own GPS receiver.

To transmit RTCM data to the rover, the base station utilizes RF communication. RF communication allows for wireless data transmission, facilitating communication between the stationary base station and the mobile rover. The base station encodes the correction data and broadcasts it to the rover's receiver. The rover receives the RTCM data transmitted by the base station. It uses this data, along with the signals received from its own GPS device, to calculate its accurate location.

C. Mathematical Analysis1) GNSS Position:

$$c\Delta t_j = \sqrt{(y - y_j)^2 + (y - y_j)^2 + (y - y_j)^2} \quad (1)$$

where:

c = speed of light

Δt_j = time travel of signal by satellite j

(y,y,y) = GPS receiver coordinates;

(y_j,y_j,y_j) = coordinates for satellite j

We know that there is time delay in these signals and it causes significant error. To eliminate these errors, there are different ways.

2) Pseudo Random Code: One of the way is to use pseudo random code: This approach involves the pseudo code used by the satellite, which is a binary sequence. The receiver generates same code on its internal clock and once the signal is received, it compares the delay.

But this delay measurement is not accurate. It involves a lot of other components that causes delay. The key difference between RTK and Pseudo Random code is that it uses phase carrier measurements to calculate the delay between the signal received from satellite to the GPS receiver.

3) Carrier Phase Measurement: In RTK, carrier phase measurement is used to eliminate the delay caused in equation 1. Here, it measures the phase from signal received by the GPS Receiver compared to the locally generated signal. By subtracting the phase errors from base and the rover, all the error gets eliminated from the readings except the integer ambiguity.

D. Measuring distances using phase

Let's use simple sinusoidal functions to explain how we can measure phase and what is the integer ambiguity.

Consider 2 sinusoidal signals, one sent by a transmitter at some unknown distance from the receiver and one generated locally at the receiver:

$$g_{\text{recv}}(u, v) = C\cos\left(2\pi k u + \frac{2\pi}{\mu} v\right) \quad (2)$$

$$g_{\text{local}}(u) = D\cos(2\pi k u) \quad (3)$$

where:

- C,D = signal's amplitude
- k = signal's frequency
- v = distance traveled by the signal
- μ = wavelength of the signal

The first equation is for the travelling wave through space, and represents what we see at the receiver. The term depending on the distance is the phase of the travelling signal relative to the receiver.

Multiplying two equations, we get the second term dependent on phase, which is in turn dependent on distance.

$$g_{\text{recv}} \times g_{\text{local}} = \frac{CD}{2}\left[\cos\left(4\pi k u + \frac{2\pi}{\mu} v\right) + \cos\left(\frac{2\pi}{\mu} v\right)\right] \quad (4)$$

However, the distance v can be written as a function of the

$$v = P\mu + \frac{\mu\theta_{\text{recv}}}{2\pi} \implies \cos\left(\frac{2\pi}{\mu} v\right) = \cos\left(2P\pi + \theta_{\text{recv}}\right) = \cos(\theta_{\text{recv}}) \quad (5)$$

signal wavelength; therefore:

where:

- P = unknown integer number of wavelengths
- θ_{recv} = signal phase measured at the receiver

So it's clear that, by just measuring the phase, we cannot determine the full distance between the transmitter and the receiver since, in reality, we can only measure the small

fractional part of the phase difference. N represents the integer ambiguity.

E. Calculating the accurate co-ordinates

There are majorly three steps:

- Calculate the inaccuracy as float numbers using pseudo range. This is the float mode.
- Find integer ambiguity near float numbers.
- Use the integers received abov to get accurate GPS Receiver position.

Once the integer ambiguity is solved, the RTK enters in Fixed mode. In this state there is high accuracy because it uses, phase measurements which has fractional errors around 3 cm and not time measurements which causes errors up-to 3 metres.

F. Comparison of GPS vs RTK

In this comparison between normal GPS, represented by Geotracker/Google Maps, and RTK Technology, we observe significant differences. In normal Google Maps or Geo-tracker, the red mark signifies the actual location where the user is positioned with their phone. However, the location indicated by the blue dot is notably distant from the user's actual position, as depicted in the figure. This inaccuracy between the observed location and the actual position measures approximately 10.36 meters, indicating substantial accuracy difference.

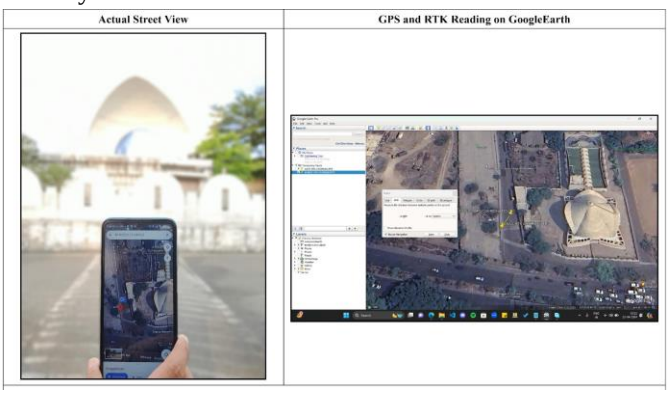


Fig. 3. Comparison of GPS with RTK.

- Red mark: GNSS-RTK coordinates (centimeter-level accuracy)
- Blue mark: Mobile GPS coordinates (meter-level accuracy)
- Inaccuracy: 10.36m, show-casing GNSS-RTK superior precision.
- Location: Dr BR Ambedkar Memorial Bhavan, Airoli, NaviMumbai.

G. Testing Scenarios

The testing process was initiated by exploring different scenarios, including urban area, open spaces, and areas near water bodies like Big Lake. The urban built-up included a 36 floored building, a big Gurudwara and an Ambedkar bhavan. The open area is used as RTO test center and has small grass and open environment. The third location had a big lake surrounded by residential area and a school named as St John High School. By examining locations, the variations in signal strength and stability across these different scenarios were observed, with an average signal strength ranging from 38-45 dB.

IV. Results

A. Testing at different times of the day:

In afternoon, around 1:30 PM, at Dr. Babasaheb Ambedkar Memorial Bhavan in Navi Mumbai, the signal strength for tracking is between 38 to 40 dB, and the tracing is done by



Fig. 4. Description of Different Test Scenarios.

walking. Both the rover and base station are within a 220meter radius, and they remain in Fixed Mode except when encountering obstacles. Later, at 3:30 PM, at the RTO Fitness Track in Airoli, Navi Mumbai, the signal strength increases to an average of 40 to 45 dB. Tracing is handheld, and again, it's always in Fixed Mode. At 4:00 PM, at Talao Pali in Thane, the signal strength is around 40 to 42 dB, and tracing is done via pedal boat, with both rover and base station within a180-meter radius, remaining in Fixed Mode.

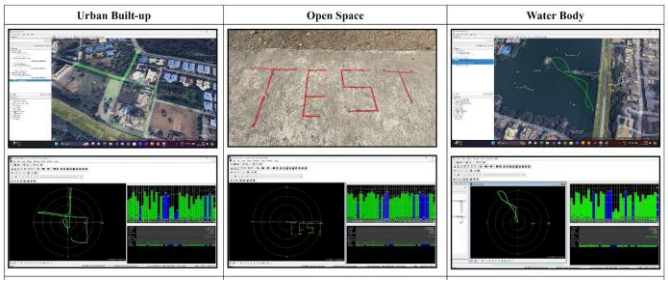


Fig. 5. Afternoon Testing Results.

In the evening, around 8:00 PM, at Dr. Babasaheb Ambedkar Memorial Bhavan, the signal strength remains consistent at 38 to 40 dB, tracing is again by walking, and both rover and base station are within a 220-meter radius. The system switches to No Fix Mode only around obstructions, otherwise staying in Fixed Mode. Meanwhile, at the RTO Fitness Track in Airoli at 5:30 PM, signal strength drops to 30 to 35 dB, tracing with the help of bike, with Float Mode and sometimes No Fix Mode occurring due to loss of RTCM Data around big trees. Lastly, at Talao Pali in Thane at 8:00 PM, signal strength maintains at 38 to 40 dB, tracing is through pedal boat, and both rover and base station are within a 180-meter radius, remaining in Fixed Mode throughout.

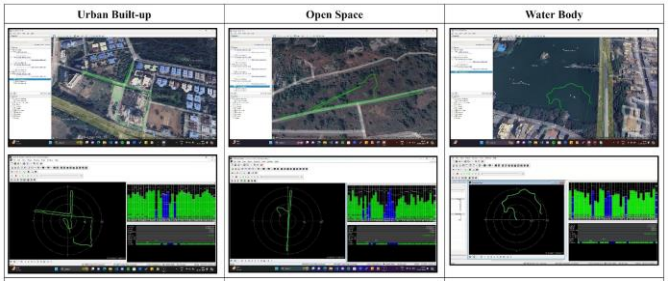


Fig. 6. Evening Testing Results.

B. System Accuracy Testing :

System Accuracy Testing involved tracing of various geometric shapes like square, rectangle and specific numeric figures (in Figure 7).

- The dimension of outer square was : Length = 152.4 cm and Breadth = 101.6 cm.
- The dimension of inner square was : Length = 101.6 cm and Breadth = 50.8 cm.
- The Figure 9 : Vertical Dimension = 70 cm Horizontal Dimension = 59 cm

The tracing done could clearly represent the inner and outer boundaries which had a spacing of 20-25 cm.

The tracking took place at specific locations and times, aiming to determine the precision with which the system could pin point positions. This analysis was crucial for applications such as navigation or surveying which require localising at centimeter level.

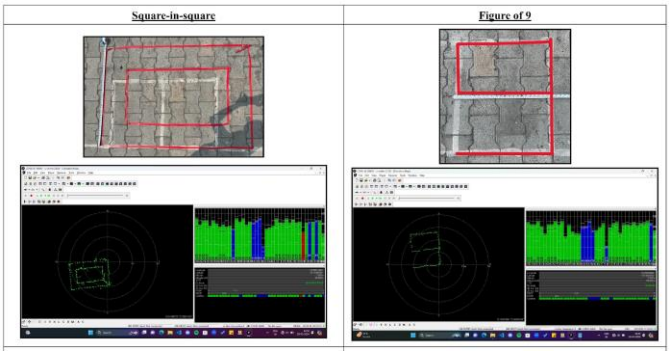


Fig. 7. System Accuracy Visualization.

C. Range Testing of Signal Transmission:

The range of the system's signal transmission was evaluated to ensure effective communication over significant distances, particularly in open areas. Range tests demonstrated (in Figure 8) successful RTCM transmission up to 430 meters in line-of-sight conditions, with consistent results achieved within a range of 180-220 meters in urban environments.

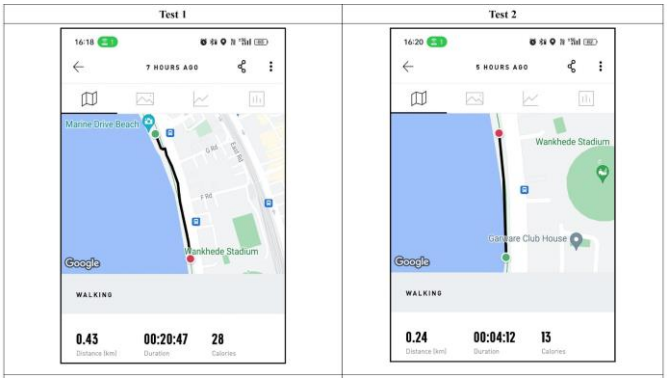


Fig. 8. Maximum distance between base and Rover to receive RTCM data.

Test 1:

- Time:8:41 AM
- Base Location A : Marine Drive (Northern End), Mumbai,Maharashtra.
- Remarks :The rover received the RTCM signal upto 410 meters. Beyond this range,the rover stopped receiving RTCM.
- Range: 430 meters

Test 2:

- Time:10:23 AM
- Base Location B: Marine Drive (Central Region), Mumbai, Maharashtra.
- Remarks: The rover received the RTCM signal upto 220 meters. Beyond this range, the rover stopped receiving RTCM.
- Range: 240 meters

D. Reliability Testing:

Finally, the reliability of the system's location readings over time was evaluated through repeated tests in the same location. Here we kept three points at a distance gap of 15cm between points A and B, and 35cm between points B and C. By conducting thirteen iterations at 30-minute intervals, we ensured that the system consistently provided accurate coordinates, with minimal variation observed at the sixth and seventh decimal places. This reliability is crucial for

applications requiring consistent and precise location data. The variations in the Latitude and the Longitude has been shown in the figure 5.8 using graphical representation.

The rover antenna is repeatedly placed at same positions A, B and C. Ideally the co-ordinates should be same. The red line shows the average of all co-ordinates for latitude and longitude respectively. The blue line shows the variation at each iteration. Variation was observed only in 6th and 7th decimal places. This verifies that the product gives consistent results at every iteration.

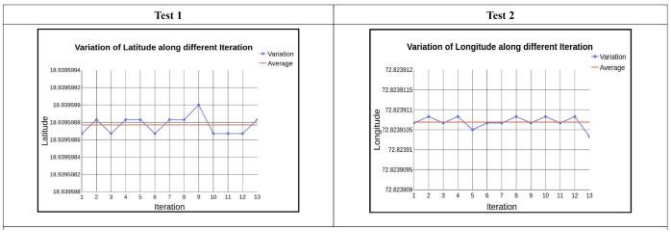


Fig. 9. System Reliability Visualization.

V. Conclusion

The project focuses on achieving centimeter level accuracy in GNSS data. It includes two boards, the Base and the Rover, each equipped with a GNSS and LoRa module. The Base board receives GPS coordinates from the GNSS receiver and compares them with the fixed coordinate which is provided via Ntrip server. Based on the comparison, the base calculates the RTCM correction data and transmits it to the rover. The rover uses the correction data and calculates centimeter level accuracy in its position.

The project has been tested under various conditions, including urban built-up, open space and across water body. It achieved consistent results across all the scenarios. The project maintained an accuracy of 10-15 centimeters. Apart from this, the project is tested on predefined paths routes in each scenario where it provided reliable centimeter accuracy. The board is also tested for maximum range between base and rover for which it provided accurate results. The results confirmed the systems capability to provide precise GNSS data across various environmental conditions. The project has achieved all its objectives but there are areas for improvement. Integrating an IMU (Inertial Measurement Unit) can improve the system's performance, in situations where GNSS signal is limited. The IMU predicts the position of the object using accelerometer, gyrometer and magnetometer in areas with no GNSS signals. Another possibility is fabrication of a custom board using GNSS and LoRa chips and using only the pins that the system requires. It will reduce the cost and make the system more efficient.

References

[1] M. Stranner, C. Arth, D. Schmalstieg, and P. Fleck. A high-precision localization device for outdoor augmented reality. In 2019 IEEE International Symposium on Mixed and Augmented Reality Adjunct (ISMARAdjunct), Oct. 2019.

[2] W. Yan, L. Wang, Y. Jin, and G. Shi. High accuracy navigation system using gps and ins system integration strategy. In 2016 IEEE International Conference on Cyber Technology in Automation, Control, and Intelligent Systems (CYBER), Jun. 2016.

[3] R. W. Ouyang, A. K.-S. Wong, and K. T. Woo. Gps localization accuracy improvement by fusing terrestrial toa measurements. In 2010 IEEE International Conference on Com- munications, May 2010

[4] H. A. A. Dafallah. Design and implementation of an accurate realtime gps tracking system. In The Third International Conference on e-Technologies and Networks for De- velopment (ICeND2014), Apr. 2014.

Development of A Container GPS Tracking System To Enhance Supply Chain Security

Sanskar Kumar[1], Russel Dmello[2], Sakshi Kaveri[3], Shreyas Nanaware[4], Freda Carvalho[5]
[1]*Department of Electronics and Telecommunication Engineering*
[1]*The Bombay Salesian Society's, Don Bosco Institute Of Technology, University of Mumbai, Mumbai India*
[1]*sanskarkumar2017@gmail.com,* [2]*russeldmello88@gmail.com,* *sakshikaveri2002@gmail.com,*[4]*shreyasnanaware2003@gmail.com*
[5]*freda@gmail.com*

***Abstract*—This paper intends to provide an innovative GPS tracking and anti-theft system for container shipments, addressing the growing concern about theft and smuggling. The suggested system uses GSM, GPS modules, and an STM32F302R8 microcontroller for better durability and cost effectiveness compared to existing alternatives. A simple current break sensor detects theft at- tempts, triggering alerts sent to the server via the GSM module. Real-time location monitoring is enabled through NMEA message format packets broadcast from the GPS module to the server, facilitating swift intervention to prevent theft. The system ensures accurate track- ing and effective theft prevention. This approach has the potential to greatly improve security in shipping operations, providing concrete benefits to society by protecting valuable cargo from unlawful activity.**

***Index Terms*—STM32 microcontroller, GSM, GPS, NMEA, asset management, tracking system, real time monitoring**

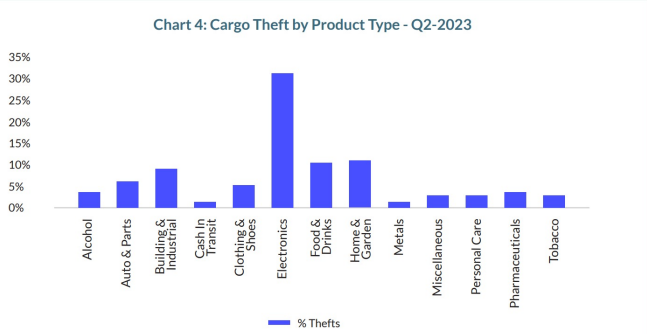


Fig. 1. Cargo Theft Statistics
[**?**]

I. Introduction

In the span of 2021 to 2022, supply networks in North America had a 13% increase in cargo theft volume, with a 16% increase in value, a trend that has persisted into 2023. While electronic products remain extremely susceptible, thieves are increasingly targeting domestic items and food and beverages, showing that increased pressures are driving shifts in criminal behavior. With a stolen product value of $107 million in 2022, a considerable rise from the $68 million recorded in 2020, cargo theft is definitely a concern that requires increased monitoring. Allianz Commercial, a worldwide maritime insurance, has observed an increase in cargo theft cases in recent years, notably in transportation and logistics. [1] Cargo theft cases increased more than 57% in 2023 compared to the previous year, according to CargoNet, a Verisk firm. According to CargoNet, about $130 million in products were stolen in 2023, but because reporting cargo theft is not mandated, the figure is likely to be greater. Cargo theft refers to the theft of products at any step during the shipping process, and instances have reached record proportions. [2] The major aim is to keep the containers and their contents safe throughout travel. The items will be transported safely, and the tracking technology will help to track the position in real-time. If the customers know the precise locations of their containers, there will definitely be a trust factor from the client side due to the reliable mode of business. The below Figure 1.1 shows the statistics of cargo thefts in year 2023.

A. Motivation

During the Covid-19 pandemic, when most modes of transportation were severely limited due to lockdowns and safety precautions, the movement of products grew more reliant on shipping containers, particularly for critical things like medical supplies, food, and other emergency goods. Shipping containers are really important for global trade, worth about $10 billion in 2024. But there are some significant challenges. One is ensuring that these containers are safe and secure. Imagine if someone stole or tampered with what's inside; that could be a major issue. So we're particularly working on keeping these containers safe and secure.That includes employing lock systems and technologies to ensure that everything stays where it is supposed to and is not tampered with

B. Scope of the Project

The project's goal is to develop a complete system capable of tracking several containers
simultaneously and individually. To achieve this, several key outcomes have been proposed.

- The project will include incorporating GPS devices into the tracking system.
  These devices will be mounted on each shipping container and will constantly collect location information. The acquired data will include latitude and longitude coordinates, allowing for accurate real-time information on the container's current location. This

connection will allow logistics managers and other stakeholders to monitor container movement throughout the shipping process, from origin to destination.

- GSM modules will add to GPS systems by allowing remote communication and data transmission over cellular networks.These modules will allow two-way communication between the tracking system and a central server or control center. They will allow the system to send alerts, receive commands, and transmit data, such as location updates and sensor readings, using standard mobile network infrastructure. This feature increases the system's versatility and allows for seamless connectivity, even in remote or inaccessible regions.
- In addition to GPS and GSM technology, the tracking system will incorporate sensor systems to enhance security and monitoring capabilities. The system includes a closed loop circuit system. It will continuously monitor the container's environment and detect any irregularities or unauthorized access attempts. When such events are detected, the system triggers an alert and notify specified persons or authorities, allowing for immediate response and intervention. By combining sensor systems, the tracking system improves theft prevention and cargo security while in transit.
- To ensure reliable and continuous functioning, the project intends on optimizing battery usage inside the tracking system. This optimization involves carrying out careful calculations to determine the power requirements of numerous components, such as GPS
devices, GSM modules, microcontrollers. The sleep and wake cycles of the GSM module, and power-saving features of other components will be considered in battery optimization strategies.
- The tracking system will be connected to a database so we can see where something is going and check if someone tries to steal it.

The ultimate objective is to develop a viable GPS and GSM tracking system for shipping containers that provides
continuous location visibility.

II. Methodology

The system begins by initializing the GPS module, which is necessary for the device to detect its accurate position. The initialization involves configuring the hardware connections and software settings to ensure proper operation. In addition, UART connection is established between the GPS module and the STM32 Microcontroller. UART is a common serial communication protocol used for transmitting data between devices. After establishing connectivity, the GPS module starts transmitting location data in NMEA. This data contains critical information such as latitude, longitude, altitude, time, and satellite status. The STM32 microcontroller then conducts the parsing process, carefully examining the NMEA words to extract relevant information, such as latitude and longitude coordinates. In addition, AT instructions are used to activate the GSM module. AT commands are standardized instructions for controlling and communicating with modems and other devices. Similar to the GPS setup, UART connection is established between the GSM module and the STM32 microcontroller. This allows data flow between the microcontroller and the GSM module. Once both the GPS and GSM modules are initialized and communication channels are established, the location data is transmitted to a mobile phone via the GSM module. This enables real-time tracking of the device's position. To ensure continuous and automated updates, the system is designed to repeat the data retrieval and transmission process hourly. This periodic procedure takes advantage of both GPS and GSM technologies to deliver efficient and dependable tracking functionality.

A. Software Used

Ansys HFSS (high-frequency structure Here is the list of softwares that have been utilized until this point of time :

1) STM32 Cube IDE : Designed for programming and developing applications for STM32 microcontrollers

2) Docklight : Docklight is a testing, analysis and simulation tool for serial communication protocols

3) KiCad : KiCad is an open-source electronic design automation (EDA) software suite for creating schematics and printed circuit boards (PCBs)

4) Putty : Putty is a free and open-source terminal emulator, serial console, and network file transfer application. It supports various network protocols like SSH, Telnet, rlogin, and raw socket connections.

5) Google Earth : Google Earth is a virtual globe, map, and geographical information program that allows users to explore the Earth's surface and view satellite imagery, maps, terrain, and 3D buildings. It enables users to navigate to different locations, view geographical features, landmarks, and even explore outer space. Google Earth is available as a web-based application, desktop software, and mobile app, providing an immersive and interactive way to discover and learn about our planet.

An important point to be noted is that all the above softwares used are open source and free of cost which means anyone can install it on their systems and work on it to develop applications free of cost.

B. Hardware Used

1) Quectel M66 GSM module: The M66 GSM module is a compact and versatile cellular communication module. It provides GSM/GPRS connectivity, allowing devices to communicate over cellular networks. The module features support for voice, SMS, data transmission, and internet connectivity, making it suitable for applications such as remote monitoring, telemetry, tracking, and control systems. With its small form factor and low power consumption, the M66 module is widely used in embedded systems where reliable and efficient cellular communication is required.

2) NEO 6M GPS module : The NEO-6M GPS module is a compact and cost-effective global positioning system (GPS) module commonly used in navigation and tracking applications. It utilizes the NEO-6M GPS chipset, which provides accurate positioning information with support for multiple satellite navigation systems, including GPS, GLONASS, and Galileo. The module communicates with external devices such as microcontrollers or computers through a serial interface, typically UART (Universal Asynchronous Receiver-Transmitter), and provides real-time latitude, longitude, altitude, time, and satellite data.

3) STM32F302R8 micrcontroller : The STM32F302R8 microcontroller is a member of the STM32F3 series of 32-bit ARM Cortex-M4 microcontrollers produced by STMicroelectronics. It features a high-performance core running at up to 72 MHz, with an extensive set of peripherals and interfaces, making it suitable for a wide range of embedded applications.

III. Implementation and Troubleshooting

To begin implementation, we initially tested the Quectel M66 GSM module, by linking its TX, RX, VCC i.e anywhere from 3.7 - 4.5V, and GND pins to a USB to TTL converter and then to the docklight. By adjusting the baud rate at 115200, selecting the suitable COM port and using AT commands, the GSM functionality was verified by acquiring the âOKâ response in return and also its operational integrity. Figure 4.1: AT commands response on Docklight Further, the GPS

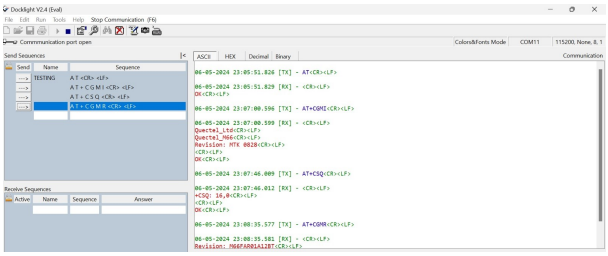


Fig. 2. AT commands response on Docklight

module was tested by linking its TX, RX, VCC i.e 3.3V, and GND pins to a USB to TTL converter, then to the docklight. By adjusting the baud rate at 9600 and selecting the suitable COM port, we observed NMEA sentences displayed on the docklight as illustrated below.

```
$GPGGA,065729.00,1900.93039,N,07305.79090,E,1,04,3.84,19.4,M,-66.1,M,,*46<CR><LF>
$GPGSA,A,3,22,05,20,24,,,,,,,,,4.99,3.84,3.19*03<CR><LF>
$GPGSV,3,1,09,05,38,176,19,11,61,002,08,12,50,332,06,13,02,172,*7F<CR><LF>
$GPGSV,3,2,09,19,19,065,08,20,64,136,29,22,21,132,23,24,31,232,32*71<CR><LF>
$GPGSV,3,3,09,25,21,322,*47<CR><LF>
$GPGLL,1900.93039,N,07305.79090,E,065729.00,A,A*68<CR><LF>
$GPRMC,065730.00,A,1900.93227,N,07305.79083,E,3.175,24.70,040524,,,A*5E<CR><LF>
$GPVTG,24.70,T,,M,3.175,N,5.880,K,A*09<CR><LF>
$GPGGA,065730.00,1900.93227,N,07305.79083,E,1,04,3.84,18.8,M,-66.1,M,,*4C<CR><LF>
$GPGSA,A,3,22,05,20,24,,,,,,,,,4.99,3.84,3.19*03<CR><LF>
$GPGSV,3,1,09,05,38,176,16,11,61,002,08,12,50,332,06,13,02,172,*70<CR><LF>
$GPGSV,3,2,09,19,19,065,08,20,64,136,29,22,21,132,24,24,31,232,33*77<CR><LF>
$GPGSV,3,3,09,25,21,322,*47<CR><LF>
$GPGLL,1900.93227,N,07305.79083,E,065730.00,A,A*6F<CR><LF>
$GPRMC,065731.00,A,1900.93327,N,07305.79080,E,3.441,7.73,040524,,,A*6D<CR><LF>
```

Fig. 3. NMEA sentences recorded on Docklight

Example of GPGGA GPS sentence:-
$GPGGA, 161229.487, 3723.2475, N, 12158.3416, W, 1, 07, 1.0, 9.0, M, , , , 0000*18

161229.487: Time of the fix in UTC.
3723.2475, N: Latitude of the fix (in degrees and minutes, with N indicating North).
12158.3416, W: Longitude of the fix (in degrees and minutes, with W indicating West).
1: Quality of the fix (1 = GPS fix).
07: Number of satellites being tracked.
1.0: Horizontal Dilution of Precision (HDOP).
9.0: Altitude of the fix in meters.
M: Units of altitude (meters).
(Empty fields): Additional information (may be empty).
0000: Differential GPS data age.
*18: Checksum for data integrity.

Example of GPRMC GPS sentence:-
$GPRMC, 161229.487, A, 3723.2475, N, 12158.3416, W, 0.13, 309.62, 120598, , *10

161229.487: Time of fix in UTC hours, minutes, and seconds.
A: Status A = active or V = void. This tells if the GPS has a valid fix at the moment.
3723.2475, N: Latitude 37 degrees 23.2475 minutes North.
12158.3416, W: Longitude 121 degrees 58.3416 minutes West.
0.13: Speed over the ground in knots.
309.62: Course over ground in degrees true.
120598: Date - 12th May 1998.
,: Magnetic variation direction (not provided in this sentence).
10: Checksum, used for error checking the data.

A ring buffer maintains continuous data flow by storing elements in a fixed-size buffer and overwriting the oldest ones when the buffer is full. Thus, the ring buffer was developed to verify UART communication, guaranteeing alignment between transmitted and received data. This establishes a groundwork for incorporating GPS functionality using this dependable communication method.

Sensing System : The STM32 board was utilized to generate an alert that displayed a message in response to a voltage drop at the RX pin. To demonstrate a prototype in which if no value is present at a pin, an alert message should be presented on the console at that time. The two pins were connected using jumper wires wherein one pin was providing the power supply to the next pin. As in when the connection of jumper wires was removed the output was displayed on the console. To use this sensing system prototype, the merging with the GSM module was done so that when the closed loop circuit used for sensing breaks the alert message will be received on the specified mobile phone whose number will be put in the program.

GSM+STM32 : Initially, the STM32F302R8 board was

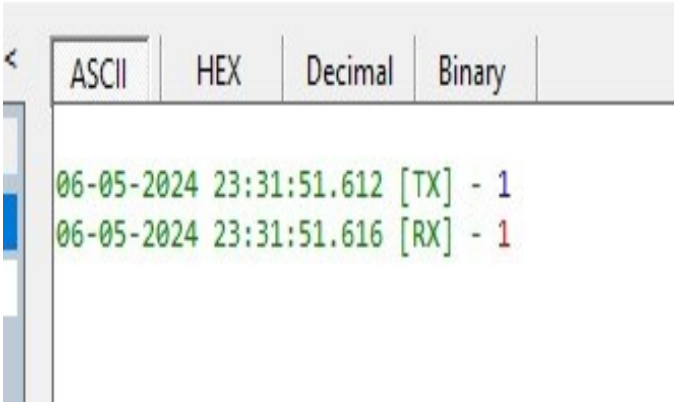


Fig. 4. Verifying UART establishment on Docklight

selected using STM32CubeIDE.
Following the micrcontroller parameters were configured and it starts with establishing clock settings and GPIO pins, which sets up the hardware environment.The baud rate for GSM is 115200. The USART3 peripheral is initialized to allow UART connectivity, which is required for dealing with external modules such as GSM devices. Before entering the main loop, the system sends a sequence of AT instructions over UART to set up the GSM module for SMS transmission. These instructions contain fundamental AT commands for setup and configuration, like "AT" for checking if the GSM module responds, ``AT+CREG?''- provides
information about the registration status and access technology of the serving cell, and
``AT+CMGF=1''- this command sets the GSM modem in SMS Text Mode.

After startup, the system constantly checks the status of a jumper pin attached to a GPIO pin (PA1). If the jumper pin is identified in a low condition (indicating a door breach), the system generates an SMS message notifying a breach attempt. The `alertMsg[]` array stores the message "Alert: Door breach detected". To send the SMS message, the system first creates the ``AT+CMGS'' (the command sends an SMS message to a GSM phone) command and specifies the recipient's phone number. This command is formatted as a string and sent to the GSM module over UART. The system then waits for the ``>'' prompt, which indicates that the GSM module is prepared to accept the SMS message payload. Once the ``>'' prompt is
received, the system sends the message content contained in the `alertMsg[]` array. Finally, the system transmits the CTRL-Z character (ASCII code 0x1A) to mark the conclusion of the message. Delays are introduced throughout the process to guarantee correct timing for command execution and message transmission.

GPS+STM32: For this process also the initialization was done for a system based on a microcontroller, most likely an STM32F3xx series device by setting up the required configurations in the STM32Cube IDE. The baud rate for GPS is 9600. Specifically, it sets up the USART1 peripheral for UART connection with the GPS module. The system then enters an indefinite loop, always waiting for and processing GPS data.

Within the loop, the system uses custom methods to handle GPS data receiving and decoding. It uses the `Wait_for` function to wait for certain GPS data phrases, such as ``GGA'' and ``RMC''. When the system detects these phrases, it replicates the incoming data into the ``GGA'' and ``RMC'' character arrays. These words usually include important GPS information like position, time, and velocity. The line `Copy_upto("*", RMC/GGA);` likely invokes a custom function called `Copy_upto` with two arguments: a character pointer "" and a destination character array. The purpose of this function call appears to be to copy characters from a source buffer up to a specified delimiter (in this case, the asterisk character) into the destination array.

Once the data has been received and copied, the system will decode it using specialized
decoding routines such as `decodeGGA` and `decodeRMC`. These routines parse GPS data from
character arrays and extract important information into a structured manner that is saved in the `gpsData` structure. The `decodeGGA` function retrieves GPS fix information from a `GGA` phrase, such as latitude, longitude, altitude, fix quality, time, and number of satellites. Similarly, the `decodeRMC` function pulls date, speed, course data, and RMC data validity from the `RMC`
statement.

After getting the coordinates from the GPS module the parsing was done and extraction of only certain sections of the NMEA format was carried out .The retrieved data must then be transferred to the GSM module for transmission.This ring buffer was created using a UART1 connection within the STM32Cube IDE environment. The ring buffer stores the coordinates received from the GPS module via Docklight-Testing, analysis and simulation tool for serial communication protocols.The algorithm for reading GPS data and writing it to the buffer was included into the loop structure, guaranteeing that it runs continuously as long as fresh data is recognized.As data comes, it is stored in the buffer before being passed to the next level of processing.

IV. Troubleshooting

The project encountered its first obstacle when the UART Tx and Rx pins of the STM32 controller malfunctioned, necessitating a switch to a different UART port due to the multiple UARTs available on the controller. Moreover, upon each restart, the GSM module defaulted back to its default baud rate of 9600, despite being previously configured to a different rate. Indoors, the GPS module struggled to obtain a fix on the antenna, requiring placement in an open area. Additionally, there was a challenge in converting the latitude and longitude
coordinates obtained from the GPS module. Compatibility issues arose between the GSM module and the high-frequency

clock of the STM32 microcontroller. Despite the GPS module's slightly inaccurate location data, which deviated slightly from the actual location but still met project requirements, a USB to TTL converter was employed to troubleshoot communication errors, with analysis performed using Docklight software.

V. Results

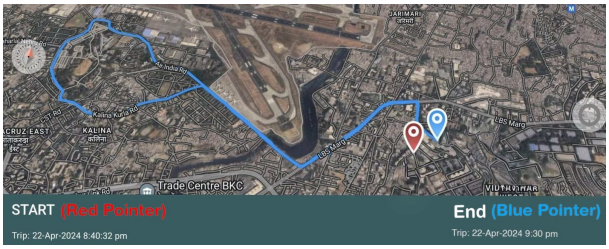


Fig. 5. Route

In Figure 5, Google Earth was used to map out the entire route, allowing for subsequent verification of the GPS coordinates' accuracy. The testing began at Holy Cross Church, highlighted in red, and concluded at the same endpoint, now marked in blue. The route included passing through the LBS area which is a high traffic zone, crossing the Mithi River to assess GPS reliability, and traveling alongside restricted zones such as Mumbai International Airport and Kalina Military Camp. Upon returning, the journey also takes place through Kalina's urban and residential areas, following the same route, crossing the Mithi River again, and navigating the congested LBS area.

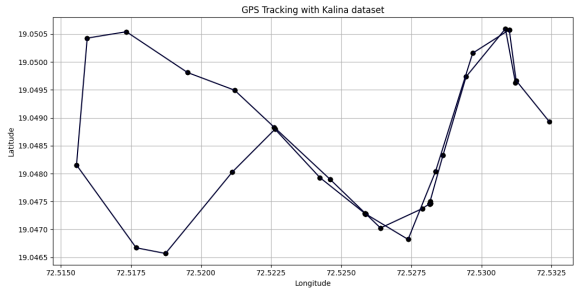


Fig. 6. Graph

Figure 6 Plotting those coordinates in Google Colab using Python and the Matplotlib module, a graph was obtained, mirroring their route, confirming GPS accuracy. Comparing their tracked path to Google Maps, a high level of consistency was found, validating the system's accuracy in tracing their journey from point A to point B.

Figure 7 shows the accuracy of the GPS module.

In the precision test of the GPS module at Don Bosco College Playground, a 5-meter path was chosen for measurement using Google Earth. Walking this path with the GPS



Fig. 7. Measurement of path

module produced latitude-longitude coordinates, which when analyzed on Google Earth, showed a traveled distance of roughly 18 meters, significantly more than the expected 5 meters. Despite this divergence, the GPS module consistently generated distinct coordinates for each point along the path.

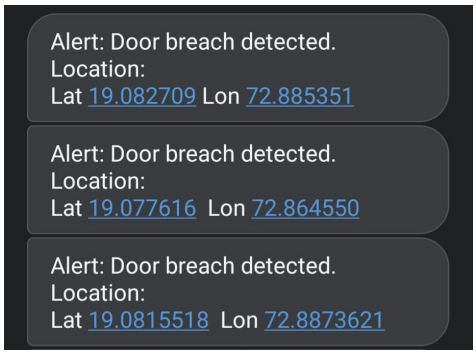


Fig. 8. Alert SMS

Further, our tracking system is incorporated with an alert sensing mechanism to promptly alert us of any intrusion during container tracking. Upon detection, the system sends real-time alert messages containing latitude and longitude coordinates to the vehicle's driver for immediate response, while simultaneously logging this information in the database so that the company which owns the cargo can conduct further inspection and take necessary actions. The above Figure 8 represents the alert SMS.

REFERENCES

[1] Abdullahi Abdirahman, Abdirahman Hashi, Ubaid Dahir, Mohamed Elmi, and Octavio Rodriguez. Enhancing vehicle tracking through sms: A cost-effective approach integrating gps and gsm. *SSRG International Journal of Electronics and Communication Engineering*, 10(9), 2023.

[2] Andrea Miller. Cargo theft spiked over 57% in 2023 vs. 2022, new data shows, 2024. [Accessed: (April 29, 2024)].

[3] Rahul Khanna. Cargo theft: An increasing concern, 2023. [Accessed: (April 29, 2024)].

[4] Thin Thin Htwe and Kyaw Kyaw Hlaing. Arduino based tracking system using gps and gsm. *International Journal for Advance Research and Development*, 4(8):11–15, 2019.

[5] Mr Saif Iqlas, Mr Owais Ahmed, Mr Mohammed Ahmed Khan, and Shilpa Mangshetty. Vehicle tracking system and theft detection.

[6] Bilkisu Jimada-Ojuolape, Oluwafunto Spencer, and Monsurat Omolara Balogun. Development of a gsm based vehicle demobilizer and tracking system. *ABUAD Journal of Engineering Research and Development*, 6(2):167–175, 2023.

[7] Kamran Khan and Shuang Wang. Vehicle security system based on stm 32 micro-controller using gsm and gps module. *International Core Journal of Engineering*, 7(4):135–140, 2021.

Design of a LiDAR System using Optisim Scans

Kanishka Aware[1], Jaipreet Singh[2], Simran Kot[3], Satyam Shukla[4], Poonam Chakraborty[5]
[1]Department of Electronics and Telecommunication Engineering,
[1]The Bombay Salesian Society's, Don Bosco Institute of Technology, University of Mumbai, Mumbai, India.
[1]kanishkaaware02@gmail.com, [2]jaipreet.saini12@gmail.com, [3]simranak164@gmail.com,
[4]satyamshukla3074@gmail.com, [5]poonam@dbit.in

Abstract - ***LiDAR (Light Detection and Ranging) systems are instrumental in distance measurement, widely employed across industries. The LiDAR system aims to deliver heightened accuracy and reliability in distance maeasurement and object detection tasks across varied environments. In this project the parameters Range, Time of Flight and FMCW are integrated. Optisim scans is an innovative optical communication system simulation package that designs, tests, and optimizes virtually any type of optical link in the physical layer of a broad spectrum of optical networks, from analog video broadcasting systems to intercontinental backbones. In this project the design centers on key parameters: Range (Phase Shift), Time of Flight (ToF), and Frequency Modulated Continuous Wave (FMCW). Range (Phase Shift) delineates the LiDAR's effective measurement distance, critical for terrain mapping and object detection. Time of Flight assesses light travel time for swift data acquisition and processing, while FMCW modulation enhances precision by emitting continuous waves with varying frequencies. This research advances LiDAR technology, promising enhanced efficiency and effectiveness in real-world applications. This report explores the crucial LiDAR parameters of range, time of flight, and FMCW technology. It covers the principles and applications of time-of-flight LiDAR, highlighting its uses in various industries. Additionally, it discusses the advantages of FMCW LiDAR and its potential in enhancing range resolution and velocity information. This report provides a concise overview of how these parameters are integral to LiDAR technology***

Keywords - Corporate Keylogger Software, Productivity assessment, Keystroke logging, Ethical and legal compliance, Data breach scenarios, Anomaly detection, Cyber threats

I. Introduction

LiDAR (Light Detection and Ranging) is a technology that uses laser pulses to measure distances with high accuracy by timing how long they take to bounce back from objects. This precision makes LiDAR crucial in fields like autonomous vehicles, urban planning, and environmental monitoring. LiDAR comes in various types: Aerial LiDAR, mounted on aircraft, is used for large-scale mapping and surveys; Terrestrial LiDAR, a ground-based system, is ideal for detailed mapping of smaller areas like archaeological sites; Mobile LiDAR, installed on moving vehicles, is used for road surveys and infrastructure inspection; and Spaceborne LiDAR, operating from satellites, is utilized for atmospheric research and global earth observation[3][14].

The key components of LiDAR systems include the laser emitter, which generates the laser pulses; the photodetector, which captures the reflected pulses and converts them into electrical signals; the scanning mechanism, which directs the laser across the target area to collect data; and the signal processing unit, which analyzes the signals to extract distance information and create 3D maps. These components work in harmony to deliver accurate, detailed mapping, offering insights into a wide range of applications. The versatility and precision of LiDAR continue to drive its adoption across industries, with ongoing advancements expanding its reach and capabilities[1][12].

II. Objective of study

The project's goal is to use cutting-edge simulation tools to build a highly precise and effective LiDAR system, with an emphasis on optimizing critical parameters for optimal performance in 3D environmental mapping, object detection, and distance measuring. The project aims to design a flexible LiDAR system that can operate reliably across a wide range of remote sensing applications, such as autonomous navigation, environmental monitoring, and industrial automation. This will be achieved by combining Time-of-Flight (ToF), Frequency Modulated Continuous Wave (FMCW), and Phase Shift techniques.

Through careful consideration of lighting and climatic conditions, the research aims to determine the best possible arrangement of system components to maximize accuracy, range, and resolution. The project endeavors to verify the operational efficacy of the planned LiDAR system through meticulous simulation and testing, hence recording the design procedure and outcomes to facilitate future advancement and implementation in practical uses. The ultimate goal is to create a solid LiDAR system that can satisfy the requirements of various industries, providing consistent performance and trustworthy data for in-the-moment analysis and decision-making.

II. Literature survey

1. Future Directions in Fiber Optics Communication

Fiber optics communication is advancing with multi-core and multi-mode optical fibers, offering enhanced data throughput for 5G and beyond[3]. Artificial intelligence (AI) and machine learning are key to network optimization, reducing latency and improving efficiency[4][5]. Quantum communications, especially Quantum Key Distribution (QKD), are gaining attention for secure data transmission. Space-based optical communication via satellites is expanding global connectivity, particularly in remote areas. Sustainability is a growing focus, with new materials aimed at reducing energy use and signal loss[2][6][13].

2. Innovations in Wavelength Division Multiplexing (WDM)

Wavelength Division Multiplexing (WDM) allows multiple data streams to travel through a single fiber, dramatically increasing bandwidth. Dense Wavelength Division Multiplexing (DWDM) has transformed high-speed internet and video streaming. Flexible grid WDM and superchannels offer dynamic resource allocation. Coherent optical transmission has extended the range and data rates of optical communication[1]. WDM-Passive Optical Network (WDM-PON) redefines last-mile connectivity with high-speed broadband.

3. Advantages of LiDAR Technology

LiDAR provides high precision with sub-centimeter accuracy, ideal for 3D mapping and infrastructure development[8]. It supports long-range detection and fast data capture, crucial for real-time applications like autonomous navigation. LiDAR's high spatial resolution allows detailed object identification. Its non-contact operation reduces risks, and it performs reliably in adverse weather. LiDAR can be customized for specific needs, with terrestrial, airborne, and spaceborne deployments.

4. Drawbacks of LiDAR Technology

LiDAR can be costly, with high power consumption, particularly for mobile systems like drones. Environmental factors like rain and fog can affect its performance, reducing accuracy and range. Limited penetration through dense vegetation and the line-of-sight requirement may result in incomplete data. LiDAR data processing is complex and resource-intensive. Safety concerns arise with high-power LiDAR systems, and regulatory constraints can complicate adoption in sensitive areas like defense and aviation[3].

III. Parameters

The parameters discussed in this section are critical for optimizing the performance and reliability of LiDAR systems. These parameters encompass various aspects of LiDAR technology, including Time-of-Flight (TOF), Frequency Modulated Continuous Wave (FMCW), and Phase Shift LiDAR, as well as ITU standards that guide the design and implementation of these systems. Each parameter plays a vital role in determining the range, accuracy, resolution, and other key characteristics of LiDAR systems[5][7].

1) Time-of-Flight (TOF) Parameters

TOF LiDAR measures the round-trip time for a laser pulse to travel from the emitter to the target and back. Essential parameters for TOF LiDAR include:

Pulse Duration: Shorter pulse durations provide higher temporal resolution but require more energy. This is crucial for accurately measuring fast-moving objects.

Pulse Repetition Rate: Higher rates support faster data acquisition and greater spatial resolution, key for detailed mapping.

Receiver Sensitivity: Higher sensitivity allows the system to detect weak signals, improving performance in low-reflectivity or long-range conditions.

Temporal Resolution: A higher temporal resolution provides finer distance measurements and better differentiation between closely spaced objects[1][[9].

2) Frequency Modulated Continuous Wave (FMCW) Parameters

FMCW LiDAR continuously modulates the frequency of the emitted laser signal. Important parameters for FMCW LiDAR are:

Frequency Modulation Range: A wider range enhances range resolution, enabling the detection of targets at varying distances.

Sweep Rate: Faster sweep rates lead to quicker data acquisition and real-time mapping.

Chirp Duration: Shorter chirp durations result in higher spatial resolution but may require more complex signal processing.

Frequency Modulation Profile: The modulation profile affects the signal-to-noise ratio (SNR) and range accuracy. Optimizing it improves performance in challenging environments[3][8].

3) Phase Shift LiDAR Parameters

Phase Shift LiDAR uses the phase difference between emitted and reflected laser signals to measure distance. Key parameters for Phase Shift LiDAR include:

Phase Resolution: Higher phase resolution allows for finer distance measurements, critical for high-precision applications.

Sampling Rate: Higher rates support more precise measurements, especially for fast-moving objects.

Signal Processing Techniques: Advanced algorithms like Fourier transforms and phase unwrapping are essential for accurate phase shift measurement[4][15].

4) ITU Standard Parameters

ITU standards guide the design and implementation of LiDAR systems to ensure interoperability and reliability. Important ITU standard parameters are:

Distance: Defines the maximum range for accurate measurement, with a standard of 45 km for long-range capability.

Signal-to-Noise Ratio (SNR): A measure of signal power compared to noise. Low SNR requires robust signal processing.

Laser Repetition Rate: Higher repetition rates support faster data acquisition. A common standard is 100 kHz.

Laser Pulse Width: Shorter pulse widths offer higher temporal resolution, typically around 0.5 ns.

Average Output Power: Indicates total energy imparted during exposure. Higher power improves range but may increase power consumption.

Angular Resolution: The smallest angle between two distinct points. Lower values indicate higher precision.

Objective Lens: Defines the focal length and diameter of the primary lens. Larger lenses can improve light collection[12][11][16].

IV. Implementation

To implement a LiDAR (Light Detection and Ranging) system using OptiSystem, a comprehensive set of steps is required to ensure the system is designed, modeled, and optimized effectively. This detailed explanation covers each step involved in the implementation process, from conceptualization to analysis and optimization.

1) Define the System Requirements

Define the context for your LiDAR system—whether it's for autonomous vehicles, industrial automation, or remote sensing. Determine key operational parameters: range, accuracy, resolution, and field of view. Factor in environmental conditions like weather, temperature, and light interference to ensure robustness.

2) Design the System Architecture

Choose the type of LiDAR system based on your requirements:

Time of Flight (ToF): Measures time taken for a laser pulse to travel to a target and return.
Frequency Modulated Continuous Wave (FMCW): Measures distance through frequency shifts.
Phase Shift: Uses phase differences between transmitted and received signals for precise measurements.
Identify core components: lasers, modulators, optical fibers, photodetectors, and signal processing elements. Design the system architecture around the chosen LiDAR type.

3) Create a Simulation Model in OptiSystem

Set up a new OptiSystem project, specifying key parameters like signal wavelength, data rate, and simulation time. Design the optical path, including the laser source, modulators, optical fibers, and photodetectors. Add signal processing components like low-pass filters, amplifiers, and phase shifters. Use measurement tools such as oscilloscopes and RF spectrum analyzers to evaluate system performance.

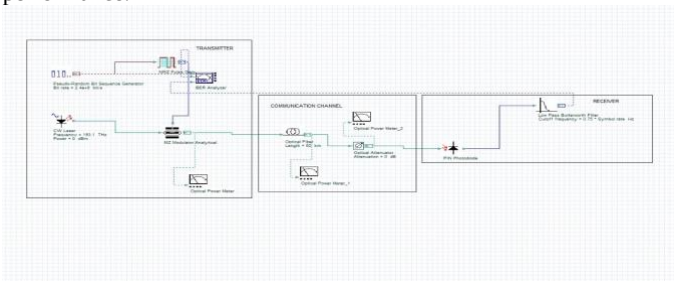


Figure 1: Implementation (Optical fibre)

Integrate optical fibers, accounting for their length, dispersion, and attenuation characteristics. For signal detection, add photodetectors to capture reflected light. To process and measure signals, include components like low pass filters, amplifiers, and phase shifters.

4) Simulate Time of Flight (ToF)

Generate laser pulses and simulate their reflection from a target. Introduce a time delay to represent the distance between the system and the target. Add a photodetector to measure the time delay and calculate distance based on the speed of light. This simulation can help evaluate accuracy and optimize ToF parameters.

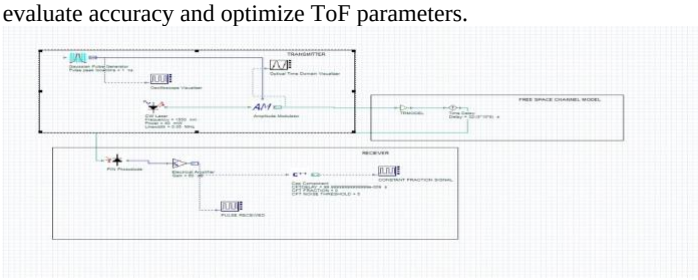


Figure 2 : Implementation (TOF)

5) Simulate Frequency Modulated Continuous Wave (FMCW)

Use a frequency modulator to create a frequency sweep with a continuous laser beam. Simulate the reflection from a target, introducing a time delay. Analyze the frequency shift using RF spectrum analyzers to calculate the range. This simulation provides a foundation for understanding FMCW LiDAR performance.

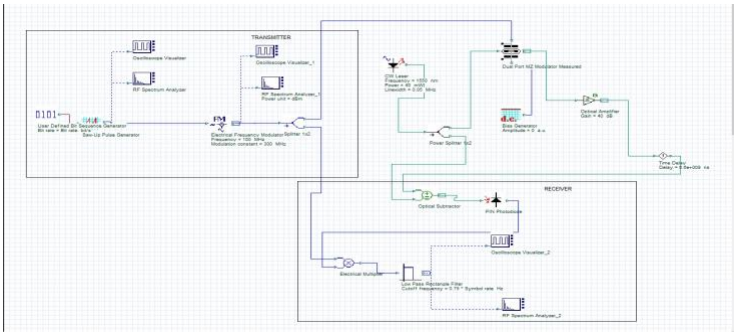


Figure 3 : Implementation(FMCW)

6) Simulate Phase Shift

Introduce phase modulation to a continuous wave signal. Simulate its reflection from a target, creating a phase difference between transmitted and received signals. Measure this phase difference to determine the time delay and calculate the range. This approach complements frequency shift analysis for high-precision measurements.

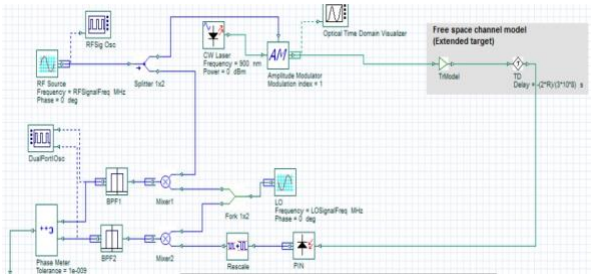


Figure 4: Implementation (Phase Shift)

7) Test and Optimize the System

After simulation, test and optimize your LiDAR system. Experiment with different configurations to improve accuracy, resolution, and range. Adjust parameters like laser power, modulation, and optical fiber length. Use Bit Error Rate (BER) analyzers, oscilloscopes, and RF spectrum analyzers to evaluate system metrics like signal quality and error rates. This iterative process helps you fine-tune the system for optimal performance before real-world deployment.

V. RESULTS

This section discusses the results obtained from the simulations and experiments conducted to evaluate the performance and effectiveness of the LiDAR system across various scenarios and applications.

1) Optical Fiber

The study on optical fiber components focused on enhancing dispersion characteristics, signal fidelity, and transmission efficiency. The data showed that specific adjustments to calibration parameters improved performance. This is evident from the bit error rate (BER)

analysis and the statistics on gain, noise figure, quality factor, and BER, which demonstrated significant gains after optimization. The complex interactions between various variables in fiber-optic communication systems were explored, highlighting the potential for a more robust and efficient communication infrastructure. The implementation of a Optical communication system is done with specifying values in Table 1 and it's resultant output is given in Table 2. With BER and EYE diagrams giving the idea about how the specified values are used to make the graphs given in the Figures 5,6 and 7.

Table 1: Parameter Table

Parameters	Value
CW Laser Power	10mW to 5W
Center Wavelength	1550nm
Center Frequency	193.414Thz
Extinction ratio of Mach-Zehender modulator	30dB

Table 2: Gain, Noise figure, Quality Factor, and BER

Length (m)	Gain (dB)	Noise figure (dB)	Quality factor	BER
10	-1.978	1.978	15.21	13.8E-54
20	-3.971	3.971	14.24	5.91E-47
30	-6.011	6.011	13.018	1.17E-40
40	-6.581	6.581	13.018	1.17E-39
50	-7.121	7.121	12.956	1.45E-38

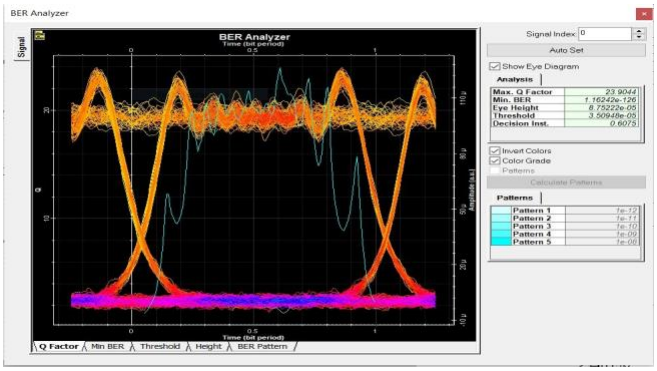


Figure 5: BER analyzer of Optical Fibre

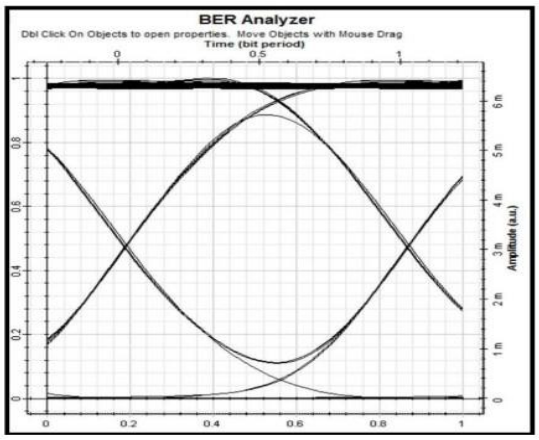


Figure 6: Eye diagram of Optical Fibre

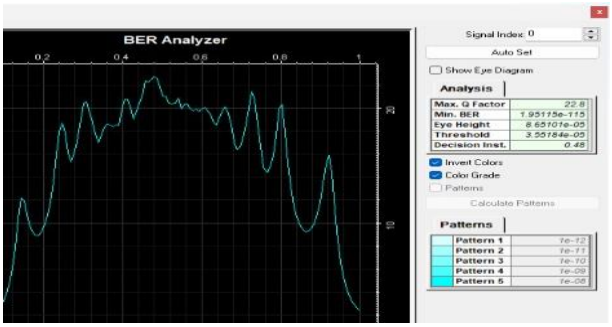


Figure 7: BER pattern of Optical Fibre

2) Time of Flight

The zero-crossing point (from negative to positive) is then found and acts as the time trigger to determine the received pulse time as shown in Figure 8 it discusses the graph obtained as successful simulation of the ToF parameter. The parameters set are of mostly of CFT Delay, Fraction and Noise Threshold with their values being fixed Table 3. Furthermore, the outputs are obtained in the form of Range, Signal index and Time in the Table 4.

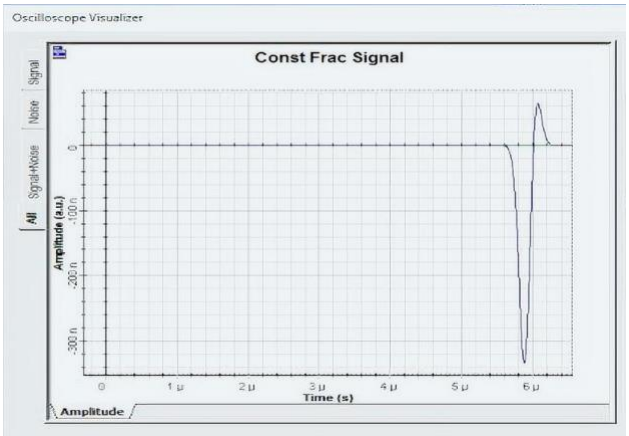


Figure 8: Oscilloscope Visualizer(Amplitude(a.u) vs Time(s))

Table 3: ToF Parameters

Parameters	Value
CFT DELAY	99.9999999E-009s
CFTNoiseThreshold	5E-009 MHZ
PulseTimeStart	1E-008s

Table 4: output

Parameters	Value
Signal Index	1970
Range (m)	751.274
Time s	6.0119E-008

3) Frequency Modulated Continuous Wave (FMCW)

The application of FMCW (frequency modulated continuous wave) radar technology in LiDAR systems resulted in significant improvements in distance measurement and information processing. The intermediate frequency signal created by combining the received and reference FM waveforms describes the implementation procedure. The computed numbers, displayed in a corresponding table, shed light on how beat frequency, time, and range are related to one another. Spectrum analyses were conducted to validate these calculations. According to the findings, FMCW provides a dependable technique for attaining precise distance measurement in LiDAR systems. As shown in the Table 5 the values are calculated for fidning the beat frequency which is then clearly explained in the Figures 10,11 and 12

Table 5 : Result Table

R/m	t/s	fb/Hz
30	$0.2*10^{-}6$	$6*10^{6}$
60	$0.4*10^{-}6$	$12*10^{6}$
90	$0.6*10^{-}6$	$18*10^{6}$

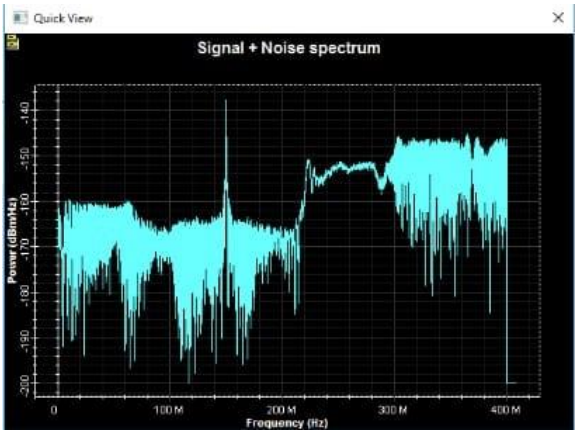


Figure 9: Signal+Noise spectrum (Power(dBmHz) vs Frequency(Hz))

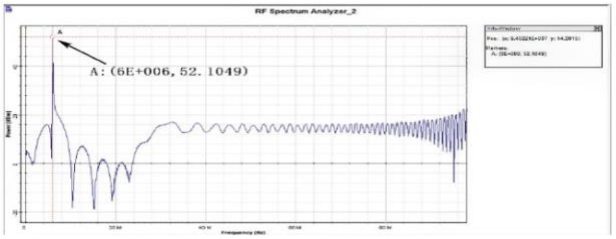


Figure 10: The beat frequency spectrum at a distance of 30 meters

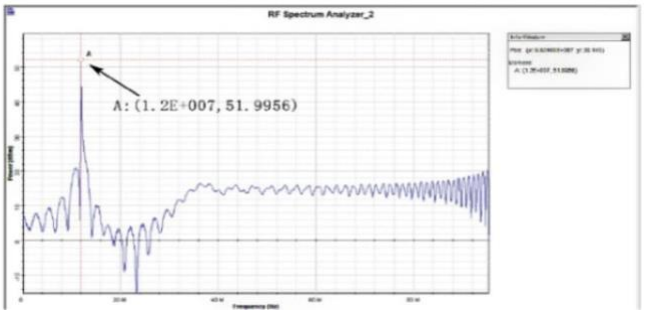


Figure 11: The beat frequency spectrum at a distance of 60 meters

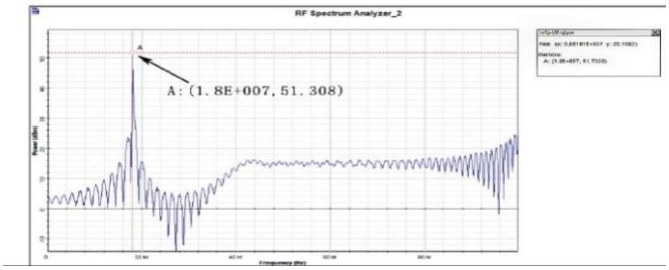


Figure 12: The beat frequency spectrum at a distance of 90 meters

4) Phase Shift (Range):

The acquired results from integrating phase shift range output techniques into Light Detection and Ranging (LiDAR) systems unveil significant advancements in range precision, target localization, and environmental mapping fidelity. These findings, substantiated by meticulously tabulated data showcasing phase shift measurements across varying distances, provide comprehensive insights into LiDAR performance. The parameters were set accordingly to get the desired output as given in Table 6 and the obtained results for finding the range and other parameters in Table 7. The range has been calculated as 0.2012 m compared to the global parameter setting of 0.2 m.

Table 6: Phase Meter

Parameters	Value
Tolerance	1E-009
ModFreq	RFSignalFreq MHZ
LOFreq	LOSignalFreq MHZ

Table 7: Output

Parameters	Value
Non Ambiguity Range (m)	2.9979246
Phase Shift (rad)	0.42184472
Range (m)	0.201277
Time received s	31.78E-009
Time Ref s	25.024E-009

VI. CONCLUSION

In conclusion, the design of a LiDAR system using OptiSystem software has proven to be a comprehensive and valuable endeavor, allowing for the analysis and optimization of criti cal parameters such as optical fibre, Time of Flight, Frequency Modulated Continuous Wave (FMCW), and Phase Shift. This software has provided us with a versatile platform to simulate and fine-tune our LiDAR system, ensuring its performance and accuracy. By carefully config uring these parameters, we can optimize the system's ability to accurately measure distances, detect objects, and create detailed 3D maps of the environment.

VII. FUTURE SCOPE

Our project has significant potential for further refinement by adopting precise methodologies in two key areas:

1) Quantifying Losses in Optical Transmission Systems

To better understand optical transmission losses, consider these approaches:Modal Analysis: Characterize the modal power distribution within optical fibers using advanced computational tools like Finite-Difference Time-Domain (FDTD) simulations. This helps pinpoint loss processes such as mode coupling and bending losses.

Scattering Description: Identify and describe scattering centers within the fiber core and cladding. Techniques like Raman spectroscopy can determine material defects, while Brillouin scattering microscopy can reveal dopant profiles, providing insights into Rayleigh and Mie scattering contributions to total loss.

2) Simple Signal Processing for Resource-Limited Settings

To address signal processing in environments with limited resources, these methods are useful:

Compressed Sensing Techniques: Reconstruct signals from sparsely sampled data, reducing processing complexity while maintaining signal fidelity. This approach is especially beneficial in bandwidth-constrained scenarios.

Fixed-Point Implementation: Implement signal processing algorithms with fixed-point arithmetic to lower power consumption and device complexity, a practical solution for resource-limited settings. Considerations include managing limited dynamic range and quantization noise.

Implementing these refined methodologies allows for a deeper understanding of optical transmission system performance while optimizing signal processing in resource-limited environments. These approaches can be customized to enhance system functionality and achieve optimal results even in constrained settings.

VIII. REFRENCES

[1] Bilik, "Comparative analysis of radar and lidar technologies for automotive applications," IEEE Intelligent Transportation Systems Magazine, vol. 15, no. 1, pp. 244–269, 2022.

[2] K. Brown, "Applications of lidar in forestry management," Forestry Science Quarterly, vol. 8, no. 4, pp. 512–527, 2022.

[3] H. Chen, "Lidar-based environmental monitoring in urban areas," Urban Studies, vol. 37, no. 2, pp. 178–193, 2024.

[4] O. Corporation, "Optisystem overview," Guide to Optisystem, vol. 20, no. 2, pp. 25–29, 2017.

[5] M. Dreissig, D. Scheuble, F. Piewak, and J. Boedecker, "Survey on lidar perception in adverse weather conditions," arXiv preprint arXiv:2304.06312, 2023.

[6] L. Garcia, "Recent advances in airborne lidar technologies," IEEE Transactions on Geoscience and Remote Sensing 2024, vol. 42, no. 3, pp. 421–436, 2024.

[7] S. Genser, S. Muckenhuber, C. Gaisberger, S. Haas, and H. Timo, "Occlusion modela geometric sensor modelling approach for virtual testing of adas/ad functions," IEEE Open Journal of Intelligent Transportation Systems, 2023.

[8] L. Giuffrida, G. Masera, and M. Martina, "A survey of automotive radar and lidar signal processing and architectures," Chips, vol. 2, no. 4, pp. 243–261, 2023.

[9] T. Gomes, R. Roriz, L. Cunha, A. Ganal, N. Soares, T. Araujo, and J. Monteiro, "Evalua- ´ tion and testing system for automotive lidar sensors," Applied Sciences, vol. 12, no. 24, p. 13003, 2022.

[10] A. Johnson, "High-resolution 3d mapping using lidar," Remote Sensing, vol. 14, no. 2, pp. 256–271, 2022.

[11] S. Kim, Y. Jung, and S. Lee, "Multipoint combined processing for fmcw lidar," IEEE Sensors Journal, vol. 22, no. 9, pp. 8933–8943, 2022.

[12] C. Liu, L. Lu, Y. Guo, X. Li, J. Chen, and L. Zhou, "Hybrid integrated frequency modulated continuous-wave laser with synchronous tuning," Journal of Lightwave Technology, vol. 40, no. 16, pp. 5636–5645, 2022.

[13] T. Nguyen, "Advances in compact lidar systems for drones," Journal of Unmanned Vehicle Systems, vol. 11, no. 3, pp. 345–359, 2023.

[14] R. Patel, "Lidar data processing techniques: A review," Journal of Applied Remote Sensing, vol. 17, no. 1, pp. 120–135, 2023.

15] R. Roriz, A. Campos, S. Pinto, and T. Gomes, "Dior: A hardware-assisted weather denoising solution for lidar point clouds," IEEE Sensors Journal, vol. 22, no. 2, pp. 1621–1628, 2021.

[16] J. Smith, "Advancements in lidar technology for autonomous vehicles," Sensors, vol. 23, no. 4, pp. 789–803, 2023.

Design and Development of Duplexer for GSM Applications

Darshan Kadlag[1], Vaishnav Nadar[2], Kajal Sathe[3], Anto Ridon0[4], Freda Carvalho[5]
Department of Electronics and Telecommunication Engineering
The Bombay Salesian Society's Don Bosco Instiute of Technology, University of Mumbai, Mumbai India
[1]*darshankadlag21@gmail.com,* [2]*vais02800@gmail.com,* [3]*121kajal0006@dbit.in,*
[4]*antoridon2002@gmail.com,* [5]*freda@dbit.in*

***Abstract*—This paper shows the design and development of duplexer for GSM applications using microstrip technology.Duplexers are crucial components in wireless communication systems, allowing simultaneous transmission and reception of signals in two different frequency bands. In the context of GSM applications, duplexers play a critical role in enabling full-duplex communication, enabling both uplink(890MHz to 915MHz) and downlink(935MHz to 960MHz)transmissions to occur simultaneously. A duplexer can be designed using various techniques, including waveguide filters, microstrip technology, and cavity filters. The microstrip duplexer offers a compact and cost-effective solution for frequency band separation within mobile devices. The simulation is done using Keysight Genesys and ANSYSS HFSS software. By employing rigorous electromagnetic simulations and optimization techniques, the duplexer's design parameters are carefully fine-tuned to achieve optimal performance characteristics, including optimised insertion loss, low return loss lesser than 10 dB.**

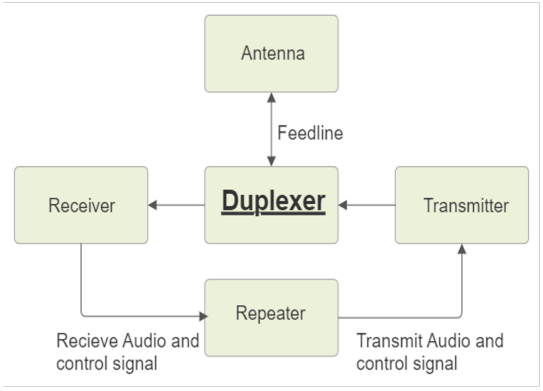


Fig. 1. Block Diagram of Repeater System

I. Introduction

A Duplexer is a 3-port device that allows the transmitter and receiver to use a single antenna, while operating at the same/similar frequencies. It is a device that allows two-way communication over a single channel by isolating the receiver from transmitter while transmitting a pulse and isolating the transmitter from receiver while receiving a pulse, allowing them to share the same antenna. A duplexer typically consists of two band pass filters connected in parallel. One filter provides a path between the transmitter and the antenna, the other provides a path between the antenna and the receiver. No direct path between the transmitter and receiver exists. It enables simultaneous duplex operation on different frequencies, thus improving the capacity and efficiency of the communication system. [1]

A. Bandpass Filter

The bandpass filter serves as a device that selectively allows a specific range of frequencies to pass through to the load while attenuating or blocking frequencies outside this range. This range is defined by two points: the lower cut-off frequency (ωc1) and the upper cut-off frequency (ωc2). Any signal falling within this frequency range, known as the passband, is transmitted efficiently to the load with minimal loss. Within the passband, there exists a central frequency denoted as ω0. This frequency is determined by calculating the geometric mean of the lower and upper cut-off frequencies. It represents the midpoint or center of the frequency range allowed by the bandpass filter.Signals outside the specified frequency range are either attenuated significantly or completely blocked. This ensures that only the desired frequencies, falling within the passband, are transmitted effectively to the load. The bandpass filter thus acts as a gatekeeper, allowing only signals within its designated bandwidth to pass through while rejecting or suppressing others.

B. Microstrip

Microstrip technology is a method of constructing electronic circuits by placing a flat conductor, typically made of metal, on top of a dielectric substrate, separated by a ground plane. The dielectric substrate is chosen based on its low-loss characteristics and may possess a relative permittivity higher than that of free space. This configuration enables guided transmission of electromagnetic signals along the strip conductor, with the ground plane serving as a return path for current. The choice of dielectric material with higher relative permittivity allows for miniaturization of the circuit, a critical aspect in modern electronics where space constraints are paramount. However,

the use of different dielectric materials above and below the strip introduces challenges in circuit analysis, particularly regarding impedance matching and signal integrity. Additionally, the presence of multiple dielectrics may lead to variations in signal propagation speed with frequency, impacting the performance of timing-sensitive applications. Despite these complexities, microstrip technology remains indispensable in achieving compact circuit designs compatible with contemporary semiconductor fabrication methods, thereby advancing high-performance electronic systems.

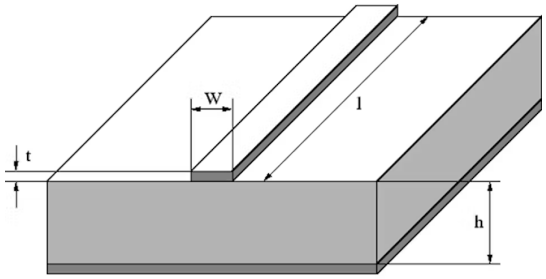


Fig. 2. Microstrip Design

Where:

- l = Length of the element.
- w =Width of the element.
- h = Height of the dielectric element.
- t = Thickness of the element.

C. Hairpin microstrip filter

A hairpin microstrip filter is a specialized microwave filter utilized in RF (radio frequency) and microwave circuits to selectively allow certain frequencies to pass through while blocking others. This is achieved through the use of hairpin-shaped resonators, which are looped structures formed from conductive material on a substrate. These resonators interact with incoming signals, permitting specific frequencies to propagate while attenuating others based on their resonant properties.The "microstrip" aspect of the hairpin microstrip filter refers to its construction using a thin strip of conductive material, typically copper, deposited on top of a dielectric substrate, with a ground plane beneath it. This design enables the filter to be compact, lightweight, and cost-effective, making it suitable for various applications in wireless communication systems, radar systems, and satellite communications.Hairpin microstrip filters play a crucial role in RF and microwave engineering, where precise signal filtering is essential. Their compact size and ease of fabrication make them the most important components in modern electronic devices, especially in scenarios where space is limited and it also ensure optimal performance and reliability.

D. Genesys

Genesys is a Electronic circuit Simulation software developed by Keysight Technologies, commonly used for RF and microwave circuit design. In duplexer design, a crucial component for sharing a single antenna between transmitter and receiver, Genesys plays a vital role. The software offers a range of tools for designing and simulating RF components like filters, amplifiers, and mixers. Its intuitive interface allows for easy circuit creation, modification, and in-depth analysis.

E. ANSYS HFSS

ANSYS HFSS (High-Frequency Structure Simulator) is a powerful electromagnetic simulation software used for the design and analysis of high-frequency electronic components and systems. ANSYS HFSS was employed for comprehensive electromagnetic simulation and analysis in the design of the duplexer circuit.

II. Design Flow

A. Design Details of order 6 filter

- Design of Uplink Frequency Bandpass Filter

1) Uplink Frequency Band: 890MHz to 915MHz
2) Lower cut-off Frequency (F_L): 890MHz
3) Upper cut-off Frequency (F_U): 915MHz
4) Centre Frequency (F_C): $(F_L + F_U)/2 = (890 + 915)/2 = 902.5$MHz
5) Percentage Frequency Band (Δ): $(F_U - F_L)/F_C \times 100 = (915 - 890)/902.5 \times 100 = 2.77\%$
6) Order of Filter (N) = 6
7) Characteristic Impedance (Z_0) = 50Ω
8) Equal ripple response = 0.1dB
9) $\Delta = 0.0277$
10) $W_0 = 2\pi f_c = 2 \times 3.14 \times (902.5 \times 10^6) = 5667700000$
11) $L_1, C_2, L_3, L_4, L_5, L_6$ are components of low pass filter.

From element value chart for equal ripple of 0.1, Value of elements of low pass filter are obtained,

$$L_1 = 1.1681$$
$$C_2 = 1.4039$$
$$L_3 = 2.0562$$
$$C_4 = 1.5170$$
$$L_5 = 1.9029$$
$$C_6 = 0.8618$$

Conversion of Low Pass Filter to Bandpass Filter:

$$L_1' = \frac{L_1 Z_0}{W_0 \Delta} = 371.8289\text{nH}, \quad C_1' = \frac{\Delta}{W_0 L_1 Z_0} = 0.083\text{pF}$$
$$L_2' = \frac{\Delta Z_0}{W_0 C_2} = 0.1739\text{nH}, \quad C_2' = \frac{C_2}{W_0 \Delta Z_0} = 178.755\text{pF}$$
$$L_3' = \frac{L_3 Z_0}{W_0 \Delta} = 654.528\text{nH}, \quad C_3' = \frac{\Delta}{W_0 L_3 Z_0} = 0.0475\text{pF}$$
$$L_4' = \frac{\Delta Z_0}{W_0 C_4} = 0.161\text{nH}, \quad C_4' = \frac{C_4}{W_0 \Delta Z_0} = 193.156\text{pF}$$
$$L_5' = \frac{L_5 Z_0}{W_0 \Delta} = 605.730\text{nH}, \quad C_5' = \frac{\Delta}{W_0 L_5 Z_0} = 0.05134\text{pF}$$
$$L_6' = \frac{\Delta Z_0}{W_0 C_6} = 0.2834\text{nH}, \quad C_6' = \frac{C_6}{W_0 \Delta Z_0} = 109.731\text{pF}$$

- Design of Downlink Frequency Bandpass Filter

1) Downlink Frequency Band (935MHz to 960MHz)
2) Lower cut-off Frequency (f_L): 935MHz
3) Upper cut-off Frequency (f_U): 960MHz
4) Centre Frequency (f_C): $(f_L+f_U)/2 = (935+960)/2 = 947.5$MHz
5) Percentage Frequency Band: $(f_U - f_L)/f_C \times 100 = (960-935)/947.5 \times 100 = 2.638\%$
6) Order of Filter (N) = 6
7) Characteristic Impedance (Z_0) = 50Ω
8) Equal ripple response = 0.1dB
9) $\Delta = 0.0263$
10) $W_0 = 2\pi f_C = 2 \times 3.14 \times (947.5 \times 10^6) = 5950300000$
11) $L_1, C_2, L_3, L_4, L_5, L_6$ are components of low pass filter.

From element value chart for equal ripple of 0.1, values for elements in low pass filter are obtained,

$$L_1 = 1.1681$$
$$C_2 = 1.4039$$
$$L_3 = 2.0562$$
$$C_4 = 1.5170$$
$$L_5 = 1.9029$$
$$C_6 = 0.8618$$

$$L_1' = \frac{L_1 Z_0}{W_0 \Delta} = 373.022\text{nH}, \quad C_1' = \frac{\Delta}{W_0 L_1 Z_0} = 0.075\text{pF}$$
$$L_2' = \frac{\Delta Z_0}{W_0 C_2} = 0.1573\text{nH}, \quad C_2' = \frac{C_2}{W_0 \Delta Z_0} = 179.329\text{pF}$$
$$L_3' = \frac{L_3 Z_0}{W_0 \Delta} = 656.629\text{nH}, \quad C_3' = \frac{\Delta}{W_0 L_3 Z_0} = 0.0429\text{pF}$$
$$L_4' = \frac{\Delta Z_0}{W_0 C_4} = 0.161\text{nH}, \quad C_4' = \frac{C_4}{W_0 \Delta Z_0} = 193.776\text{pF}$$
$$L_5' = \frac{L_5 Z_0}{W_0 \Delta} = 607.730\text{nH}, \quad C_5' = \frac{\Delta}{W_0 L_5 Z_0} = 0.0464\text{pF}$$
$$L_6' = \frac{\Delta Z_0}{W_0 C_6} = 0.256\text{nH}, \quad C_6' = \frac{C_6}{W_0 \Delta Z_0} = 110.083\text{pF}$$

After completing the design and simulation of a sixth-order filter, we discovered that its group delay was significantly higher than anticipated. Consequently, we opted to design a third-order filter for comparison purposes and to determine the most suitable option for our project.

B. Design Details of order 3 filter

- Design of Uplink Frequency Bandpass Filter

1) Uplink Frequency Band: 890MHz to 915MHz
2) Lower cut-off Frequency (F_L): 890MHz
3) Upper cut-off Frequency (F_U): 915MHz
4) Centre Frequency (F_C): $(F_L + F_U)/2 = (890 + 915)/2 = 902.5$MHz
5) Percentage Frequency Band (Δ): $(F_U - F_L)/F_C \times 100 = (915-890)/902.5 \times 100 = 2.77\%$
6) Order of Filter (N) = 3
7) Characteristic Impedance (Z_0) = 50Ω
8) Equal ripple response = 0.1dB
9) $\Delta = 0.0277$
10) $W_0 = 2\pi f_c = 2 \times 3.14 \times (902.5 \times 10^6) = 5667700000$
11) L_1, C_2, L_3 are components of low pass filter.

From element value chart for equal ripple of 0.1, Value of elements of low pass filter are obtained,

$$L_1 = 1.0316$$
$$C_2 = 1.1474$$
$$L_3 = 1.0316$$

$$L_1' = \frac{L_1 Z_0}{W_0 \Delta} = 328.54\text{nH}, \quad C_1' = \frac{\Delta}{W_0 L_1 Z_0} = 947.52\text{pF}$$
$$L_2' = \frac{\Delta Z_0}{W_0 C_2} = 212.974\text{nH}, \quad C_2' = \frac{C_2}{W_0 \Delta Z_0} = 146.16\text{pF}$$
$$L_3' = \frac{L_3 Z_0}{W_0 \Delta} = 328.54\text{nH}, \quad C_3' = \frac{\Delta}{W_0 L_3 Z_0} = 974.52\text{pF}$$

- Design of Downlink Frequency Bandpass Filter

1) Downlink Frequency Band (935MHz to 960MHz)
2) Lower cut-off Frequency (f_L): 935MHz
3) Upper cut-off Frequency (f_U): 960MHz
4) Centre Frequency (f_C): $(f_L+f_U)/2 = (935+960)/2 = 947.5$MHz
5) Percentage Frequency Band: $(f_U - f_L)/f_C \times 100 = (960-935)/947.5 \times 100 = 2.638\%$
6) Order of Filter (N) = 3
7) Characteristic Impedance (Z_0) = 50Ω
8) Equal ripple response = 0.1dB
9) $\Delta = 0.0263$
10) $W_0 = 2\pi f_C = 2 \times 3.14 \times (947.5 \times 10^6) = 5950300000$
11) L_1, C_2, L_3 are components of low pass filter.

From element value chart for equal ripple of 0.1, values for elements in low pass filter are obtained,

$$L_1 = 1.0316nH$$
$$C_2 = 1.1474pF$$
$$L_3 = 1.0316nH$$

$$L_1' = \frac{L_1 Z_0}{W_0 \Delta} = 329.6\text{nH}, \quad C_1' = \frac{\Delta}{W_0 L_1 Z_0} = 856.91\text{pF}$$
$$L_2' = \frac{\Delta Z_0}{W_0 C_2} = 192.60\text{nH}, \quad C_2' = \frac{C_2}{W_0 \Delta Z_0} = 146.63\text{pF}$$
$$L_3' = \frac{L_3 Z_0}{W_0 \Delta} = 329.6\text{nH}, \quad C_3' = \frac{\Delta}{W_0 L_3 Z_0} = 856.91\text{pF}$$

After we finished designing and simulating the third-order filter, we noticed a big improvement in the group delay compared to the sixth-order one. This made us decide to stick with the third-order filter

III. Implementation of Passive Filter in Keysight Genesys

To design a duplexer, two parallel combinations of band-pass filters are used. Both the uplink and downlink band-pass filters, each with an order of 6, are connected together. The same procedure is applied for filters with an order of 3.

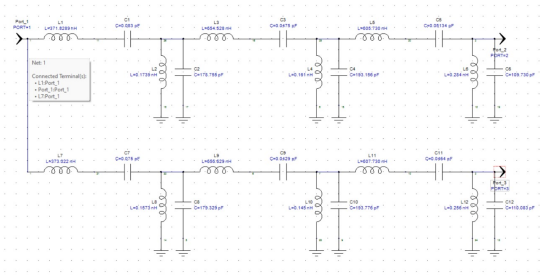


Fig. 3. Schematic of order 6 duplexer

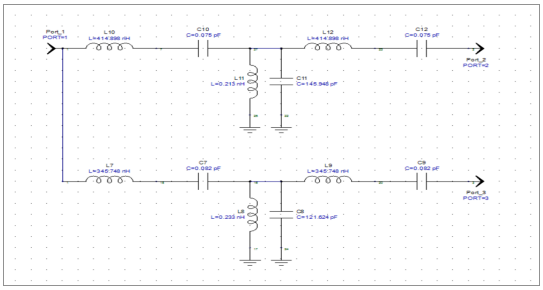


Fig. 4. Schematic of order 3 duplexer

Figures 3 and 4 show the designs of order 3 and order 6 duplexers. They're made using passive elements in Keysight Genesys. These filters are set up with different impedance levels, with 100 ohms at the input and 50 ohms at the output for each one.

Figure 5 illustrates the duplexer's performance of order 6, with the uplink filter operating within the 890-915MHz band and the downlink filter within the 935-960MHz band. Notably, it achieves significant isolation between uplink and downlink frequencies. The return loss is measured to be below -10 dB, with a ripple of less than -0.5 dB.

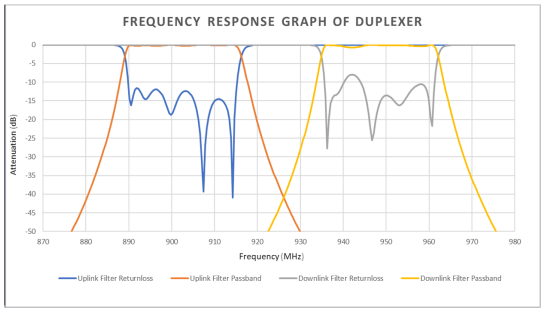


Fig. 5. Response of order 6 duplexer

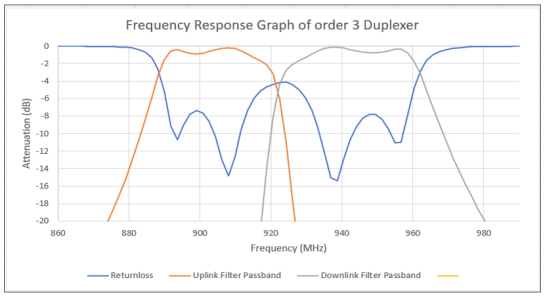


Fig. 6. Response of order 3 duplexer

Figure 6 illustrates the duplexer's performance of order 3, with the uplink filter operating within the 890-915MHz band and the downlink filter within the 935-960MHz band. Notably, it achieves significant isolation between uplink and downlink frequencies. The return loss is measured to be below -10 dB, with a ripple of less than -0.5 dB.

IV. Analysis of Graph of this Project

A. Conversion of Passive filter to Microstrip filter

After the completion of initial design of a passive bandpass filter, we attempted to convert it into a microstrip filter using Kuroda's identities. However, we encountered a challenge because Kuroda's identities only provide a method for converting low-pass filters into microstrip filters, not highpass filters.So it became difficult for us to convert the passive filter into microstrip filter.Kuroda's identities are mathematical transformations that enable the conversion of lumped-element (e.g., capacitors and inductors) low-pass filter designs into microstrip filter designs. However, these identities do not provide a direct method for converting bandpass filters.The difficulty arises because bandpass filters typically require a more complex design approach compared to low-pass filters. Converting a bandpass filter to a microstrip implementation involves additional considerations such as coupling structures, resonators, and impedance matching networks, which are not directly addressed by Kuroda's identities.

B. Implementation of Passive Filter

Due to the issues in conversion of passive filter to microstip, we tried to implement passive filter.After designing of the passive filter, implementation of the filter became difficult as the required values of inductors and capacitors were not readily available in the market. So we decided to search for standard available values of inductors and capacitors that were closest to the required values, it was challenging to find inductors and capacitors with precise values that match the design requirements. We opted to search for standard available values of inductors and capacitors that were closest to the required values. This approach involved consulting standard component value charts or databases provided by manufacturers to identify commercially available components that are the best match for the design specifications. While these standard available values may not perfectly match the required values, they are chosen based on their proximity to the desired specifications and their availability in the market. However, upon simulating the filter using the readily available inductors and capacitors on the market, we found that the response we obtained was unsatisfactory. Consequently, we opted to design an air core inductor with the specific value we needed.

UPLINK FILTER			
Capacitor (Req.)	Available	Inductor (Req.)	Available
0.075pF	1 pF	414.898nH	390 nH
145.948pF	150 pF	0.213nH	1nH
0.075pF	1pF	414.898nH	390 nH

TABLE I
CAPACITOR AND INDUCTOR VALUES FOR UPLINK FILTER

DOWNLINK FILTER			
Capacitor (Req.)	Available	Inductor (Req.)	Available
0.082pF	1pF	345.748nH	330nH
121.624pF	120pF	0.233nH	1 nH
0.082pF	1pF	345.748nH	330nH

TABLE II
CAPACITOR AND INDUCTOR VALUES FOR DOWNLINK FILTER

C. Design of Inductor

Inspite of using standard values of inductors and capacitors, we did not get our expected outcome.

Hence , we decided to design the inductors on our own.

N = Number of turns.

L = Inductor value

l = Length of the coil = 1.5 $\times 10^{-3}$

r = Radius = 0.5×10^{-2}

L = $\pi r^2 \mu_e N^2$

N = L$\times l$

$$N^2 = \frac{L^* I}{\pi r^2 \mu_0},$$
$$L = \frac{\pi r^2 \mu_0 N^2}{l},$$
$$r = 0.5'' 10^{-2}, \quad I = 1.5^* 10^{-3},$$
For $L = 0.1573$nH,
$$N^2 = \frac{0.1573 \times 10^{-9} \times 0.5 \times 10^{-2}}{\pi \times 1.5 \times 10^{-3} \times 4\pi \times 10^{-7}},$$
$$N = 0.2975,$$
For $L = 0.1739$nH,
$$N^2 = \frac{0.1739 \times 10^{-9} \times 0.5 \times 10^{-2}}{\pi \times 1.5 \times 10^{-3} \times 4\pi \times 10^{-7}},$$
$$N = 0.3128,$$
For $L = 0.145$nH,
$$N^2 = \frac{0.145 \times 10^{-9} \times 0.5 \times 10^{-2}}{\pi \times 1.5 \times 10^{-3} \times 4\pi \times 10^{-7}},$$
$$N = 0.2856,$$
For $L = 0.161$nH,
$$N^2 = \frac{0.161 \times 10^{-9} \times 0.5 \times 10^{-2}}{\pi \times 1.5 \times 10^{-3} \times 4\pi \times 10^{-7}},$$
$$N = 0.3010,$$
For $L = 0.256$nH,
$$N^2 = \frac{0.256 \times 10^{-9} \times 0.5 \times 10^{-2}}{\pi \times 1.5 \times 10^{-3} \times 4\pi \times 10^{-7}},$$
$$N = 0.3796,$$
For $L = 0.284$nH,
$$N^2 = \frac{0.284 \times 10^{-9} \times 0.5 \times 10^{-2}}{\pi \times 1.5 \times 10^{-3} \times 4\pi \times 10^{-7}},$$
$$N = 0.3997.$$

After completing the calculations for the inductor design, we found that the necessary number of turns fell within the range of zero to one, making it impractical for manufacturing. Then the study on different type of microstrip filter is made.

V. DESIGN OF HAIRPIN MICROSTRIP FILTER

We designed hairpin filters using Genesys by entering specific details like the frequency range, filter type, order, and input/output impedance. Once we have the design, we run simulations to see how it performs, especially when using the FR-4 substrate. We developed an uplink hairpin filter covering frequencies from 890 to 915 MHz and a downlink hairpin filter spanning from 935 to 960 MHz. Their simulations were conducted to assess their performance.

A. Analysis of the results of hairpin microstrip filter

Based on the simulations of both filters, we observed that the response did not meet our expectations, with higher losses than anticipated. Additionally, we determined that the

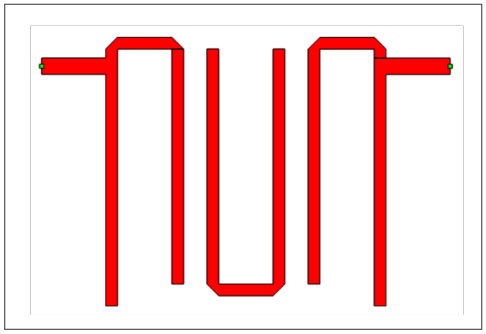


Fig. 7. Uplink hairpin microstrip filter

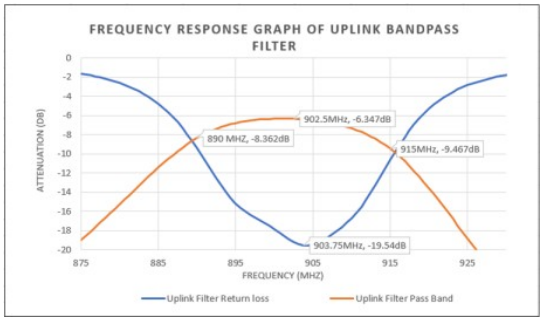


Fig. 8. Response of uplink hairpin microstrip filter

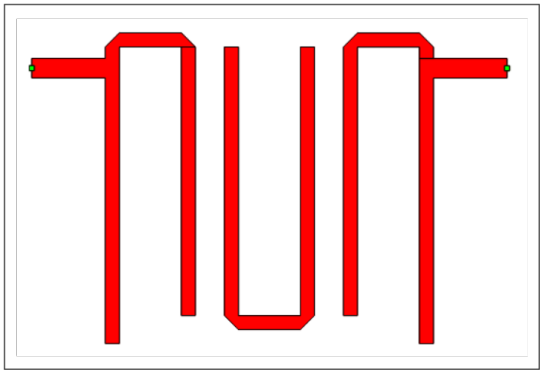


Fig. 9. Downlink hairpin microstrip filter

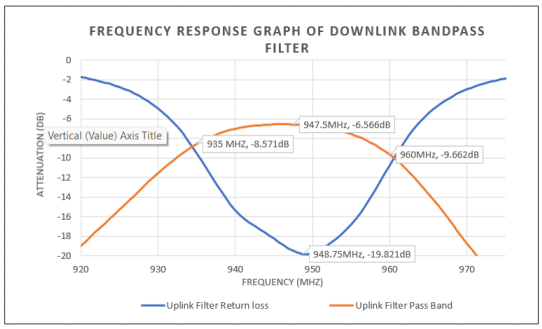


Fig. 10. Response of downlink hairpin microstrip filter

decline in response was due to the dielectric constant of the FR-4 substrate used in the simulation process. Therefore, we conducted a survey by simulating the filter with various substrates/boards and examined the response at the center frequencies of both the uplink and downlink filters, namely 902.5 MHz and 947.5 MHz.. The substrates we utilized are listed below, along with their respective dielectric constants.

1) Fr-4 Rolled Cu @1000 Mhz 1oz - 4.50.
2) Rogers R04350 1oz ED 60 mil-3.48.
3) Rogers R04003 1oz ED 60 mil- 3.38.
4) Rogers RO3203 1 oz ED 60mil- 3.02.
5) Rogers RTD5870 2oz Rolled 62 mil- 2.33.

B. Results after simulating on different types of substrate

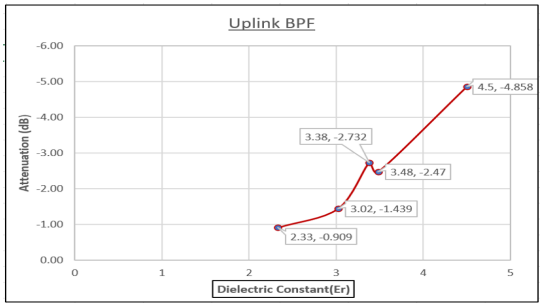


Fig. 11. For uplink filter

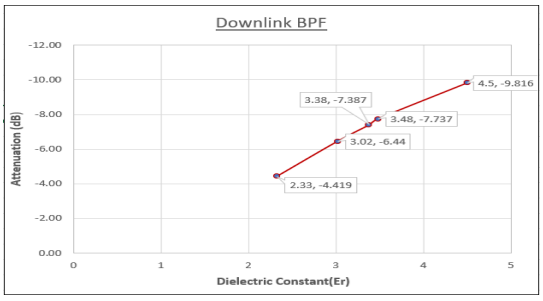


Fig. 12. For downlink filter

After looking at our results, it's clear that the Rogers RTD5870 2oz Rolled 62 mil substrate has much lower losses than the Fr-4 Rolled Cu @1000 MHz 1oz board. However, since the Rogers RTD5870 2oz Rolled 62 mil board is harder to find and more expensive, we decided to focus on optimizing our simulation using the Fr-4 Rolled Cu @1000 MHz 1oz board, which is more widely available and cost-effective.

VI. Simulation of Duplexer in HFSS

For connecting two hairpin microstrip filters, a power divider is essential in RF and microwave systems for efficient signal distribution and system integration.We chose to use a

quarter-wave power transformer power divider because it's really good at giving us the output we need within our frequency range. In our simulation, we evaluated a duplexer by linking two bandpass filters in parallel with a power divider. This arrangement enables simultaneous signal transmission and reception via a single antenna. The obtained results affirm the efficiency of our duplexer design in isolating signals and refining frequencies for both uplink and downlink transmissions.

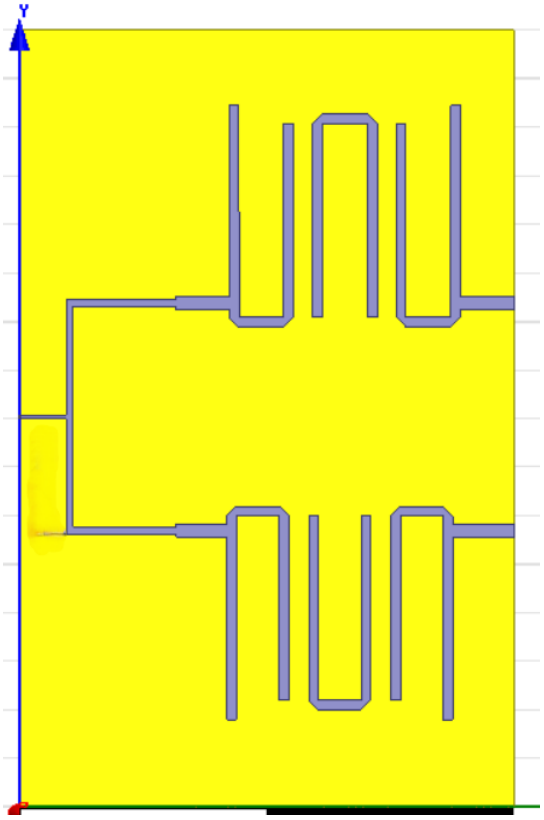


Fig. 13. Integration of Duplexer on ANSYS HFSS

In Figure 13 we've set up a system where two bandpass hairpin filters are connected in parallel, with one inverted to enhance isolation, as they're linked to a power divider. To address impedance matching, we've introduced capacitance in shunt. Due to unavailability of specific capacitor values, we've combined four capacitors in series for each connection to achieve the desired impedance characteristics. This approach ensures effective signal distribution and impedance matching within the system.

Figure 14 represents the achieved performance of the duplexer designed in HFSS. The frequency response illustrates how the duplexer behaves across different frequencies, showcasing its ability to effectively isolate and filter signals for both uplink and downlink transmissions. The response graph provides valuable insights into the duplexer's performance

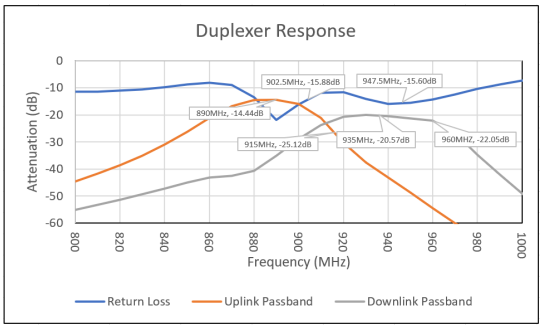


Fig. 14. Frequency response of the duplexer

characteristics, including return loss and isolation, ensuring reliable signal management in RF systems.

VII. Fabrication and Results

We have fabricated a hairpin microstrip filter designed for a frequency range of 800MHz to 1000MHz. The substrate employed in our fabrication process is FR-4, with a dielectric constant of 4.4 and a thickness of 1.6mm. The hairpin microstrip filter design offers several advantages, including compactness, ease of manufacture, and good reliability.To integrate the uplink and downlink filters, we have utilized power dividers, facilitating the connection and signal distribution between the two sections effectively. Following fabrication, we conducted measurements and observed the response using a Vector Network Analyzer (VNA). The VNA is a precision instrument used to measure the scattering parameters of electrical networks. It provides insights into the filter's performance, including characteristics such as insertion loss, return loss, and bandwidth. The fabricated hairpin filter image is shown below.

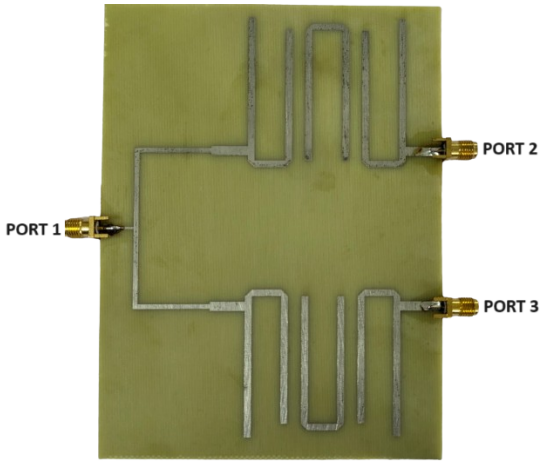


Fig. 15. Fabricated hairpin microstrip duplexer

- The responses observed in Vector Network Analyzer is shown below.

Figure 16 shows the return loss observed at the filter is a highly desirable -10dB, indicating that the filter effectively



Fig. 16. Return Loss (S11) of a Duplexer



Fig. 18. Downlink Passband (S31) of a Duplexer

reduces the amount of signal reflected back from the input port. This level of return loss is important for ensuring optimal performance and minimal signal loss within the filter circuit. The -10dB return loss demonstrates the filter's ability to efficiently transmit signals while minimizing reflections, resulting in improved overall filter performance.



Fig. 17. Uplink Passband (S21)of a Duplexer

Figure 17 shows the response observed for the uplink frequency band at port S21 is not desirable, as the response falls behind the frequency range of 890MHz to 915MHz and registers a -20dB signal level. This deviation from the desired response can negatively impact the filter's performance within the specified frequency band, leading to signal loss or distortion. In order to improve the filter's response within the uplink frequency band, adjustments may need to be made to the filter's design or components. Addressing this issue will be crucial to ensure the filter meets performance requirements and effectively filters out unwanted signals within the specified frequency range.

Figure 6.4 shows the response observed for the uplink frequency band at port S31 is not desirable, as the response differs the frequency range of 935MHz to 960MHz and registers a -28dB signal level. Deviation from the desired response can detrimentally affect the filter's performance within the designated frequency band, potentially resulting in signal loss or distortion.

VIII. Conclusion

For the proposed project 'design and development of duplexer for GSM applications,' various literature surveys have been conducted, leading to several inferences. The calculations for the design of bandpass filters in the duplexer have been successfully achieved with the assistance of the book 'Microwave Engineering' by David M. Pozar. Simulations were performed using Genesys, ensuring that the calculated bandpass filter specifications meet all the necessary requirements for GSM applications. However, the conversion of passive filters to microstrip was not feasible due to limitations in Kuroda's identity. Subsequently, a study on hairpin filters was conducted, and filters were designed to meet our specific requirements. These designs were then simulated and optimized until achieving an improved response. The simulated filters were fabricated, and the fabrication process was completed successfully, resulting in proper functionality but the results were not desirable.

References

[1] S. Li, L. Luo, and W. Cao, "A compact microstrip duplexer," in IEEE 3rd International Conference on Electronic Information and Communication Technology (ICEICT). IEEE, Nov. 2020

[2] J. E. Portune. The cavity duplexer, 2019

[3] D. M. Pozar, Microwave Engineering, 4th ed., Dec. 2011

[4] L. Suresha, S. Kn, U. Kumar, S. Kumar, R. K. Manjunath, and K. Nagamani, "Design and fabrication of duplexer for gsm900 band applications," 2015.

[5] V. Vineeth, "Design of duplexer using waveguide filters for gsm applications," International Journal of Engineering and Technical Research (IJETR), 2014

[6] Wireless Planning and Coordination Wing, Department of Telecommunications, "National Frequency Allocation Plan - 2022," 2022, 26 October 2022

Analysis and Comparison of Methods of Speech Recognition Using Neural Network

Divya Sharma[1], Dhanshree Pansare[2], Gracy Borra[3], Ms. Madhavi S. Pednekar[4]
[1] *Department of Electronics and Telecommunication Engineering*
[1] *The Bombay Salesian Society's, Don Bosco Institute of Technology, University of Mumbai, India*
[1] divyasourabh01@gmail.com, [2] dhanshree.pansare002@gmail.com, [3] 121gracy0018@dbit.in, [4] madhavi@dbit.in

Abstract **- Speech recognition is a process by which the elements of spoken language can be recognized, analysed, and transposed into a meaningful form so that a machine can respond correctly to spoken commands. This project evaluates the various methods of Speech Recognition based on the analysis done by measuring the performance parameters using Neural Network. It aims to identify the most suitable and efficient techniques among Random Forest (RF), Radial Basis Function (RBF) and Multi-Layer perceptron (MLP) used for speech Recognition. These methods are evaluated based on their performance parameters like Accuracy, Precision, Specificity, Recall, False Negative Ratio (FNR), False Positive Ratio (FPR) etc. using Neural Network models. This study helps the researchers to identify the most suitable Speech Recognition method for their research application.**

Keywords: Speech Recognition, Feature Extraction, MFCC, Neural Network, MLP, RBF, RF

I INTRODUCTION

Speech Recognition is a crucial technology that enables computers to understand human speech. This project aims to enhance the accuracy of Speech Recognition using advanced computer models known as Neural Networks.

Our methodology involves the collection and preprocessing of recorded Marathi speech audio signals. We utilize techniques such as pre-emphasis filtering, adaptive thresholding, framing, and windowing to refine the data. Subsequently, we conduct feature extraction using Fast Fourier Transform (FFT) and Mel Frequency Cepstral Coefficients (MFCC). To optimize feature selection, we employ a hybrid approach combining Fennec Fox Optimization (FFO) and Tuna Swarm Optimization (TSO).

The selected features are then classified using Random Forest (RF), Radial Basis Function (RBF), and Multi-Layer Perceptron (MLP) classifiers. These trained models are evaluated using performance metrics such as Accuracy, Precision, Specificity, False Negative Rate (FNR), and False Positive Rate (FPR). A comparative analysis of these methods allows us to identify the most suitable and efficient Speech Recognition technique for Marathi.

This project is significant as it contributes to the advancement of Speech Recognition technology specifically tailored for the Marathi language. By enhancing accuracy and efficiency, our efforts aim to improve user experience and effectiveness in Human-Computer interaction within Marathi-speaking communities.

II LITERATURE SURVEY

The Reserch Paper discusses feature extraction technique for speech recognition, focusing on Mel Frequency Cepstral Coefficients (MFCC) and its various steps like pre-emphasis, frame blocking, windowing, and triangular bandpass filtering. MFCC is a mathematical representation of speech data used in speech processing, synthesis, and speaker recognition. Steps involved in MFCC extraction include pre-emphasis to minimize high frequencies, frame blocking to divide audio into frames, and applying a Hamming window for continuity. Triangular bandpass filters are used to moderate the magnitude spectrum of speech signals, compress harmonics, and obtain the envelope of the spectrum. Mel frequency warping is applied to scale frequency nonlinearly to match human auditory perception, leading to Mel Frequency Cepstral Coefficients (MFCC) extraction. [1]

The paper explores speech recognition systems for mathematical expressions, highlighting dataset creation and information fusion to improve accuracy. It categorizes these systems based on speech patterns, speaker mode, and vocabulary size, offering insight into their diverse applications. Additionally, it explains the architectural framework of these systems, detailing interactions among components. The paper also discusses various approaches for feature extraction and classification in mathematical expression recognition. By examining these aspects, it provides valuable insights into the functioning of speech recognition systems for math. The paper is a valuable resource for researchers and practitioners,

equipping them with foundational knowledge to advance speech recognition technology in mathematical contexts. [2]

The paper discusses different approaches and models for speech recognition. It compares the strengths and weaknesses of each approach and provides insights into their applications. The main findings include the use of template-based approach with accurate word models and segmentation, the insensitivity of pattern recognition approach to speech-specific knowledge, the explicit modeling of variation in speech in the knowledge-based approach, the frequency-based measurement in the dynamic time warping-based approach, and the use of hidden Markov models for piecewise stationary signals. The document also mentions the JAWS software for blind users and the use of MATLAB for sound recording and speech recognition. [3]

The paper presents the development of a Marathi numeral recognition system utilizing automatic speech recognition (ASR) techniques. It targets Marathi numerals from zero to nine and utilizes a database comprising recordings from male and female speakers for training and testing. Feature extraction methods, including Mel-frequency Cepstral coefficient (MFCC) and Low pass filter and zero Interpolation (LFZI), are employed for pattern classification. Experimental findings demonstrate the efficacy of these techniques in achieving high recognition rates. [4]

.

III METHODOLOGY

The process begins with the creation of a comprehensive database, featuring carefully recorded speech samples from a diverse group of speakers. To ensure the data's clarity, pre-processing steps are taken to remove any unwanted noise. This refined dataset is then used to extract features using Mel Frequency Cepstral Coefficients (MFCC), involving procedures such as pre-emphasis, windowing, Fast Fourier Transform (FFT), Mel-Scale conversion, and coefficient extraction, resulting in an MFCC output stored as matrices. The data is split into two parts: 70% for training and 30% for testing. Three neural network model Random Forest (RF), Radial Basis Function (RBF), and Multi-Layer Perceptron (MLP) are utilized for this process. These models are evaluated based on performance metrics including Accuracy, Recall, Precision, Specificity, False Positive Ratio, Kappa statistic, error rate, and Matthews Correlation Coefficient. This analysis helps identify the most effective approach for speech recognition.

Database Creation**:** The initial phase involved the creation of a comprehensive database, consisting of recorded Marathi speech audio signals from various speakers. This diverse dataset was crucial for developing robust speech recognition models Pre-processing: To ensure data quality, the recorded audio signals underwent a series of pre-processing steps. These included pre-emphasis filtering to enhance signal-to-noise ratio, adaptive thresholding for noise reduction, and framing and windowing techniques to segment the audio signals effectively.

Feature Extraction: Subsequent to pre-processing, feature extraction was carried out using Fast Fourier Transform (FFT) and Mel Frequency Cepstral Coefficients (MFCC). These techniques were selected for their ability to capture the spectral characteristics of the speech signals. The extracted features were further refined using a hybrid approach combining Fennec Fox Optimization (FFO) and Tuna Swarm Optimization (TSO), ensuring optimal feature selection.

Classification: The refined features were classified using three distinct neural network models: Random Forest (RF), Radial Basis Function (RBF), and Multi-Layer Perceptron (MLP). These models were trained and tested on the dataset, with 70% allocated for training and 30% for testing.

Performance Parameters (Evaluation): The performance of the models was evaluated based on several metrics, including Accuracy, Precision, Recall (Sensitivity), Specificity, False Negative Rate (FNR), and False Positive Rate (FPR). These metrics provided a comprehensive assessment of each model's effectiveness in recognizing Marathi speech.

IV IMPLEMENTATION

4.1 Speech Recognition System Overview

This initial step provides a high-level view of the entire speech recognition system. The system starts with the speech signal (audio input) which undergoes pre-processing to enhance the quality of the signal. The pre-processed signal is then passed through feature extraction to derive meaningful features. These features are then used in the training and testing phase

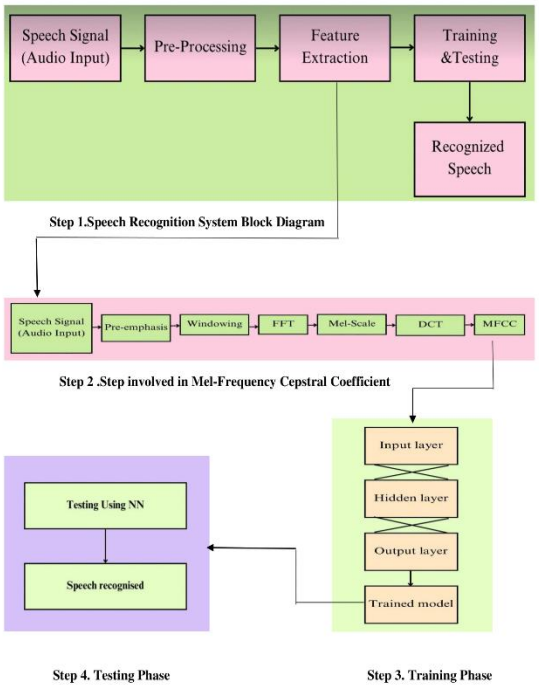


Fig No.1 Block diagram of Speech Recognition

4.2 MFCC Feature Extraction

In this step, the audio signal is processed to extract Mel-Frequency Cepstral Coefficients (MFCC), which are crucial features for speech recognition.

MFCC utilized for spectral feature extraction from speech signals in both training and testing phases. MFCC transforms time-based signal into frequency domain, capturing spectral characteristics efficiently.

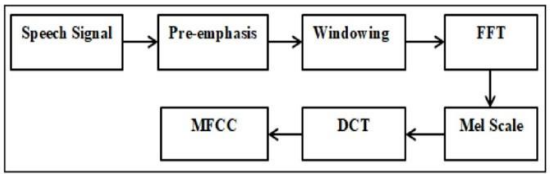


Fig no.2 Block diagram MFCC

Pre-processing: Enhancements like pre-emphasis for noise reduction.

Windowing: Divides signal into frames for analysis, applying a window function.

FFT: Converts framed signal from time to frequency domain, revealing spectral characteristics.

Mel Filter Bank: Groups DFT spectrum into distinct frequency bands based on human auditory perception. Inverse

DFT: Reconstructs signal from modified frequency representation.

Dynamic Transform: Techniques like CMVN normalize cepstral coefficients for robustness against variations.

4.3 Training Phase

The MFCC features are used to train the data with the help of Neural Network models that are MLP (Multi-Layer Perceptron), RBF (Radial Basis Function), RF(Random Forest)

4.3.1 Neural Network

Neural Network is a computational learning system that uses a network of functions to understand and translate a data input of one form into a desired output, usually in another form.

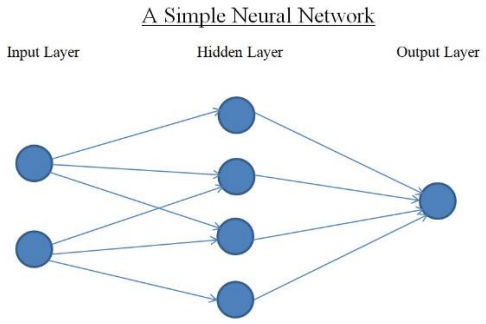


Fig no.3 Neural Network

The concept of the artificial neural network was inspired by human biology and the way neurons of the human brain function together to understand inputs from human senses. Neural networks are just one of many tools and approaches used in machine learning algorithms. The neural network itself may be used as a piece in many different machine learning algorithms to process complex data inputs into a space that computers can understand.

4.3.1 Random Forest

Random Forest (RF) is an ensemble learning method that constructs multiple decision trees during training.

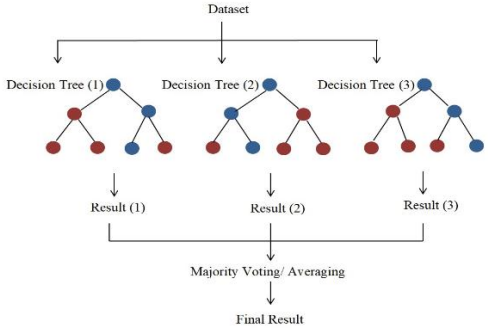


Fig no.4 Random Forest

It outputs the mode of classes for classification or the mean prediction for regression. It employs bootstrapping to create random samples of the training dataset and random feature selection at each node to reduce overfitting. Decision trees are constructed recursively based on split criteria, and the final prediction is determined by voting (classification) or averaging (regression) the predictions of individual trees.

4.3.2 Radial Basis Function

Radial Basis Function (RBF) is a kernel function used in SVMs and other ML algorithms. It transforms input data into higher-dimensional space, aiding in capturing complex decision boundaries. RBF kernels are valued for their effectiveness in making data linearly separable or more easily approximated.

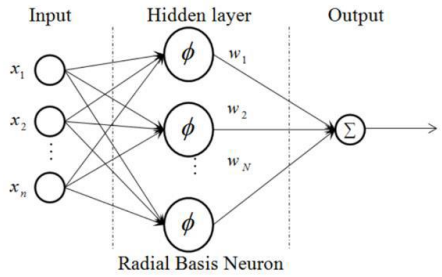


Fig no.5 Radial Basis Function

The Kernel Trick: RBF kernel computes similarity between points in original space, avoiding explicit mapping to higher dimensions for efficient computations.

4.3.3Multi-Layer Perceptron

A Multilayer Perceptron (MLP) is an artificial neural network with multiple layers of neurons arranged in a feedforward manner. Each neuron in one layer connects to every neuron in the next layer, forming an input layer, one or more hidden layers, and an output layer

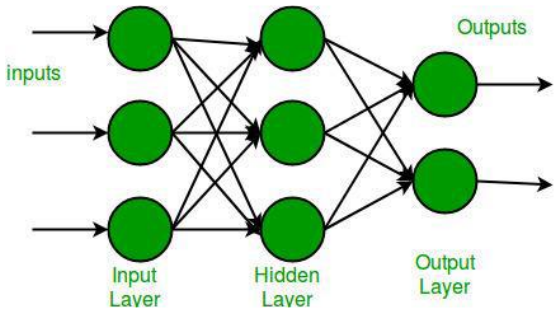


Fig no.6 Multi-Layer Perceptron

An MLP consists of layers: input, hidden, and output. Input neurons represent features, hidden neurons process data via weighted sums and activation functions, and output neurons produce final results. During training, weights are adjusted via backpropagation to minimize error. Once trained, MLPs can predict on new data, making them valuable for various tasks like classification, regression, and pattern recognition

4.4 Testing Phase

The performance is evaluated based on parameters such as Accuracy, Precision, Specificity, MCC, Recall, and Kappa. The results are then analyze through graphs to determine which method performs better based on these performance parameters.

4.4.1 Performance Parameters

Accuracy: Accuracy gives an overall measure of how often the model is correct. However, it can be misleading if the dataset is imbalanced (e.g., if there are many more negative cases than positive cases).

Precision: Precision is crucial when the cost of false positives is high. For example, in medical diagnoses, a high precision means that when the model predicts a disease, it is likely to be correct.

Recall (Sensitivity): Recall is important when the cost of missing positive cases is high. For instance, in disease detection, high recall means that most of the patients with the disease are identified.

Specificity: Specificity is useful when the cost of false positives is high. It reflects the model's ability to correctly identify negative cases.

Error: Error rate provides a general measure of how often the model makes mistakes. It's the complement of accuracy (i.e., Error Rate = 1 - Accuracy).

Cohen's Kappa: Kappa takes into account the possibility of agreement occurring by chance and provides a more robust measure of model performance, especially when dealing with imbalanced datasets.

Matthews Correlation Coefficient (MCC):
MCC is particularly useful for imbalanced datasets because it provides a single score that balances all four confusion matrix categories. It ranges from -1 (perfect disagreement) to 1 (perfect agreement), with 0 indicating no better than random prediction.

False Negative Rate (FNR): FNR measures the proportion of actual positives that are incorrectly predicted as negative.

V. RESULTS AND DISCUSSION



Fig no.7 Accuracy

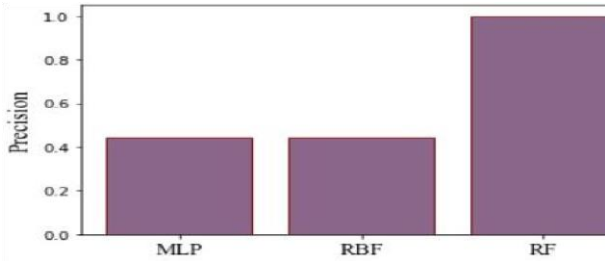


Fig no. 8 Precision

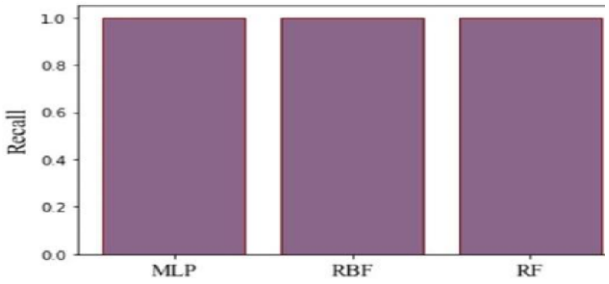


Fig no 9 Recall

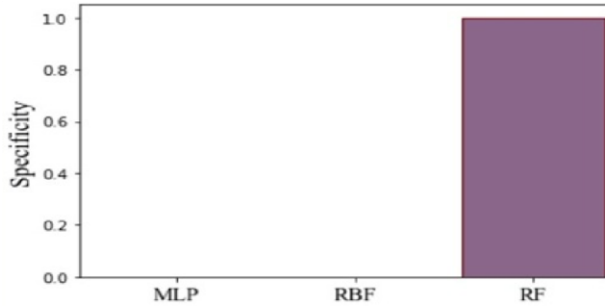


Fig no .10 Specificity

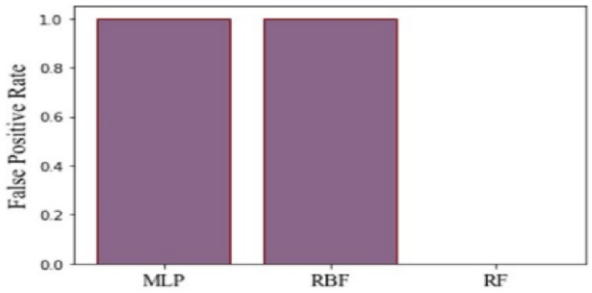


Fig no. 11 False Positive Rate

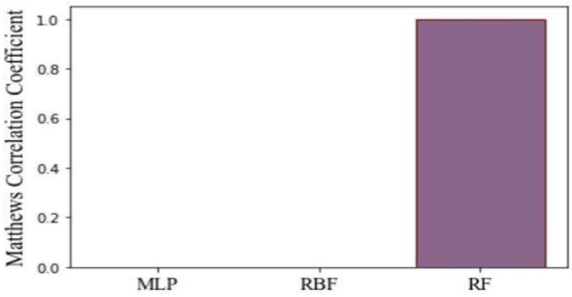


Fig no. 12 MCC

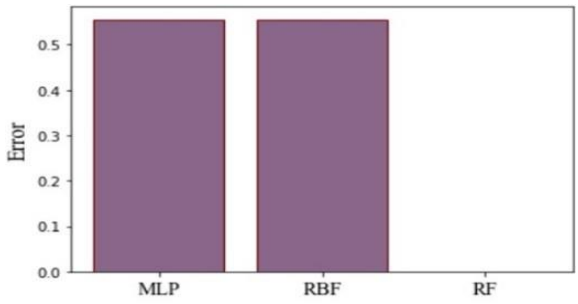


Fig no. 13 Error

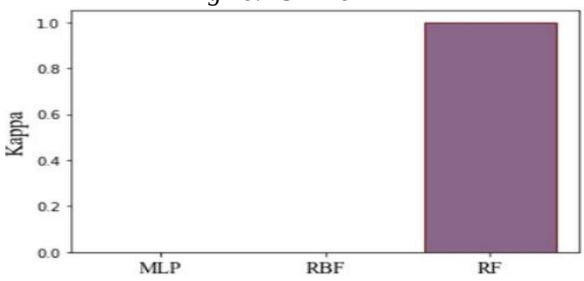


Fig no .14 Kappa

MODAL	ACCURACY	PRECISION	RECALL	SPECIFICITY	FPR	ERROR	KAPPA	MCC
MLP	0.46	0.4	0.99	0.10	0.99	0.54	0.02	0.02
RBF	0.44	0.4	0.99	0.10	0.99	0.55	0.02	0.02
RF	1.0	1.0	1.0	0.99	0.01	0.01	0.99	0.99

Table No. 1 Result: Performance Parameters

The results indicate that the Random Forest model significantly outperforms the other two models in this classification task, achieving a perfect accuracy of 1.0. This implies that it correctly classified all instances in the dataset. However, it is crucial to consider the limitations of evaluating model performance using a single dataset, as the Random Forest model might have overfitted to this specific data and may not perform as well on unseen data. In contrast, the MLP and RBF models exhibit very low accuracy, precision, Kappa, and MCC scores. Although these models show high recall, this accompanied by a very high false positive rate, indicating that they classify many negative cases as positive. This suggests that MLP and RBF are not suitable for this particular classification task.

VI. CONCLUSION

In this project, we compared the performance of three neural network models: Random Forest (RF), Radial Basis Function Network (RBF), and Multi-Layer Perceptron (MLP) using various performance parameters. The Random Forest (RF) model stood out for its high accuracy in recognizing both positive and negative cases. While each model had its strengths, RF demonstrated a strong overall performance, effectively balancing accuracy, precision, and recall. This makes RF a robust choice for applications requiring reliable classification across diverse scenarios.

VII. REFERENCES

[1] V. A. Kherdekar and S. A. Naik, "Speech Recognition System Approaches, Techniques And Tools For Mathematical Expressions: A Review," in INTERNATIONAL JOURNAL OF SCIENTIFIC TECHNOLOGY RESEARCH, vol. 8, no. 08, pp. 2277-8616, August 2019.

[2] S. Gupta, J. Jaafar, W. F. Wan Ahmad, and A. Bansal,"Feature Extraction using MFCC," Signal Image Processing: An International Journal (SIPIJ), vol. 4, no. 4, August 2013[3] R. Ranjan and A. Thakur, "Analysis of Feature Extraction Techniques for Speech Recognition System," in International Journal of Innovative Technology and Exploring Engineering (IJITEE), vol. 8, no. 7C2, pp. 2278-3075, May 2019.

4] D. Gupta and A. Madan," Speech Feature Extraction and Classification: A Comparative Review," International Journal of Computer Applications, vol. 90, no. 9, pp. 0975 – 8887, March 2014.

[5] H. Dudhrejia and S. Shah, "Speech Recognition using Neural Networks," in International Journal of Engineering Research Technology (IJERT), vol. 7, no. 10, pp. 2278-0181, October 2018. Published by www.ijert.org.

[6] D. Nagajyothi, P. Siddaiah,"Speech Recognition Using Convolutional Neural Networks", in International Journal of Engineering Research Technology (IJERT), pp .133-137, year 2018

[7] Mohit Bansal, Dr. T. K. Thivakaran ,"ANALYSIS OF SPEECH RECOGNITION USING CONVOLUTIONAL NEURAL NETWORK", International Journal of Engineering Research Technology (IJERT), pp.0377-9254 , Vol.11,Issue.1,Jan 2020

[8] A. Khan, et al ,"Speech Recognition: Increasing Efficiency of Support Vector Machines,", A. Khan, et al ,International Journal of Computer Applications , Vol.35, dec 2011

Implementation of Mesh Topology for IoT Network

1st Aniket Pawar
Department of Electronics and Telecommunications
Don Bosco Institute of Technology
Mumbai, India

2nd Anushk Sawant
Department of Electronics and Telecommunications
Don Bosco Institute of Technology
Mumbai, India

3rd Omkar Bidwai
Department of Electronics and Telecommunications
Don Bosco Institute of Technology
Mumbai, India

4th Aparna M. Telgote
Department of Electronics and Telecommunications
Don Bosco Institute of Technology
Mumbai, India
aparna@dbit.in

***Abstract*—This project explores the practical implementation of a mesh network topology in the context of Internet of Things (IoT) devices. Mesh topology offers redundancy and scalability, making it well-suited for IoT applications. We discuss the benefits, challenges, and key considerations in deploying a mesh network for IoT, and provide insights into real-world scenarios where this topology can enhance connectivity and reliability. This research aims to contribute to the growing field of IoT networking, offering valuable insights for developers and engineers looking to optimize their IoT deployments.**

***Index Terms*—IoT, ESP32, Mesh topology**

I. Introduction

The implementation of mesh topology in IoT networks has become a crucial endeavor in the realm of interconnected devices. IoT, with its vast and diverse ecosystem, demands resilient, self-healing, and scalable network architectures, making mesh topology an attractive choice. This introduction delves into the practical application of mesh topology within IoT networks, shedding light on the advantages, challenges, and real-world implications of this network configuration. By embracing mesh topology, IoT networks can achieve enhanced reliability and adaptability, fostering the growth of the Internet of Things.

Additionally, to address the issue of delayed rescues during crises in mining operations, we propose a health monitoring system using ESP32. The primary goal of this system is to transmit information about the worker to a centralized system, which will send alert messages, track the worker's location, and enable the rescue team to respond swiftly.

Section 2 describes the project overview and problem statement, outlining the specific challenges and issues this project aims to address. Section 3 provides a literature review, examining previous research and developments in the field of IoT and mesh network topologies. Section 4 details the methodology and implementation of the project, explaining the steps and processes involved in deploying the mesh network and health monitoring system. Finally, Section 5 presents the results, showcasing the outcomes and effectiveness of the proposed solutions.

A. Problem Statement

The wide range of IoT devices requires reliable, self-repairing, and scalable networks. However, current network architectures often fall short in these areas. Therefore, exploring the implementation of mesh topology in IoT networks is essential to address these needs and improve connectivity, resilience, and scalability.

B. Scope of the project

- Reliable Communication: Mesh topology offers robust communication pathways by allowing IoT devices to connect directly with one another.
- Self-Healing: Mesh networks have self-healing capabilities, automatically rerouting data in case of node failure, making them ideal for applications where continuous connectivity is essential.
- Continuous Monitoring: Implement a system capable of real-time tracking of patient movements.
- Coverage and Range: Mesh topology can provide extended coverage and range, particularly useful in large-scale IoT deployments, such as smart cities or agricultural monitoring.
- Low Power Consumption: Devices can operate at lower power levels since they only need to transmit short distances to nearby nodes
- Device Data: Sensor readings, device status, and any other data generated by IoT devices.
- Immediate Response: Enable ground team to take swift action based on the received alerts.

II. Literature Survey

There has been a significant rise in the educational technology sector over the last few years. Numerous software solutions have been developed to meet the needs of a variety of educational institutions. Most of these solutions aim not only to address or enhance various practical administrative issues and internal processes but also to support and promote the goals and objectives of the institutions.

A. Coal Mine Safety Monitoring and Alerting System

Security is a fundamental concern across all industries, with safety being paramount in the mining sector. In mining operations, numerous safety measures are implemented to prevent accidents, such as those caused by steel malfunctions, methane gas leaks due to temperature increases, and rising water levels in underground mines. Protecting workers is a primary focus, and mechanisms like panic switches are employed to alert workers and manage dangers they can address themselves.

To enhance safety among employees in underground mines and ensure continuous communication with stationary systems, a reliable communication network is essential. Any interruption in this network can compromise safety. This project proposes a robust wireless supervision system with early warning capabilities, leveraging IoT technology. This system will enable real-time monitoring of worker status and ensure that communication remains uninterrupted, thus improving overall safety and operational efficiency in mining environments[2].

B. IoT based Smart Security Helmet for Miner's Safety

In the coal mining industry, safety remains a significant concern due to frequent accidents. To address this issue, researchers have focused on developing wireless network solutions that provide real-time data to alert officials about accidents, allowing for timely intervention. A major cause of accidents in mining is falling rubble, which can be mitigated by innovative technologies.

One such innovation is the IoT-based helmet project designed to enhance worker safety. This project aims to address the safety gaps in the mining industry by introducing SMART HELMETS. Unlike other industries, the mining sector has been slower to adopt new technologies. To improve safety conditions, SMART HELMETS have been developed as a life-saving tool for workers operating deep within mines.

The SMART HELMET prototype incorporates several key components: an ESP8266 for wireless communication, an accelerometer sensor to detect sudden movements or impacts, a gas sensor to monitor harmful gas levels, and a buzzer to alert workers of potential hazards. This integration of IoT technology into mining safety equipment represents a significant step forward in reducing accidents and improving overall worker protection in hazardous environments[3].

C. A Wearable Alert System for Underground Mining Workers based on Arduino with GSM

The mining sector places a high priority on coal mine safety due to the severe risks associated with mining accidents, which can lead to catastrophic failures, substantial financial losses, and, most critically, harm to human life. Efforts to enhance mine safety through monitoring are crucial for advancing safety surveillance and maintenance. Many researchers have developed wearable alert systems aimed at improving miner safety in coal mines. Despite the substantial body of literature addressing miner security, existing systems face significant challenges due to unpredictable environmental changes and machinery failures within the mines.

To address these challenges, there is a need for efficient monitoring and alert systems tailored to the underground mining environment. This work focuses on the design and development of a smart alert system for miners that is both wearable and capable of ensuring safety by issuing clear alerts in case of worker illness or other issues. The proposed system integrates various components, including a temperature sensor, heartbeat sensor, gas sensor, display unit, and GSM module, all interfaced through an Arduino. This approach aims to provide a more reliable and effective safety solution for mining workers[4].

D. Power Efficient Intelligent Helmet for Coal Mining Security and Alerting

India is endowed with a rich variety of mineral resources, including the world's fourth-largest coal deposits. The demand for domestic use has driven commercial coal mining in India for a significant period. The mining industry involves complex processes carried out underground, including tunnels and caverns, and is subject to numerous hazardous conditions that impact miners' health. Despite following safety procedures to prevent accidents, issues such as surface warming, methane hydrate leaks, and carbon dioxide emissions continue to pose risks.

Recent advancements in technology, particularly in IoT and wireless communication, offer new ways to enhance safety and communication in mining operations. The earlier the control room receives updates, the more effectively damage can be mitigated. To address the persistent safety challenges, a Smart Helmet for mining safety and alerting has been proposed. This helmet integrates IoT-based surveillance systems that monitor the mining environment and alert users to critical situations. It is equipped with pre-installed safety modules and smart sensors.

The Smart Helmet uses Wi-Fi networks to exchange data with various sensors and tracking devices. In the event of hazardous conditions, the helmet's indicator takes necessary precautions and issues warnings through a buzzer for the miner and via the cloud to the control room. Both the miner and the control room supervisor are informed of dangerous situations through the helmet's devices. Additionally, the helmet features a Pulse and SPO2 sensor to monitor the miner's health and alert the supervisor in case of any health issues. A tracking system is also incorporated to provide real-time location information of the miner, enhancing the ability to respond promptly in emergencies[5].

III. IMPLEMENTATION

For the implementation of the project, we developed a wireless system integrating the ESP32 with various modules, including GPS, pulse, and heart rate sensors. In this setup, we utilized three modules as client devices and one module as a server connected to a PC.

The implementation process involves several key steps: hardware setup, software development, testing, and calibration.

Each step is essential to ensure the system's functionality, accuracy, and reliability.

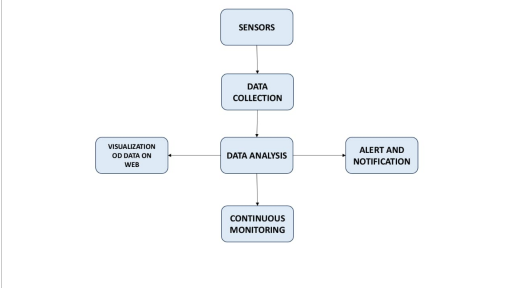


Fig. 1. Flowchart

Flow Chart Description:

Figure 1 illustrates the overall flow of the project, divided into five main parts:

Data Gathering: Sensors collect data from their respective sources. Data Transmission: The collected data is transmitted to the server, typically over a network connection. Data Analysis: The server analyzes the incoming data using various algorithms to interpret it, identify patterns, detect anomalies, or determine if any values exceed predefined thresholds. **Display on Monitor:** The analyzed data is then displayed on a monitor, potentially in the form of graphs, charts, or other visual formats. **Alerts and Notifications:** If the analyzed data reveals that certain values surpass predefined thresholds or if anomalies are detected, alerts and notifications are generated. **User Notification:** These alerts and notifications are sent to the relevant users, informing them of the situation through means such as email, SMS, push notifications, or a dedicated application.

BLOCK DIAGRAM

Figure 2 illustrates the block diagram of the entire project. It shows the ESP32 module connected to sensors, forming the client modules. We have used three client modules, each sending data to the ESP32 server. The server processes this data and displays the results on a monitor after analysis, thus forming a mesh network.

Hardware Setup Hardware set up requirements are as follows

ESP32 Development Boards: We use three ESP32 development boards because the ESP32 is a cost-effective, low-power microcontroller with integrated Wi-Fi and Bluetooth, making it ideal for IoT applications.

Power Supply: Each ESP32 board is powered using a USB cable.

Programming Environment: We use the Arduino IDE or Platform IO with the ESP32 board support package to program the ESP32 devices. This setup enables us to write and upload code to control the behavior of the ESP32.

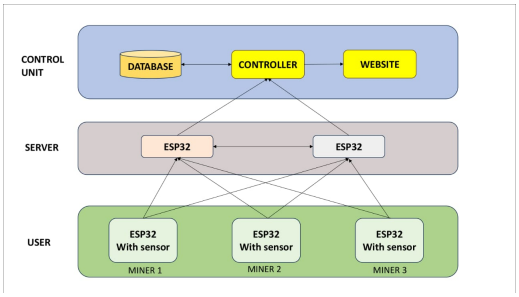


Fig. 2. Block Diagram

Mesh Networking Library: We utilize a mesh networking library compatible with the ESP32, such as the ESP-MESH framework from Espressif Systems, the manufacturer of the ESP32. ESP-MESH facilitates the implementation of mesh networking on ESP32 devices.

IV. Results

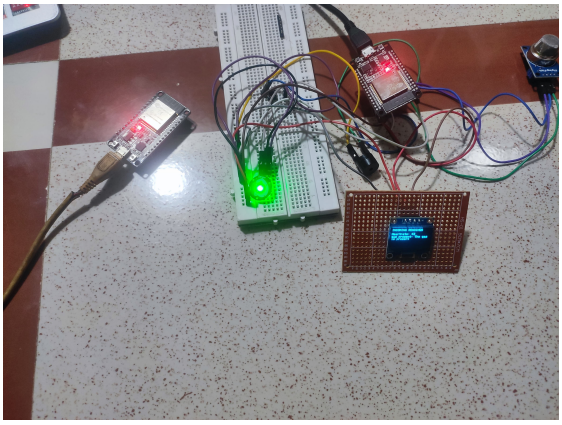


Fig. 3. Client Modules

Figure 3 illustrates the Mesh Topology, comprising the sensor module and a client module. The server module collects data from the client module, analyzes it, and presents it. Figure 4 showcases the server module's display monitor, revealing the detection of hazardous gases within the mine environment. Sensors play a crucial role in monitoring environmental conditions within mines, including factors such as toxic gases, temperature, humidity, and air quality. Furthermore, we've implemented a system to track the location of mine workers, ensuring their safety and enabling swift location in emergencies or if they become trapped. This IoT mesh network project aims to implement a real-time monitoring system to provide information about environmental gas levels, monitor miners'

Figure 3 depicts the Mesh Topology, which includes both sensor and client modules. The server module collects data from the client modules, processes it, and presents the results.

Figure 4 shows the server module's display monitor, which indicates the detection of hazardous gases within the mining environment. Sensors are essential for monitoring environmen-

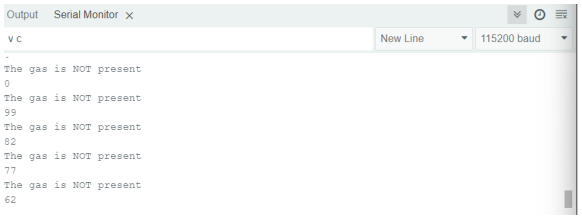


Fig. 4. Display monitor at server Module

tal conditions in mines, including toxic gases, temperature, humidity, and air quality.

Additionally, we have implemented a tracking system for mine workers to ensure their safety and enable quick location in emergencies or if they become trapped.

The IoT mesh network project aims to establish a real-time monitoring system that provides information about environmental gas levels, monitors miners' temperature and heart rate, and tracks their location during emergencies.

The results presented in Figures 3 and 4 highlight the effectiveness of the IoT mesh network in improving safety measures in mining environments. Figure 3 illustrates the foundational architecture of the Mesh Topology, showing how sensor and client modules work together for data collection and transmission. This setup allows the server module to analyze and present real-time data, facilitating informed decision-making and proactive hazard management.

Figure 4 demonstrates the server module's capability to detect and display hazardous gas levels, emphasizing the system's effectiveness in monitoring and alerting personnel to environmental risks. Sensors play a critical role in continuously tracking various environmental factors, including toxic gases, temperature, humidity, and air quality. This comprehensive monitoring helps stakeholders implement targeted interventions to reduce risks and protect workers.

Furthermore, the tracking system for mine workers enhances safety by providing real-time location information. This feature aids in efficient resource allocation, task coordination, and swift emergency response, potentially saving lives and reducing the impact of critical incidents.

Conclusion

In this project, we implemented a mesh topology within an IoT network specifically for mine worker rescue operations. This setup provides a resilient, adaptable, and real-time communication system, greatly enhancing safety measures and enabling swift responses to emergencies in challenging underground environments. By improving rescue operations and potentially saving lives, the health monitoring system proves to be crucial for miners working in caves, addressing various health risks they may face. Its efficiency and user-friendly interface offer significant flexibility, marking a substantial advancement over traditional monitoring systems.

Future Scope

The future scope of this project includes several potential avenues for further development and refinement. One promising direction is the integration of advanced sensor technologies to improve the accuracy and range of environmental monitoring in mining operations. This could involve sensors capable of detecting a wider variety of gases, as well as monitoring additional factors such as seismic activity and ground stability.

Another area for advancement is the incorporation of predictive analytics algorithms. These algorithms could help the system anticipate potential hazards and implement proactive safety measures, thus reducing risks to mine workers. Additionally, integrating machine learning algorithms could enhance the system's ability to analyze historical data, identify patterns and trends, and improve its predictive capabilities.

Exploring wearable technologies for mine workers, such as smart helmets or vests with built-in sensors, represents another significant opportunity. These wearables could continuously monitor vital signs, physical exertion, and exposure to hazardous substances, enabling timely intervention in emergencies or health issues.

Moreover, advancements in communication technologies, such as integrating 5G networks or satellite communication systems, could further enhance connectivity. This would ensure seamless communication between mine workers, supervisors, and rescue teams, even in remote or underground locations.

Overall, the future scope of this project involves leveraging emerging technologies to develop a more comprehensive and proactive safety and monitoring system for mining operations, ultimately improving worker safety and operational efficiency.

V. Acknowledgment

A project is a teamwork which involves the contribution of many people. We would like to thank everyone who have contributed by taking interest in our work and motivating us all the way through. Our sincere thanks to our project guide Ms.Aparna Telgote, for motivating, co-operating and guiding us throughout the project work, with his effective skills and huge knowledge base. We would like to thank Dr. Sudhakar Mande, Head of Department and Ms. Aparna Telgote, Project Coordinator for their continuous valuable guidance, support, suggestions and their precious time in every possible way throughout the project activity

References

- Rahul M, Vinoth Kumar N,"Live Health Monitoring and Menace Detection Using Lifi And Blockchain Encryption", 2023 2nd InternationaConference on Advancements in Electrical, Electronics, Communication, Computing and Automation (ICAECA).
- Dhanalakshmi V, Vimalraj S, Praveen Raj B,"Keeping Track of Coal Mine Safety using IoT Technology", 2023 Eighth InternationalConference on Science Technology Engineering and Mathematics (ICONSTEM).
- Rohan Paul, Arpan Karar, Abhirup Datta, Sumit Kumar Jindal,"Smart Helmet For Coal Miners", 2022 1st International Conference onthe Paradigm Shifts in Communi-

cation, Embedded Systems, Machine Learning and Signal Processing (PCEMS).

- N.Surendranath Reddy, MSrinivasa Saketh, Sourav Dhar,"Review of sensor technology for mine safety monitoring systems: A holistic approach ",2016 IEEE First International Conference on Control,Measurement and Instrumentation (CMI).
- Sufia Banu, Rashmi Rani Samantaray, Hajira Zaiba, Abdul Rehaan, Mansha Yasin, Arun Kumar,"Power Efficient Intelligent Helmet forCoal Mining Security and Alerting", 2023 International Conference on Sustainable Computing and Smart Systems (ICSCSS).
- Suk Hyun Yoon, Jong Ha Moon, Myung Hoon Sunwoo, "Efficient DSP architecture for high-quality audio algorithms", Circuits and Systems, 2005. ISCAS 2005. IEEE International Symposium 2005Huili Zhang, Binghao Li, Mahmoud Karimi, Serkan Saydam, Mahbub Hassan,"Recent Advancements in IoT Implementation forEnvironmental, Safety, and Production Monitoring in Underground Mines", IEEE Internet of Things Journal, vol.10, no.16.

Multi-Object Detection in Operation Theatre

Disha Maggu[1], Nitish Chavan[2], Rohit Gupta[3], Yash Sonavane[4], Hemalata Mote[5], Satishkumar Chavan[6]
[1]*Department of Electronics and Telecommunication Engineering*
[1]*The Bombay Salesian Society's, Don Bosco Institute Of Technology, University of Mumbai, Mumbai India*
[1]*dishamaggu12@gmail.com,* [2]*nitishchavan937@gmail.com,* [3]*rohitgupta0663149@gmail.com,* [4]*yashsonavane62@gmail.com,*
[5]*hemalata@dbit.in,* [6]*satyachavan@gmail.com*

***Abstract*—Within the dynamic and critical environment of the operation theatre, safety and precision are paramount. It introduces an innovative solution aimed at enhancing patient safety and optimizing resource utilization by implementing object detection technology combined with intelligent lighting control. The primary goal of this project is to create a sophisticated multi-object detection system that leverages Infrared (IR) and Light Detection and Ranging (LIDAR) sensors integrated with Arduino technology. The proposed system is designed not only to identify the presence of objects, particularly medical staff and equipment within the operation theatre but also to dynamically control lighting based on detected objects. When an object is detected, the system will intelligently adjust the lighting by dimming in the specific area where objects are present and increasing the intensity of other lights. [4], [6]**

***Index Terms*—Multi Object Detection, IR sensor, LIDAR sensor, Operation Theatre**

I. Introduction

Multi-object detection refers to a physical setup and elements utilized in constructing the system detecting multiple objects. Multi object detection in an operation theatre revolves around the need to enhance patient's safety, optimize workflow and improve surgical outcomes. Their latest estimate found that approximately 9.5 % lives are claimed each year because of medical error. The motivation for undertaking this project stems from the desire to address critical issues such as the inadvertent retention of surgical instruments and the unintentional rupture of arteries or veins. [1], [5]

Accidental retention of surgical instruments: This is a serious issue that can lead to complications such as infection, internal organ damage, or even death if not promptly detected and addressed. Multi-object detection systems can help mitigate this risk by continuously monitoring the presence and location of instruments throughout the surgical procedure. Alerts can be triggered if an instrument is inadvertently left inside a patient before the incision is closed, enabling swift action by the surgical team to retrieve the object. Accidental rupture of artery or vein: During surgical procedures, inadvertent damage to blood vessels can occur, leading to bleeding and potential life-threatening complications. Multi object detection systems can aid in preventing such incidents by providing real-time feedback on the proximity of surgical instruments to critical anatomical structures. For example, if a tool approaches a major blood vessel, the system can issue warnings to the surgical team, prompting them to adjust their approach or reposition the instrument to avoid potential harm. [2], [3]

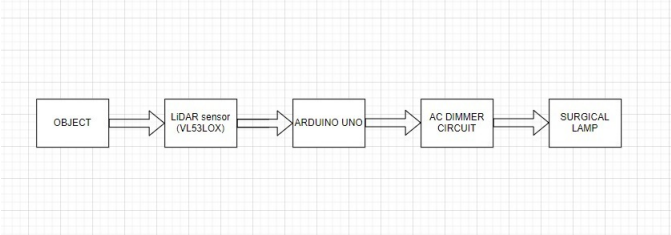


Figure 1. Block Diagram

We have developed a AC Dimmer circuit comprising components like a triac, optocoupler, and resistors, designed specifically for precise brightness control. With this circuit, we can finely adjust the brightness level to our preference. Additionally, We have integrated a Lidar sensor for object detection, seamlessly incorporated with an Arduino board. Using the Arduino IDE software, we have coded the functionality. Upon detecting an object, the Lidar sensor swiftly communicates the information to the Arduino board, which in turn sends a signal to the AC Dimmer circuit, facilitating the gradual dimming of the light. Initially, the bulb emits high brightness, providing ample illumination. However, as an object approaches within Lidar's proximity, the light dims gradually, ensuring a smooth transition. This setup not only showcases technological innovation but also addresses practical concerns, such as safety and energy efficiency, in real-world applications. [3], [6]

II. Methodology

- AC Dimmer Circuit Development using components such as a triac , optocoupler, and resistors for precise control of brightness levels.
- Integrated a Lidar sensor into the system for object detection.
- Upon detecting an object, the Lidar sensor rapidly transmits the information to the Arduino board.
- Utilized the Arduino IDE software for programming and coding the functionality of the system.
- Implemented gradual dimming controlled by AC Dimmer circuit.
- Bulb starts with high brightness for ample illumination. As object nears Lidar, light dims smoothly.

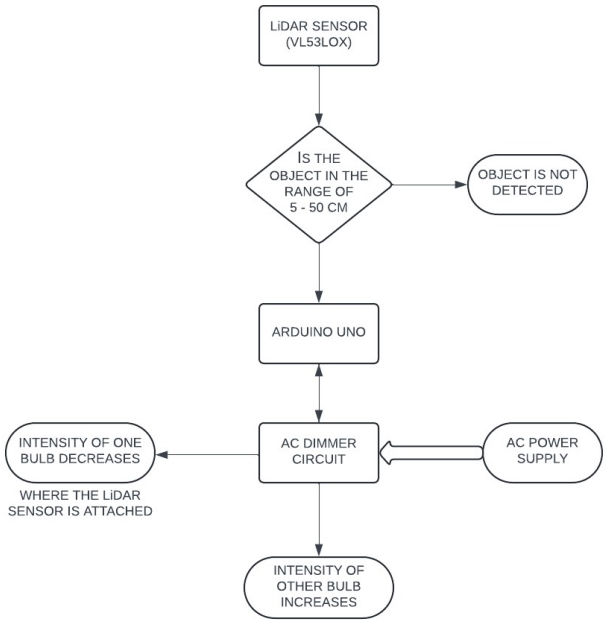


Figure 2. Methodology

III. Implementation

The implementation of the project for multi-object detection in the operation theatre involves a comprehensive approach, integrating AC Dimmer circuit building and LiDAR (Light Detection and Ranging) interfacing [1] [2]. The AC Dimmer circuitry serves as a crucial component for efficient signal processing and control within the system. The primary goal of this project is to design a system that detects objects interfering with LED lights in operation theatres and adjusts the lighting to minimize shadows. It involves integrating LiDAR sensors with Arduino UNO, using AC dimmer circuits to control LED lights, and conducting testing and calibration [1] [2].

Recent advancements in LiDAR technology have facilitated its integration into various applications, including object detection and ranging. Beltran et al. (2018) discussed the utilization of LiDAR for object detection in dynamic environments. Their study highlighted the effectiveness of LiDAR in accurately detecting objects and obstacles, making it a suitable choice for the proposed project [1].

Furthermore, Kim et al. (2021) explored the integration of LiDAR sensors with microcontroller platforms for real-time object detection and tracking. Their research demonstrated the feasibility of using LiDAR in combination with Arduino for applications requiring precise distance measurements and object detection [2].

The integration of AC dimmer circuits adds another layer of functionality to the system by enabling dynamic control of LED lighting. AC dimmers allow for the adjustment of light intensity, which is crucial for minimizing shadows caused by objects in the operation theatre.

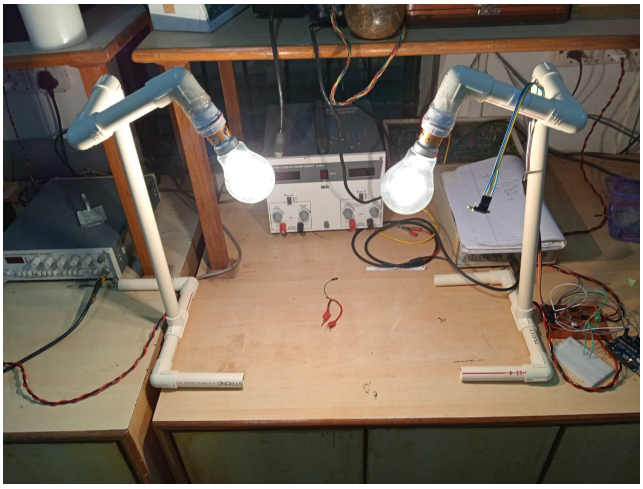


Figure 3. Hardware Setup

This integration enhances the adaptability and efficiency of the overall system, ensuring optimal lighting conditions during surgical procedures.

In addition to hardware integration, comprehensive testing and calibration are essential steps in validating the performance and reliability of the proposed system. Rigorous testing procedures, including scenario simulations and real-world testing in operation theatres, are necessary to evaluate the system's accuracy, responsiveness, and robustness in detecting and mitigating shadows.

In summary, the project entails a multidisciplinary approach, combining LiDAR interfacing, AC dimmer circuitry, and Arduino programming to develop a sophisticated system for object detection and lighting control in operation theatres. By leveraging state-of-the-art technologies and conducting thorough testing, the proposed system aims to enhance the safety and efficiency of surgical procedures while minimizing potential risks associated with inadequate lighting and object interference.

IV. Results

The implementation of the multi-object detection system in the operation theatre yielded promising results. The following sections detail the outcomes of integrating AC Dimmer circuitry and LiDAR interfacing, as well as the testing and calibration procedures conducted.

A. AC Dimmer Circuit Performance

The AC Dimmer circuits effectively controlled the LED lighting in the operation theatre. By adjusting the dimming level based on object detection data, the system successfully minimized shadows caused by objects interfering with the LED lights. The dimming process was smooth and responsive, ensuring optimal lighting conditions during surgical procedures.

B. LiDAR Interfacing Results

The integration of LiDAR sensors with Arduino UNO facilitated accurate object detection and distance measurements. LiDAR data provided real-time information about the presence and location of objects in the operation theatre. The system demonstrated high precision in detecting objects and effectively identified potential shadow areas.

Table I
OBSERVATION TABLE

Sr. No.	Distance (cm)	Brightness
1	5	127
2	10	110
3	15	98
4	20	82
5	25	75
6	30	59
7	35	40
8	40	26
9	45	15
10	50	3

C. Comprehensive Testing and Calibration

Rigorous testing and calibration procedures were conducted to evaluate the performance and reliability of the multi-object detection system. Scenario simulations were performed to assess the system's responsiveness to different object configurations and lighting conditions. Real-world testing in operation theatres further validated the system's accuracy and robustness in detecting and mitigating shadows.

D. Overall System Performance

The integrated system successfully achieved its primary goal of detecting objects interfering with LED lights and adjusting the lighting to minimize shadows. It demonstrated consistent performance across various testing scenarios and proved to be an effective solution for enhancing the safety and efficiency of surgical procedures in operation theatres.

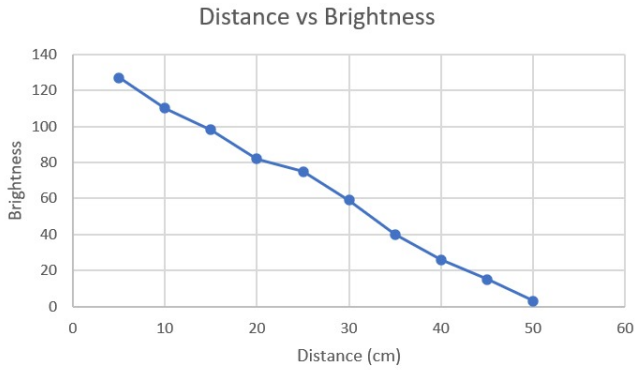


Figure 4. Resultant Graph

In summary, the results obtained from the implementation of the multi-object detection system highlight its effectiveness in addressing the challenges associated with inadequate lighting and object interference in operation theatres. The combination of AC Dimmer circuitry, LiDAR interfacing, and comprehensive testing procedures has resulted in a reliable and efficient solution for optimizing lighting conditions during surgical procedures.

V. CONCLUSION

The successful development of our system marks a pivotal advancement in operation theatre technology, offering a solution that can intelligently sense the presence of objects within a predefined range and dynamically adjust surgical lamp lighting accordingly. This innovation holds immense potential to significantly enhance patient safety during surgeries by minimizing the risk of shadows and ensuring optimal illumination for medical procedures.

Looking ahead, there are several key recommendations for further enhancing operation theatre lighting systems. Firstly, exploring advanced object detection techniques such as machine learning algorithms or advanced sensor technologies could augment the system's capabilities, enabling more precise and efficient detection of objects in the surgical environment. Additionally, improvements to the user interface can streamline operation and make the system more intuitive for medical personnel to use, ultimately enhancing workflow efficiency during surgical procedures. Moreover, investing in research and development efforts to enhance system durability and implement proactive maintenance practices can prolong the lifespan of the equipment and minimize downtime, ensuring uninterrupted support for critical surgical operations.

In essence, the successful implementation of our project represents a significant milestone in the ongoing pursuit of optimizing operation theatre environments. By harnessing the power of technology and innovation, our project has not only addressed a critical need in surgical settings but has also paved the way for safer, more efficient, and ultimately more effective surgical practices. As healthcare continues to evolve, projects like ours serve as beacons of progress, driving positive change and improving the lives of patients worldwide.

REFERENCES

[1] J. Beltrán, C. Guindel, F. M. Moreno, D. Cruzado, F. García, and A. D. L. Escalera, "Birdnet: A 3d object detection framework from lidar information," in *21st International Conference on Intelligent Transportation Systems (ITSC)*, Maui, HI, USA, 2018, pp. 3517–3523.

[2] A. Kim, A. Ošep, and L. Leal-Taixé, "Eagermot: 3d multi-object tracking via sensor fusion," in *IEEE International Conference on Robotics and Automation (ICRA)*, Xi'an, China, 2021, pp. 11 315–11 321.

[3] S. K. Manghat and M. El-Sharkawy, "A multi sensor real-time tracking with lidar and camera," in *10th Annual Computing and Communication Workshop and Conference (CCWC)*, Las Vegas, NV, USA, 2020, pp. 0668–0672.

[4] R. Ravindran, M. J. Santora, and M. M. Jamali, "Multi-object detection and tracking, based on dnn, for autonomous vehicles: A review," *IEEE Sensors Journal*, vol. 21, no. 5, pp. 5668–5677, 2021.

[5] J. J. Sun and C. M. Huang, "Multi-target detection and tracking with semantic segmentation by using lidar sensor," in *IEEE International Conference on Consumer Electronics - Taiwan (ICCE-Taiwan)*, Taoyuan, Taiwan, 2020, pp. 1–2.

[6] X. Zhao, P. Sun, Z. Xu, H. Min, and H. Yu, "Fusion of 3d lidar and camera data for object detection in autonomous vehicle applications," *IEEE Sensors Journal*, vol. 20, no. 9, pp. 4901–4913, 1 May 2020.

Design and Development Of A Ultra Wide Band Antenna Configuration For Radio Jamming Applications

Hasan Ali Dalal[1],Rishi Dubey[2],Sakshi Morey[3],Zoya Shaikh[4],Ashwini Kotrashetti[5]
[1]*Department of Electronics and Telecommunication Engineering*
[1]*The Bombay Salesian Society's, Don Bosco Institute Of Technology, University of Mumbai, Mumbai India*
[1]*faizaldalal184@gmail.com,* [2]*rishidubey@gmail.com,* [3]*sweetymorey@gmail.com,* [4]*zoyashaikh1026@gmail.com,* [5]*ashwini@dbit.in*

***Abstract*—This project elucidates the design and development of a ultra wide band antenna configuration specifically tailored for radio jamming applications at uplink and downlink bands of GSM, UMTS, LTE. In recent years, the need for efficient and versatile radio jamming systems has become paramount, especially in defence, security, and tactical operations. The ultra wide band antenna presented herein is meticulously designed to operate over multiple frequency bands, ensuring a wider coverage and enhanced jamming capabilities. By leveraging simulation tools and iterative prototyping, the proposed configuration ensures optimized performance across different frequency bands from 0.7 to 5.9 GHz . Detailed analysis of the antenna's radiation patterns, gain, bandwidth, axial ratio, polarization and return loss is provided, confirming its suitability for robust and effective radio jamming operations.**

***Index Terms*—return loss, gain, antenna.**

I. Introduction

RF Jamming, or radio frequency jamming, is the concept of blocking a wireless device from communicating with other devices or a wireless network. This is usually done in environments that require high security, and any undesired communication needs to be stopped. Radio jamming, a critical component in modern electronic warfare and defense strategies, requires sophisticated equipment to ensure efficient and effective disruption of targeted communication channels. Traditional antennas, predominantly designed for singular frequency bands, often fall short in offering comprehensive jamming capabilities, particularly in scenarios where threats span a multitude of frequencies. Recognizing this technological gap, this project embarks on an exploration into the design and development of a ultra wide band antenna configuration specifically crafted for radio jamming applications. By transcending the limitations of single-band antennas, this innovative configuration seeks to provide broader frequency coverage. This report digs into the difficulties of the design, simulation, prototyping, and validation of this ultra wide band antenna. For making the Radio Frequency Jammer these elements are are supposed to be considered which are mentioned in the Figure 1.1

Identify applicable funding agency here. If none, delete this.

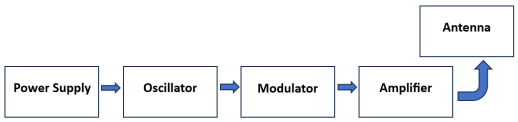


Fig. 1. Block Diagram of Radio Frequency Jamming.

II. Literature Survey

A. Design Of A UWB Unidirectional Radiation Compound Spiral Antenna

This paper presents the design of a modified unidirectional radiation miniaturized compound spiral antenna fed by an exponentially tapered balun. The antenna design combines an equiangular spiral antenna with an Archimedean spiral line and incorporates a modified reflector to achieve a microstrip form. Simulation results demonstrate favorable radiation patterns, axial ratio plots, and VSWR plots across the 5 to 20 GHz range, indicating improved performance compared to traditional UWB antennas. The proposed antenna offers enhanced axial ratio characteristics suitable for UWB communication applications. The growing demand for UWB electronic systems necessitates antennas with superior performance. While equiangular spiral antennas are known for their wide bandwidth and circular polarization, their large dimensions at low frequencies prompt the exploration of miniaturization techniques. Compound spiral antennas, achieved by adding terminals such as an Archimedean spiral line, offer a solution. Unidirectional radiation is essential for specific applications like UWB communication, typically achieved through methods like cavity placement or microstrip configuration. This paper focuses on a unidirectional radiation compound spiral antenna with a metal plane reflector, providing UWB and unidirectional radiation characteristics suitable for specialized applications.The simulated performance of the proposed compound spiral antenna demonstrates its suitability for specialized UWB applications, offering improved axial ratio characteristics compared to traditional UWB antennas. This design integrates miniaturization techniques, unidirectional radiation, and wide

bandwidth operation, catering to the evolving demands of UWB electronic systems.

B. Practical Jamming of a Commercial 5G Radio System at 3.6 GHz

This research paper explores the vulnerability of 5G radio systems, particularly focusing on jamming attacks at the 3.6 GHz frequency. It highlights the increasing interest of global armed forces in adopting 5G technology due to its advanced communication capabilities. However, it acknowledges the significant challenges posed by threats such as intentional radio jamming in the electromagnetic spectrum.The paper specifically examines the impact of jamming on a commercial 5G system, with a focus on determining the required jamming signal strength to disrupt its operation. The study utilizes a 5G base station equipped with massive Multiple Input Multiple Output (MIMO) antenna technology operating at 3.6 GHz frequency.Findings from the study reveal that the 5G system under examination demonstrated adaptive behavior in response to jamming, adjusting its modulation until reaching a threshold point, beyond which communication ceased. The paper discusses how 5G's New Radio (NR) interface incorporates features such as massive MIMO technology, which could potentially enhance its resistance to jamming compared to earlier generations of cellular technology. However, it also acknowledges that despite these advancements, 5G, primarily designed for civilian applications, may still be vulnerable in challenging radio frequency (RF) environments.To empirically assess the resilience of commercial 5G systems to jamming attacks, the paper describes a practical jamming experiment, which it claims is the first of its kind. The experiment aims to evaluate the system's performance under jamming conditions and determine the required jamming power to disrupt its function.The paper provides a comprehensive overview of the theoretical background, experimental setup, performance metrics, results, and discussions on the findings. It concludes with recommendations for future research aimed at enhancing the resilience of 5G systems against radio jamming and other potential threats.

C. Design, Analysis and Construction Of An Archimedean Spiral Antenna and Feed Structure

The research paper delves into the critical role of frequency-independent antennas in a variety of applications, ranging from wideband measurement systems to spread spectrum communication and radar technologies. These antennas, characterized by their ability to maintain consistent patterns, impedance, and polarization across broad frequency spectrums, offer significant advantages over conventional antennas.One of the key advantages highlighted in the paper is the superior performance of wideband arrays compared to individual antennas.The paper then transitions to discussing the design and testing of a specific type of frequency-independent antenna: the Archimedean spiral antenna. Utilizing computational tools like the Electromagnetic Surface Patch Code (ESP), the researchers were able to evaluate the performance of the Archimedean spiral antenna across a wide frequency range. Despite some limitations in accurately predicting antenna patterns at higher frequencies, ESP proved to be a valuable tool in the antenna design process. An Archimedean spiral antenna consists of two arms, with the width between arms defining its characteristics. When the width matches the spacing between arms, it becomes self-complimentary, exhibiting an input impedance. Circular plates at its center facilitate feed attachment. This active region's circumference, typically one wavelength, determines the antenna's low-frequency limit. Orthogonally directed currents along the arms, spaced at quarter-wavelength intervals, produce circular polarization in the radiation, aligned with the spiral's winding direction. For loosely wound spirals, subsequent active regions may form if attenuation is minimal, with each active region expanding the antenna's operational bandwidth. In conclusion, while acknowledging the constraints of ESP in accurately predicting antenna performance, the paper underscores its significance as a valuable aid in designing frequency-independent antennas like the Archimedean spiral. This research contributes to advancing the understanding and development of antennas capable of operating efficiently over exceptionally large bandwidths, thereby addressing the evolving demands of modern communication and sensing systems.

D. An Optimized and Integrated Antenna Design for the Future Jamming System against RCIEDs

In this research paper an integrated antenna has been designed for the future jamming system. It discusses the challenges and design considerations for jamming antennas used to counter Radio-Controlled Improvised Explosive Devices (RCIEDs). There are some advantages of it.Radio-frequency jammers are discussed as an effective response to RCIED threats, interfering with communication between remote controls and detonators. The requirements for jamming antennas, wideband operation from (20 MHz to 6 GHz) and omnidirectional radiation at every single frequency in the bandwidth. The main aim of project is to design a broadband jamming antenna system , for the high frequency range (500 MHz to 6 GHz).The jamming antenna bandwidth is divided into 2 sub-bands: low band(from 20 MHz to 700 MH) and high band(500 MHz to 6 GHz). Focusing on the high bang range, which can cover the most popular frequencies available in the commercial band . The project has been started with the platform modelling. Several host vehicles were modelled in 3D by the mean of FEKO. A monopole antenna which has an ideal omnidirectional pattern was simulated on top of a military vehicle , located at different locations and the antenna size is adapted according to the simulated frequency. Spiral antenna is designed for the high frequency range from 500 MHz to 6 GHz.It is mentioned that a jamming system may consist of multiple antennas to effectively cover 360 degrees around the vehicle. The host platform changes significantly the antenna radiation. The antenna performance should be optimised in the integration with its platform instead of stand-alone antenna. Most of the area is covered by sufficient electric fields at 500 MHz. The research should be continued with

others frequencies in the bandwidth of interest and with other possible combinations of antennas.

E. Low-cost Jamming System Against Small Drones Using a 3D MIMO Radar Based Tracking

The paper introduces a sophisticated yet economical drone tracking and jamming system leveraging a combination of a 3D Multiple Input Multiple Output (MIMO) radar and an RF jammer. Comprising three primary components, the system exhibits a robust architecture: Firstly, a 3D Frequency-Modulated Continuous Wave (FMCW) MIMO radar, which diligently scans the designated area and generates comprehensive three-dimensional images of detected targets.The signal generator is adept at producing a band-limited noise signal (5MHz), modulated on a carrier within the 2.4GHz to 2.5GHz spectrum. Thirdly, a laptop assumes the responsibility of radar signal processing, executing the tracking algorithm, and generating control signals for both the MIMO radar and the servo controller board. Operational functionality unfolds as follows: The radar initiates the detection process, identifying drones within the monitored area. Subsequently, upon drone detection, the tracking algorithm commences, diligently monitoring and tracing the drone's position. In tandem, the laptop generates control signals, steering the directional antenna via the servo controller board to align with the drone's coordinates. The jamming signal, emitted through the directional antenna, disrupts the drone's communication link effectively. The versatility of the system extends to shielding predefined areas against unauthorized drone intrusions, proving invaluable for long-term security surveillance or the temporary fortification of mass gatherings and events. In essence, the proposed system offers a comprehensive solution, seamlessly integrating detection, tracking, and jamming functionalities, thus meeting the escalating demand for robust countermeasures against illicit drone activities.

F. Rectangular microstrip antenna with ISM band.

The research paper emphasizes the significance of antennas in communication systems, particularly highlighting the growing popularity of microstrip antennas for their compact size and ability to operate across multiple bands. Recent advancements have rendered these antennas both efficient and cost-effective, making them indispensable in wireless applications. Designing microstrip antennas using simulation programs is a common practice, typically involving dielectric constants ranging from 2.2 to 3.7. Adjusting the substrate height is a crucial factor that can enhance antenna efficiency and bandwidth, although excessive height may lead to surface wave issues. Minimizing losses, including dielectric and conductor losses, is paramount to achieving optimal antenna performance. The focus of this article is on the design of a rectangular microstrip antenna with the objective of boosting gain while minimizing reflection attenuation to ensure efficient radiation.Various techniques for powering microstrip antennas are discussed, including contacting and non-contacting types. Contacting types employ a microstrip line and probe to supply current to the radiating patch, while non-contacting types rely on electromagnetic field coupling. Common feeding mechanisms such as coaxial probe and microstrip line are examined, with Microstrip Line Feeding highlighted for its direct connection between the conductive microstrip and the patch, simplifying manufacturing and impedance matching processes.The design optimization targets a rectangular patch coil operating at 2.4GHz frequency. FR4, characterized by a permittivity of 4.6, is chosen as the dielectric substrate due to its cost-effectiveness and widespread availability. This selection underscores the practical considerations in substrate choice, balancing performance requirements with economic factors. In conclusion, the paper presents a comprehensive overview of the design considerations and techniques employed to optimize the performance of microstrip antennas, offering insights into enhancing gain and minimizing attenuation for efficient radiation in wireless communication systems.

G. Ultra-Wideband Low-Cost High-Efficiency Cavity-Backed Compound Spiral Antenna.

This research paper elaborates on Imaging and detection radars often use narrow pulses with wide frequency bandwidths, requiring antennas meeting challenging ultra-wideband (UWB) design specifications. Spiral antennas, especially when circular polarization (CP) is needed, are preferred for their mechanical robustness and relative cost-effectiveness. However, they require balanced feeds to high input impedances, necessitating UWB baluns to match the typical 50-ohm feed. Compound spirals, which combine equiangular and Archimedean spirals, offer a compromise between radiation efficiency and size. Achieving unidirectional radiation with compound spirals is challenging, with various methods proposed including complex cavities and resistive terminations. An absorber-free cylindrical cavity with simple center-raised geometry is proposed here, providing unidirectional patterns and a wide impedance bandwidth from 350 MHz to 5.5 GHz while maintaining efficiency and avoiding additional losses, even with low-cost substrates. However, the absorber-free cavity affects the uniformity of gain and AR patterns, particularly at higher frequencies. The proposed antenna comprises a compound spiral, cavity, and balun, meeting design requirements in the 500 MHz to 5 GHz bandwidth, including a return loss of 10 dB or better, front-to-back ratio of 6 dB or more, and minimum axial ratio within 45 degrees of boresight less than 6 dB. Fabrication must be low-cost and straightforward, with design conducted using HFSS and verified with CST. Both right-hand and left-hand polarized antennas were implemented, showing similar performance. Spiral parameters were optimized for impedance match from 500 MHz to 5 GHz, achieving better than 10 dB reflection loss from 350 MHz to 5.5 GHz. The Archimedean portion of the spiral is crucial for wideband impedance matching, enabling gradual current decay towards the arms' ends within a compact diameter of 360 mm. This ensures minimal impact on efficiency, particularly when using FR-4 substrate, where material losses outweigh copper trace losses. The antenna's gain remains fairly consistent regardless

of the proportion of area occupied by the Archimedean spiral, as long as impedance match requirements are met.

III. Problem Statement

To design and develop a configuration of the antenna operating in the frequency band of the range 0.7 GHz to 5.9 Ghz with a minimum gain of 5dB and -10dB Return Loss.

IV. Proposed System

Radio Jamming Requires Circular Polarized antenna, with high gain as 5dB, and the antenna is required to be directional.

A. Antenna Feed Line

In a radio antenna, the feed line (feed line), or feeder, is the cable or other transmission line that connects the antenna with the radio transmitter or receiver. In a transmitting antenna, it feeds the radio frequency (RF) current from the transmitter to the antenna, where it is radiated as radio waves.

B. Antenna Cavity

Rectangular and circular cavity. Antennas performance can be improved using two kinds of backing structure like cavity antennas. Cavity backing helps to reduce back radiation. The antenna consists of a slot cut in a ground plane and backed by shorting strips, forming a backing cavity. The volume of the cavity typically influences the bandwidth. A larger volume often yields a higher bandwidth. The material within the cavity, can be replaced with a dielectric medium.

V. Software and Hardware Used

Software used-
Ansys HFSS for Windows 11 and AutoCAD version 18.4

Hardware used-
FR-4 (PCB Material), Connectors, Fabrication.

VI. Implementation

Designing and developing an ultra-wide band (UWB) antenna configuration for radio jamming applications involves several steps, including antenna design, simulation, prototyping, and testing. The frequency range on which the antenna is going to operate is 0.7GHz to 5.9 GHz the radiation pattern is circular polarized and it is directional antenna with the gain of 5dB and return loss less than -10dB. The structure of Archimedean Spiral Antenna is designed and simulated through software HFSS (High Frequency Structure Simulator). Simulation of the design of antenna is configured to analyse its performance across the desired frequency range. To improve the performance we have designed the cavity. Parameters such as return loss, radiation pattern,gain and impedance matching is evaluated. We designed the antenna on Auto CAD for fabrication purpose. Fabricated the prototype of the designed antenna using PCB and copper material and with manufacturing techniques. Also conducted laboratory testing of the prototype antenna to validate its performance. Measured the key parameters such as return loss, bandwidth, and radiation pattern using vector network analyzers and antenna measurement chambers. Compared the measured results with simulation data to verify the accuracy of the design. Identified if any discrepancies between simulated and measured results and iterate on the design. To improve the performance we have designed the cavity.

SR.NO	Parameters	Formula
1	Inner Radius (r1)	$\frac{c}{2\pi \times Fh}$
2	Outer Radius (r2)	$\frac{c}{2\pi \times Fl}$
3	Wavelength(λ)	$\frac{c}{F}$
4	Spacing	$2\pi \times a \times sin\psi$
5	Width	$a \times \delta \times sin\psi$
6	Log Spiral Curve	$r^{-1}e^{(a(\psi+\delta)}$

Fig. 2. Parameter and Formula for design details

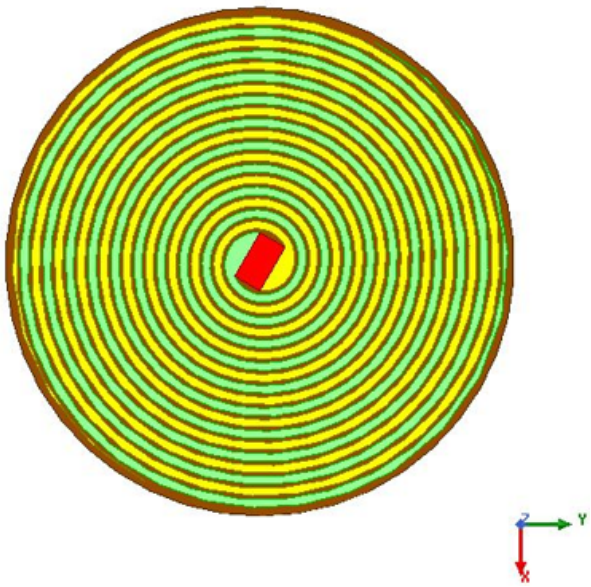


Fig. 3. Simulated Archimedian Spiral Antenna

Simulation result of Archimedian spiral antenna top view is shown in the Fig 4.1. By adding required parameters on HFSS that is mentioned in design details which are frequency band that ranges between 0.7 - 5.9 GHz, wavelength of 0.3703 metre, inner radius of 0.8 cm, outer radius of 6.8 cm, diameter of 13.6510 cm, no. of turns are 9.59.

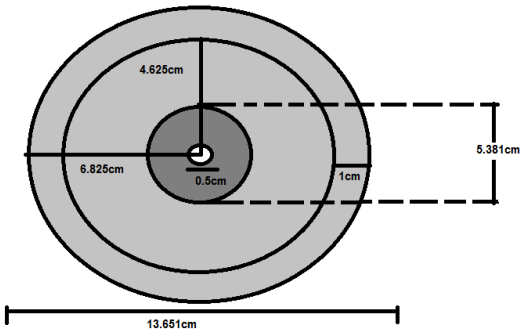


Fig. 4. Simulated Archimedian Spiral Antenna

Formula and calculation for spiral antenna is given-
For Inner Radius: r1= $\frac{c}{2\pi \times F \times h}$

r1= $\frac{3\times10^8}{2\pi\times5.9\times10^9}$=0.8cm

For Outer Radius: r2= $\frac{c}{2\pi \times F \times l}$

r2= $\frac{3\times10^8}{2\pi\times0.7\times10^9}$=6.8cm

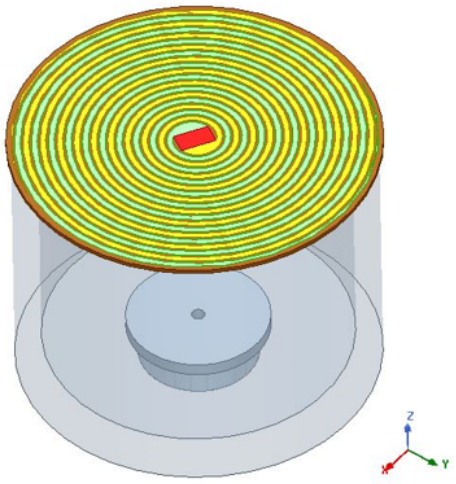


Fig. 5. Top view Design of Archimedean Spiral Antenna

With the current design of antenna, the result of the gain was not as expected. For improving gain a cavity backed is made. Cavity backed has inner radius is 6.6255cm and outer radius is 6.825cm. Also inner height is 9.7 cm and outer height is 10.7 cm

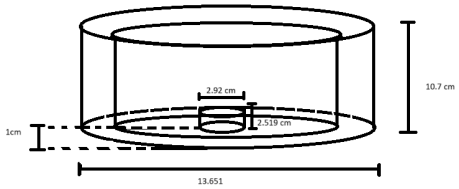


Fig. 6. Simulated Archimedian Spiral Antenna

Formula and calculation for design cavity backed is given-

For inner height i.e $\lambda max = c/f.$

$\lambda max = \frac{3\times10^8}{5.9\times10^9} = 5.08cm$
$\frac{\lambda max}{4} = \frac{5.08}{4} = 1.27cm$

For outer height i.e $\lambda max = c/f.$
$\lambda max = \frac{3\times10^8}{0.7\times10^9} = 42.8cm$

$\frac{\lambda max}{4} = \frac{5.08}{4} = 10.7cm$

A. Abbreviations

RF-Radio Frequency, NR-New Radio, MIMO-Multiple-input multiple-output, RCIEDs-Radio Controlled Improvised Explosive Devices, RCS-Radar Cross Sectio

VII. Results

*A. **Simulation Results On HFSS***

We used HFSS Software to design the sprial antenna for which frequency band ranges from 0.7GHz - 5.9 GHz. By using Design Parameters mentioned in Fig.2 we did simulation and created Spiral Antenna. After creating Spiral Antenna we got results of the return loss, gain and Axial ratio.

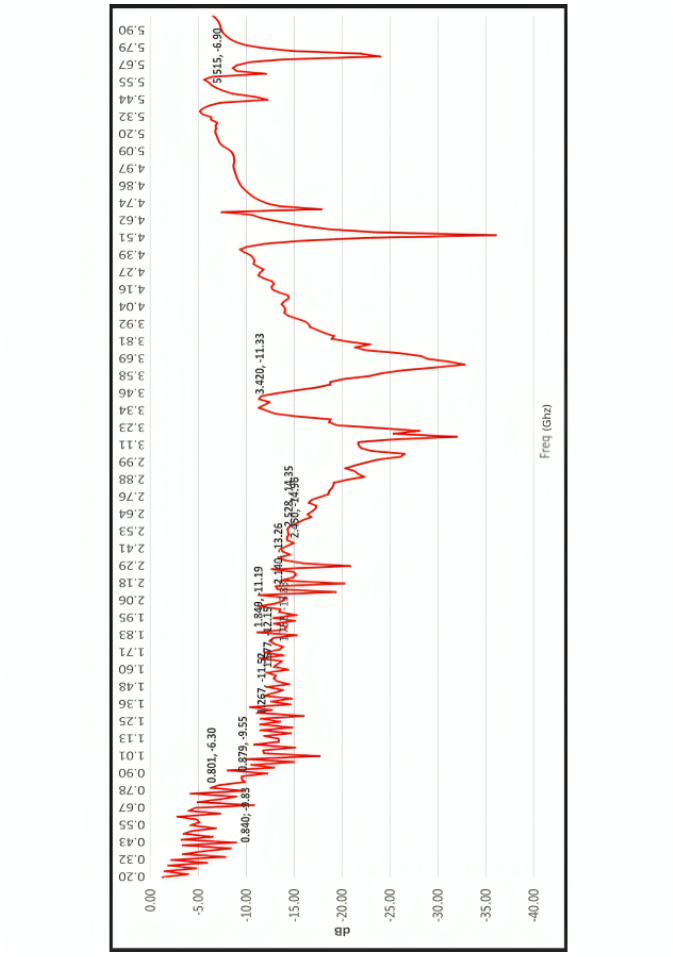


Fig. 7. **Result of Return Loss.**
Return loss is the measurement of the reflected wave or signal strength traveling or returning back to a transmitter from an antenna.
We achieved return loss of -10 db for frequency band that ranges from 0.7 GHz to 5.9 GHz. With the above Fig the result of return loss is clearly visible which is represented in graphical manner.

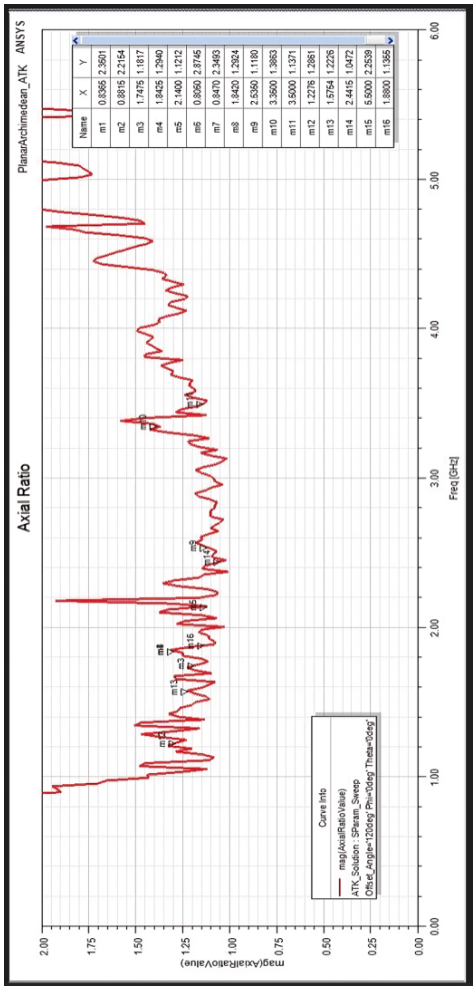
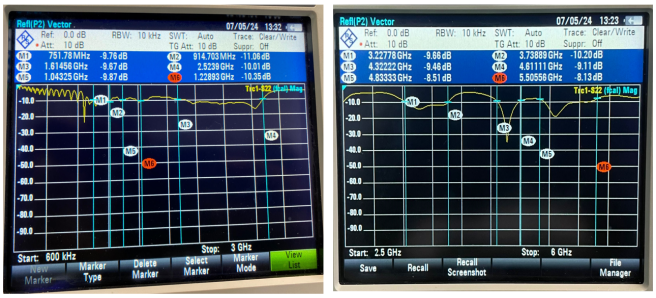


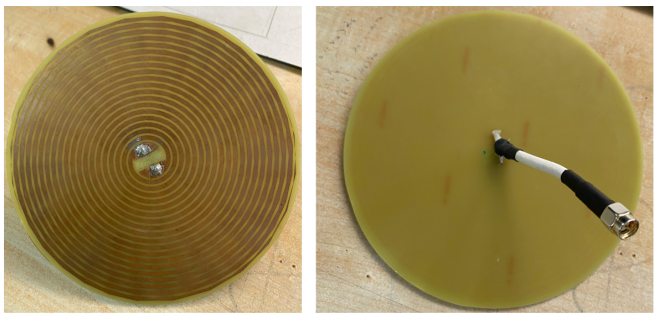
Fig. 9. **Result of Axial Ratio**
The axial ratio of an antenna is defined as the minor axis to major axis ratio of an electromagnetic wave. It is a measure of the deviation from an ideal circular polarized antenna pattern over a given angular range.This is the Axial Ratio that we achieved for the frequency band ranging between 0.7GHz to 5.9Ghz. With the above Fig the result of return loss is clearly visible which is represented in graphical manner.



➢ Fig 1. Return Loss measured from 0.7GHz to 3GHZ

➢ Fig 2. Return Loss measured from 2.5GHz to 6GHZ

Fig. 8. Measured Return Loss On VNA after fabrication



➢ **After Fabrication Antenna Design.**

Fig. 10. Fabricated Spiral Antenna top view and bottom view

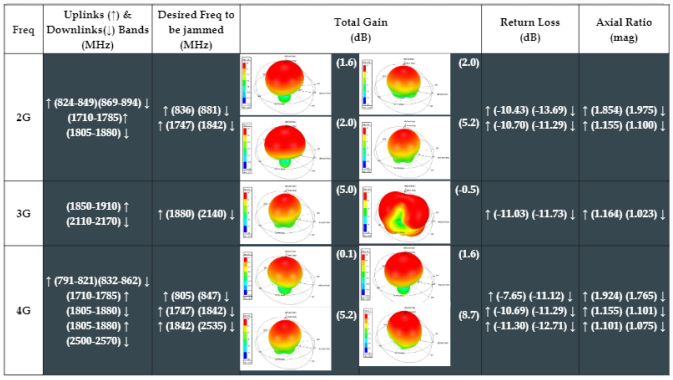


Fig. 11. **Result of Gain through simulation**
Gain of Antenna is a key performance parameter which combines the antenna's directivity and radiation efficiency.

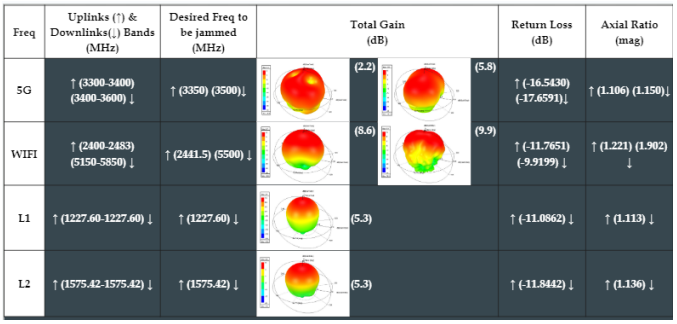


Fig. 12. **Result of Gain through simulation**
We achieved desired average gain of 5 db for frequency band that ranges from 0.7 GHz to 5.9 GHz



Fig. 13. Measured result of Antenna on VNA

VIII. Conclusion

We have designed ultra wide band antenna configuration for radio jamming applications with frequency band that ranges from 0.7 GHz - 5.9 GHz. With the help of simulation we got results on gain, return loss, axial ratio. The average gain of 5 dB is achieved and return loss less than -10 dB on simulation is achieved. After testing the Fabricated Spiral Antenna, we compared the simulation results with it and got return loss of -10db.

Acknowledgment

A project is a teamwork that involves the contribution of many people. We would like to thank everyone who has contributed by taking an interest in our work and motivating us all the way through. Our sincere thanks to Dr. Ashwini Kotrashetti, project guide, for guiding us throughout the project and also for helping us with all the difficulties we faced throught out the project work. We would like to thank Ms. Namita Agarwal, Head of Department for supporting us and helping us for project. We would also like to thank Dr. Sudhakar Mande, Principal and Management of Don Bosco Institute of Technology for allowing us to use the college campus and infrastructure throughout our project.

References

- [1] C. Baard, Y. Liu, and N. Nikolova, "Ultra-wideband low-cost high-efficiency cavity-backed compound spiral antenna," Electronics, vol. 9, no. 9, p. 1399, 2020
- [2] M. A. Birutis and A. Mykkeltveit, "Practical jamming of a commercial 5g radio system at 3.6 ghz," Procedia Computer Science, vol. 205, pp. 58–67, 2022.
- [3] T. Multerer, A. Ganis, U. Prechtel, E. Miralles, A. Meusling, J. Mietzner, M. Vossiek, M. Loghi, and V. Ziegler, "Low-cost jamming system against small drones using a 3d mimo radar based tracking," in 2017 European radar conference (EURAD). IEEE, 2017, pp. 299–302
- [4] V. Ramamurthy and S. Patel, "Design of planar archimedean spiral antenna for wi-max us- ing different materials," International Journal of Engineering development and Reserach, vol. 02, pp. 1947–1951, 04 2014.
- [5] G. B. TR et al., "Rectangular microstrip patch antenna at ism band," in 2018 second inter- national conference on computing methodologies and communication (ICCMC). IEEE, 2018, pp. 91–95.
- [6] T. M. Tran and M. Piette, "An optimized and integrated antenna design for the future jam- ming system against rcieds," in 2018 IEEE-APS Topical Conference on Antennas and Propagation in Wireless Communications (APWC). IEEE, 2018, pp. 862–865.
- [7] P. Werntz and W. Stutzman, "Design, analysis and construction of an archimedean spiral antenna and feed structure," pp. 308–313 vol.1, 1989
- [8] Y. Zhao and W. Hu, "Design of a uwb unidirectional radiation compound spiral antenna," in 2015 IEEE 6th International Symposium on Microwave, Antenna, Propagation, and EMC Technologies (MAPE). IEEE, 2015, pp. 158–161

Real Time ICU Patient Monitoring & Visualisation Of Critical Parameters Of Patients Health For Hospital Professionals

Kshitij Bare[1], Jignesh Bhandi[2], Aditya Moozhayil[3], Omkar Mundhe[4], Hemalata Mote[5]
[1] Department of Electronics and Telecommunication Engineering
[1]The Bombay Salesian Society's, Don Bosco Institute Of Technology, University of Mumbai, Mumbai India
[1]barekshitij90@gmail.com, [2]jigneshbhandi18@gmail.com, [3]adityasaju071@gmail.com, [4]omkarmundhe0509@gmail.com, [5]hemalata@dbit.in

***Abstract*—During the COVID-19 pandemic, healthcare systems faced unprecedented strain, resulting in challenges in providing adequate treatment. To address this, we initiated a project aimed at alleviating the burden on healthcare workers and ensuring all patients receive timely care. Our solution involves the development of a real-time patient monitoring system for intensive care units (ICUs). Utilizing sensor technologies like the ESP8266, we collect vital patient data and transmit it via the MQTT protocol. A web interface enables easy access to this data, aiding hospital authorities in visualizing patient health. Additionally, the data is stored on ESP32 modules for future analysis. By streamlining data collection, analysis, and visualization, this project facilitates quicker medical decision-making and enhances resource utilization within healthcare environments, ultimately mitigating strain on the healthcare system during times of crisis.**

***Index Terms*—Data Analytics, Data Visualization, MQTT protocol, Web interface, Micro SD card, Healthcare system**

I. Introduction

Real-time ICU monitoring is a critical aspect of modern healthcare, allowing for continuous surveillance and analysis of patients within the Intensive Care Unit (ICU). This dynamic approach to patient care has become indispensable for improving outcomes and guiding medical decision-making in critical settings. The imperative of real-time ICU patient monitoring lies in its ability to provide clinicians with timely and accurate information about patients' physiological status. By continuously monitoring parameters such as heart rate, blood pressure, oxygen saturation, and respiratory rate, healthcare providers can identify changes in patients' health status and intervene swiftly to prevent adverse outcomes. Database systems play a crucial role in real-time ICU monitoring by enabling the storage, management, and analysis of vast amounts of patient data collected from various monitoring devices and sensors. These databases serve as repositories of valuable information, allowing healthcare teams to track patient progress over time, identify trends, and make informed decisions about their care. Moreover, the visualization of patient data through advanced database visualization tools is essential for rendering complex medical information comprehensible and actionable for clinicians.

II. Acknowledgement

A project is a teamwork which involves the contribution of many people. We would like to thank everyone who have contributed by taking interest in our work and motivating us all the way through. Our sincere thanks to our project guide Ms. Hemalata mote, for motivating, co-operating and guiding us through- out the project work, with his effective skills and huge knowledge base. We would like to thank Ms. Namita Agarwal, Head of Department and Ms. Madhavi S. Pednekar, Project Coordinator for their continuous valuable guidance, support, suggestions and their precious time in every possible way throughout the project activity. We would like to thank Mr. Ravi Hedau for his continued support in helping us out with the troubleshooting of errors. Also, we are very grateful to the design and development EPMD Pvt Ltd.

III. Project Overview

In our project we have undertaken a thorough analysis to define its parameters. We've crafted a framework that identifies the problem statement and defines the scope of our undertaking.

A. Aim

Our project focuses on developing a real-time ICU patient monitoring system to address healthcare challenges during

COVID-19. Using sensor technologies and data analysis, it streamlines processes and optimizes resource allocation. Real-time visualization aids in identifying health trends, like heart rate and oxygen levels. An Alerts and Notifications system promptly notifies providers of critical conditions. Prioritizing critical patient data facilitates quick access for urgent care. This system aims to improve patient care and enable faster medical decisions. By enhancing resource visualization, it supports healthcare professionals in delivering quality care during the pandemic.

B. Problem Statement

To build an user friendly interface for healthcare professionals which will collect data of patients health and will provide information regarding patient's health for quick and informed decision making.

C. Scope of the project

- Continuous Monitoring: Implement a system capable of real-time tracking of patient movements.
- Notification System: Establish a mechanism to promptly alert doctors and staff members upon detection of abnormal activity.
- Immediate Response: Enable healthcare professionals to take swift action based on the received alerts.
- Enhanced Patient Safety: Improve patient safety by actively monitoring their health status and movements.
- Resource Optimization: Optimize resource allocation by directing attention and resources to patients requiring immediate intervention, thereby improving overall efficiency.

D. Motivation

The motivation behind our project "Real-time ICU Patient Monitoring and Visualization of Critical Parameters of Patients' Health for Hospital Physicians" stems from the urgent need to improve healthcare delivery, especially during critical situations like the COVID-19 pandemic. We aim to provide hospital physicians with real-time access to vital health data such as temperature, blood pressure, and heart rate, gathered through advanced sensors. By presenting this data through an web interface with clear visualizations like graphs and charts, our goal is that doctors to make quicker and more informed medical decisions. Ultimately, our project works to enhance patient care outcomes in ICUs by ensuring timely interventions based on accurate, up-to-date health information. This approach not only supports healthcare professionals in delivering personalized care but also contributes to better management of hospital resources, thereby improving overall efficiency and patient outcomes.

E. Challenges

Our project "Real-time ICU Patient Monitoring and Visualization of Critical Parameters of Patients' Health for Hospital Physicians" faces several challenges that need careful consideration. These include:

1. Data Accuracy and Reliability: Ensuring that the sensors accurately capture and transmit critical health parameters such as temperature, blood pressure, and heart rate without errors or interruptions is crucial. Any inaccuracies could potentially lead to incorrect medical decisions.

2. Data Security and Privacy: Handling sensitive patient data requires stringent measures to protect confidentiality and comply with healthcare regulations. Safeguarding information from unauthorized access or breaches is essential to maintain trust and legality.

3. Integration and Compatibility: Coordinating various sensors, data transmission protocols like MQTT, and the web interface seamlessly can be technically complex. Ensuring all components work together effectively without compatibility issues is a significant challenge.

4. Real-time Monitoring and Response: Providing instant access to data and ensuring that healthcare professionals can interpret and respond to it promptly is critical. Delays or inefficiencies in data transmission or visualization could impact patient care.

5. User Interface Design: Designing a user-friendly interface that presents complex medical data in a clear and intuitive manner for busy healthcare professionals is challenging. The interface must support quick decision-making while accommodating diverse user needs and preferences.

6. Scalability and Maintenance: As the system is deployed in ICUs, scalability to handle increasing data volumes and the ongoing maintenance to ensure reliability and performance are ongoing challenges.

Addressing these challenges requires a multidisciplinary approach involving healthcare professionals, engineers, data scientists, and designers to create a robust and effective solution that truly enhances ICU patient monitoring and care.

F. Objectives

- To select the sensors sensors, such as pulse oximetry and LM35 for temperature monitoring, to collect patient data.
- To choose the ESP32 microcontroller for gathering sensor data because it's reliable and works well with various sensors.
- To use the ESP32's Wi-Fi feature to send data securely through the MQTT protocol.
- To create a simple web interface for accessing and visualizing real-time patient health data.
- To set up an Alert and Notification system to quickly alert healthcare providers about critical conditions.
- To data prioritization method is added in order to make critical patient top in created database.

G. Outcome

- Implementing a system capable of continuously monitoring patient data, such as vital signs and sensor readings, in real-time.
- Ensuring the secure transmission of patient data between devices using the MQTT protocol over a secure connection.

- Developing a web interface for healthcare professionals to access and visualize patient data in real-time, facilitating remote monitoring.
- Setting up an alert system to promptly notify healthcare providers of any critical conditions or anomalies detected in the patient data.
- Establishing a reliable data storage mechanism, such as using an SD card module, to securely store patient data for future analysis and reference.

IV. Literature Survey

There has been an upsurge in the educational technology sector over the last few years. Plenty of software solutions have been designed to serve the needs of a wide range of educational institutions. The majority of such solutions are focused not only on resolving or further improving a wide range of practical administrative issues and internal processes, but also on supporting and promoting the goals and objectives of the Institute.

A. Fall Prevention from Scaffolding Using Computer Vision and IoT-Based Monitoring

In [1] the author suggested that the integration of computer vision and IoT-based monitoring for scaffolding safety offers valuable insights applicable to real-time patient monitoring systems. By deploying sensors and devices to collect vital data such as heart rate, blood pressure, and activity levels, healthcare providers can leverage real-time information transmission to a centralized platform. This approach enables continuous analysis of patient metrics using machine learning algorithms to detect anomalies and trigger timely alerts for healthcare interventions. Similar to identifying unsafe behaviors in scaffolding scenarios, computer vision techniques can be employed to recognize concerning patterns in patient data, facilitating proactive care and risk management. Overall, adopting a comprehensive framework that integrates diverse sensor data allows for more effective and personalized patient monitoring, ultimately improving healthcare outcomes and patient safety.

The integration of computer vision enables automated analysis of patient behavior and vital signs, complementing traditional monitoring methods to create a comprehensive and efficient patient safety framework. Ultimately, adopting these technologies fosters a more responsive and preventive healthcare environment, optimizing patient outcomes and promoting a higher standard of care.

B. Automatic and Continuous Blood Pressure Monitoring

In [2] L. Li suggests that ensuring monitoring of automatic and continuous blood pressure monitoring is imperative in the prevention of cardiovascular diseases, particularly hypertension. The ongoing assessment of medication effects and the accurate diagnosis of clinical hypertension greatly benefit from continuous monitoring. However, existing wearable blood pressure monitors face challenges related to portability, electrical safety, accuracy, and precise position alignment.

The author introduces a solution to these limitations through the development of an optical fiber sensor-assisted smartwatch designed for precise and continuous blood pressure monitoring.The innovation lies in the incorporation of a fiber adapter within the smartwatch, enabling the detection of pulse wave signals. Hence with the help of such sensor we can help establish a good baseline of the patients underlying data and this can be crucial in assessment of medications to be delivered.

To enhance the sensing area's coverage and ensure optimal conformity to the body, a liquid capsule is utilized.The integration of optical fiber technology into the smartwatch presents a promising paradigm for digital health. By offering a practical and reliable solution to the limitations of current wearable blood pressure monitors, this optical fiber sensor-assisted smartwatch can be used as an innovative contribution to the field of continuous health monitoring. Such devices help in gaining an understanding of patient health accurately and precisely.

C. A Survey on Ambient Intelligence in Healthcare

In [3] Acampora suggests to use Ambient Intelligence in information technology which can be aimed at empowering people's capabilities by means of digital environments that are sensitive, adaptive,and responsive to human needs, habits, gestures, and emotions. This futuristic perspective envisions daily environments that enable innovative human-machine interactions characterized by pervasive, unobtrusive, and anticipatory communications. AmI technology stands out as a promising tool for developing real-life solutions, particularly within the healthcare domain.Even in our project we can use this as a major contribution.

This survey delves into the emergence of AmI techniques in healthcare, providing the research community with essential insights. The author begins with an examination of the infrastructure and technology necessary for realizing the vision of AmI, encompassing smart environments and wearable medical devices. These components lay the foundation for creating digitally intelligent spaces that seamlessly integrate with human activities. It then delves into the state of the art artificial intelligence (AI) methodologies deployed in developing AmI systems in healthcare.

This includes an overview of various learning techniques, crucial for adapting to user interactions, reasoning techniques for understanding user's goals and intentions, and planning techniques for orchestrating activities and interactions. Furthermore, the survey addresses the potential applications of AmI technology in supporting individuals affected by physical or mental disabilities or chronic diseases. By leveraging AmI capabilities, tailored solutions can be devised to enhance the quality of life for individuals facing health challenges. The discussion encompasses how AmI technology can provide personalized assistance and intervention, making it an invaluable asset in healthcare scenarios.

D. Design of a Physiological Monitoring Device for Holistic Telemedicine Applications

In [4] Kullayappa suggests to focus on enhancing the telehealth experience to closely resemble direct in-person appointments, particularly within the realm of real-time ICU patient monitoring and database visualization. Our initiative aligns with the recognition that a comprehensive understanding of patient information is pivotal for effective medical care, prompting the development of a novel prototype that integrates state-of-the-art software and hardware components.

It incorporates a multifaceted approach to physiological monitoring crucial for ICU patients. This encompasses the measurement of skin temperature, SpO2 (oxygen saturation), pulse rate, heart rate, breath rate, and Non-invasive Blood Pressure (NIBP). The precision of SpO2 measurements is ensured through the application of Beer-Lambert's law, while a single synchronous ECG and PPG sensor is employed for accurate NIBP measurements. This holistic approach enables real-time monitoring of critical parameters, enhancing the quality of remote healthcare.Moreover it integrates high-quality video conferencing capabilities, facilitating seamless communication between patients and healthcare practitioners.

This feature aims to create an immersive telehealth experience, allowing practitioners to visually assess patients in real time, thereby bridging the gap between traditional face-to-face consultations and remote telemedicine appointments. By integrating advanced software and hardware components, focusing on critical physiological parameters, and incorporating video conferencing capabilities, our initiative represents a significant step forward in the application of telehealth for critical care scenarios.

V. Methodology

The mainly process for making the Real Time ICU Patient Monitoring and Visualization of Critical Parameters of Patients Health for Hospital Professionals consist of three steps: Data Collection Data storage Data Processing and analysis.

A. Data Collection

1) Sensor Integration: Various sensors are integrated into the monitoring system to capture a wide range of physiological parameters. Including

- Electrocardiogram (ECG) sensors for monitoring heart activity.
- Blood pressure sensors for measuring arterial blood pressure.
- Temperature sensors for monitoring body temperature.
- Pulse oximeters for measuring oxygen saturation levels in the blood.
- Other specialized sensors as required by specific patient conditions.

The sensors continuously collect patient data, which is transmitted in real-time to the monitoring system via wired or wireless connections. This ensures that hospital professionals have access to up-to-date information about the patient's condition.

B. Data Storage

1) SD Card Module: The monitoring system is equipped with a dedicated SD card module for storing the vast amount of patient data collected over time. The SD card offers ample storage capacity and is easily accessible for data retrieval and analysis. Redundancy Measures: To ensure data integrity and reliability, redundant storage mechanisms may be implemented, such as backup SD cards or cloud-based storage solutions.

C. Data Processing and Analysis

At the process of an Upon receipt, the raw data undergoes preprocessing to remove noise, artifacts, and other disturbances that may affect the accuracy of the measurements. Relevant features are extracted from the preprocessed data to characterize various aspects of the patient's health status, such as heart rate variability, blood pressure trends, and respiratory patterns. Algorithmic Analysis:Advanced algorithms are employed to analyze the extracted features and detect anomalies, trends, and patterns indicative of changes in the patient's condition. These algorithms may include machine learning techniques for predictive modeling and classification.

D. Data Visualization

The processed data is visualized in real-time through a user-friendly interface, which may include graphical representations, trend charts, and alert notifications for abnormal findings. This enables hospital professionals to monitor the patient's health status at a glance and take timely action as needed.

The Real-Time ICU Patient Monitoring System combines advanced sensor technology, robust data storage capabilities, and sophisticated data processing algorithms to deliver actionable insights into patients' health status in the ICU setting. By providing real-time monitoring and visualization of critical parameters, it empowers hospital professionals to deliver high-quality care and improve patient outcomes.

VI. Approach & Analysis

A. Data collection

Sensors in the ICU collect patient data, including vital signs, ECG, blood pressure, temperature, and more. This data can be collected continuously and transmitted to a central system. Data Processing involves microcontrollers running algorithms to process and analyze the collected data in real time. Anomalies and trends are detected. Data is stored in a secure and scalable database, ensuring that it's easily accessible and can handle a large volume of information. Data is processed to remove noise, perform real-time analytics, and extract valuable insights.

B. Alert and notification

The system continuously monitors patient data, including vital signs and sensor readings, in real time. Algorithms and predefined thresholds are used to detect critical conditions or anomalies.When an abnormality or critical event is detected, the system . triggers an alert.

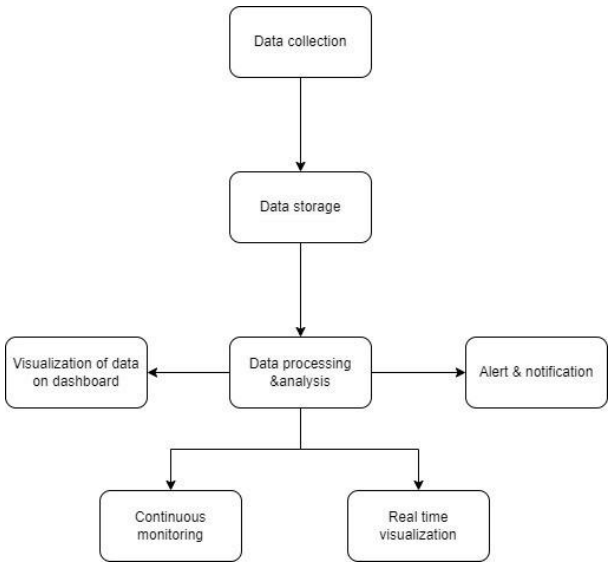


Fig. 1. Flow chart of process of monitoring and visualization patients health

C. Continuous monitoring

In a real-time ICU patient monitoring and database visualization system with cloud storage involves the uninterrupted and real-time collection, processing, and analysis of patient data from sensors and monitoring devices in the ICU. Real time visualization: Real-time visualization in a real-time ICU patient monitoring and database visualization system with cloud storage refers to the dynamic and instantaneous presentation of patient data through graphical and interactive displays. Visualization of data on dashboard: Patients all data will be visible on dashboard as graphs etc.

D. Visualization of data :

The web server serves as a platform for showcasing real-time patient data collected from temperature and pulse sensors, enabling hospital professionals to remotely monitor patients' health. Upon accessing the website, users are directed to a login page where they can create an account to store patient data in an Excel database updated every 2 seconds. Once logged in, users can navigate through tabs such as "Real-time Data," where temperature and pulse readings are graphically displayed, complete with a threshold feature triggering email alerts to hospital professionals upon crossing. Finally, the "Logout" option ensures data integrity and security by enabling doctors to conclude their session and transition to another patient's database as needed.

VII. Implementation

To implement the project, start by wiring the LM35 temperature sensor to GPIO pin 36 and the pulse sensor to GPIO pin 39 on the ESP32. GPIO pins 36 and 39 are chosen for their analog input capability, ideal for reading data from these sensors. Ensure proper connections for accurate sensor data acquisition. Next, establish inter-device communication using the MQTT protocol, with MQTTX serving as the broker.

This setup enables seamless data exchange between the interconnected ESP32 units, facilitating message transmission and command sharing. Through MQTTX, a robust and organized connection is established, enhancing coordination and collaboration in project operations.

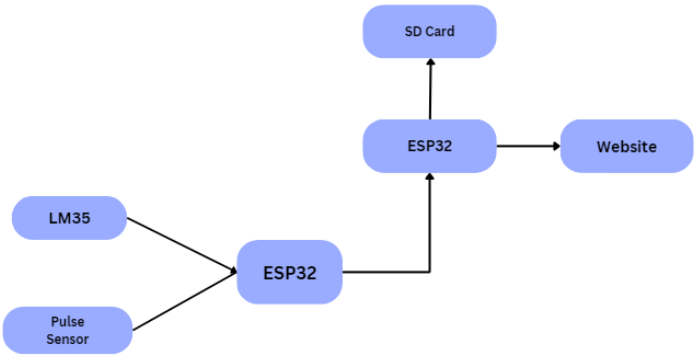


Fig. 2. Block Diagram

1) Block Diagram: LM35 and Pulse Sensor are connected to an STM32 microcontroller, which communicates with a central node via the MQTT protocol. Data collected is stored on an SD card module and eventually visualized on a webpage.

2) Historical patient data using SD card module: By using the MQTT protocol, we've established a communication framework enabling the transmission of sensor data from an ESP32 sensor node to a central node, which is another ESP32 device. This central node acts as a hub, receiving the incoming sensor data and facilitating its storage onto an SD card module. This architecture enables the logging of patient data, creating a repository of historical records that can be accessed and reviewed as needed.

TABLE I
COMPONENTS & THEIR USES

Sr no.	List of components	Uses
1	LM35	Temperature Sensor
2	ESP32	Send & receive data
3	Pulse sensor	Heart rate sensor
4	SD card module	Store patient data

LM35 Temperature Sensor: This sensor helps measure the patient's body temperature. It's important because changes in body temperature can indicate health conditions, so monitoring it accurately is crucial for patient care. ESP32 Microcontroller: Think of this as the brain of the system. It collects data

from sensors like the LM35 and Pulse Sensor, processes this information, and controls how the system works. It's like the coordinator that makes sure everything runs smoothly. Pulse Sensor: This sensor monitors the patient's heart rate and blood oxygen levels. It's vital for understanding cardiac health and can alert healthcare providers to any abnormalities that need attention. SD Card Module: This module acts like a digital storage locker. It stores all the data collected by the ESP32 from sensors like the LM35 and Pulse Sensor. This stored data is crucial for doctors to review later to track patient progress or analyze trends over time.

VIII. FLOWCHART

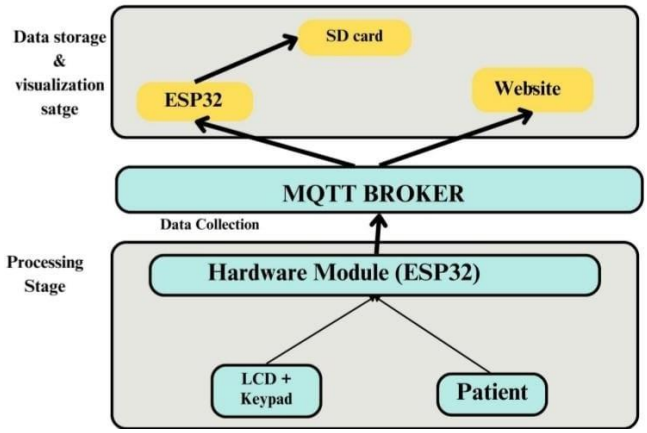


Fig. 3. Flow chart

The LCD screen and keypad are like the system's communication buddies for patients. They help patients tell the system what's going on and give important info. These parts talk to the ESP32, which is like the brain of the whole system. It handles what the LCD and keypad say, deals with info from sensors, and runs everything smoothly.

The ESP32 also talks to a storage module called an SD card. It saves all the important data about patients. So, if we need to check something later, it's all safely stored.

Then there's this thing called an MQTT broker. It helps the system talk to a website. This website does a lot of cool stuff like showing data in real-time, letting us see past info, making graphs, and managing who can access what.

So, with this setup, doctors and nurses can see what's happening with patients right away. They can also look back at past info to see how things have been going. And the website makes all this info easy to understand and keep safe.

IX. SOFTWARE IMPLEMENTATION

In the software implementation of the describe project sensors such as temperature sensor(LM35) and pulse oximeter sensor are connected to the ESP32 microcontroller, which is programmed by using Arduino IDE (Integrated Development Environment).

The Arduino IDE is used to develop the firmware that interface with the sensors, collect the data from them and process it necessary. The ESP32 then communicates the data with Node.js server application using visual studio code(vscode), serves as a backend of a system.

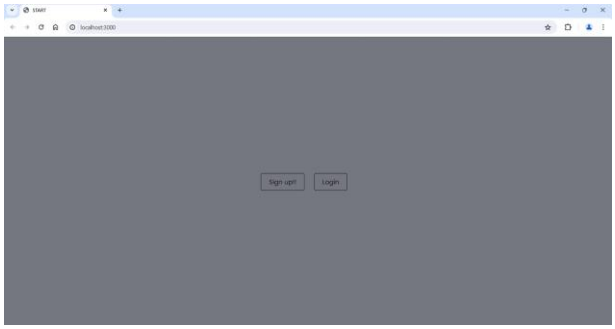


Fig. 4. Home Page

As per figure 4 A user-friendly login page has been created for doctors and hospital staff to register patients and add them to the database. This system allows healthcare providers to begin recording patients' health information as soon as they are registered. This setup ensures continuous monitoring and management of patients' health records, keeping their medical histories complete and up-to-date.

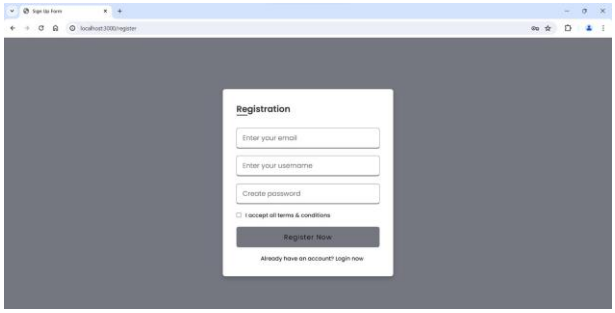


Fig. 5. Registration page

As per figure 5 the login page is illustrated where users are prompted to enter two specific pieces of information: their email ID and password. This setup is designed so that individuals who want to access the system or application must first verify their identity by providing these credentials. Here's why each piece of information is important:

Email ID: This serves as a unique identifier for each user. It ensures that the system can distinguish between different individuals who are attempting to log in.

Password: This is a secret code that only the authorized user should know. It acts as a form of security to protect the user's account from unauthorized access.

Together, the email ID and password work as a dual-factor authentication mechanism, where the email ID provides identification, and the password provides authentication.

As per figure 6 In Figure 6, the process for users to create a new account is illustrated. If someone doesn't already have

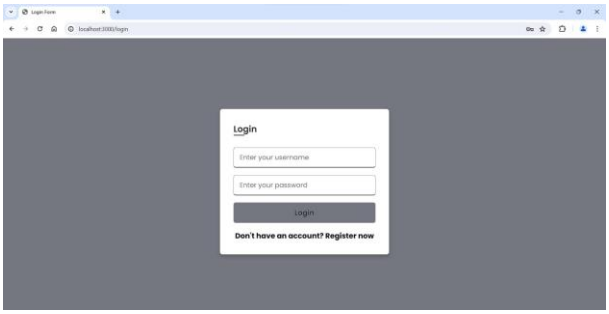


Fig. 6. Login page

an existing account, they have the option to easily register by providing a few specific pieces of information:

1. Email: This serves as a unique identifier for the user's account. It ensures that the system can communicate important information and verify the user's identity when necessary.

2. Username: Users can choose a username that will represent them within the system. This username is often displayed publicly or to other users, depending on the system's settings.

3. Password: A password is chosen by the user to secure their account. It's important for this password to be strong and unique to prevent unauthorized access.

This streamlined registration process is designed to make it easy for new users to sign up and start using the system quickly. By collecting this information upfront, the system can manage and organize each user's health data securely.

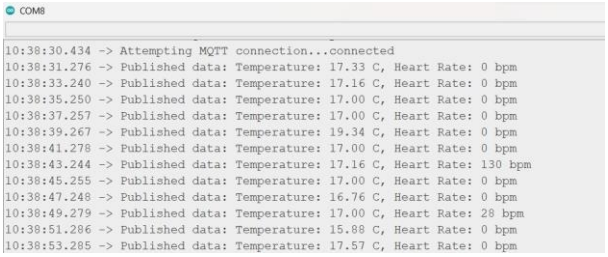


Fig. 7. Arduino IDE serial monitor

As per the figure 7 The MQTTS protocol is employed in our project to ensure secure communication and data transmission between devices in real-time ICU monitoring.

To display real-time data for temperature and pulse oximeter readings, MQTTS topics are utilized to publish the data from the sensors to the central monitoring system. The sensors continuously measure the temperature and pulse oximeter readings of the patient, which are then transmitted securely using the MQTTS protocol.

As per the figure 8 Fig 8 The terminal in figure 8 utilizes MQTT (Message Queuing Telemetry Transport) alongside HTML, CSS, and JavaScript to enable efficient real-time patient monitoring. MQTT is a lightweight messaging protocol ideal for scenarios where bandwidth and device resources



Fig. 8. VS code terminal

are limited, such as in IoT (Internet of Things) applications. In this context, MQTT facilitates the seamless transmission of patient data updates between the monitoring devices and the web interface. This protocol ensures that updates are delivered promptly and reliably, allowing hospital professionals to access the latest patient information without delays. By integrating MQTT with HTML for structure, CSS for styling, and JavaScript for interactivity, the terminal offers a comprehensive solution that enhances user experience and supports timely decision-making in healthcare settings.

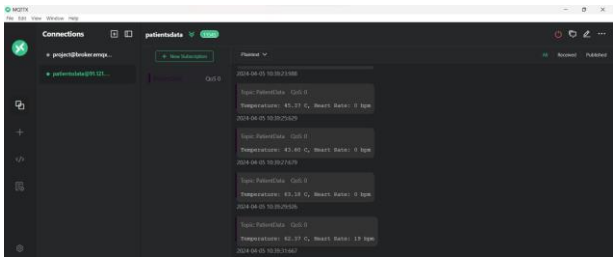


Fig. 9. MQTTSBroker

As per the given fig 9 normal data of temperature of server running on Node.js platform server as the host for visualization of data on a MQTTS broker. This local host setup allows hospital professionals to access and monitor temperature data in real-time within the hospital,s network, facilitating prompt decision-making and interventions based on the patient's health status.



Fig. 10. Graphical representation of patient's data

As for figure 10 MongoDB Compass is linked to the local host of the webpage, serving as a bridge between the login page and the local host. Patient login information is stored

securely using MongoDB, while MQTTSS ensures the data's security. This integration acts as a connection point between patient accounts and the web server, facilitating proper access to patient data while ensuring its confidentiality and integrity.

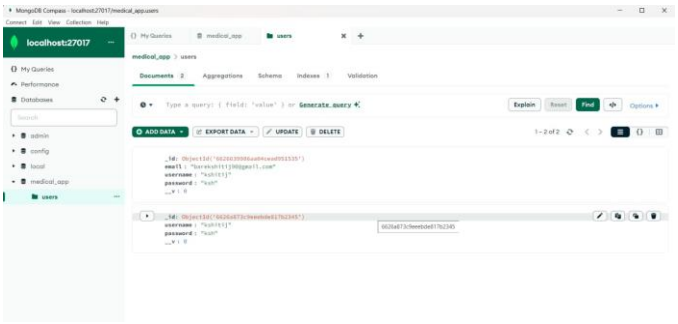


Fig. 11. Store Login data

As per figure 11 Demonstrates a platform designed to securely store patients' login IDs exclusively on its website using "software storage." This method involves using backend technologies like encrypted databases or secure storage systems to manage and protect login credentials. By storing this data within the website's infrastructure, the platform ensures sensitive patient information remains confidential and accessible only through secure login procedures. This approach is crucial for maintaining data integrity and complying with privacy regulations, safeguarding patient login details from unauthorized access or potential security breaches.

X. Conclusion

The project focuses on building a system with data collection system by integrating various sensors like the LM35 for precise temperature monitoring and the MAX30102 for tracking vital signs. These sensors gather crucial parameters such as blood pressure, temperature, and heart rate, forming a crucial database for informed medical decision-making. Physicians can access real-time data through a secure and user-friendly web interface, featuring intuitive visualization methods like bar graphs. This integration of sensor technology, data science, and user-centric design aims to enhance ICU patient care by providing healthcare professionals with actionable insights for timely interventions and significantly improved patient outcomes. By using advanced monitoring capabilities and intuitive data visualization, our system aims to ensure that every patient receives optimal care during critical moments, ultimately saving lives and improving recovery rates.

References

[1] Uen, S., Fimmers, R., Brieger, M., Nickenig, G., Mengden, T. (2009). Reproducibility of wrist home blood pressure measurement with position sensor and automatic data storage. BMC Cardiovascular Disorders, 9, 1-9.

[2] Li, L., Sheng, S., Liu, Y., Wen, J., Song, C., Chen, Z., ... Shum, P. P. (2023). Automatic and Continuous Blood Pressure Monitoring Via an Optical-Fiber-Sensor-Assisted Smartwatch.

[3] Hameed, Rasha Talal, Omar Abdulwahabe Mohamad, Omar Talal Hamid, and Nicolae T¸ a˘pus¸. "Patient monitoring system based on e-health sensors and web services." In 2016 8th International Conference on Electronics, Computers and Artificial Intelligence (ECAI), pp. 1-6. IEEE, 2016.

[4] Patel, Shyamal, et al. "A review of wearable sensors and systems with application in rehabilitation." Journal of neuroengineering and rehabilitation 9.1 (2012): 1-17.

[5] Kullayappa, G. R., Kumar, C. M., Alam, K. T. (2023). Design of a Physiological Monitoring Device for Holistic Telemedicine Applications. MAPAN, 38(1), 1-19.

[6] Acampora, G., Cook, D. J., Rashidi, P., Vasilakos, A. V. (2013). A survey on ambient intelligence in healthcare. Proceedings of the IEEE, 101(12), 2470-2494.

[7] Islam, M. M., Rahaman, A., Islam, M. R. (2020). Development of smart healthcare monitoring system in IoT environment. SN computer science, 1, 1-11.

[8] Al-Khafajiy, M., Baker, T., Chalmers, C., Asim, M., Kolivand, H., Fahim, M., Waraich, A. (2019). Remote health monitoring of elderly through wearable sensors. Multimedia Tools and Applications, 78(17), 24681-24706.

[9] Mohammadzadeh, N., Gholamzadeh, M., Saeedi, S., Rezayi, S. (2020). The application of wearable smart sensors for monitoring the vital signs of patients in epidemics: a systematic literature review. Journal of ambient intelligence and humanized computing, 1-15.

[10] Zhang, Q., Zhou, D., Zeng, X. (2017). Highly wearable cuff-less blood pressure and heart rate monitoring with single-arm electrocardiogram and photoplethysmogram signals. Biomedical engineering online, 16(1), 1-20.

[11] 1-Kumar, S., Bhagat, V., Sahu, P., Chaube, M. K., Behera, A. K., Guizani, M., ... & Alsamhi, S. H. (2024). A novel multimodal framework for early diagnosis and classification of COPD based on CT scan images and multivariate pulmonary respiratory diseases. Computer Methods and Programs in Biomedicine, 243, 107911.

Design And Implementation Of Low Power MAC Unit For Image Processing On FPGA

Bhagyesh Manjrekar
Dept. of Electronics and Telecomm
Don Bosco Institute of Technology
Kurla(W), Mumbai-400070, India
manjrekarbhagyesh@gmail.com

Jay Dulange
Dept. of Electronics and Telecomm
Don Bosco Institute of Technology
Kurla(W), Mumbai-400070, India
dulangejay01@gmail.com

Pratham Amare
Dept. of Electronics and Telecomm
Don Bosco Institute of Technology
Kurla(W), Mumbai-400070, India
amarepratham007@gmail.com

Pratham Koturwar
Dept. of Electronics and Telecomm
Don Bosco Institute of Technology
Kurla(W), Mumbai-400070, India
pratham1102koturwar@gmail.com

Dr.Sudhakar Mande
Dept. of Electronics and Telecomm
Don Bosco Institute of Technology
Kurla(W), Mumbai-400070, India
ssmande@yahoo.com

***Abstract*—The paper explores the implementation of a Multiply Accumulate (MAC) unit to enhance performance through Sobel edge detection in digital VLSI circuits. It addresses the challenge of managing large pixel datasets efficiently within strict timing constraints. By leveraging the parallel processing capabilities of reconfigurable FPGA devices, the study accelerates algorithms, particularly edge detection crucial for image analysis. Sobel edge detection, which utilizes gradients, aids in identifying edge pixels, with FPGA implementation maximizing the benefits of parallel processing. The coding is executed in Verilog, and synthesis along with FPGA implementation is carried out using Xilinx tools. The research findings demonstrate significant improvements in delay and speed compared to traditional methods. The results indicate that designing a MAC unit using Sobel Edge Detection is notably more efficient in terms of delay and speed when compared to conventional multiplication techniques. This study showcases the effectiveness of utilizing Sobel edge detection in conjunction with a MAC unit to enhance performance and efficiency in digital VLSI circuits, particularly in image processing applications.**

***Index Terms*—Mac Unit, FPGA, Sobel Edge Detection, Verilog, Xilinx**

I. INTRODUCTION

In the domain of digital VLSI circuits, the pivotal roles of adders and multipliers are indisputable for ensuring computational efficiency. Particularly, Multiply-Accumulate (MAC) units stand out as indispensable components for real-time signal processing endeavors, notably in digital image processing applications. The MAC operation encompasses two vital phases: computing the product and subsequently accumulating it. This sequential process significantly influences the overall efficiency of computational tasks, especially when dealing with large datasets within stringent timing constraints.

The core aim of this research project revolves around the development and implementation of a low-power MAC unit customized explicitly for image processing tasks. A specific emphasis is placed on enhancing the performance of the Sobel edge detection algorithm, which holds paramount importance in the domain of computer vision. Sobel edge detection, being a gradient-based method utilized for detecting edge pixels in images, is essential for a myriad of computer vision applications. By harnessing advanced software tools and innovative design methodologies, the primary objective is to devise an energy-efficient solution capable of reducing power consumption significantly in real-time scenarios. This research endeavor is particularly geared towards addressing the escalating demand for power-efficient solutions, especially in embedded systems and portable devices.

The overarching goal of this project is to develop and deploy a low-power MAC unit optimized explicitly for image processing tasks, with a strong emphasis on advancing the Sobel edge detection algorithm. This endeavor is propelled by the increasing need for power-efficient solutions, particularly in the context of embedded systems and portable devices. Through the application of innovative design methodologies and optimization techniques, the project endeavors to realize a low-power MAC unit tailored for real-time image processing applications. Leveraging software algorithms and exploring the capabilities of reconfigurable devices such as FPGAs, the research aims to demonstrate the practical feasibility and effectiveness of the proposed solution in enhancing computational efficiency and reducing power consumption in image processing tasks.

II. THEORETICAL CONCEPTS

A. MAC Unit

The MAC unit is pivotal in DSP, swiftly multiplying and adding numbers for computational efficiency. Customizable for various tasks, it's crucial in real-time processing. Designing a low-power MAC for image processing addresses energy concerns in power-limited environments. Image algorithms heavily depend on MAC operations, demanding energy-efficient solutions for battery-powered devices. Methodology involves precise control, optimization, and integration of components like the Vedic Multiplier and Brent-Kung Adder. The MAC

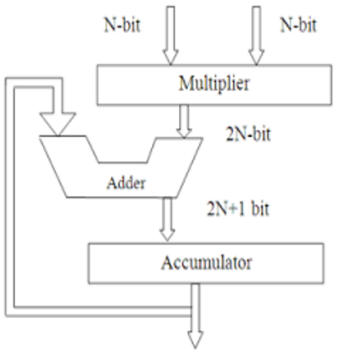


Fig. 1. MAC Unit

unit is designed using VHDL and synthesized in Xilinx. This high speed low power multiplier can be apply to the DSP application. It can be used to introduce parallel processing speeder output. The MAC unit is designed using Verilog and synthesized in Xilinx. This high speed low power multiplier can be apply to the DSP application. It can be used to introduce parallel processing speeder output. This enhances performance while minimizing power consumption. The project's goal is to advance energy-efficient computing for embedded systems and portable devices, ensuring optimal performance in image processing tasks.

B. Sobel edge detection operation

The Sobel edge detection algorithm detects changes in intensity to identify edges. It utilizes derivatives for edge detection. The first derivatives are implemented using the magnitude of the gradient. They must satisfy the following conditions:

1) It must be zero in the areas of constant intensity.
2) It must be nonzero at the onset of intensity step or ramp.
3) It must be nonzero at points along an intensity ramp.

The gradient of the image f at (x, y) is defined as:

$$\text{grad}(f) = [G_x, G_y]^T = \left[\frac{\partial f}{\partial x}, \frac{\partial f}{\partial y}\right]^T$$

G_x is the gradient in the horizontal direction, and G_y is the gradient in the vertical direction.

The gradient magnitude G is given by:

$$G = \sqrt{G_x^2 + G_y^2}$$

Here, G represents the rate of change in the direction of the gradient vector.

Leveraging the Xilinx ISE Design Suite-14 software platform, the Sobel edge detection algorithm is implemented using Verilog. The system takes a grayscale image of size $m \times n$ as input and produces an edge-detected grayscale image of the same dimensions as the output.

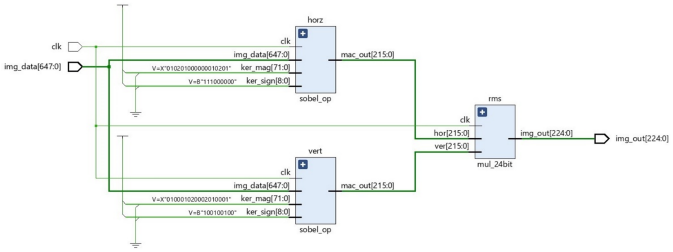


Fig. 2. Sobel edge architecture

III. LITERATURE REVIEW

The research paper delves into the innovative application of Vedic Mathematics principles to optimize Multiply-Accumulate (MAC) units in real-time signal processing tasks. By incorporating the "Urdhav Triyagbhyam" sutra, specifically Vertical and Crosswise multiplication, the study aims to enhance efficiency, speed, and power consumption compared to traditional methods. The critical role of multipliers in MAC operations within digital signal processing systems is emphasized, with a focus on improving power consumption and speed. Traditional methods like Booth's Multiplier and Wallace Tree are contrasted against Vedic Mathematics-based designs, which demonstrate advantages in speed, area requirements, delay, and power consumption. The research presents these Vedic multipliers as promising solutions for high-performance digital signal processing applications requiring low-power operation. [1]

The research presented at the 2020 International Conference on Emerging Trends in Information Technology and Engineering explores the analysis of a 32-bit Multiply and Accumulate (MAC) unit utilizing Vedic Multiplier techniques. Authored by K. Lilly, K. Lekhya, S. Nagaraj, and B. Manvitha, the study delves into the critical role of MAC units in digital signal processing and the implications of their design on system performance. The incorporation of Vedic Multipliers and Carry Save Adders in the MAC unit is discussed to enhance efficiency and reduce delay, aligning with current trends in VLSI design for low-power, low-area, high-speed devices. The emphasis on MAC units' influence on power consumption and system performance underscores the relevance of exploring Vedic Mathematics principles to address these challenges. [2]

The research paper "Implementation of Pipelined Sobel Edge Detection Algorithm on FPGA for High-Speed Applications" delves into the development of a pipelined Sobel edge detection algorithm on an FPGA for efficient processing in high-speed applications. The paper highlights the significance of edge detection in various domains and emphasizes the computational challenges faced by traditional processors in real-time image processing tasks. FPGAs are identified as a promising solution due to their re-programmability and parallel processing capabilities. The Sobel edge detection algorithm's pivotal role is elucidated, focusing on detecting changes in intensity to identify edges within images. The hardware implementation involves key components such as block

memory, Sobel enhancement operator module, and binary segmentation module, tailored for processing grayscale images efficiently. The paper demonstrates notable improvements in efficiency through simulation results, showcasing reduced propagation delay and enhanced performance compared to existing implementations. [3]

The research paper titled "Design of Sobel Operator based Image Edge Detection Algorithm on FPGA" delves into the implementation of the Sobel edge detection algorithm on Field Programmable Gate Arrays (FPGAs). It underscores the significance of image processing in various applications, highlighting the importance of edge detection for extracting meaningful information from images. The theoretical underpinnings of Sobel edge detection, including gradient computations and the functionality of Sobel operators, are expounded upon. The paper elucidates the advantages of utilizing FPGAs for image processing, emphasizing their efficiency in executing functions in fewer clock cycles and their parallel processing capabilities. The system architecture of the Sobel edge detection system, comprising 3x3 pixel data generation and Sobel edge detection operation modules, is detailed. Experimental results demonstrate the algorithm's efficacy on different FPGA devices, meeting real-time processing requirements for various image sizes. [4]

IV. Methodology

The methodology involves the conversion of the gray image into a .hex file and the utilization of an Image Reading Module in MATLAB to facilitate data handling. The primary stages include parallel convolution using a low-power MAC unit in a single machine cycle and the implementation of the Sobel edge detection operation module employing Root Mean Square calculations. The resulting edge-detected image is then converted back to .hex format using the Xilinx Vivado Design Suite, ensuring seamless integration and compatibility for further processing and analysis in MATLAB.

A. Stage I

In the first stage of our project, we focus on implementing parallel convolution using low-power Multiply-Accumulate (MAC) units. Convolution is a fundamental operation in image processing, essential for tasks such as filtering, feature extraction, and edge detection. By employing parallel convolution, we aim to enhance computational efficiency and reduce processing time, crucial for real-time image processing applications.

The primary objective of Stage 1 is to design and implement a parallel convolution module that utilizes low-power MAC units to perform convolution operations efficiently. This module will form the foundation of our image processing pipeline for Sobel edge detection.

B. Stage II

The Sobel operator, a first-order derivative operator, detects intensity changes in images through gradient calculations. It satisfies conditions such as being zero in areas of constant intensity and non-zero at intensity changes. G_x and G_y are computed using finite differences, and the gradient magnitude (G) is the sum of their absolute values.

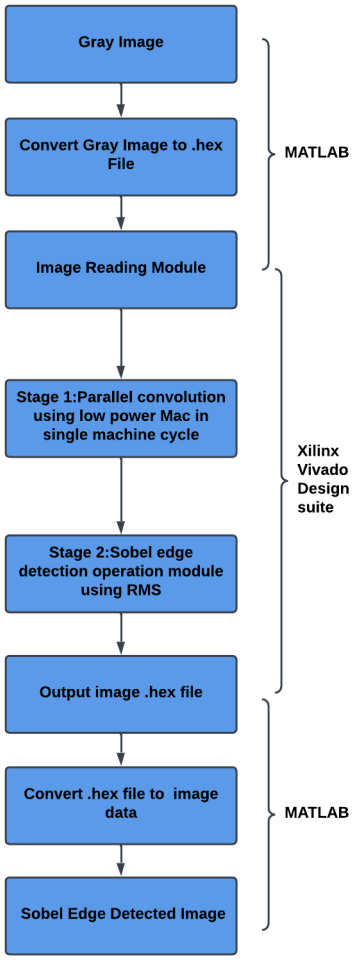


Fig. 3. Flowchart

$$G_x = \frac{\partial f}{\partial x} = \begin{pmatrix} -1 & 0 & 1 \\ -2 & 0 & 2 \\ -1 & 0 & 1 \end{pmatrix} * \text{image} \quad (1)$$

$$G_y = \frac{\partial f}{\partial y} = \begin{pmatrix} -1 & -2 & -1 \\ 0 & 0 & 0 \\ 1 & 2 & 1 \end{pmatrix} * \text{image} \quad (2)$$

The two gradients are calculated using the partial derivatives to identify edge pixels in the image efficiently.

V. IMPLEMENTATION

In Digital Signal Processing (DSP), the Multiply-Accumulate (MAC) unit plays a crucial role in swiftly performing mathematical operations, particularly in tasks like audio and video processing. Customizable for diverse applications, MAC units enhance computational efficiency, making them indispensable for real-time processing. A project on

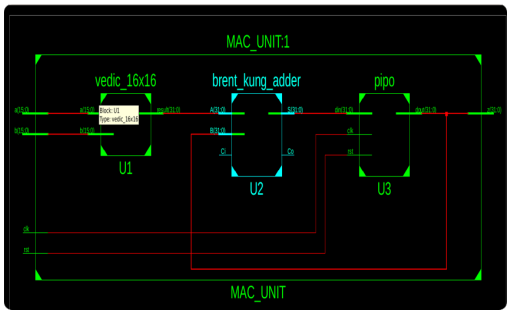


Fig. 4. MAC Unit Schematic

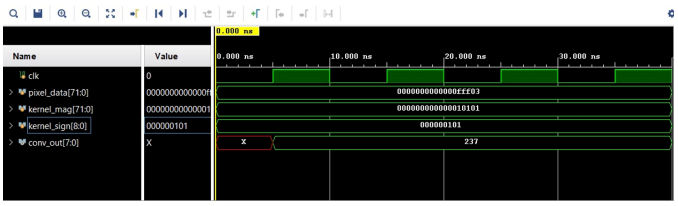


Fig. 5. Waveform MAC Unit 16x16

low-power MAC units should introduce their importance in energy-efficient image processing, discuss image processing requirements, delve into low-power design techniques, and present integration, validation, and performance evaluation methodologies, showcasing significant power savings and efficacy.

VI. RESULTS

A. Comparison of Adder Architectures

The comparison of different adder architectures, including Brent-Kung, Kogge-Stone, and HanCarlson, reveals varying performance metrics crucial for evaluating their efficacy within the Multiply-Accumulate (MAC) unit. Among these architectures, Brent-Kung stands out for its low average power consumption and power-delay product, coupled with a relatively low delay. These characteristics position Brent-Kung adders as a favorable choice for integration in the MAC unit, offering significant power savings and improved performance. The regular structure and efficient carry propagation further endorse Brent-Kung adders for high-speed arithmetic operations, aligning them well with the optimization goals of the MAC unit for image processing tasks.



Fig. 6. MAC Unit Simulation Result

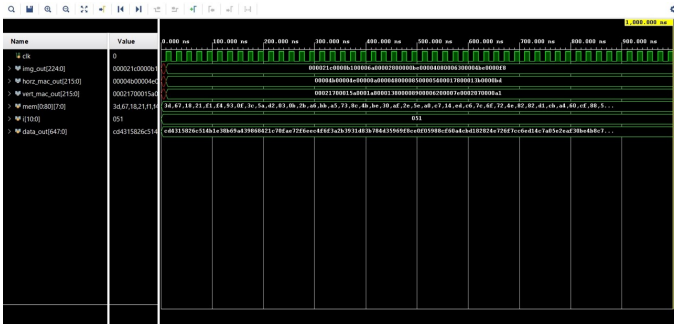


Fig. 7. sobel Edge Detection Simulation Result

The table compares various adder architectures, including Brent-Kung, Kogge-Stone, and Han-Carlson, based on their average power consumption (µW), delay (ns), and power-delay product (X 10^{-15} Joules). Brent-Kung demonstrates an average power consumption of 102.2749 µW with a delay of 0.88 ns, resulting in a power-delay product of 88.001912 × 10^{-15} Joules. Kogge-Stone shows higher power consumption at 140.9152 µW with a delay of 0.93 ns, resulting in a power-delay product of 90.685056 × 10^{-15} Joules. Han-Carlson exhibits an average power consumption of 111.5113 µW with a delay of 0.94 ns, resulting in a power-delay product of 93.669492 × 10^{-15} Joules. This comparison provides valuable insights into the performance disparities among these adder architectures.

B. Comparison of Multiplier Architectures

The comparison table provides a thorough evaluation of the Vedic multiplier's exceptional qualities compared to traditional multiplier architectures. Its outstanding swiftness, achieved through a single clock cycle requirement, establishes it as a prime candidate for time-sensitive applications necessitating rapid computations. Additionally, its minimal hardware usage highlights its efficiency in resource allocation, making it highly suitable for integration into intricate digital systems with space constraints. Leveraging the Vedic multiplier's inherent benefits, such as rapid operation and optimal resource utilization, within Multiply-Accumulate (MAC) units can significantly enhance system speed and efficiency. This is particularly advantageous in domains like image processing where real-time processing capabilities are pivotal for seamless performance. The Vedic multiplier's versatility, accommodating various number representations and formats seamlessly, from binary to decimal and signed to unsigned, exemplifies its flexibility. This adaptability makes it a valuable asset across diverse domains, from digital communications to scientific computing, promising enhanced capabilities and efficiency in a wide array of applications.

The table compares different parameters of various multiplier architectures, including Vedic Multiplier, Array Multiplier, Wallace Tree Multiplier, and Booth's Multiplier. It assesses factors such as clock cycle, delay, operating speed, power consumption in comparison to Vedic Multiplier, and FPGA implementation efficiency. Vedic Multiplier exhibits a clock cycle of 1 and the highest operating speed, while the Array Multiplier requires N clock cycles and has the highest

delay at N². The Wallace Tree Multiplier operates at N/2-1 clock cycles and shows high operating speed, whereas Booth's Multiplier operates at N/2 clock cycles and offers higher operating speed. In terms of power consumption, the Vedic Multiplier consumes less power compared to others, while the Array Multiplier consumes the most. FPGA implementation efficiency varies, with Vedic Multiplier being the most efficient and Wallace Tree Multiplier being the least efficient. This summary encapsulates the comparative analysis of these multiplier architectures.

C. Hardware Resources Utilisation

The hardware resource utilization summary offers insights into the FPGA's capacity and efficiency in executing the edge detection algorithm. Specifically, it outlines the utilization of key components such as slice logic, 4-input look-up tables (LUTs), slice flip-flops, bonded input/output blocks (IOBs), and BUFGMUXs. Understanding these utilization metrics is essential for evaluating the algorithm's feasibility and scalability across different FPGA platforms.

The table provides a summary of hardware resource utilization for the MAC Unit architecture on Spartan-6. It includes parameters such as the number of Slice Registers, Slice LUTs, fully used LUT-FF pairs, bonded IOBs, and BUFG/BUFGCTRLs. For each parameter, it presents the utilization by the MAC unit and Simple Multiplier, along with the total available resources. The utilization is expressed as a percentage. Notably, the majority of Slice LUTs are utilized, accounting for 59% of the available resources, while other resources exhibit varying degrees of utilization. This summary offers insights into the efficient allocation of hardware resources for the MAC Unit architecture on Spartan-6.

Logical Utilization	Used by MAC unit	Used by Simple Multiplier	Available	Utilization
Number of Slice Registers	257	787	42000	0%
Number of Slice LUTs	12424	2376	21000	59%
Number of fully used LUT-FF pairs	177	396	12504	1%
Number of bonded IOBs	258	258	210	122%
Number of BUFG/BUFGCTRLs	1	2	32	3%

TABLE I
HARDWARE RESOURCES UTILIZATION SUMMARY OF SPARTAN-6 FOR MAC UNIT ARCHITECTURE

VII. CONCLUSION

Image processing algorithm for image edge detection using Sobel operator is successfully designed on target FPGAs. Developed algorithm takes advantages of parallelism possible in FPGA. The Xilinx Spartan-6 device is well suited for implementing imaging functions such as edge detection. The FPGA supports high levels of parallel processing data flow structures that are important for efficient implementation of image processing algorithms. Reconfigurable device like FPGA can be a very useful device to implement real-time image processing algorithm. Uses of complex mathematical operations are avoided to achieve real-time timing constraints. Drawback of proposed method is that detected edges are thicker. The algorithm designed in this paper is basic image processing algorithm, this work can be further extend to developed real-time complex image processing algorithms such as feature detection, feature extraction, target tracking.

REFERENCES

[1] R. Pawar and S. S. Shriramwar, "Design and implementation of area efficient low power high-speed MAC unit using FPGA," 2017 IEEE International Conference on Power, Control, Signals and Instrumentation Engineering (ICPCSI), Chennai, India, 2017, pp. 2683- 2687.

[2] K. Lilly, S. Nagaraj, B. Manvitha and K. Lekhya, "Analysis of 32-Bit Multiply and Accumulate unit (MAC) using Vedic Multiplier," 2020 International Conference on Emerging Trends in Information Technology and Engineering (ic-ETITE), Vellore, India, 2020, pp.1-4

[3] Vanishree and K. V. Ramana Reddy, "Implementation of pipelined sobel edge detection algorithm on FPGA for High speed applications," 2013 International Conference on Emerging Trends in Communication, Control, Signal Processing and Computing Applications (C2SPCA), Bangalore, India, 2013, pp. 1-5.

[4] G. Chaple and R. D. Daruwala, "Design of Sobel operator based image edge detection algorithm on FPGA," 2014 International Conference on Communication and Signal Processing, Melmaruvathur, India, 2014, pp. 788-792.

PUBLISHED AND ACCEPTED PAPERS

Evaluating the Effectiveness of Machine Learning Models for Early Diagnosis of Chronic Kidney Disease

Siddhant Kedar
Pranjali Raval
Amogh Workilar

Sarika Galphade
Pratibha Dumane
Satishkumar Chavan

Dept. of Electronics and Telecomm
Don Bosco Institute of Technology
Mumbai, Maharashtra

ABSTRACT

Chronic Kidney Disease (CKD) is one of the most arising as concerning health issues among many others due to the gradual damaging of the kidney, causing it to slowly reduce its ability to perform essential and fundamental functions of the body. It tends to go undetected in the early stages. The early detection and prediction of Kidney diseases becomes extremely helpful in such cases for diagnosing the problem. A Glomerular Filtration Rate (GFR) is an evaluation test that is used to check functioning of kidney. Based on the different GFR ratios, the severity of kidney disease can be diagnosed.

The performance Assessment using ML Models for early prediction of kidney disease is a system designed by assessing and evaluating the attributes provided to the system. The system utilizes Logistic regression, Support Vector Machine, Random Forest, and Decision Tree Algorithms for the assessment. This study proposes using ML to diagnose the Kidney disease. The mentioned algorithms were trained using the data gathered with different attributes.

KEYWORDS *: Machine learning, Chronic kidney disease, Feature selection, Logistic regression, Support vector machine, Decision tree, Random forest, F1 score, Precision, Accuracy.*

INTRODUCTION

Kidney Disease is one of the most important health problems as it is an increasing disease worldwide and is a disease that eventually through a slow process damages the kidneys in the long term and reduces the ability of the kidneys to function in the body. Kidney Disease is interconnected with complications such as renal failure which causes it to lose its ability to filter blood properly, hypertension, anaemia which is a deficieny of blood, and neurological damage. A GFR ratio of 90+ is stage 1 and is considered as normal for healthy people. GFR ratio between 60 to 89 is stage 2 and a constant ratio for more than 3 months might be a sign of early CKD with very few symptoms observed. The range of 30 - 59 is stage 3 and is common in Kidney Disease. The stage 4 with GFR ranges in between 15-29 has fatal severity Kidney Disease and most likely needs dialysis.The stage 5 with GFR ratio of 15 and below is end stage renal disease and the kidney would have almost lost all of its ability to function properly and it needs to undergo dialysis or kidney transplant to survive.As the study done by National Medical Journal of India in 2023, the CKD prevalence is increased to nearby 30% in 2020 as compared to 1990. The same study also showed the 4% to 20% prevalence of CKD in India.

The goals of the research is to show how Kidney Disease can be diagnosed more accurately through prediction

and classification by using ML algorithms. To achieve the aim we have used Linear regression, Support Vector Machine (SVM), Decision Tree, Random Forest for accurate prediction of the disease as proposed in this study.

The scope of Performance Assessment of Machine Learning Models for Early Prediction of Chronic Kidney Disease is to provide a more targeted and more effective methodology to identify the individuals at the risk of CKD by assessing various attributes. This utilises the Machine Learning models and algorithms like SVM,Logistic Regression, Decision Tree to analyse and assess the risk of Kidney Disease. It aims to address the evaluation of individuals having risk of CKD. This system can provide cost effective analysis as well as accurate results serving the medical field.

This system can be used by Healthcare Professionals in the medical field such as Nephrologists who specialise in treating kidney conditions. The general practitioners, nurses, healthcare staff working with CKD patients and healthcare administrators who regulate and manage such types of illness also benefit from this. The other beneficiary audience could be the Machine Learning researchers who are willing to apply Machine Learning knowledge in the medical field and healthcare problems. The patients and caregivers could also benefit from this to diagnose individuals at risk of CKD. Caregivers could monitor the individual from time to time to maintain records. The government bodies and agencies could use this system to keep track, monitor and regulate the statistics of CKD and to oversee the healthcare and medical care.

II. LITERATURE SURVEY

Related work

According to the research that has been already carried out shows that many medical features were used in utilisation with Machine Learning algorithms to implement the system for chronic kidney detection. The main challenges and problems that was observed in earlier work is that the datasets were not available or the datasets were not sufficiently large. Weilun et al [1] proposed the use of contracting network by successive layers and replaced the pooling by up-sampling and extensive use of data augmentation. Three machine learning models viz. a bagging tree model named Random Forest, a boosting tree model named XGBoost, and a neural network based model named ResNet were utilized in their work. Debal and Sitole [2] focused on cross validation based performance evaluation and comparing models by dividing data into partitions. The machine learning algorithms were applied to original datasets with all 19 features. The prediction models preferred are Random Forest (RF), Support Vector Machine (SVM) and Decision Tree (DT). Applying the models on the original dataset, the highest accuracy with RF, SVM, and XGBoost were observed. The feature selection is done using two methods i.e UFS and RFECV and two binary classifiers for 18 models. Training and testing on these models have been executed using tenfold cross-validation. In tenfold cross-validation, the dataset is partitioned randomly into ten equal size sets.

Akter et al. [3] used seven DL algorithms viz. ANN, LSTM, GRU, Bidirectional LSTM, Bidirectional GRU, MLP, and Simple RNN for CKD for discussion on the various clinical features of CKD. GRU, Bidirectional LSTM, Bidirectional GRU, MLP, and Simple RNN were implemented for early prediction of CKD. These algorithms were implemented on the pre-processed fitted CKD dataset. This study involves the measurement of accuracy, recall, precision and calculates loss and validation loss in the prediction. The accuracy that was observed during the training and testing was 99%, 96%, 97% for ANN, Simple RNN, and MLP respectively. In addition, the AdaBoost and Perceptron algorithms are applied to find the significant risk factors of CKD. However, the dataset that is used to train the model is small which could eventually cause the result to be unreliable. Finding the dataset with more attributes and higher instances is difficult as the dataset of patients are kept private due to privacy issues.

Ebiaredoh-Mienye et al. [4] have segregated the data for it to be used for Logistic Regression and SVM and Random Forest. Six other Machine Learning classifiers were implemented as the baseline for performance comparison. The classifiers include logistic regression, decision tree, random forest, SVM, XGBoost, and the traditional AdaBoost.

Machine Learning Model

1) Logistic regression: Logistic regression is one of

the highly accurate statistical analysis methods in Machine Learning algorithms that is mainly focused on the probability as a binary outcome. It is a type of supervised learning. It predicts whether the given instance belongs to the given class or not. It mainly focuses on solving problems based on the classification. The logistic regression fits the regression line to an "S" shaped logistic function which predicts the value based on the maximum values that typically range from 0 to 1. The logistic regression gives us the probabilistic value of the prediction between 0 and 1. This algorithm is simple and straightforward for the outcomes that lie between two classes.

2) Support Vector Machine: SVM stands for Support vector Machine. It is one type of machine learning algorithm that is proficient in analyzing data not only for classification but also for regression problems. The main goal of SVM is to form the best hyperplane for the separation of the data. The key purpose of SVM is to categorize or classify the data in two different categories by means of a hyperplane or decision plane. The hyperplane or decision plane is the best boundary or space that segregates the set of objects. For deciding the hyperplane, the extreme cases are considered as support vectors. The margin is the gap that is located in between the two lines on the closest point of difference.

3) Decision Tree: Decision trees belong to the supervised learning category of ML and are used for classification and regression problems. They are visualized as a tree-like structure, where the root node represents the starting point of the decision-making process using the dataset, while the split points resemble nodes where the root node is characterized into two sub-nodes based on feature selection and criteria. This step is important in constructing classification or regression tasks. Decision nodes are used to make decisions in the algorithm, while leaf nodes denote the final output that cannot be further divided. One of the main benefits of using the decision tree algorithm is that it imitates human thinking, making it easy to understand.

4) Random Forest: The Random Forest is a supervised Machine Learning algorithm used for classification and regression. It is based on ensemble learning, which combines the predictions of multiple neural networks to improve model performance and reduce variance.

Random Forest comprises of multiple decision trees, and the more trees it has, the higher the accuracy and the lower the over-fitting. This algorithm has several advantages, including a shorter training time compared to other algorithms, high accuracy in predicting outputs, and excellent performance on large datasets.

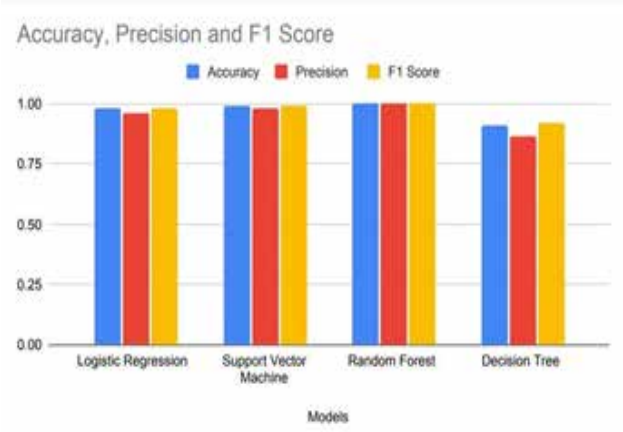
PROPOSED SYSTEM

The work intends to evaluate the performance of Machine Learning models to diagnose patients who are at risk of developing CKD well before clinical symptoms are recognized. The proposed system makes use of different Machine Learning algorithms to visualize graphs of various parameters required for diagnosis of CKD. The Performance Assessment using Machine Learning Models for Early Prediction of Chronic Kidney Disease is a system designed for early prediction of CKD by assessing the attributes provided to the system. The system utilises Logistic Regression, SVM, Random Forest and Decision Tree algorithms for the assessment. The above mentioned models were trained using the data gathered with different attributes and comparative analysis of the various models was carried out.

Collected CKD data is used by the University of California, Irvine (UCI) Repository. Prior to use, the original dataset—which included unique values and missing values—was pre-processed. The data set contains 400 patient records, some of which have missing values. It consists of 24 clinical characteristics that show up in the diagnosis of chronic kidney disease (CKD), with one class attribute acting as a predictor of the patient's propensity for chronic renal failure. The predicted feature diagnostic has two different sorts of values: "ckd" and "notckd." There are 250 values (62.5%) of the "ckd" class in the data set. 250 values from the "ckd" class (62.5%) and 150 values from the "notckd" class (37.5%) make up the data set.

RESULTS AND DISCUSSION

Models	Accuracy (%)	Precision	F1 Score
LogReg	98	0.9629	0.98113
SVM	99	0.9811	0.9904
RF	100	1.000	1.000
DT	91	0.8644	0.9189



The above table presents the performance assessment with metrics like Accuracy, Precision, and F1 Score. The accuracy is the measurement of the overall correctness of the model. Accuracy is given by:

$$Accuracy = \frac{TP + TN}{TP + TN + FP + FN} \quad (1)$$

TP stands for True Positive whereas TN is True Negative. The term False Positive is abbreviated to FP and FN is an abbreviation of False Negative.

Precision is the ratio between true positive values to all the positive values. It is calculated by:

$$Precision = \frac{TP}{TP + FP} \quad (2)$$

F1 score is the combination of recall and precision. It typically ranges from 0 to 1 where 1 is considered as better. It is given by:

$$F1 = \frac{2 * Precision * Recall}{Precision + Recall} \quad (3)$$

As seen above, Random Forest turns out to be the best-suited algorithm for diagnosis of CKD. The Random Forest has Accuracy, Precision, and F1 Score of 1 making it better in performance than other algorithms that are being used in our work.

In addition, after Random Forest, Support Vector Machine is most preferred with an accuracy of 0.99, precision of 0.9811, and F1 score of 0.9904

The Logistic Regression algorithm has an accuracy of 0.98, precision of 0.9629, and F1 score of 0.9811 The Decision Tree algorithm gave an accuracy of 0.91, precision of around 0.8644, and F1 score of 0.9189.

REFERENCES

1. Wang W, Chakraborty G, Chakraborty B. Predicting the Risk of Chronic Kidney Disease (CKD) Using Machine Learning Algorithm. Applied Sciences. 2021; 11(1):202. https://doi.org/10.3390/app11010202

2. Debal, D.A., Sitote, T.M. Chronic kidney disease prediction using machine learning techniques. J Big Data 9, 09(2022). https://doi.org/10.1186/s40537-022-00657-5

3. S. Akter et al., "Comprehensive Performance Assessment of Deep Learning Models in Early Prediction and Risk Identification of Chronic Kidney Disease," in IEEE Access, vol. 9, pp. 165184-165206, 2021, doi: 10.1109/ACCESS.2021.3129491

4. Ebiaredoh-Mienye SA, Swart TG, Esenogho E, Mienye ID. A Machine Learning Method with Filter-Based Feature Selection for Improved Prediction of Chronic Kidney Disease. Bioengineering (Basel). 2022 Jul 28;9(8):350. doi: 10.3390/bioengineering9080350. PMID: 36004875; PMCID: PMC9405039.

5. Tekale, Siddheshwar & Shingavi, Pranjal & Wandhekar, Sukanya. (2018). Prediction of Chronic Kidney Disease Using Machine Learning Algorithm. IJARCCE. 7. 92-96. 10.17148/IJARCCE.2018.71021.

6. S. Akter et al., "Comprehensive Performance Assessment of Deep Learning Models in Early Prediction and Risk Identification of Chronic Kidney Disease," in IEEE Access, vol. 9, pp. 165184-165206, 2021, doi: 10.1109/ACCESS.2021.3129491.

7. Kanda, E., Suzuki, A., Makino, M. et al. Machine learning models for prediction of HF and CKD development in early-stage type 2 diabetes patients. Sci Rep 12, 20012 (2022). https://doi.org/10.1038/s41598-02224562-2

8. Khamparia, A.; Saini, G.; Pandey, B.; Tiwari, S.; Gupta, D.; Khanna, A. KDSAE: Chronic kidney disease classification with multimedia data learning using deep stacked autoencoder network. Multimed. Tools Appl. 2020, 79, 35425–35440. [Google Scholar] [CrossRef]

9. Bikbov, B.; Purcell, C.A.; Levey, A.S.; Smith, M.; Abdoli, A.; Abebe, M.; Adebayo, O.M.; Afarideh, M.; Agarwal, S.K.; Agudelo-Botero, M.; et al. Global, regional, and national burden of chronic kidney disease, 1990–2017: A systematic analysis for the Global Burden of Disease Study 2017. Lancet 2020, 395, 709–733. [Google Scholar] [CrossRef]

10. Suresh, C.; Pani, B.C.; Swatisri, C.; Priya, R.; Rohith, R. A Neural Network based Model for Predicting Chronic Kidney Diseases. In Proceedings of the 2020 Second International Conference on Inventive Research in Computing Applications (ICIRCA), Coimbatore, India, 15–17 July 2020; pp. 157–162. [Google Scholar].

IEEE TECHNICOKNOCKDOWN-2024 (TKD-24)

Design of Web based Student Information System

Shivam Sharma
Department of Electronics and Telecommunication
Don Bosco Institute of Technology
Mumbai, India
sharmashiva4423@gmail.com

Anuj Dhumal
Department of Electronics and Telecommunication
Don Bosco Institute of Technology
Mumbai, India
dhumal04anuj@gmail.com

Vivek Kamble
Department of Electronics and Telecommunication
Don Bosco Institute of Technology
Mumbai, India
vivekkamble356@gmail.com

Namita Agarwal
Department of Electronics and Telecommunication
Don Bosco Institute of Technology
Mumbai, India
namita@dbit.in

***Abstract*— "Web-Based Student Information System" is an online, web-based platform that serves as a valuable resource for both faculty members and students within the department. This system is structured with three distinct modules: student, admin, and faculty, each of which is endowed with specific permissions tailored to their respective roles and responsibilities. These unique rights and access levels ensure that the system operates efficiently and securely, meeting the diverse needs of the users. This system is designed to securely store both academic and non-academic data of students, offering valuable reference and insight for faculty members in the event they need to access information about students, particularly for addressing any future needs. Additionally, the system incorporates a feature of sending important notices to parents via email. Email notifications can be a convenient and efficient way to ensure that parents stay updated about important information and events. The system also contains a notice board feature for communication of important notices within the department.**

I. Introduction

The conventional method of handling student information relied on paper-based systems, it required significant physical storage space. This approach limited the exchange of information and increased the risk of document loss. A student management system acts as an all-encompassing tool for documenting, analyzing, and managing information within educational institutions. Without a student management system, schools would face disorganization, leaving staff members without clear visibility into scheduling and student involvement. Additionally, school districts would struggle to utilize data efficiently for decision-making.

The "Design of Web based Student Information System" is an online platform designed to meet the various needs of both faculty members and students in the department. The system is divided into three distinct modules—student, admin, and faculty—each equipped with specific permissions tailored to their respective roles. This detailed control ensures that academic and non-academic data is managed efficiently, providing faculty members with a valuable resource. Such capabilities are particularly crucial when addressing future academic requirements, providing faculty with insightful information about students.

Furthermore, the system incorporates a feature for sending emails to parents, enhancing communication between the stakeholders. This functionality ensures timely delivery of important announcements, updates, and notifications, fostering effective information exchange between the faculty and parents.

II. Literature Survey

Over the past few years, there has been a surge in the educational technology industry. Numerous software programs have been developed to meet the requirements of various educational establishments. Most of these solutions are aimed at supporting and advancing the aims and objectives of the Institute in addition to further refining administrative problems and internal processes.

In [1] the authors have suggested a program that combines all the modules and features of the Department in a single system that administrators can manage and that faculty and students with a working login and password may access. The primary objective of the entire system was to offer an intuitive user interface and a robust data system that enhance its utility. There are four main user categories in the system: administrators, teachers, operators, and students. The student user can see notes and assignments, check academic performance, monitor attendance information, and add other student details for further analysis. The teacher user can submit assignments and notes, add attendance information for the relevant subjects, and enter grades for various subjects.

This system has an extra user called operator which may give burden to system or complicate the system also the rights given to "operator" is not effective it can be given to other users like "admin" or "faculty".

The authors in [2] have proposed an information system application which is useful for staff, faculty, and principal to deal with students details, academic reports, college informa tion, course specifics etc. It serves as a web-based application

IEEE TKD-24/ISBN No. 978-81-992245-6-7

enabling staff, faculty, and the principal to manage comprehensive information regarding student profiles, academic reports, college specifics, course details, batch information, and related data. College staff have the capability to securely access and review all facets of a student's academic progress using an online interface seamlessly integrated within the college website.

The authors have also included some administrative functionalities like managing fee details, managing leaves, managing admission. This system also includes principal module which have rights to approve leave, viewing details of student as well as faculties.

The authors in this paper have four user modules namely Faculty Module, Staff Module, Student Module, Principal Module. In this paper, three modules are being used .

A comprehensive tool for managing the activities of a specific department within a college has been proposed by authors in [3]. Their primary objective was to streamline and enhance departmental operations, and it caters to various users, including administrators, faculty members, and students. This has been developed with aim to provide information to all the levels of department in an organization. This system consist of three users Admin Staff and student. System administrator is the one who create, update, delete as well as manages the database of the whole system. In this module some of the activities done by the admin are managing library, keeping records of placements, rooms and labs etc, adding faculty details in the system as well as updating the same.

The system appears to be relatively complex, involving different user roles, extensive data management, and integration with SMS and email notifications. This complexity may not be suitable for smaller educational institutions or projects with limited resources.

In [4] authors compared the implementation of the ModelView-Controller (MVC) architecture in ASP.NET and PHP frameworks for web application development. The study concludes that ASP.NET excels in implementing MVC architecture compared to PHP.

In [5] authors proposed a online delivery website with a focus on providing a seamless user experience. This system is developed using ASP.Net, same technology we have used to develop our system.

An automated student database management system for a university, aiming to replace manual paper-based processes with a user-friendly web application has been proposed by authors in [6]. Through the utilization of Agile Software Development methodology, the system covers various modules including student enrollment, attendance tracking, grades management, lab scheduling, library resources, faculty details, and administrative tasks. The article details each phase of the software development life cycle, from requirement analysis to deployment, and provides insights into future enhancements such as mobile application integration and artificial intelligence utilization. By centralizing student information and streamlining administrative tasks, the system offers improved accessibility, efficiency, and potential for further development.

The systems database is managed using MySql and front end is developed using HTML, CSS, JavaScript.

In [7] the author presents an automated Student Management System designed for a college, aiming to replace traditional paper-based methods with an online platform. Utilizing role-based access control, the system caters to students, teachers, and college management, offering functionalities such as profile management, attendance tracking, fee payment, and event organization. Leveraging HTML, CSS, JavaScript, Java, MySQL, and PHP technologies, the system streamlines administrative tasks, enhances data accessibility, and improves overall efficiency within the educational institution. Through a prototyping model approach, the system's development focuses on iterative enhancements based on user requirements. The proposed system aims to address the limitations of manual record-keeping, streamline information exchange, and enhance the overall management of student data, contributing to a more efficient and accessible educational environment.

In [8] describes a College Management System developed using PHP programming language. It aims to manage various aspects of college information, including student records, placement details, event information, and notice board updates.

Key modules of the system include the Student Module for managing student records, Placement Module for tracking student placements, Notices Module for event updates, Registration Module for hostel fee management, Hostel Management Module for managing hostel facilities, Room Allotment Module for allocating rooms to students, Mess Module for handling mess transactions, and Room Fees Module for describing fee structures.

The system utilizes technologies such as PHP, SQL Server, HTML, JavaScript, and CSS. It offers a graphical user interface and allows for registration, login, password change, detail viewing/editing, feedback submission, and admin functionalities. The paper concludes that the web-based information management system reduces paperwork, manpower requirements, and communication costs while providing accurate and accessible information for stakeholders.

III. Proposed System

The proposed Student Information System is a web-based system that offers a comprehensive solution to address key objectives such as secure data management, efficient communication, and streamlined departmental operations. With an intuitive and user-friendly interface, the system ensures that students, teachers, and administrators can effectively utilize it. It will securely store the academic, co-curricular, and extracurricular data of all the students in the department, allowing for easy access and reference in the future. Academic data, including student profiles, academic records, extracurricular activities, and co-curricular information, will be systematically organized, providing faculty members with a comprehensive resource for any future academic requirements.

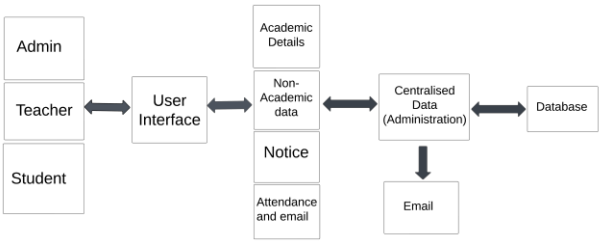


Fig. 1. Block diagram of the system

Figure [1] shows the block diagram of various modules in the system and the relationship between them. There are mainly three modules-Student, Faculty, and Admin.

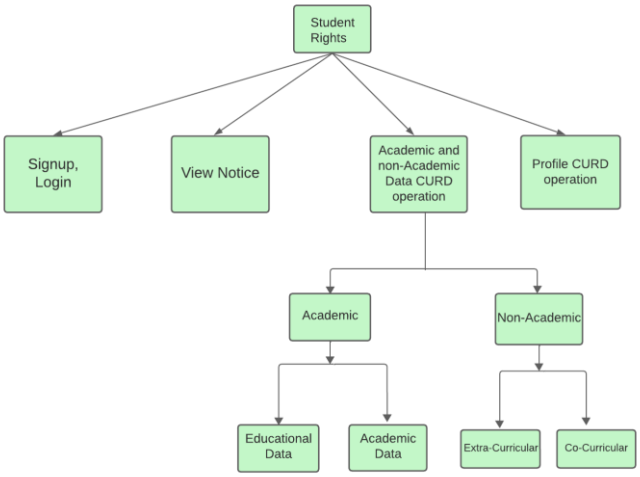


Fig. 2. Student's rights

Figure [2] represents rights assigned to the student. Students can upload their profiles, academic data, and co-curricular and extracurricular activities. They are also able to view notices uploaded by the faculty and admin.

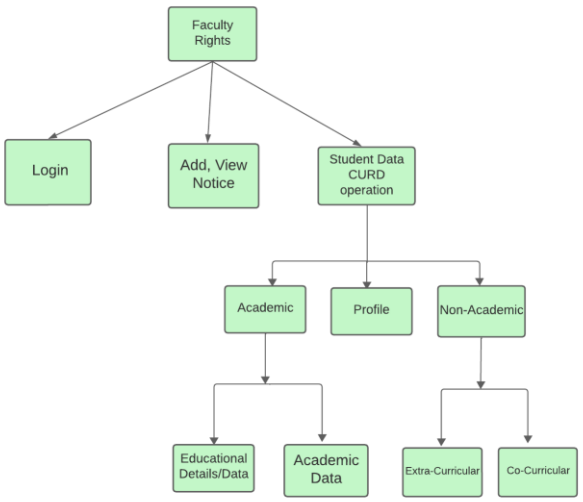


Fig. 3. Faculty rights

Figure [3] represents the rights that are assigned to the faculty. This student information system includes a faculty module that allows the faculty to carry out a number of important duties related to their instruction. Upon gaining access to their account, they can specifically browse student profiles that encompass all the necessary information about their students.

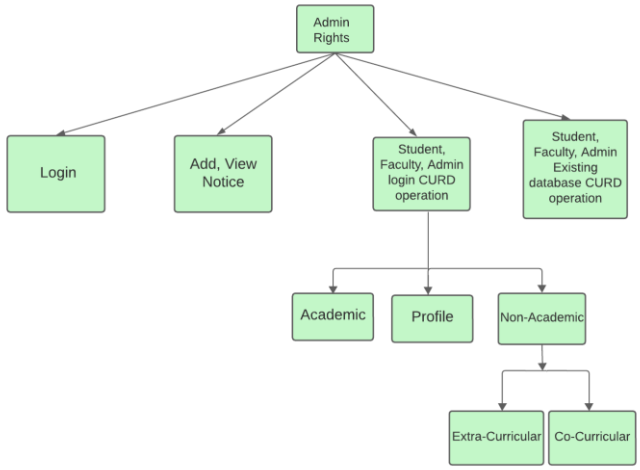


Fig. 4. Admin Rights

Figure [4] represents rights assigned to the Admin. Admin can view and add notices and can view and edit the academic and non-academic data of students. Also can view and edit the login credentials of all users.

IV. Implementation

The system has been built using the ASP.NET MVC (Model View Controller) framework. HTML, CSS, and JavaScript are utilized for the front end, while C-sharp programming language is employed for the back end. To manage data storage

and retrieval from the SQL Server database, SQL Server is utilized to store all system data.



Fig. 5. OTP validation

Figure [5] illustrates the process of OTP (One-Time Password) validation during the sign-up procedure for new users. The system restricts user registration to email addresses from the ”dbit.in” domain, which is the domain associated with the Institute. This limitation ensures that only individuals with valid college affiliations can create accounts within the system.

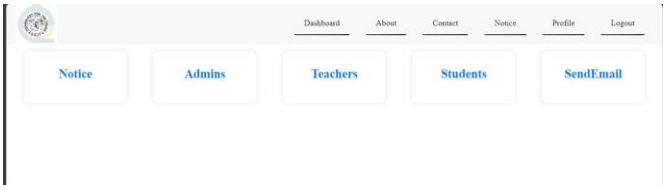


Fig. 6. Admin dashboard

Figure [6] represents the admin dashboard. Where the admin can view and edit the login credentials of other admins, teachers, and students.



Fig. 7. Adding notice

Figure [7] represents the form used specifically to add notices to the notice board of the website. This form allows department administrators or authorized personnel to input and submit notices, announcements, or updates relevant to the Department.



Fig. 8. Notice board

Figure [8] represents the notice board.

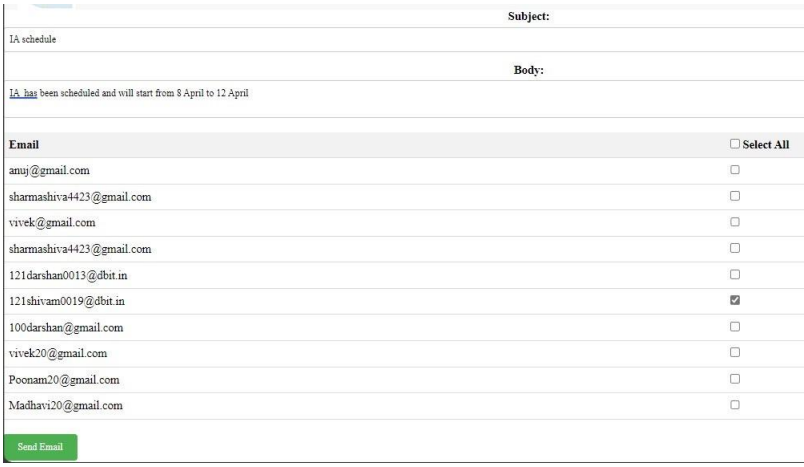


Fig. 9. Selection for email recipients

Figure [9] illustrates the feature enabling the sending of important notices to parents. Within this feature, administrators or faculty members can select the recipients to whom the email will be sent. This functionality allows for targeted communication, ensuring that relevant information reaches the intended recipients efficiently.

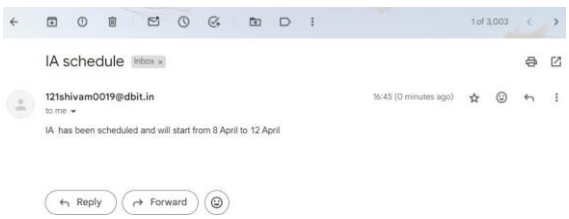


Fig. 10. Received mail

Figure [10] Shows the mail received by the parent.



Fig. 11. Student dashboard

Figure [11] depicts the student dashboard, providing a centralized interface for students to access and manage their academic and non-academic data. Within this dashboard, students can view their academic records, add new academic data such as grades or coursework, as well as input their curricular and extracurricular activities.

FUTURE SCOPE

In the future, access to login credentials can be extended to parents of students, enabling them to monitor their child's academic progress along with his/her participation in events and activities. The system can be extended to encompass features for managing data for attendance along with academic and non-academic records for students. Additionally, administrative features like fees and library management can be incorporated into the system to increase the functionality of the current system.

REFERENCES

[1] Jhanvi Agarwal, Renuka Singh, Mansi Singh, Mansi Raghav (2020), DEPARTMENT MANAGEMENT SYSTEM, International Journal of Engineering Applied Sciences and Technology.
[2] Chaitra B. S. (2018), An Innovative Information System for College Management, International Journal of Management, Technology.
[3] Ms.Swati S. Shintre, Ms.Shubhangi B. Bagul, Ms.Ashwini B. Kanawade Ms. Shital B. Tajanpure, Mr.Kishor N. Shedge (2020), DEPARTMENT ACTIVITY MANAGEMENT SYSTEM, International Journal of Creative Research Thoughts.
[4] Sonal J. Patel1 and Pooja D. Pancholi (2018), Implementation and Comparison of MVC Model in ASP.net Framework and PHP Framework, IJRAR- International Journal of Research and Analytical Reviews.
[5] Utkarsh Chauhan (2023), E-SHOPPING WEBSITE USING ASP.NET, International Research Journal of Modernization in Engineering Technology and Science [Digests 9th Annual Conf. Magnetics Japan, p. 301, 1982].
[6] Development of a Student Database Management System for a University (2016), Int. Journal of Engineering Research and Application.
[7] Student Management System (2021), Deepak Saini, Payal, Mansi Ghadigaonkar, Prof. Sujata Kadu. IJARIIE.
[8] College Management System (2016), Srikant Patnaik, Khushboo Kumari Singh, Rashmi Ranjan, Niki Kumari. International Research Journal of Engineering and Technology (IRJET)

A-eye: Attendance monitoring using face detection and recognition from CCTV footage

Nimesh Ambre[1], Raveena Pitale[2], Prajeet Rao[3], Satishkumar Chavan[4], Hemalata Mote[5]

[1]*Department of Electronics and Telecommunication Engineering*

[1]*The Bombay Salesian Society's, Don Bosco Institute of Technology, Mumbai, India*

[1]*nimeshambre08@gmail.com,* [2]*pitaleraveena@gmail.com,* [3]*raoprajeet7@gmail.com,*

[4]*satyachavan@gmail.com,* [5]*hemalata@dbit.in*

***Abstract*—Monitoring and updating attendance records of students is an integral part of activities in schools and colleges. To mitigate the laborious work of keeping attendance records, we propose an automated method of attendance monitoring using face as biometrics. In this paper, face detection and recognition for maintaining student attendance using deep learn- ing methodology is presented. Face detection in low-resolution CCTV footage is achieved using the Haar Cascade algorithmwith 88.59% detection accuracy. The detection is not limited to frontal face detection. It also has side face selection along with varied illumination situations. These detected faces are then used to create a student face database. The Convolutional Neural Network (CNN) is trained on this face database for student recognition to mark attendance. A total of 60 students' face data is used in this for recognition and updating attendance for5 subjects. The proposed CNN provided 76% face recognition accuracy for the implemented network.**

***Index Terms*—Face detection, face recognition, Haar cascade, Convolutional neural network, deep learning, Closed-circuit television.**

I. Introduction

The use of face biometrics systems in surveillance, particularly in the context of analyzing CCTV footage, has become increasingly pivotal in modern security applications [1], [2]. However, these systems encounter a myriad of challengessuch as poor resolution, varied lighting conditions, unwanted background and variation in size which can significantly impact their efficacy [3], [4]. To overcome these challenges, we propose an attendance monitoring system that integrates face detection and recognition algorithms with advanced image processing techniques along with video augmentation.

Face detection algorithms typically involve several steps to identify and locate faces within an image or video frame [5]. These steps often include pre-processing to enhance image quality, followed by feature extraction and classification to determine the presence of a face. Similarly, face recognition algorithms utilize intricate processes to match detected faces with known identities or stored templates, typically involving feature extraction, comparison, and verification [6].

However, challenges such as low image resolution, background clutter, and lighting variations can impede the effectiveness of these algorithms in CCTV footage analysis [7]. Low image resolution may lead to inaccurate detection and recognition results, while background clutter can obscure or interfere with the detection of faces. Additionally, lighting variations, including shadows and uneven illumination, pose significant challenges for accurate face detection and recognition.

To overcome these challenges, this paper proposes the application of histogram equalization to enhance image contrast and improve the visibility of facial features within CCTV footage. Additionally, localized histogram equalization techniques can be employed to selectively enhance regions of interest within the footage for better accuracy of face detection and recognition. Furthermore, video augmentation techniques can beutilized to generate additional training data by extracting facesfrom CCTV footage at various angles and orientations, thereby enhancing the robustness of face detection and recognition algorithms.

By integrating these advanced image processing techniques with face detection and recognition algorithms, this paper aims to provide a comprehensive solution to the challenges encountered in analyzing CCTV footage for the detection of faces, recognition, and updating attendance. The proposed methodology offers the potential to improve accuracy, reliability, and efficiency.

II. Literature Survey

The integration of face recognition into attendance monitoring system is an essential transformative shift for attendance tracking and management. This literature survey delves into approaches for attendance monitoring system using face recognition. Automatic monitoring of attendance based on face

Accepted: International Conference, eSmarTA-2024

recognition is a need of an hour. Such system detects and localizes the faces from closed circuit television (CCTV) anda person is recognized based on face is required in educational institutions. Powale et al. [8] trained and validated 62 student faces for attendance monitoring using 6 layers of CNN framework using low-resolution closed-circuit television (CCTV) footage. Bhatti et al. [9] proposed an automatic attendance monitoring system in which face detection is achieved using histogram-oriented gradients (HOG) and 128-d facial points are extracted for face matching. Yang and Han [10] developed the attendance system based on face recognition using a real-time video acquisition with 82% accuracy of face recognition.The neural network extracts a variety of features that distinguish one face from another. These features are useful setsfor identifying each person's face and are saved in a databasefor potential recognition [6]. Face detection looks for the face,its location, and putting the bounding box around the faces.Dong et al. [11] presented an intelligent face detection system which cascading multiple feature layers in video surveillancecameras to localize a face accurately. Shukla and Tiwari et al.
[12] provided an extensive survey of deep learning methods for face detection and recognition. Face detection using Haar features and Adaboost face detector and face recognition using Seetaface and YouTu methods are proposed by Lu and Yan [13].

Face recognition is the authentication of every individual's identity. Facial features are effectively used to discern one person from another [8]. Face Recognition poses various challenges such as occlusions, pose shifts, expressions, aging, and variations in facial information [14]. The deep learning approach is a preferred choice for such an application provided the availability of huge data. Deep learning can produce astonishing results in face recognition by increasing the number of layers to provide a decent approximation of a complex function [15]. The superposed linear representation approach, inspired by a linear discriminant analysis (LDA), is devel- oped for face recognition in [16]. There are limitations for available face recognition and detection algorithms to correctlyrecognize faces under diverse circumstances such as different lighting and backgrounds [17]. Kashyap et al. [18] developed aCNN model for classifying faces in three categories (face with-out mask, face with mask and face with incorrect mask). The work also tested their model for different lighting conditions. Rostami et al. [19] proposed a Mobile Net-based model for facedetection and recognition on Drone Face and ATT datasets for recognizing the scaled and occluded faces from aerial images. Khan et al. [20] presented the MTCNN++ Deep learning model for face recognition in face density images. Ullah etal. [21] developed a system for face detection and recognition from CCTV images wherein face features are extracted using principal component analysis (PCA) and convolutional neural network (CNN) and faces are classified using machine learning and deep learning techniques. Arsenovic et al. [22] developed a face recognition attendance system in which face detection, face embedding, and face recognition is achieved using CNN cascade, Face Net CNN, and SVM, respectively. Jafri et al. [23] developed a CNN-based liveliness detection system in which only faces in photographs should not be detected as living human faces.

III. Methodology

In the proposed system, we created a database of faces captured from low-resolution CCTV cameras. Haar feature-based cascade classifier, an efficient method of object identification, is used for the detection of faces [24]. The algorithm looks for features like the eyes, nose, and mouth [6] for face detection purposes. The Haar Cascade is performed by superimposing the positive image over a set of negative images [15]. In this work, faces with various orientations after augmentation are also detected and added to the database. The images are pre-processed to resize each image to an appropriate size for the CNN models [19]. This dataset is used for the training of the convolutional neural network (CNN) model.

Convolutional neural networks are commonly employed in tasks involving image and video classification. They are specifically designed to learn spatial hierarchies of features from raw input data automatically and adaptively [24]. CNN models are used for the speedy face detection that evaluates low-resolution input images and eliminates non-face sections because of which highly precise detection is possible [18]. The system for attendance monitoring using face detection and recognition is presented in Fig. 1. It follows a struc-tured process comprising three primary steps namely database creation using the Haar cascade algorithm, face recognition from detected faces, and maintaining attendance records in a database management system.

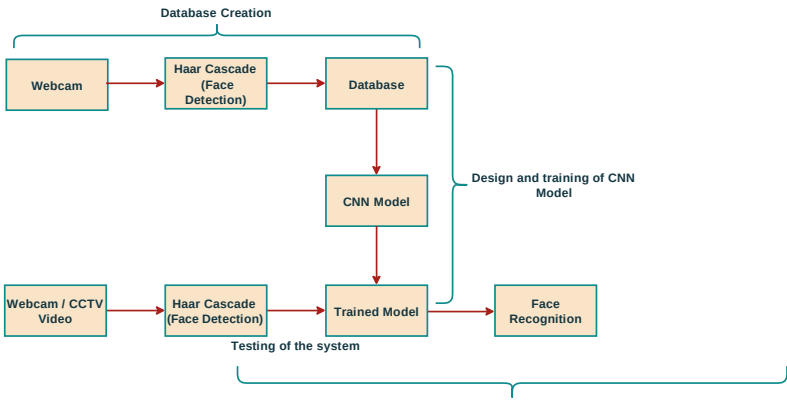


Fig. 1. General block schematic of face detection and recognition system

Haar cascade algorithm detects and crops the faces from image frames of CCTV footage to form a comprehensive collection of facial data. The CNN model, designed to analyze visual data, learns to identify and extract distinctivefeatures from the faces. This training process involves feedingnumerous labeled images to the network which may help in improving its accuracy of recognizing individual faces. The outcome is a trained CNN model capable of accurate face

recognition. The trained network is tested on real-time images captured from webcams or CCTV cameras. This real-time functionality is crucial for applications like attendance monitoring, where the system must reliably identify individualsto log attendance accurately. Combining database creation,model training, and real-time testing ensures the system isboth accurate and capable of performing in various conditions, from high-quality images to lower-resolution CCTV footage.

A. Augmentation

Video augmentation [25] is a pivotal process in enhancing the robustness and effectiveness of face recognition systems applied to CCTV footage. The augmentation begins by extracting individual frames containing faces from the video footage. Subsequently, these frames undergo a series of transformations to simulate diverse real-world scenarios and ensure the recognition model's resilience to variability. These transformations may include changes in facial orientation, lighting conditions, facial expressions, and occlusions. Additionally, augmentation techniques like rotation, scaling, translation, and flipping are applied to simulate variations in viewing angles and distances.Furthermore, synthetic noise or distortions may be introduced to emulate adverse conditions such as blurriness or sensor noise. Once augmented, the frames are reassembled into a video sequence, creating a diverse dataset that challenges the recognition model to generalize across different environmental conditions and facial appearances. Through this iterative process of augmentation, the face recognition system becomes more robust, adaptive, and capable of accurately identifying faces across a wide range of scenarios encountered in real- world surveillance applications. Figure 2 shows the dataset created by extracting the faces of students after augmentation of video from the CCTV footage.

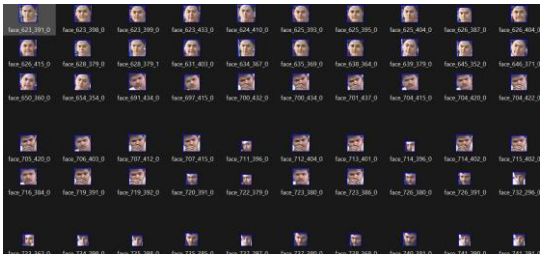


Fig. 2. Cropped faces after extracting them from augmented CCTV footage

B. Haar Cascade

In this work, the Haar cascade algorithm is used for detecting the faces in images that are scale-invariant and location-independent [26]. It is simple, fast, and works well in a real-time. It functions as a classifier to identify the face in cascading windows by computing features in that particular window. It selects matching features for detecting faces as wellas rejecting a face for non-matching features. Haar cascade gives a lot of false positives. The various masks used in face detection while implementing the Haar cascade algorithm are displayed in Fig. 3.

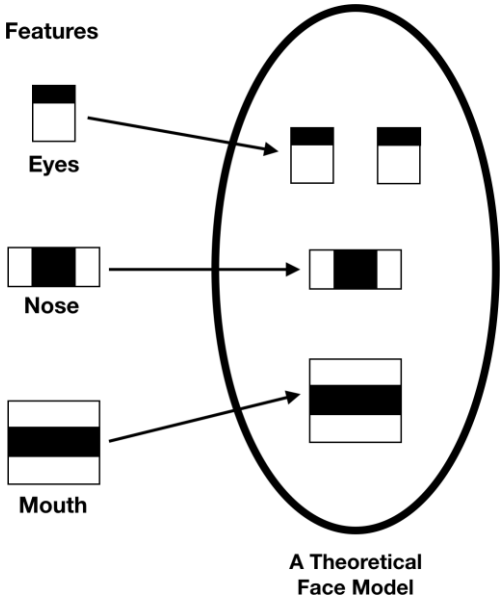


Fig. 3. Haar Facial Parameters

In the proposed system, we have used the existing infrastructure of our college. The CCTV cameras installed in the classroom are used to capture the footage of the classroom while the lecture is going on. We worked on recorded CCTV footages. Applying the Haar cascade to the video directly, we did not get the promising results of detection. So, we applied histogram equalization to the video frames. The detection accuracy is improved compared with detection from normal video. However, some faces were not being detected. This is due to uneven illumination conditions, random noise, and varied contrast. So, we applied a localized histogram to the video. Localized histogram is an adaptive histogram equalization process to mitigate illumination and contrast variations. This made the video very much useful for face detection as theimproved face detection accuracy is achieved in low-resolutionCCTV cameras. Fig. 4 shows the detected faces from low- resolution CCTV cameras. The extracted faces are extremely small and a bit blurry because of long-distance image capture and low-resolution camera as shown in Fig. 5.

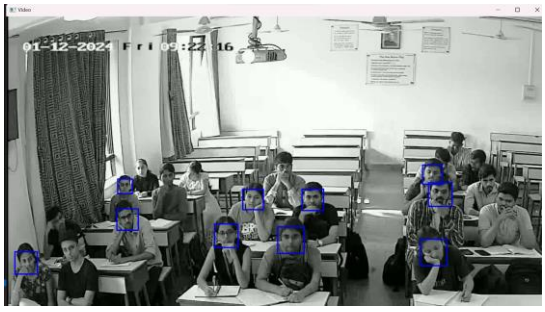


Fig. 4. Face Detection using Haar Cascade

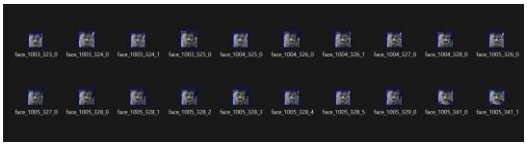


Fig. 5. Face Extraction using Haar Cascade

C. Convolutional Neural Network (CNN):

CNN is used for the classification of faces to map students' attendance in the record. It is a feed-forward neural network comprised of convolutional layers and fully connected layers. Input images are applied to train a CNN resulting in the feature maps. It extracts hierarchical patterns and characteristics from given images similar to the visual cortex ofthe human brain. Convolution operation preserves the spatial relationship between pixels by the use of tiny input squaresto learn image properties. A variety of learning neurons canbe used to transform the image into the input. This results inan activation map or map on the output image and then the function maps are fed into the next convolution layer as input data [23]. The general CNN architecture is given in Fig. 6. Theframework consists of 4 convolutional layers along with ReLUand 1 flatten layer and 1 fully connected layer with dropout layers at each convolution layer and final softmax layer. Batchnormalization and max pooling are used in a few layers. The detailed architecture is presented in Table I.

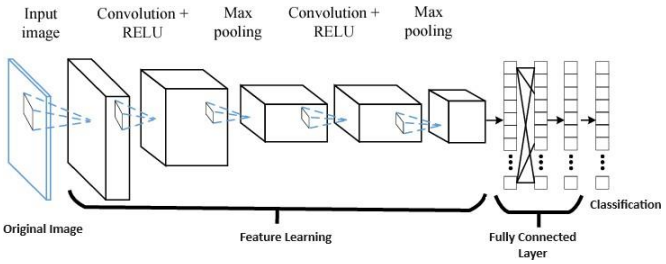


Fig. 6. Layers of CNN

TABLE I
PROPOSED CNN ARCHITECTURE DETAILS

Layer	Tensor Size
Input image	64 × 64
Conv-I	64×64×64
MaxPool-I	32×32×64
Conv-II	32×32×128
MaxPool-II	16×16×128
Conv-III	16×16×512
MaxPool-III	8×8×512
Conv-IV	8×8×512
MaxPool-IV	4×4×512
Flatten	512×1
Dense	256×1
Output	60×1

IV. IMPLEMENTATION

The CCTV video was downloaded from the college server. Adaptive histogram equalization is applied on the video frames to improve contrast to get better detection accuracy. Then, the augmentation process is implemented to increase the sample size in the database of faces. The Haar cascade classifier detects student's face in a class. The bounding box is put on the face detected. These detected faces are extracted and storedin a local storage device as a database. The image size of the extracted faces from the video frame is varying in size (from 32×32 to 64×64). These images are tiny faces.

TABLE II
PERFORMANCE OF HAAR CASCADE FACE DETECTION

Video No.	Frame No.	# Students	Detected faces	% Accuracy
1	15	31	29	93.54
2	22	42	38	90.48
3	39	40	34	85.00
4	5	26	21	80.77
5	74	44	41	93.18
Average Detection Accuracy				88.59

Haar cascade provides an average detection accuracy of 88.59% as presented in Table II. It took less than 15 seconds to extract 50 images per student. These faces are segregated and divided into train and test folders. The training and testing sets are mutually exclusive sets. In the training dataset, a total 7788 images are stored in 34 classes i.e. (Students), and in the test dataset, 1947 images are stored in 26 classes i.e. (Students). Each folder name is a label for a class (i.e. names of the students).

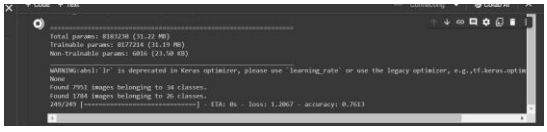


Fig. 7. Result of CNN Output

A. Results and Discussion

The facial images of 60 students were captured using low-resolution CCTV cameras. A minimum of 100 images per person were stored in respective labeled folders. We varied the dataset i.e. no fixed numbers of images were stored in the folders. We split the dataset in the train-test set as 80:20 which gave the highest accuracy. A total of 9735 images of 60 students were used from training and testing of CNN with 249 epochs. CNN was tested on 1947 images and gained an accuracy of 76%.

The same model was tested on publicly available tiny faces dataset [3] for face recognition and received a recognition accuracy of 84%. The accuracy of recognition for this dataset is comparatively better as these images are high quality images. Table III presents a comparative evaluation of face recognition using the proposed model for two datasets namelyour college dataset (DBIT) and tiny face dataset [3].

TABLE III
COMPARATIVE EVALUATION OF CNN ALGORITHM FOR COLLEGE DATASETS AND ONLINE DATASET

Dataset	*Accuracy*	*Recall*	*Precision*	*F1score*
DBIT dataset	76	78	71	74.33
Tiny Faces [3]	84	85	82	83.47

We have experimented the face recognition algorithms and tested on DBIT college dataset. The comparative evaluation is presented in Table IV.

TABLE IV
COMPARATIVE EVALUATION OF FACE RECOGNITION ALGORITHM FOR DBIT COLLEGE DATASETS

Method	*Accuracy*	*Recall*	*Precision*	*F1score*
CNN [8]	76	78	71	74.33
SIAMESE CNN [27] [3]	84	85	82	83.47
[28]	84	85	82	83.47

B. Student Attendance Monitoring System (SAMS)

This student attendance monitoring system (SAMS) incorporates an interactive dashboard to support students making them aware of their attendance data throughout the semester. The dashboard offers two approaches. First, it presents a detailed breakdown of individual attendance records for each subject in a tabular format. Second, the dashboard leverages graphical representations to depict a student's cumulative attendance percentage for the entire semester. This visual approach facilitates easy comprehension of attendance trends and allows students to readily identify courses in which attendance needs to be improved. Furthermore, the system employs a unique login identification (ID) for each student. This ensures the security and privacy of individual attendance data by restricting access solely to the student. Figure 8 shows the dashboard for students after login.

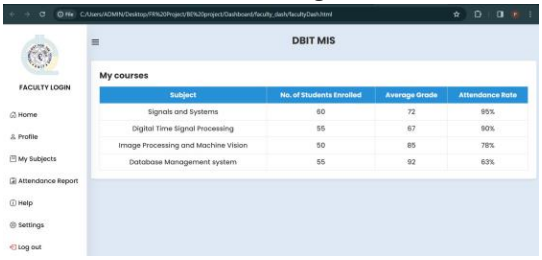


Fig. 8. Screenshot of Student Dashboard

This faculty dashboard serves the purpose of facilitating instructor overview of students' attendance patterns as shown in Figure 9.

The dashboard offers a comprehensive suite of features designed to streamline attendance monitoring by faculty members to take corrective action in time. It also displays students' grades. This targeted view allows instructors to easily identify students who might be falling short of attendance for a course along with the performance of the student. This granular

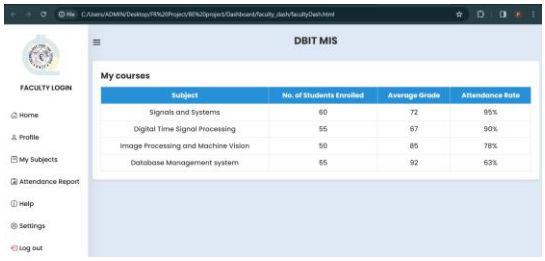


Fig. 9. Screenshot of Faculty Dashboard

level of information allows instructors to pinpoint specific instances of absence and address any potential attendance concerns promptly. Finally, recognizing the possibility of data discrepancies, the system incorporates a mechanism for manual correction of attendance records. This helps faculty members to rectify any errors that might arise. This system isa useful tool for the early identification of potential attendanceissues and for monitoring students' performance.

V. CONCLUSION

Face detection and recognition have been evolving and challenging research over the years. Many methodologies are developed and available to accomplish this task. In this paper, face detection and face recognition in low-resolution frames from CCTV footage is achieved. We have created our dataset of 60 students from the CCTV footage in which the faces of the students are extracted using the Haar Cascade Classifier and classified using the CNN model. The developedCNN pipeline is also tested for an online dataset for facerecognition. The system provided 88.59% detection accuracy and 76% recognition accuracy for the college dataset. This system worked well for our dataset even though very low- resolution images and blurry faces. The algorithm worked verywell on tiny face images as the quality of tiny face dataset images is comparatively better than the college dataset. This work can be useful for surveillance and tracking of suspicious activity.

REFERENCES

[1] B. Kranthikiran and P. Pulicherla, "Face detection and recognition for use in campus surveillance," *International Journal of Innovative Technology and Exploring Engineering*, vol. 9, no. 3, pp. 2908–2913, 2020.

[2] A. Jaiswal and S. Tarar, "Real-time biometric system for security and surveillance using face recognition," in *Advances in Computing and Data Sciences: 4th International Conference, ICACDS 2020, Valletta, Malta, April 24–25, 2020, Revised Selected Papers 4*. Springer, 2020, pp. 293–304.

[3] Z. Cheng, X. Zhu, and S. Gong, "Low-resolution face recognition," in *Computer Vision–ACCV 2018: 14th Asian Conference on Computer Vision, Perth, Australia, December 2–6, 2018, Revised Selected Papers, Part III 14*. Springer, 2019, pp. 605–621.

[4] M. O. Oloyede, G. P. Hancke, and H. C. Myburgh, "A review onface recognition systems: recent approaches and challenges," *MultimediaTools and Applications*, vol. 79, no. 37, pp. 27 891–27 922, 2020.

[5] S. Minaee, P. Luo, Z. Lin, and K. Bowyer, "Going deeper into face detection: A survey," *arXiv preprint arXiv:2103.14983*, 2021.

[6] B. Koodalsamy, M. B. Veerayan, and V. Narayanasamy, "Face recognition using deep learning," in *E3S Web of Conferences*, vol. 387, 2023, p. 05001.

[7] H.-J. Mun and M.-H. Lee, "Design for visitor authentication basedon face recognition technology using cctv," *IEEE Access*, vol. 10, pp. 124 604–124 618, 2022.
[8] S. Powale, A. Dhanawade, S. Bagwe, S. Kawale, N. L. Chutke, and S. Chavan, "Person identification in low resolution cctv footage using deep learning," in *2020 2nd International Conference on Advances in Computing, Communication Control and Networking (ICACCCN)*, 2020, pp. 236–240.
[9] K. L. Bhatti, L. Mughal, F. Y. Khuhawar, and S. A. Memon, "Smart attendance management system using face recognition," *EAI Endorsed Transactions on Creative Technologies*, vol. 5, no. 17, 10 2018.
[10] H. Yang and X. Han, "Face recognition attendance system based on real-time video processing," *IEEE Access*, vol. 8, pp. 159 143–159 150,2020.
[11] Z. Dong, J. Wei, X. Chen, and P. Zheng, "Face detection in security monitoring based on artificial intelligence video retrieval technology," *IEEE access*, vol. 8, pp. 63 421–63 433, 2020.
[12] R. Kumar Shukla and A. Kumar Tiwari, "Comparative analysis of machine learning based approaches for face detection and recognition," *Journal of Information Technology Management*, vol. 13, no. 1, pp. 1–21, 2021.
[13] D. Lu and L. Yan, "[retracted] face detection and recognition algorithm in digital image based on computer vision sensor," *Journal of Sensors*, vol. 2021, no. 1, p. 4796768, 2021.
[14] P. Melzi, R. Tolosana, R. Vera-Rodriguez, M. Kim, C. Rathgeb, X. Liu, I. DeAndres-Tame, A. Morales, J. Fierrez, J. Ortega-Garcia *et al.*, "Frcsyn challenge at wacv 2024: Face recognition challenge in the era of synthetic data," in *Proceedings of the IEEE/CVF Winter Conference on Applications of Computer Vision*, 2024, pp. 892–901.
[15] K. Teoh, R. Ismail, S. Naziri, R. Hussin, M. Isa, and M. Basir, "Face recognition and identification using deep learning approach," in *Journal of Physics: Conference Series*, vol. 1755, no. 1, 2021, p. 012006.
[16] W. Deng, J. Hu, and J. Guo, "Face recognition via collaborative representation: Its discriminant nature and superposed representation," *IEEE transactions on pattern analysis and machine intelligence*, vol. 40, no. 10, pp. 2513–2521, 2017.
[17] S. Hangaragi, T. Singh, and N. Neelima, "Face detection and recognition using face mesh and deep neural network," *Procedia Computer Science*, vol. 218, pp. 741–749, 2023.
[18] G. S. Kashyap, J. Sohlot, A. Siddiqui, R. Siddiqui, K. Malik, S. Wazir, and A. E. Brownlee, "Detection of a facemask in real-time us- ing deep learning methods: Prevention of covid 19," *arXiv preprint arXiv:2401.15675*, 2024.
[19] M. Rostami, A. Farajollahi, and H. Parvin, "Deep learning-based face detection and recognition on drones," *Journal of Ambient Intelligence and Humanized Computing*, vol. 15, no. 1, pp. 373–387, 2024.
[20] S. S. Khan, D. Sengupta, A. Ghosh, and A. Chaudhuri, "Mtcnn++: A cnn-based face detection algorithm inspired by mtcnn," *The Visual Computer*, vol. 40, no. 2, pp. 899–917, 2024.
[21] R. Ullah, H. Hayat, A. A. Siddiqui, U. A. Siddiqui, J. Khan, F. Ullah, S. Hassan, L. Hasan, W. Albattah, M. Islam *et al.*, "A real-time framework for human face detection and recognition in cctv images." *Mathematical Problems in Engineering*, 2022.
[22] M. Arsenovic, S. Sladojevic, A. Anderla, and D. Stefanovic, "Face-time—deep learning based face recognition attendance system," in *2017 IEEE 15th International symposium on intelligent systems and informatics (SISY)*. IEEE, 2017, pp. 000 053–000 058.
[23] S. Jafri, S. Chawan, and A. Khan, "Face recognition using deep neural network with LivenessNet," in *2020 International Conference on Inventive Computation Technologies (ICICT)*, 2020, pp. 145–148.
[24] S. Mansoora, G. Sadineni, and S. H. Kauser, "Attendance management system using face recognition method," in *Journal of Physics: Conference Series*, vol. 2089, no. 1, 2021, p. 012078.
[25] N. Cauli and D. Reforgiato Recupero, "Survey on videos data augmentation for deep learning models," *Future Internet*, vol. 14, no. 3, p. 93, 2022.
[26] L. Cuimei, Q. Zhiliang, J. Nan, and W. Jianhua, "Human face detection algorithm via haar cascade classifier combined with three additional classifiers," in *2017 13th IEEE international conference on electronic measurement & instruments (ICEMI)*. IEEE, 2017, pp. 483–487.
[27] W. Wang, J. Yang, J. Xiao, S. Li, and D. Zhou, "Face recognition based on deep learning," in *Human Centered Computing: First International Conference, HCC 2014, Phnom Penh, Cambodia, November 27-29,2014, Revised Selected Papers 1*. Springer, 2015, pp. 812–820.
[28] H. Wang and L. Guo, "Research on face recognition based on deep learning," in *2021 3rd International Conference on Artificial Intelligence and Advanced Manufacture (AIAM)*, 2021, pp. 540–546.